University of Glasgow | School of Chemistry

# The Investigation and Development of IGD Peptidomimetics as Wound Healing Agents

Mhairi Matheson

MSci

This thesis is submitted in part fulfilment of the requirements for the Degree of Doctor of Philosophy

June 2015

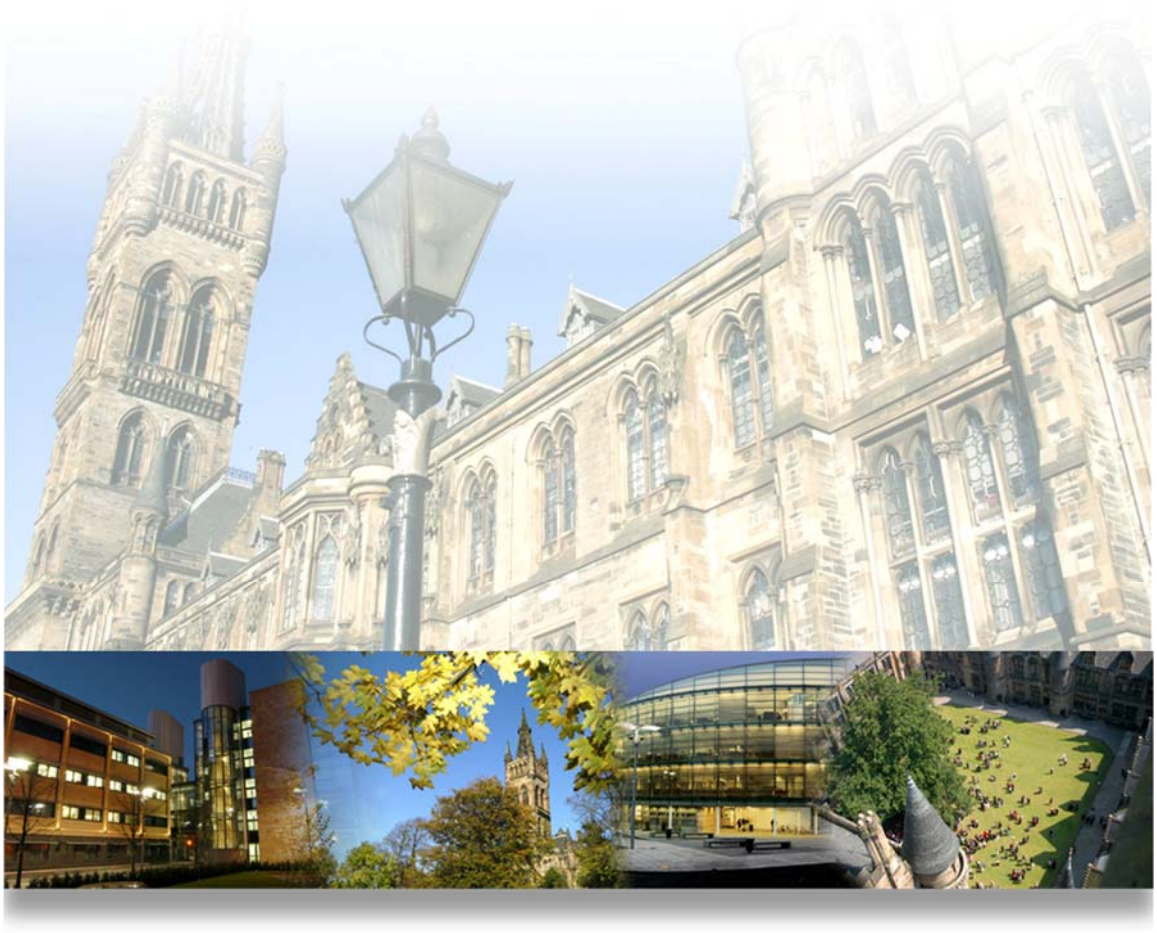

## Abstract

An ever increasing incidence of diabetes has resulted in an epidemic of chronic wounds. Few therapies effectively promote wound healing, and thus, health care budgets are faced with an unsustainable burden and patients with poor quality of life.

Recently, the isoleucine-glycine-aspartic acid (IGD) tripeptide motif of Migration Stimulating Factor (MSF) has been found to be responsible for the wound healing properties of this protein. Modelling studies of the IGD motif of MSF have lead to the design and synthesis of a benzodiazepinone core, which displays wound healing properties *in vitro* and *in vivo*. This thesis discusses the optimisation of the synthetic route to this exciting IGD peptidomimetic and investigations into the activity and the method of action of this molecule through scratch assays and qRT-PCR studies.

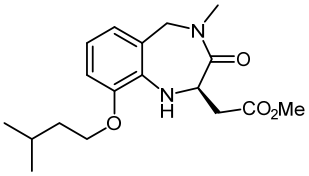

Analogues of this benzodiazepinone with varying synthetic handles have been developed and used to tag the active bicyclic core with desired technologies. In one such example, BODIPY tagging and confocal microscopy allowed the investigation of fibroblast uptake of the BODIPY IGD peptidomimetic. An IGD peptidomimetic with a triethylene glycol synthetic handle has been developed for increased hydrophilicity and is envisioned to be used in the development of a therapeutic hydrogel.

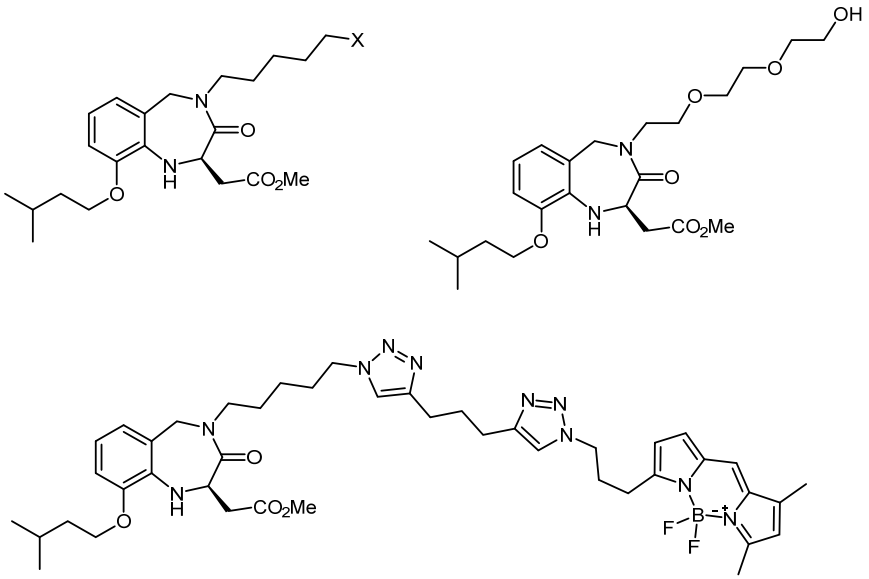

Contents


Acknowledgements v

Abbreviations vii

Authors Declaration x

1.0 Introduction

1.1 Wound Healing 1

1.2 Wound Healing In Relation to Diabetes 3

1.3 The Extra Cellular Matrix and Fibroectin 6

1.4 Migration Stimulating Factor 9

1.5 First Generation IGD Peptidomimetic 12

1.6 Synthesis of the First Enantiomerically Pure IGD Peptidomimetic 14

1.7 *In Vitro* and *In Vivo* Testing of the IGD Peptidomimetics 16

2.0 Project Aims

2.1 Development and Investigation of Methyl IGD Peptidomimetics 18

2.2 IGD Peptidomimetics with Synthetic Handles 19

3.0 Results and Discussion

3.1 Optimisation of IGD Peptidomimetic Intermediates 20

3.2. Methyl IGD Peptidomimetics 24

3.3 Biological Assessment of Methyl IGD Peptidomimetics 27

3.4 Scratch Assays and RT-qPCR for the Investigation of (*R*)- and (*S*)-IGD Peptidomimetics 32

3.5 Polymerase Chain Reaction Experiments 38

3.6 Implications of RT-qPCR 44

3.7 IGD Peptidomimetics with Synthetic Handles 46

3.8 Benzodiazepinone Cyclisation 53

3.9 Diverging From IGD Peptidomimetic Alcohols 24 and 26 63

3.10 IGD Peptidomimetic Immobilisation 70

3.11 Synthesis of BODIPY IGD Peptidomimetic *via* an Amide Coupling 74

3.12 Synthesis of BODIPY IGD Peptidomimetic *via* Meso Substitution 80

3.13 Synthesis of BODIPYFluorescent IGD Peptidomimetics *via* Huisgen Cyclisation 83
3.14 Confocal Microscopy with MM-IGD-FL1 and MM-IGD-FL2 96
3.15 Iodine Containing IGD Peptidomimetic 100
3.16 Difunctionalised BODIPY Tagged IGD Peptidomimetic 102
3.17 Ethylene Glycol IGD Peptidomimetics 110

4.0 Future Directions and Conclusions

4.1 Methyl IGD Peptidomimetics 115
4.2 Pentyl IGD Peptidomimetics 116
4.3 BODIPY Tagged IGD Peptidomimetics 116
4.4 Difunctionalised BODIPY Tagged IGD Peptidomimetics 117
4.5 Triethylene Glycol IGD Peptidomimetics 118
4.6 Biotinylated IGD Peptidomimetics 120

5.0 Experimental

5.1 Chemistry General Infromation 121
5.2 Reaction Procedures and Compound Analysis 122
5.3 Biology General Information 175
5.4 General Protocols for Splitting and Maintaining Human Fibroblast Cultures 175
5.5 HDFn Scrape Wounds General Procedure 175
5.6 RNA Extraction Protocol 176

6.0 Appendices

6.1 Serum Free vs Complete DMEM Scratch Assay Results 178
6.2 Determination of Optimal Dose (*S*)-Methyl IGD Peptidomimetic 179
6.3 Determination of Optimal Dose (*R*)-Methyl IGD Peptidomimetic 180
6.4 Solid Supported IGD Peptidomimetic NMR 181
6.5 Absorption and Emission Spectra 183
6.6 Genes Investigated in Human Cell Motility RT-qPCR Array 186

7.0 References 187

## Acknowledgements

Thank you to my mentor Dr. Marquez whose kindness and faith has encouraged me all the way from the undergraduate labs. I've learned so many things from you Rudi: which layer is which; obscure 90s American film references and that red wine looks exactly like black coffee in the right mug.

Further thanks must go to my secondary supervisors; Prof. Hartley and Prof. Dalby; for lending me their expertise and a big thank you to Carol-Anne Smith for support with the cell migration assays. I am also extremely grateful to Dr. Kate Wright for the many hours of help and training she invested in this chemist dabbling in the biology occult. Thanks to all of the support staff in the Joseph Black Building, particularly Jim and Harry in mass spec, David in NMR, Ted and Bruce in stores and Margaret for keeping me up to date with the gossip.

I gratefully acknowledge The Kelvin-Smith Scholarship for funding. I cannot express enough appreciation to Prof. Graeme Cook and Prof. Stephen Clark for their reassurance and additional financial support, enabling me to complete this thesis.

To Marquez group members, past and present, Ben, Alasdair, Jen, Anna, Faustine, Colin, Alan, Tom, Hugh, Riccardo, Sean, Liam, Alejandro, Ricardo and Ezequiel and to the Prunet and France groups, thank you for all of your help and support. I'll miss the Raphael lab. From rugby tackles to big mince; I'll miss your hilarious stories, questionable music, cakings, Anthea Turner jibes, whiteboard diagrams, but most of all I'll miss writing passive aggressive notes to you.

To my heroes, Mum, Dad and Emma, thank you for all of the many ways you've gone through the last few years with me and for being by my side…even when I leave the continent. Thank you to Shaun for keeping me company in the department far too late on so many weekend nights. To my lovely family and friends, particularly Agnes, Caroline, Wilma, Dave, Kerry, Ross, Jamie, James, Gemma, Laura and Jen, thank you for always being around. It's time for a wee pint in the Anchor.

Thanks goes to JSPS, for allowing me to have an incredible Japanese adventure. I am very grateful to Suzuki Sensei and Ohmori Sensei for allowing me to work in their prestigious laboratory.

Finally, thank you to the staff at the Beatson and Maggie's Centre, particularly Dr Pamela McKay, Julie Cain, Dr Debbie Roebuck and Fiona Murdoch whose calm dedication and insight allowed me to get well and complete this thesis.

Chemistry is…

Well, technically, chemistry is the study of matter.
But I prefer to see it as the study of change.
Now just just think about this:

Electrons.
They change their energy levels.

Molecules.
Molecules change their bonds.

Elements.
They combine and change into compounds.

Well, that's…that's all of life.
Right? I mean, it's just…

It's the constant.
It's the cycle.

It's solution, dissolution, just over and over and over.
It is growth, then decay, then transformation.

It is fascinating, really.

Walter H. White

## Abbreviations

| | |
|---|---|
| Ac | acetyl |
| ACTN3 | actnin alpha 3 |
| AIBN | azobisisobutyronitrile |
| AKT | protein kinase B |
| Asc | ascorbate |
| AZADO | 2-azaadamantane *N*-oxyl |
| BAIB | bis(acetoxy)iodobenzene |
| Boc | *tert*-butyloxycarbonyl |
| BODIPY | 4,4-difluoro-4-bora-3a,4a-diaza-*s*-indacene |
| BSA | bovine serum albumin |
| cDMEM | complete Dulbecco's modified Eagle's medium |
| cDNA | complementary |
| cFN | cellular fibronectin |
| COSY | correlation spectroscopy |
| CuTC | copper (I)-thiophene-2-carboxylate |
| DCM | dichloromethane |
| DIPEA | di*iso*propylethylamine |
| DMAP | dimethylaminopyridine |
| DMEM | Dulbecco's modified Eagle's medium |
| DMF | dimethylformamide |
| DMSO | dimethylsulfoxide |
| DNA | deoxyribonucleic acid |
| ECM | extra cellular matrix |
| ED-A | extra domain A |
| ED-B | extra domain B |
| FAK | focal adhesion kinase |
| FBS | fetal bovine serum |
| Fmoc | fluorenylmethyloxycarbonyl |
| HBTU | *N,N,N′,N′*-tetramethyl-*O*-(1*H*-benzotriazol-1-yl)uronium hexafluorophosphate |
| HDFn | human dermal fibroblasts neonatal |
| HEK | human embryonic kidney cells |
| HIF-1 | hypoxia-inducible factor 1 |

| | |
|---|---|
| HPLC | high performance liquid chromatography |
| HRMS | high resolution mass spectroscopy |
| HSQC | heteronuclear single quantum correlation |
| hTERT | telomerase reverse transcriptase (human) |
| IBX | 2-iodoxybenzoic acid |
| IGD | isoleucine-glycine-aspartic acid |
| IGDQ | isoleucine-glycine-aspartic acid-glutamine |
| IGDS | isoleucine-glycine-aspartic acid-serine |
| IGF1 | insulin like growth factor 1 |
| Ms | mesyl |
| MSF | migration stimulating factor |
| NBS | *N*-bromo succinimide |
| NIS | *N*-iodo succinimide |
| NMO | *N*-methyl morpholine |
| NMR | nuclear magnetic resonance |
| PBS | phosphate buffered solution |
| PCR | polymerase chain reaction |
| PDGF | platelet derived growth factor |
| PDGF-BB | B chain homodimer of PGDF |
| pFN | plasma fibronectin |
| qRT-PCR | real time reverse transcriptase polymerase chain reaction |
| rpm | revolutions per minute |
| RGD | arginine-glycine-aspartic acid |
| RGDS | arginine-glycine-aspartic acid-serine |
| RT | room temperature |
| SCX | strong cation exchange |
| SDGI | serine-aspartic acid-gycine-isoleucine |
| sfDMEM | serum free Dulbecco's modified Eagle's medium |
| TBAF | tetra-*N*-butylammonium fluoride |
| TBAI | tetrabutylammonium iodide |
| TBDPS | *tert*-butyldiphenylsilyl ether |
| TEA | triethylamine |
| TEMPO | 2,2,6,6-tetramethylpiperidinyloxy |
| TFA | trifluoroacetic acid |
| THF | tetrahydrofuran |
| TLC | thin layer chromatography |

| | |
|---|---|
| (TGF)$\beta$1 | transforming growth factor |
| TPAP | tetrapropylammonium perruthenate |
| Ts | tosyl |
| VEGF | vascular endothelial growth factor |

Authors Declaration

I declare that, except where explicit reference is made to the contribution of others, that this dissertation is the result of my own work and has not been submitted for any other degree at the University of Glasgow or any other institution. All chemical synthesis and analysis was carried out in the Raphael lab at the University of Glasgow. All biological testing and data analysis was carried out at the University of Glasgow or Caledonian University by the author unless otherwise stated in the text.

Mhairi Matheson

June 2015

# 1.0 Introduction

## 1.1 Wound Healing

Impaired wound healing is a significant cause of morbidity and mortality for a large proportion of the population. With the ever increasing incidence of diabetes and other diseases that blight wound healing it is now believed that 1% of the European population are affected by chronic wounds and that 2% of health budgets are devoted to their care.[1] [2] Patients with chronic wounds suffer from a significant decrease in quality of life, however, to date the choice of wound healing promoting drugs can be described as limited at best. [2]

### 1.1.1 Physiological Wound Healing

There are four overlapping phases of normal healing: haemostasis; inflammation; migration proliferation and remodeling (**Figure 1.1.1**).[3]

### 1.1.2 Haemostasis and Inflammation

Haemostasis involves vasoconstriction and platelet activation, very quickly after the injury has occurred a fibrin plug forms and inflammatory cells are activated. The fibrin plug has several components; essentially it is a meshwork of polymerised fibrinogen, fibronectin, vitronectin and thrombospondin, amongst others.[4] Platelets are embedded within this meshwork. The primary role of this plug is to provide a barrier to prevent infection and to provide temporary coverage.[3]

Second to this the platelets trapped within the meshwork secrete a number of growth factors, two of the most notable being platelet derived growth factor (PDGF) and transforming growth factor (TGF)$\beta$1.[5]These growth factors are involved in several stages of wound healing, having an early role in cell recruitment and later helping to form the extra cellular matrix (ECM).[6]

The inflammatory response is instigated as fibrinogen polymerises to fibrin, in this process fibrinopeptides A and B are formed and they are responsible for recruiting inflammatory cells. At this point white blood cells are able to move into the extracellular space (this is stimulated by the expression of selectins by endothelial cells and enabled by integrin binding). Again these white blood cells have many functions within the initial stage of wound healing. Neutrophils and macrophages aid in wound debridement, they are also key as they produce growth factors and mediators that are essential for the healing process.[3]

At this stage wounds are hypoxic in nature, due to vascular damage. This hypoxia acts as a stimulus for further healing, as it increases keratinocyte migration, angiogenesis, proliferation of fibroblasts, synthesis of cytokines and the biosynthesis of growth factors, such as, PDGF, vascular endothelial growth factor (VEGF), and TGFβ1. The synthesis of growth factors and cytokines continues for 2-3 days. At this stage macrophages collect at the injury site along with fibroblasts and endothelial cells which form early granulation tissue.[3, 7]

### 1.1.3 Migration, Proliferation and Remodeling

In the later stages of wound healing the inflammatory response becomes less intense, this allows wound closure and contraction to begin. In this phase of healing ECM proteins are formed, angiogenesis occurs, as does contraction and keratinocyte migration. Several of these processes will form the backbone of this discussion.

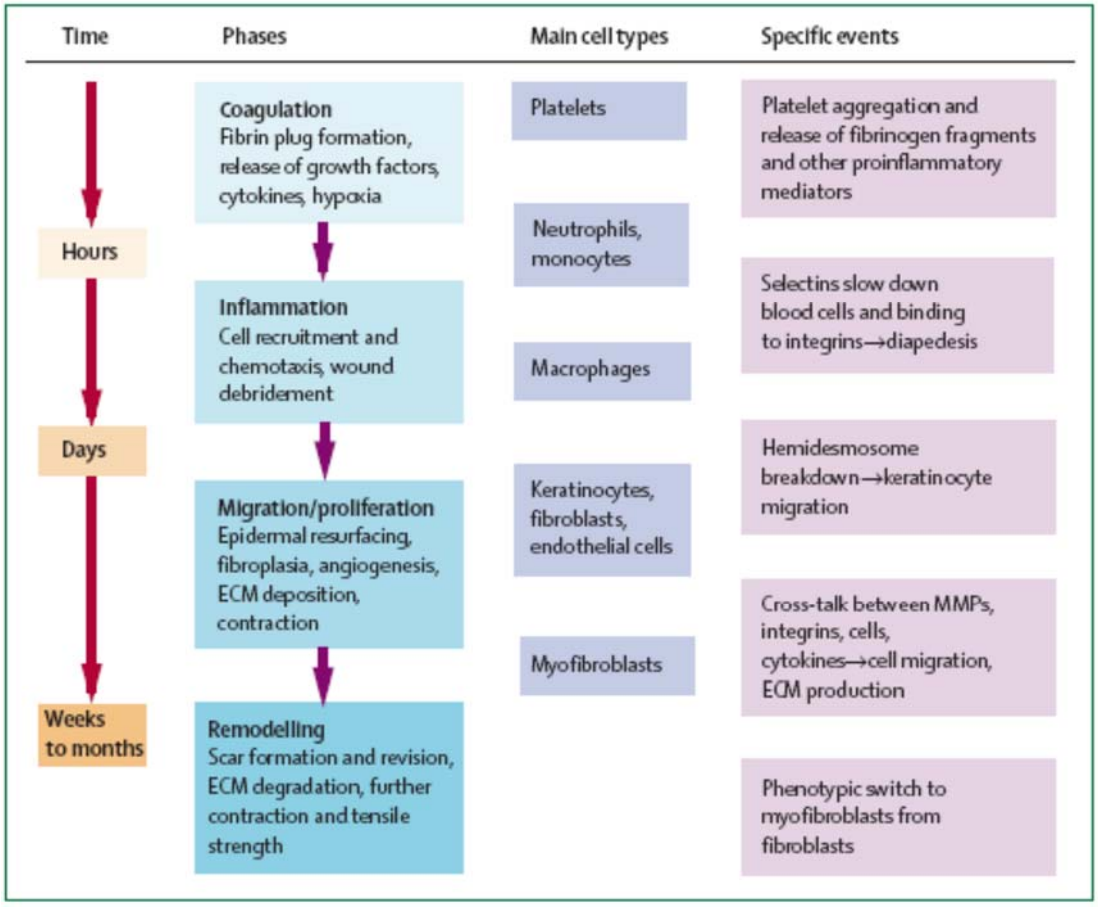


**Figure 1.1.1**: Events in physiological Wound Healing.[8]

## 1.2 Wound Healing in Relation to Diabetes

Diabetes is a disease that requires no introduction and whose prevalence is increasing at an alarming rate, driven by increasing life expectancy and obesity epidemics. It was estimated that in 2000 there were 151 million cases of diabetes worldwide, in 2010 285 million were estimated, and shockingly, by 2030 it is thought that there will be a staggering 438 million cases[9-10]

Diabetes mellitus is a term used to encompass the many kinds of diseases characterised by chronic hyperglycaemia and which are caused by a variety of underlying factors. There are many illnesses that diabetic patients are predisposed to including the significantly increased risk of developing micro- and macro-vascular diseases.[10] The macrovascular effects of diabetes are numerous, and are the cause of significant health problems in the diabetic population. Significantly, poor peripheral vascular circulation contributes to further complications.[10]

Peripheral vascular disease in diabetes patients is of the same nature as it is in the general population, however, it is said to be more aggressive and will occur at a much younger age. The development of this vascular disease is thought to be largely due to impaired endothelial cell function. However, an even more crucial factor appears to be the thickening of the basement membrane of capillaries. This thickening inhibits white blood cell migration, compromising the sufferer's immune response to injury. This reduced immune response then leaves any injured limbs, most usually feet, more at a higher risk of infection.[10] This problem is compounded by the reduced ability of diabetics to vasodilate in response to injury, leaving the sufferer vulnerable to trauma and at a further increased risk of infection. As a whole, this often leads to a great amount of pain and poor quality of life. [11]

### 1.2.1 Biological Treatment of Diabetic Foot Ulcers

One of the most problematic manifestations of diabetes is the infamous diabetic foot ulcer. Diabetic foot ulcers occur in 15% of diabetic patients and are a major cause of lower limb amputation.[12] A diabetic foot ulcer is defined as any skin breakdown in the foot of a diabetic. This is complicated by the fact that non-healing foot ulcers act as portals of entry for systemic infection, which given the impaired nature of diabetics immune response is a very serious health issue. A diabetic foot ulcer can then be described as a chronic non-healing wound, when it does not undergo the linear wound healing events outlined in **Figure 1.1.1**.[3]

With rigorous care including proper dressings, debridement, and off-loading many ulcers can heal in time.[13] However, foot ulcers that display less than 10% closure within a three week time period are currently treated with biological therapies.[14]

Physiologically, diabetic foot ulcers exhibit a decreased expression of growth factors and consequently a reduced angiogenic response.[14] There are two methods of applying biological treatments, the first is through cell therapy which involves the application of a living human skin equivalent, for example Apligraf®, onto the wound. This therapy has been shown to increase the healing rate of diabetic foot ulcers by 55%.

The utilization of a human skin equivalent promotes wound healing through many mechanisms: promoting angiogenesis, increasing growth factors and cytokines, as well as increasing matrix proteins. Human skin equivalents also provide and providing a physical and biological barrier against wound infection.

Another strategy using biological agents to increase wound healing is the use of synthetic growth factors. The only current example of this technology is Becaplermin (Regranex®) which is a growth factor generated from recombinant DNA technology. It is a homodimer of the B chain of human platelet-derived growth factor (PDGF-BB), and is marketed as a gel with the active ingredient preserved in a sodium carboxymethylcellulose based gel.

### 1.2.1 Becaplermin (PDGF-BB)

Becaplermin is sold as Regranex® in a gel form of 100 μg/g.[15] There are a number of growth factors present in the wound healing process. Any drug containing or acting on growth factors is likely to be more clinically useful if it has a broader spectrum of activity. This makes the use of a PDGF a good choice for a drug of this kind.

Platelet-derived Growth Factor is produced by many cells in the wound healing process e.g. macrophages, endothelial cells, fibroblasts and keratinocytes. It acts on many of these same cells as a mitogen and induces the production of fibronectin and hyaluronic acid. This particular growth factor works in synergy with others such as transforming growth factor (TGF-$\beta$), giving it an active role throughout the wound healing process.[15]

In double-blind clinical trials Regranex® performed well, significantly decreasing the number of days required for healing, and possibly also having an effect on wound size compared to a carboxymethylcellulose gel placebo. Becaplermin was also found

to have an excellent safety profile and good cost effectiveness (which is not to say that this is a cheap drug). However, despite all of these positive attributes Regranex® has failed to stand up in actual clinical practice, and consequently, it is not widely used.[15]

There are a few hypotheses as to why this drug is not currently clinically useful. One school of thought is that the gel preparation does not ensure good delivery to the wound, while some research suggests that other growth factors present my hinder the therapeutic potential of PDGF-BB.[16] Alternatively, it has been suggested that clinicians require more information on when to use Becaplermin.[15] Whatever the reason for this disappointing clinical response, it has to be noted that this approach to wound healing is a promising one and drugs of this nature are likely to be the subject of significant investigation for the foreseeable future.

## 1.3 The Extra Cellular Matrix and Fibronectin

For many years it was believed that the extra cellular matrix (ECM) was an inert scaffold, however, the ECM is much more complex and dynamic than it might at first appear to be. The ECM is essential for the organisation of tissues, stem cell niches and cellular microenvironments and it contains many growth factors. The importance of this network is highlighted when we consider that problems with assembly of the ECM can lead to scarring, tumorigenesis and fibrotic disease.[6]

Two structural components of the ECM, the interstitial matrix (stroma) and the basement membrane (basal lamina) can be visualized using electron scanning microscopy. The interstitial matrix is a fibrous and porous network of threadlike fibrils that surround cells. The basement membrane, on the other hand, is sheet like in nature, and acts as a platform for cells and forms a boundary that separates tissue compartments. Both of these ECM components are made of similar types of proteins, such as collagens, proteoglycans and cell adhesive glycoproteins.[6]

Matrix proteins are crucial for normal cell behaviour to take place; collagens, fibronectin and vitronectin allow cell movement which, allow tissues to regain their function after injury. Wound contraction is an efficient way of closing an injured site and this is enhanced by the reformation of the ECM.

### 1.3.1 Fibronectin

Fibronectin was discovered by Richard Haynes in the early nineteen seventies.[17] At this point in time it was the only known difference in surface chemistry between tumour and healthy cells, and its discovery was received with great excitement.

Although the discovery of was an important find, although it was not the pivotal switch turning healthy cells into cancerous forms as was hoped at the time. Today, it is considered to be an extremely important milestone in the elucidation of the very complex processes associated with tumour proliferation, and integrin signaling.[17]

### 1.3.2 Fibronectin in the Extra Cellular Matrix

Fibronectin can exist as two main types of dimer: the first, plasma fibronectin (pFN), is soluble and exists in body fluids. The second, cellular fibnonectin (cFN), is an insoluble multimeric component of the extra cellular matrix. pFN is produced in the liver by hepatocytes and is involved in wound healing in conjunction with fibrin.

Cellular Fibronectin is a large extracellular matrix glycoprotein, of around 440 kDa in weight and, amazingly, around three nanometres in width. cFN is secreted by various cells as a globular molecule which has the ability to quickly assemble into fibrils, which are the main constituent of the extra cellular matrix along with collagen. Not surprisingly, cFN is essential for life as it is assembled into a fibrillar matrix in all tissues.[18] This fibrillar matrix connects neighbouring cells and forms mesh works around them (**Figure 1.3.1**).[6]

cFN also has other crucial functions including cell migration, growth, wound healing and embryonic development. cFN mainly binds to integrins, however importantly, it also binds to components of the extracellular matrix (ECM) such as collagen and fibrin.

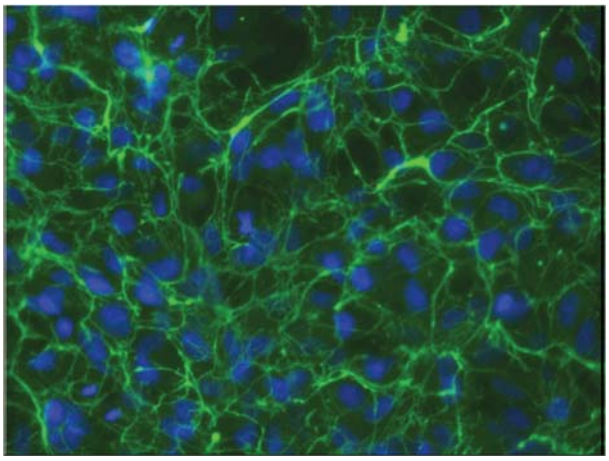

**Figure 1.3.1**: Fibronectin Surrounds Cells in Culture. Fibrils are shown in green, cell nuclei are stained blue.[6]

Ten years after the isolation of fibronectin the three-amino-acid sequence that is required for fibronectin to attach to cells was discovered. This tripeptide, RGD, lead the way to the discovery of integrins as the link between structural glycoproteins and the cytoskeleton.[17]

### 1.3.3 The Structure of Fibronectin

The significant interest that followed the discovery of fibronectin lead to the rapid elucidation of its structure. As previously stated, fibronectin exists as a dimer. This fibronectin dimer is composed of two subunits both weighted from 220-250 kDa.

These two subunits are covalently linked by a pair of disulfide bonds near their C-termini of the monomers. Each of the two subunits is comprised of three repeating types of modules, analogous to beads on a string (**Figure 1.4.2**). There are twelve type I modules, two type II, and fifteen to seventeen type III modules. In addition to these, each subunit also contains a variable sequence that is not homologous to the other parts of FN. Two of the type III domains are subject to alternative splicing, these extra domains (ED-A and ED-B) are only found in cellular fibronectin. A further difference between cFN and pFN is the variable region (V) which is only found in one of the subunits of pFN, but is present in nearly all cFN subunits.

Fibronectin binds to $\alpha_5\beta_1$ and $\alpha_{IIb}\beta_3$ integrins through the III8-III10 modules. The III10 module houses a critical binding site, the Arg-Gly-Asp (RGD) module. Excitingly, synthetic RGD peptides block integrin mediated cell adhesion to FN.

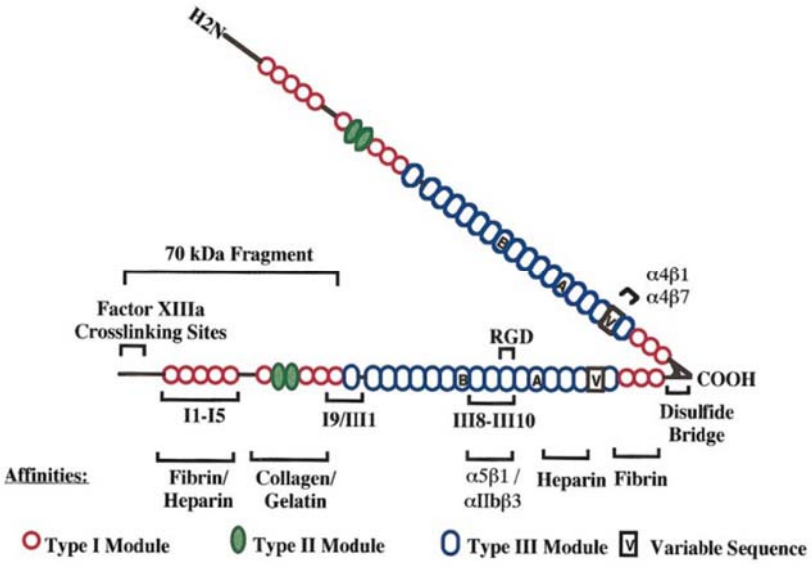


**Figure 1.3.2**: Schematic Diagram of the Modular Structure of the Fibronectin Dimer.[19]

## 1.4. Migration Stimulating Factor

Migration Stimulating Factor (MSF) is a truncated isoform of fibronectin and was first isolated from fetal calf serum in 1974.[20] As such, it is produced from the primary fibronectin gene transcript.

MSF is a motogenic protein, which stimulates the migration of a number of cells including epithelial cells, fibroblasts, vascular endothelial cells and pericytes. MSF is also involved in the upregulation of hyaluronan synthesis, proteolysis and the upregulation of angiogenesis.[21]

MSF is commonly expressed by fibroblasts, keratinocytes, and vascular endothelial cells in foetal skin.[22] It is not normally found in healthy adult skin in noteworthy amounts, but is expressed during wound healing and is expressed by over 80% of human tumours.[22] As such, it is currently being investigated as a target for prevention of novel angiogenesis in tumours.[23]

The activity of this protein comes from its IGD (Ile-Gly-Asp) tripeptide motifs. This motif is a highly conserved feature of the fibronectin type I modules and is present in the third, fifth, seventh and ninth type I modules of MSF (**Figure 1.4.1**). Although Fibronectin does contain this motif it does not display any MSF like activity. It is most likely that protein folding makes the IGD motifs cryptic.[21] [24]


**Figure 1.4.1**: The primary sequence of fibronectin/ MSF type I modules with highlighted IGD sequences.[24]

### 1.4.1 Origin of Biological Activity of the IGD Tripeptide Motif and MSF

*In vitro* mutagenesis studies have shown that the motogenic activity displayed by MSF is due to the IGD amino acid motif. However, the biological activity of the IGD motif found in fibronectin and MSF is still relatively undefined. Work by Schor indicated

that MSF promotes fibroblast and endothelial cell migration, at least partially, by inhibiting protein kinase AKT.[25]

Work within the Schor group found that the IGD peptides stimulated fibroblast migration. IGDS was found to be the most active, followed by IGDQ and then IGD, while the scrambled peptides SDGI and RGDS did not display activity. This work found that the observed cell activation and enhanced migration upon treatment with IGD-containing peptides occurs within minutes, and involves the tyrosine phosphorylation of focal adhesion kinase. Furthermore, this work found the activity is dependent on integrin $\alpha_5\beta_3$ functionality, and is inhibited by signaling through integrin $\alpha_5\beta_1$.[24, 26]

### 1.4.2 MSF in Relation to Wound Healing

The cell migratory properties of the IGD motif of MSF make it a good model for a therapeutic agent, whose applications would be based in patients with impaired wound healing and other diseases requiring the stimulation of cell migration and angiogenesis. The Marquez, Norman and Schor groups recognised that design of an IGD peptidomimetic would allow the development of a small molecule with increased stability with respect to MSF. Any peptidomimetic generated could be the structural basis for a new family of analogues, allowing optimisation of activity.

Initially, the dihedral angles of the IGD turn in the fnI-5 and fnI-7 modules of MSF were studied via NMR measurements, showing the IGD sequence as a highly structured turn (**Figure 1.4.2**). The angles were found to be very similar in both cases, enhancing the belief that they were good models for peptidomimetics

It was hypothesized that the highly structured nature of this motif would lend itself to easy recognition by the relevant cell receptors. Consequently, any peptidomimetics that mimic this turn would also have the potential to bind to these receptors.[27]

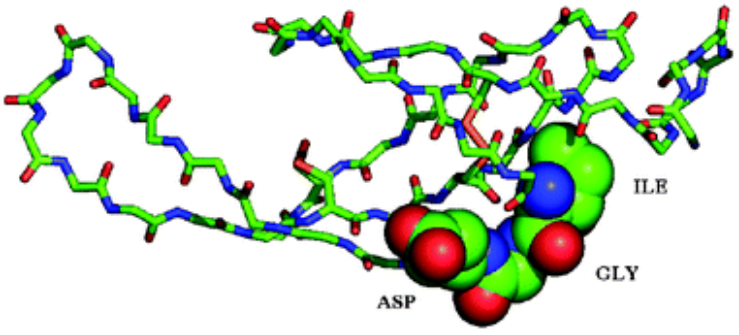


**Figure 1.4.2**: Space Filling Representation of the IGD motif on the FnI-7 backbone.[27]

## 1.5 First Generation IGD Peptidomimetics

AB-Initio level-modeling studies indicated that the IGD tripeptide motif of MSF could be closely mimicked by a benzodiazepinone bicyclic ring structure, specifically benzodiazepinone **2** (**Figure 1.5.1**). To best imitate the aspartic acid residue the stereocentre of the peptidomimetic should have an (*S*)-configuration. The IGD peptidomimetic **2** also incorporated an ester functionality, providing a handle through which the molecule could be modified, depending on the pharmacological traits required.[27]

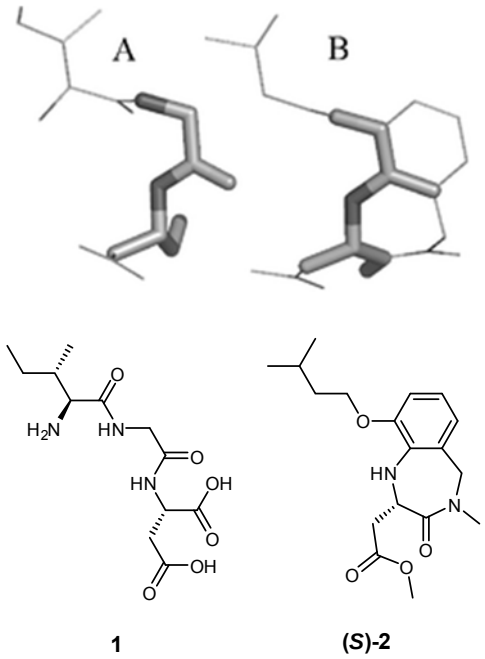


**Figure 1.5.1**: IGD Peptide Sequence **A**/**1** and Racemic IGD peptidomimetic **B**/(***S***)-**2**.

The proposed benzodiazepinone core is particularly interesting, a number of RGD peptidomimetics are also based around this privileged moiety (**Figure 1.5.2**). The similarity in structure could be indicative of binding to similar biological targets.

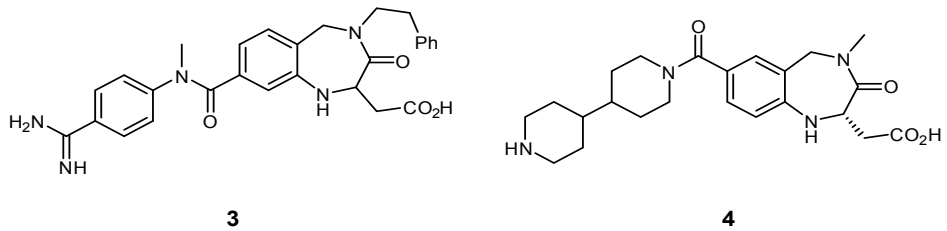


**Figure 1.5.2:** Benzodiazepinone RGD Peptidomimetics.

1.5.1 Synthesis of the First IGD Peptidomimetic

The synthesis of the first IGD peptidomimetic **(±)-2** began with the alkylation of nitro-cresol **5**. The product of this reaction was then brominated under radical conditions giving the desired benzylic bromide **6** along with a small amount of the undesired double brominated adduct **7** in moderate yield over two steps. These compounds could not be separated at this point and were reacted with methyl amine to give amines **8** and **9**. BOC protection of the benzylic amine gave intermediates **10** and **11** in good yield over both steps. Subsequent hydrogenation gave aniline **12** as a single compound in good yield (**Scheme 1.5.1**).[27]

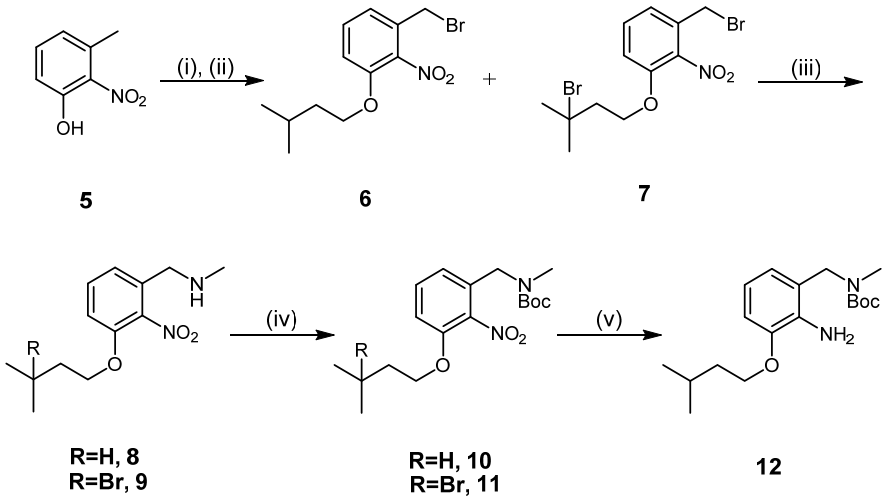


**Scheme 1.5.1**: Synthesis of Aniline **12**. *Reagents and Conditions*: (i) 1-bromo-3-methyl butane, $K_2CO_3$, DMF, RT, 24 h; (ii) NBS, AIBN, $CCl_4$, reflux, 12 h, (43% over two steps); (iii) $CH_3NH_2$ (40% in $H_2O$), THF, RT, 12 h; (iv) $BOC_2O$, TEA, DMAP, $CH_2Cl_2$, 0 °C-RT, 12 h (84% over two steps); (v) Pd/C (10%), $H_2$, $CH_3OH$, RT, 3 h (75%).

Aniline **12** was then condensed with dimethyl acetylenedicarboxylate to give dimethyl diester **13** in excellent yield. Reduction of the double bond using palladium and hydrogen gave the desired racemic dimethyl diester **(±)-14**. Deprotection of diester **(±)-15**, followed by cyclisation afforded the first IGD peptidomimetic **(±)-2** as a racemic mixture in variable yields (**Scheme 1.5.2**).[27]

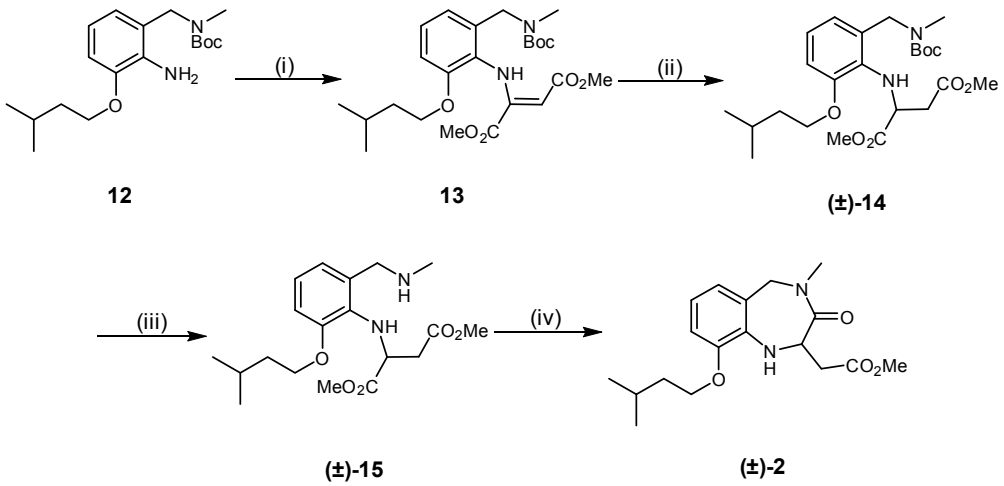


**Scheme 1.5.2**: Completion of Synthesis of IGD Peptidomimetic **(±)-2**. *Reagents and Conditions*: (i) $MeO_2CCCCO_2Me$, $CH_3OH$, reflux, 1 h (85%); (ii) Pd/C (10%), $H_2$, $CH_3OH$, RT, 30 min (58%); (iii) TFA, $CH_2Cl_2$, 0 °C, 1 h (96%); (iv) $NaOCH_3$ (25% in $CH_3OH$), RT, 1 h (45-77%).

The motogenic activity of the newly synthesized IGD peptidomimetic (**(±)-2 = BDP1**, **Figure 1.5.3**) was assessed alongside 2 amino acid sequences with known activity. Human skin fibroblasts were treated with the peptidomimetic or the peptide sequences in a 3D collagen gel assay. Pleasingly, the IGD peptidomimetic **(±)-2** was found to be as effective as IGDS in stimulating the migration of human skin fibroblasts. The control reverse peptide SDGI was devoid of any motogenic activity as expected.[27]

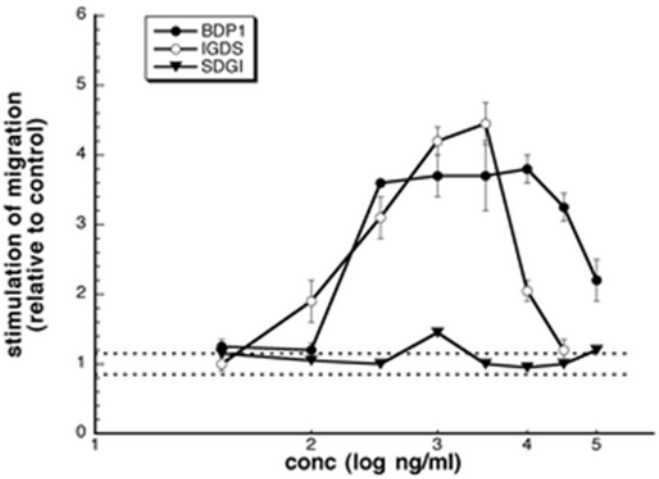


**Figure 1.5.3**: The Motogenic Activity of IGD Peptidomimetic **(±)-2**.

## 1.6 Synthesis of the First Enantiomerically Pure IGD Peptidomimetic

Further exploration of the IGD peptidomimetic **(±)-2** has been carried out within the Marquez group with the synthesis of the IGD peptidomimetics in the enantiomerically pure forms. The route to the (*R*) and (*S*)-IGD peptidomimetic esters was developed from the original methodology to ensure higher yields throughout the synthesis but also to allow the inclusion of the desired chiral functionality.[28]

The enantiomerically pure synthesis began with the alkylation of benzophenol **16** to afford clean **17**. Treatment of ether **17** with nitronium tetrafluoroborate proved very temperamental yielding nitrobenzaldehyde **18** in working yield (53%). Methylamine was then reacted with nitrobenzaldehyde **18** under reductive amination conditions to give amine **8** in excellent yield over two steps (94%). Subsequent protection (93%) and reduction (100%) gave aniline **11** near quantitative yield (**Scheme 1.6.1**).[28]

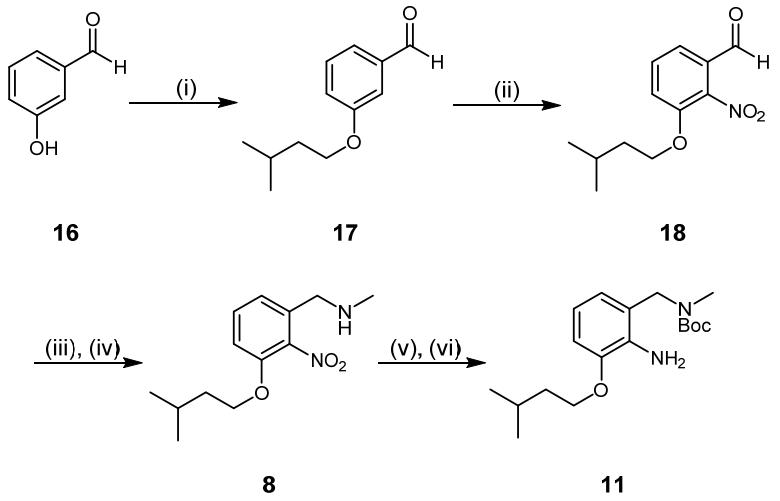


**Scheme 1.6.1**: Second Route to Aniline **11**. *Reagents and Conditions*: (i) DMF, $K_2CO_3$, 1-bromo-3-methyl butane, RT, 1h (96%); (ii) DCM, $NO_2BF_4$, -28 °C, 22h (53%); (iii) $MeNH_2$, heptane, RT, 2h; (iv) MeOH, $NaBH_4$, 1h, 0 °C (94% over two steps); (v) DMF, TEA, $BOC_2O$, 2.5 h, RT (93%); (vi) Pd/C (10%), MeOH, $H_2$, 15 h (100%).

It was found that the chiral centre could be introduced through the generation of chiral triflate **(*S*)-20** from (*S*)-(-)-dimethyl malate (**(*S*)-19**). The reaction of triflate **(*S*)-20** with aniline **11** proceeded in excellent yield (100%). Subsequent deprotection (82%) and cyclisation (85%) gave the desired benzodiazepinone core **(*R*)-2** (**Scheme 1.6.2**).[28]

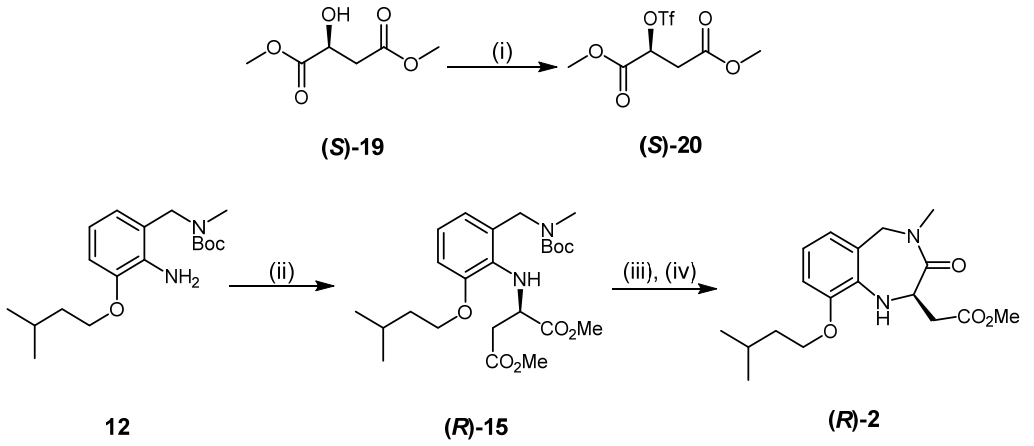


**Scheme 1.6.2.**: Synthesis of the Enantiomerically Pure **(*R*)-2**. *Reagents and Conditions*: (i) $Tf_2O$, 2,6-lutidine, DCM, 2 h, -78 °C (100%); (ii) Triflate **(*S*)-20**, DCM, reflux (100%); (iii) TFA, DCM, 20 h, RT (82%); (iv) NaOMe, MeOH, reflux (85%).

For a more complete assessment of the biological and chemical properties of the peptidomimetics it was decided to synthesize the corresponding carboxylic acids **(*R*)-22**. Thus, ester **(*R*)-2** was then converted to the desired carboxylic acid **(*R*)-22** through treatment with potassium trimethylsilanolate (97%) (**Scheme 1.6.3**). The (*S*)-IGD peptidomimetic ester was isolated and the enantiomeric excess defined by chiral HPLC through comparison with the racemic product.[28]

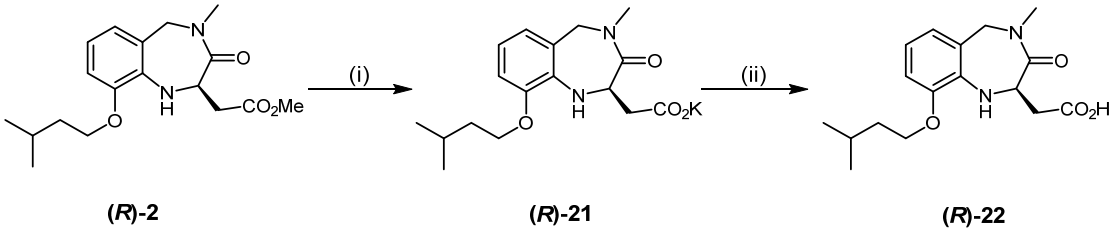


**Scheme 1.6.3**: Saponification of IGD Peptidomimetic **(*R*)-2**. *Reagents and Conditions*: (i) $KOSiMe_3$, $Et_2O$; (ii) 1M HCl (97% over two steps).

## 1.7 *In Vitro* and *In Vivo* Testing of IGD Peptidomimetics

The newly synthesised enantiomerically pure peptidomimetics then underwent biological testing to get a clearer picture with regards to the biological activity of each enantiomer. Initially, the peptidomimetics were tested *in vitro* in the transmembrane and 3D collagen gel assays.

Surprisingly, contrary to what was expected from the modeling studies the (*R*)- IGD peptidomimetic methyl ester (**(*R*)-2**) displayed noteworthy activity on fibroblasts and endothelial cells whereas the (*S*)-IGD peptidomimetic methyl ester (**(*S*)-2**) was inactive. The (*R*)-IGD peptidomimetic acid (**(*R*)-22**) was found to have activity but this was significantly less than the corresponding ester, and again the (*S*)-IGD peptidomimetic acid (**(*S*)-22**) showed no motogenic activity on cells.[28]

*In vivo* testing followed with the compounds being tested on the wounds of C57BLKs/Bom diabetic mice. A single wound (10 mm × 10 mm) of standard thickness was made on the back of several diabetic mice. The experimental animals then had their wounds treated either with a control preparation or an (*R*) or (*S*)-IGD peptidomimetic preparation along with an appropriate dressing. The treatments were reapplied on days 2, 4, 7 and 10 after wounding.[28]

The results were pleasing, the (*R*)-IGD peptidomimetic methyl ester (**(*R*)-2**) was shown to promote wound healing in the diabetic mice, having an effect on wound closure, wound contraction, re-epithelialisation and cellular maturity where healing was increased to 77% ±3 of levels displayed by healthy mice. Activity was also seen in acid (**(*R*)-22**), with this molecule allowing for faster healing times and significant reduction in wound size compared to the control group, however, this activity was less than that observed for the corresponding ester. This could allow us to conclude that the (*R*)-IGD peptidomimetics promote wound contraction in the diabetic mouse model (**Figure 1.7.1**).[28]

(*R*)-IGD Peptidomimetic Wound

Day 0

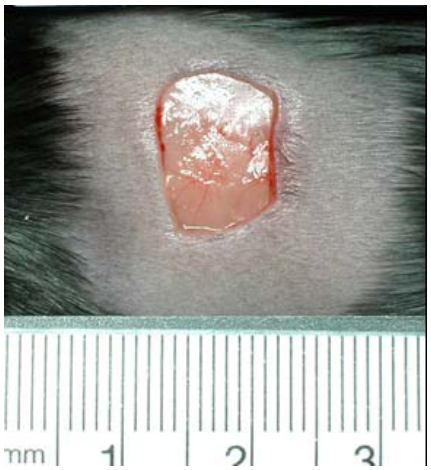

(*R*)-IGD Peptidomimetic Wound

Day 10

Control Wound

Day 0

Control Wound

Day 10

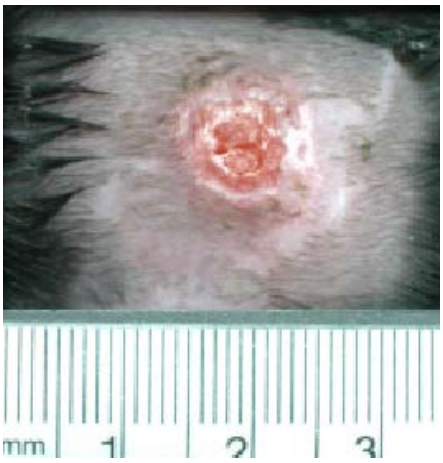

**Figure 1.7.1**: Examples of Wound Healing in Test Mice Treated with (*R*)-IGD Peptidomimetic (**(*R*)-2**) or Control Treatment.

It was also found that the (*S*)-IGD peptidomimetic acid (**(*S*)-22**) promoted wound contraction in the diabetic mouse model, relative to the control groups, although not to the same extent as the (*R*)-IGD peptidomimetics. It is possible that epimerisation of the (*S*)-IGD acid is the cause of these unexpected results, alternatively, it may be acting through an different biological mechanism.[28]

# 2.0 PROJECT AIMS

## 2.1. Development and Investigation of Methyl IGD Peptidomimetics

The initial aim of the project was to optimise the synthesis of the (*R*)- and (*S*)-methyl IGD peptidomimetics ((***R*)-2**) and ((***S*)-2**) (**Figure 2.1.1**), in order to generate enough material for biological testing. An improved synthetic route to the IGD peptidomimetics would greatly facilitate the generation of future analogues.

Once the synthesis of **(*R*)-2** and **(*S*)-2** had been optimised, biological testing was planned to confirm the relative activity of each enantiomer. Observation of "wound healing" activity would allow us to confidently to harvest samples for Polymerase Chain Reaction arrays, with the hope that these tests would divulge the origin of activity. Further to this, each enantiomer would be submitted for toxicology studies.

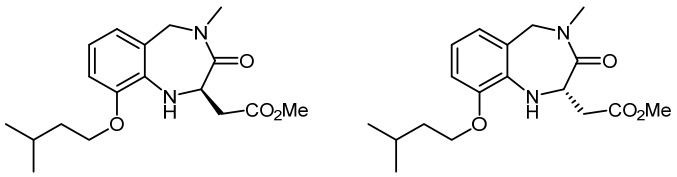


**(*R*)-2** **(*S*)-2**

**Figure 2.1.1:** Methyl IGD peptidomimetics **(*R*)-2** and **(*S*)-2**.

## 2.2. Functionalised IGD Peptidomimetics

Analogues of **(*R*)-2** and **(*S*)-2** could also be used to gain new insight into the biological mode of action of the IGD peptidomimetics. Thus, analogues could be designed to incorporate a moiety that could facilitate drug delivery. Each of these goals wa envisioned to proceed via common intermediate **(*R*/*S*)-23**/**(*R*/*S*)-24** or **(*R*/*S*)-25**/ **(*R*/*S*)-26** (**Figure 2.2.1**).

It was postulated that an alcohol functionality would allow efficient divergence to afford a small library of IGD peptidomimetics with varying functionalities. These functional groups would be capable of attaching the mimetic to other structural units for development and investigation, such as fluorophores and solid supports. The alkyl chain in the 4 position was designed to allow distance between any potential new support and our active IGD mimetic core.

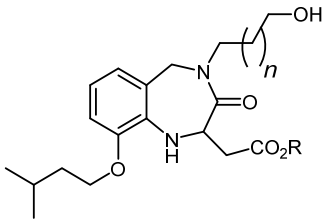


*n* = 1: R = H **(*R*/*S*)-23**, R = Me **(*R*/*S*)-24**
*n* = 3: R = H **(*R*/*S*)-25**, R = Me **(*R*/*S*)-26**

**Figure 2.2.1:** IGD Peptidomimetic Mimetic with Incorporated Alkyl Chain and Alcohol.

## 3.0 Results and Discussion

### 3.1. Methyl IGD Peptidomimetic Route Optimisation

#### 3.1.1 Optimisation of IGD Peptidomimetic Intermediates

As referred to in the introduction, the original synthesis of the methyl IGD peptidomimetics **(*R*)-2** and **(*S*)-2**, was let down by one crucial step.[27] Intermediate **18** (**Scheme 3.1.1**) was accessible only through nitration of the 2 position of benzaldehyde **17** and this strategy presented several issues which made the reaction incompatible with the scale-up required to generate sufficient material for the subsequent steps of the synthesis.

The synthesis of **18** starts with alkylation of phenol **16**, in excellent yield to generate the desired ether **17** (83%). With the ether **17** in hand the addition of the nitro group was explored. Unfortunately, nitration of ether **17** proved to be extremely challenging. Setting aside the cost and sensitivity of the nitrating agent, nitronium tetrafluoroborate, the most significant problem comes from the isolation of the desired product from the reaction mixture. The conversion of starting material **17** to a nitrated species is good, generally around 75%, however, there is no selectivity shown for the desired C2 position and several mono- and di- nitrated isomers are also formed. This problem is compounded by the similar chemical properties of these isomers meaning that flash column chromatography is often extremely lengthy and unsuccessful in giving pure material. Thus, the 53% yield previously demonstrated was irreproducible, with 26% being the highest yield of **18** observed via this route.

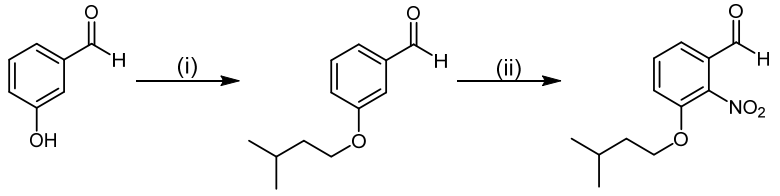


**16** **17** **18**

**Scheme 3.1.1**: The Synthesis of Nitrobenzaldehyde Intermediate. *Reagents and Conditions*: (i) DMF, $K_2CO_3$, 1-bromo-3-methyl butane, 83%; (ii) DCM, $NO_2BF_4$, - 20 ºC, 26%.

It was apparent that this method of accessing **18** was unsuitable for such an early intermediate and alternative strategies were sought. Initially, it was thought that the synthesis of aldehyde **18** by oxidation of the benzylic methyl group of the

commercially available 3-methyl-2-nitrophenol may be a convenient route (**Scheme 3.1.2**).

The first step in this alternative strategy was the alkylation of phenol **5**, which proceeded in excellent yield to give ether **27** (89%) (**Scheme 3.1.2**). Selenium dioxide was then employed in an endeavour to access nitrobenzaldehyde **18**. The reaction mixture was heated to 100 ºC for forty eight hours, yet no conversion was observed.[29] It is known that extremely high temperatures are necessary in many selenium dioxide reactions, and thus, it was thought that an alternative reagent may achieve successful conversion. A subsequent oxidation attempt was carried out with 2-iodoxybenzoic acid in dimethylsulfoxide, the reaction mixture was heated to 75 ºC for fifteen hours, however, thin layer chromatography and NMR analysis showed only starting material.[30] In a final attempt, oxone and $MnSO_4.H_2O$ were reacted with **5** and **27** in an attempt to oxidize the benzylic position, however, despite consumption of starting material in each case, no product was observed.[31]

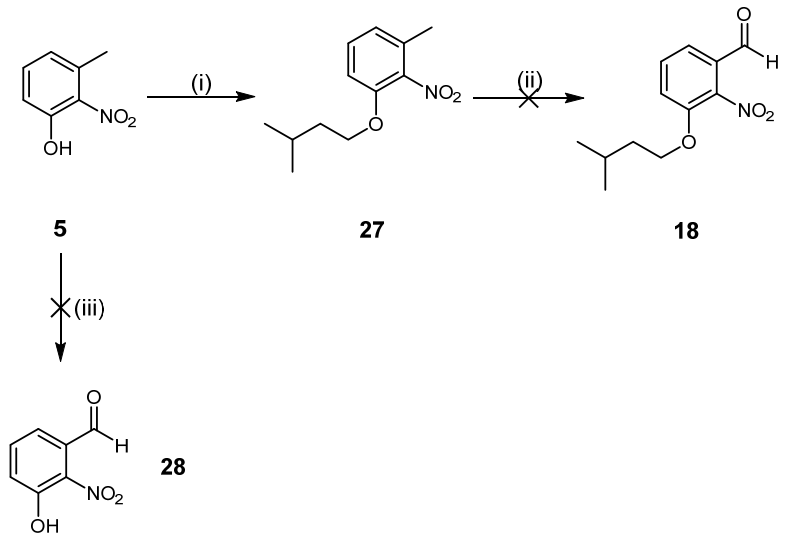


**Scheme 3.1.2**: Benzylic Oxidation Strategy for the Synthesis of Nitrobenzaldehyde **18**. *Reagents and Conditions*: (i) DMF, $K_2CO_3$, 1-bromo-3-methylbutane, 89%; (ii) IBX, DMSO (failed); $SeO_2$, dioxane (failed); $MnSO_4.H_2O$, Oxone, $H_2O$ (failed); (iii) $MnSO_4.H_2O$, Oxone, $H_2O$ (failed).

It was hypothesised that the electron withdrawing nature of the nitro group may be hindering the oxidation of the methyl group and so compound **27** was reduced under hydrogenation conditions in good yield (69%) (**Scheme 3.1.3**). However, subsequent oxidation of the methyl with selenium dioxide in dioxane was unsuccessful, thus, this route was abandoned.

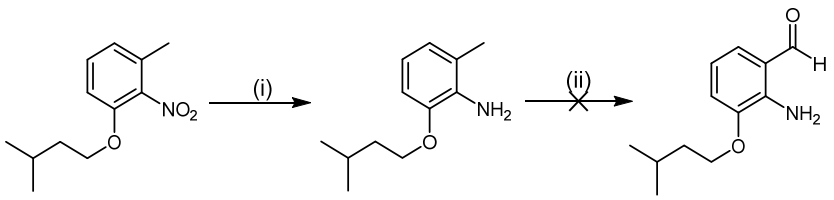


27 29 30

**Scheme 3.1.3**: Attempted Synthesis of Nitrobenzaldehyde **30**. *Reagents and Conditions*: (i) $NH_4CO_2H$, MeOH, Pd/C, 69%; (ii) $SeO_2$, dioxane (failed); $MnSO_4.H_2O$, Oxone, $H_2O$ (failed).

In an alternative strategy, a double SNAr approach was envisioned starting with commercially available 2,6-difluoronitrobenzene (**31**). However, no conversion of starting material was witnessed upon treatment of **31** with 3-methylbutanol under basic conditions (**Scheme 3.1.4**).

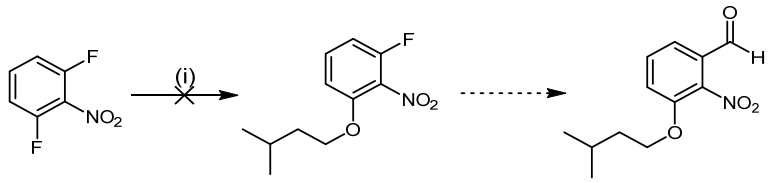


31 32 18

**Scheme 3.1.4**: SNAr Approach for the Synthesis of Nitrobenzaldehyde **18**. *Reagents and Conditions*: (i) 3-methylbutanol, $K_2CO_3$, DMF, 110 °C, (failed); (ii) 3-methylbutanol, NaOMe, DMF, 110 °C, (failed).

Faced with the low selectivity of the nitration and low reactivity of the 2,6-difluoro nitrobenzene (**31**) towards nucleophilic displacement, a new approach was sought. The new approach envisioned having the nitro and aldehyde groups in place from the start of the synthesis in order to avoid selectivity issues. Thus, it was decided to attempt the demethylation of 3-methoxy-2-nitrobenzaldehyde (**32**) (**Scheme 3.1.5**).[32]

Gratifyingly, treatment of 3-methoxy-2-nitrobenzaldehyde (**32**) with boron tribromide gave 3-hydroxy-2-nitrobenzaldehyde (**33**) in excellent yield (89%). Phenol **33** was then alkylated using 1-bromo-3-methyl-butane in high yield (83%), giving **18** quickly and efficiently in 73% yield over two steps. This straightforward synthesis allowed the multigram preparation of the key intermediate **18**, accelerating access to subsequent intermediates.

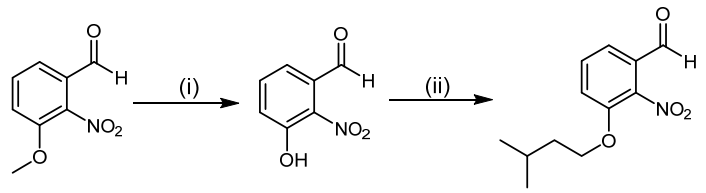


**32** **33** **18**

**Scheme 3.1.5**: Improved Route to Nitrobenzaldehyde **18**. *Reagents and Conditions*: (i) $BBr_3$, $CH_2Cl_2$ (89%); (ii) DMF, $K_2CO_3$, 1-bromo-3-methyl butane (83%).

## 3.2 Methyl IGD Peptidomimetics

### 3.2.1 Synthesis of Methyl IGD Peptidomimetics

The newly developed, efficient and reliable synthesis of intermediate **18** allowed focus to shift towards the methyl IGD peptidomimetics **(*R*)-2** and **(*S*)-2** (**Figure 3.2.1**). As previously discussed, the synthesis of these analogues is necessary to generate sufficient material for further biological tests, firstly to reconfirm which enantiomer is biologically active, and secondly, to expand our knowledge of the origin of this activity via PCR studies.

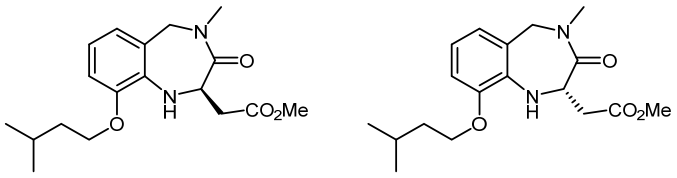


**(*R*)-2** **(*S*)-2**

**Figure 3.2.1:** Methyl IGD peptidomimetics **(*R*)-2** and **(*S*)-2**.

The synthesis of **(*R*)-2** and **(*S*)-2** proceeded from intermediate **18** as in the previous approach (**Scheme 3.2.1**).[27] Reductive amination of aldehyde **18** using methyl amine and sodium borohydride gave the benzylic amine, which upon subsequent protection gave compound **8** in 99%. Hydrogen gas and 10% palladium on activated charcoal were then used to reduce the nitro group to the corresponding aniline, however, despite previously reported success with these conditions, reaction progress was slow. Increasing the reaction time from three hours to four days, failed to achieve total conversion and these conditions were abandoned. Hydrogen gas was substituted with ammonium formate, and the reaction temperature was increased to 55 °C. This gave the desired aniline in quantitative yield after forty eight hours stirring. Subsequent alkylation of aniline **12** with triflate **(*S*)-20** proceeded in 70% to afford key intermediate **(*R*)-14**.

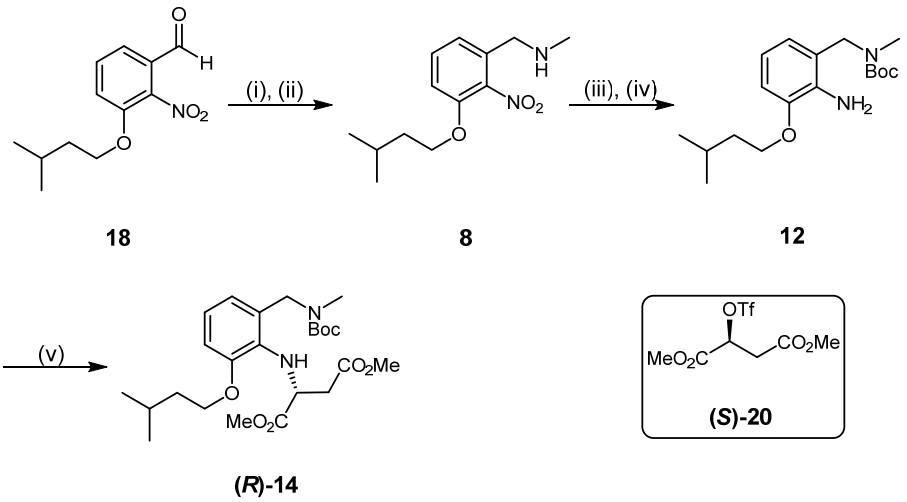


**Scheme 3.2.1**: Optimised Synthesis of Intermediate **(*R*)-14**. *Reagents and Conditions*: (i) $NH_2Me$ (aq.)(40%), heptane; (ii) $NaBH_4$, MeOH; (iii) $Boc_2O$, $NEt_3$, DCM (99% over three steps); (iv) $NH_4CO_2$, Pd/C, MeOH (quant.); (v) 2,6-lutidine, **(*S*)-20**, DCM (71%).

Deprotection of **(*R*)-14** with trifluoroacetic acid, followed by cyclisation with sodium methoxide then gave the desired methyl IGD peptidomimetic (**(*R*)-2**) in 85% over the two steps (**Scheme 3.2.2**).

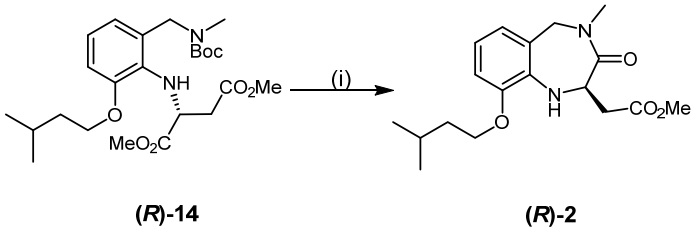


**Scheme 3.2.2:** Synthesis of (*R*)-Methyl IGD Peptidomimetic (**(*R*)-2**). *Reagents and Conditions*: (i) TFA, $CH_2Cl_2$; (ii) NaOMe (25% wt in MeOH), 65 °C (85%).

These synthetic conditions were applied to the synthesis of the *S*-enantiomer, with the alkylation proceeding in good yield (86%) (**Scheme 3.2.3**). The deprotection and cyclisation steps occurred in yields analogous to the (*R*)-IGD peptidomimetic (86%).

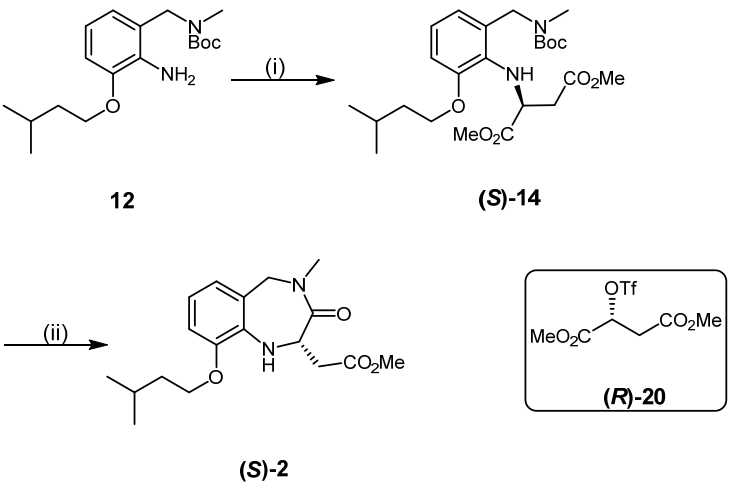


**Scheme 3.2.3**: Synthesis of (*S*)-Methyl IGD Peptidomimetic (**(*S*)-2**). *Reagents and Conditions*: (v) 2,6-lutidine, **(*R*)-20**, DCM (86%). (i) TFA, $CH_2Cl_2$; (ii) NaOMe (25% wt in MeOH), 65 °C (**86%**).

Using this optimised approach the peptidomimetics **(*R*)-2** and **(*S*)-2** could be generated in significant amounts (around 1 g) in a short amount of time (approximately two weeks). With reliable access to the methyl IGD peptidomimetics we were able to focus on the biological testing testing of these molecules.

## 3.3 Biological Assessment of Methyl IGD Peptidomimetics

In order to confirm the biological activity previously seen with the IGD peptidomimetics **(*S*)-2** and **(*R*)-2**, a reliable method of assessment was needed. The wound healing activity of our peptidomimetic compounds originates from their ability to induce migration, motogeniticity or cell proliferation. Thus cell migration was used as a measure of the efficacy of our compounds.

### 3.3.1 Time Lapse Studies

Work proceeded in collaboration with Prof. Matt Dalby and Carol-Anne Smith (University of Glasgow). The Dalby group have studied the migration and adhesion ability of cells as they respond to changes in microtopography by timelapse microscopy.[33] It was believed that a similar approach using time lapse microscopy may be useful to quantify the migration of cells treated with the (*R*)- or (*S*)-methyl IGD peptidomimetics.

Carol-Anne Smith carried out the cell culture and time lapse incubation. Due to the limitation of access to only two microscopes with time-lapse capabilities it was not possible to study cells treated with the *R* enantiomer, the *S* enantiomer and a control simultaneously. Therefore, the (*R*)-methyl IGD peptidomimetic was studied alongside a control, this was repeated for the (S)-methyl IGD peptidomimetic and a control. The control values were used to normalise the *R* and *S* results so that direct comparison became possible.

hTERT Fibroblasts were seeded at 5000 cells per 5 mL in complete Dulbecco's modified eagle's medium (cDMEM), into two T25 vented culture flasks and incubated at 37 °C for 24 hours. (*R)*-Methyl IGD peptidomimetic of (**(*R*)-2**) was then added to the culture flask at the desired concentration as a DMSO solution, while the control flask was left unmodified. Both flasks were incubated at 37 °C and recorded over twenty four hours with photographs being taken every two or three minutes. This process was repeated with the (*S*)-methyl IGD peptidomimetic (**(*S*)-2**) and a further control.

hTERT fibroblasts were selected due to their ease of handling (longevity in aerobic conditions) and their relevance to wound healing.[3] The initial experiments were run with 100 ng/mL concentration of the IGD peptidomimetic as this was the most efficacious concentration in previous experiments. [27]

ImageJ (version 1.49t) with Manual Tracking plug-in and Axiovert25 Timelapse were used to compile the images captured from the timelapse incubations and turned into video footage. The movement of each trackable cell was then followed, generating data of the cells XY coordinates in the flask over the twenty four hour period. This approach allowed us to measure the number of micrometres moved by each cell on each axis.

Five cells from each of four time lapse videos were tracked. The data was used to generate XY plots of cell movement (**Graphs 3.3.1-3.3.4**) and plots of distance from origin (**Graphs 3.3.5-3.3.8**).

**Graphs 3.3.1-3.3.4**: XY Coordinates of Fibroblast Movement (μm) Over 24 h.

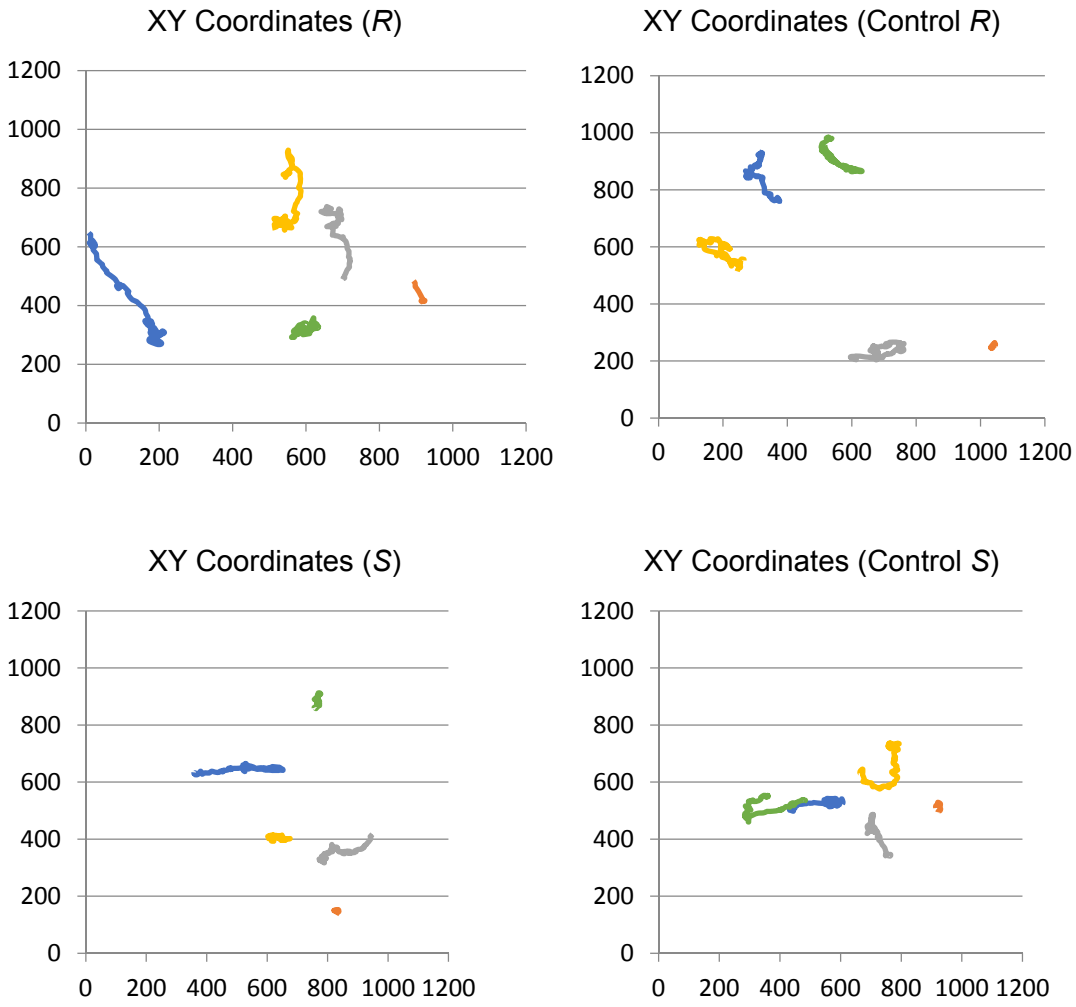

**Graphs 3.3.5-3.3.8**: Distance From Origin of Fibroblasts (μm) Over 24 h.

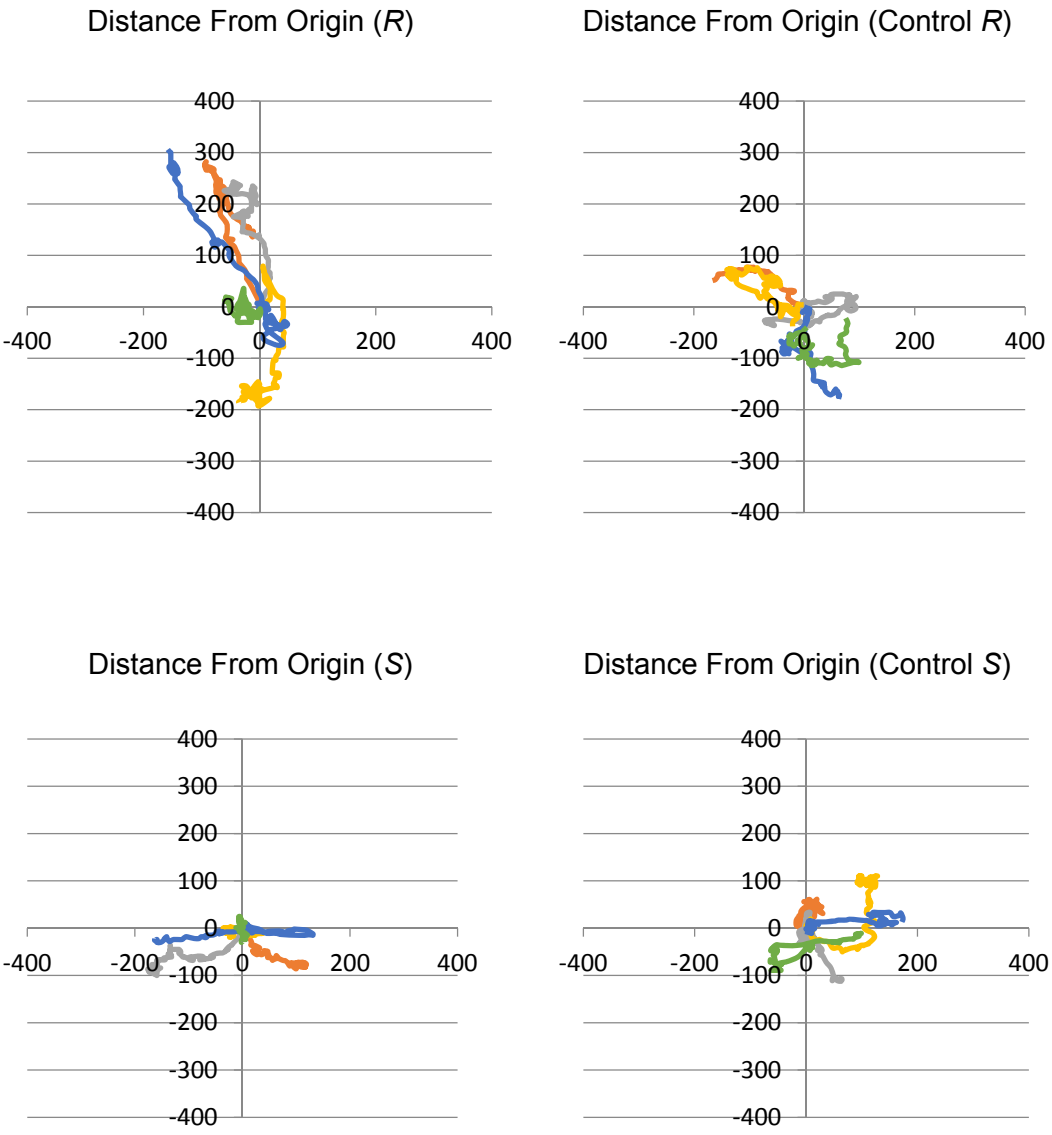


Inspection of the **Graphs 3.3.1-3.3.4** show no striking differences between the experiments, with cells in each experiment travelling a range of distances. **Graphs 3.3.5-3.3.9** are a useful alternative representation of cell movement. In these graphs we can get a clearer image of the micrometres moved by all cells. This is useful to visualise cells that don't travel far but may move forwards and backwards relative to ther starting positon. Again, we see no obvious difference in cells movement between experiments.

However, upon inspection of the mean cell movement for each experiment (**Entry 1**, **Table 3.3.1**) we do see an increase in the number of micrometres moved by the cells

treated with (*R*)-methyl IGD peptidomimetic (**(*R*)-2**) compared to those treated with the (*S*)-Methyl IGD peptidomimetic (**(*S*)-2**) and the control experiments.

While these results were encouraging, they were not statistically significant. In order to increase the likely hood of statistical significance in these results, the number of cells tracked would have to be increased. With the number of trackable cells in each experiment being small (generally between 5 and 7), each experiment was repeated in order to gain enough data.

However, the new set of results were not as hoped. The cells treated with the (*R*)-methyl IGD peptidomimetic showed a large reduction in cell movement despite experimental conditions remaining unchanged (**Entry 2**, **Table 3.3.1**).

In order to encourage a more consistent result, the concentration of the peptidomimetics used was increased to 1000 ng/mL and the experiments were repeated (**Entry 3**, **Table 3.3.1**). The (*R*)-IGD peptidomimetic showed a slight increase in movement compared to the control, however, the (*S*)-IGD peptidomimetic showed a large decrease in activity.

Upon examination of the results, we can see there is large variability within the data obtained in each experiment (as shown by high standard deviation), even in control groups. This raises the possibility that the values gained may not be reliable indications of the motogenic effect of the peptidomimetics.

**Table 3.3.1**: Summarised Results of Micrometres moved by each hTERT cell in Timelapse Studies.

| | Surface | [*R*/*S*] (ng/mL) | Cell Line | Mean Cell movement (μm) | | | |
|---|---|---|---|---|---|---|---|
| | | | | *R* | Control *R* | Corrected *S* | Corrected Control *S* |
| 1 | Flask | 100 | hTERT | 901±195 | 791±132 | 636±124 | 791±92 |
| 2 | Flask | 100 | hTERT | 489±150 | 701±334 | 662±186 | 701±131 |
| 3 | Flask | 1000 | hTERT | 724±245 | 671±273 | 490±38 | 671±284 |

The small sample size of five cells is not enough to allow to achieve a median population and to remove outliers, thus, we have data with large variations within groups. In order to increase the number of cells tracked from each experiment we would have to pursue one of two undesirable options. Firstly, decreasing our magnification would increase the number of cells in view, however, this would

decrease the accuracy of the measurements. Alternatively, we could increase the cell density within the flask, however, due to likely increased cell interactions this is unlikely to be successful in increasing the number of trackable cells.

In order to track enough cells to increase the likelihood of gaining statistically significant results we would be required to repeat each experiment around ten times, however, with demand on the time lapse microscopes and time constraints this was not viable. Nor would this give us an experiment that could quickly and reliably be used to check the activity of any new compounds synthesised. It was clear at this point that a change in experimental design was required.

It was hypothesised that the poor reliability of previous results gained may be due to the nature of the flask surface. Schor and Schor have previously shown IGD tripeptides to have "substratum dependant" activity, with cellular stimulation by the peptide being noted on native collagen but not denatured collagen.[26] Thus, it was decided to coat culture flasks with rat tail collagen, and to repeat the experiments (Entries 1-4, **Table 3.3.2**). Unfortunately, upon examination of the results it was clear that the data lacked any clear trend, and was still subject to large variations.

It was decided at this point that no further tests of this kind would be carried out and a new method of measuring cell motility would be investigated.

**Table 3.3.2**: Mean Micrometres Moved by Each hTERT Cell on Collagen in Timelapse Studies.

| | Surface | [*R*/*S*] (ng/mL) | Cell Line | Mean Cell movement (μm) | | | |
|---|---|---|---|---|---|---|---|
| | | | | *R* | Control *R* | Corrected *S* | Corrected Control *S* |
| 1 | Collagen | 1000 | hTERT | 1002±418 | 765±218 | 681±84 | 765±199 |
| 2 | Collagen | 1000 | hTERT | 680±178 | 775±93 | - | - |
| 3 | Collagen | 1000 | hTERT | 851±162 | 1100±653 | - | - |
| 4 | Collagen | 1000 | hTERT | 805±102 | 797±58 | - | - |

## 3.4 Scratch Assays and RT-qPCR for the Investigation of (*R*)- and (*S*)–IGD Peptidomimetics

Martin and Wright at Glasgow Caledonian University have reported the use of scratch assays to study the efficacy of Gap27. Gap27 is a connexion mimetic peptide with wound healing implications which increases the migration of human keratinocytes and dermal fibroblasts. Dr Martin and Dr Wright were able to conclude that Gap27 increased cell migration in conditions mimicking healthy and diabetic physiological conditions.[34-36] Further to this, they were also able to investigate what effect Gap27 treatment has on gene regulation under varying physiological conditions through Polymerase Chain Reaction (PCR) arrays.

Working in collaboration with the Wright group we were able to apply these techniques in our own investigations. Initially, scratch assays were used to quantify the effects of our (*R*)- and (*S*)- IGD peptidomimetics and subsequently, RT-qPCR was used to investigate the implications of these molecules on gene expression.

### 3.4.1 Scratch Assays for the Quantification of Cell Migration

Scratch assays are a convenient and low cost way of measuring cell migration.[37] Monolayers of cells are grown to around 80% confluency in a 12 well plate, and an artificial wound is created in each well with a pipette tip. The wound is immediately photographed and the denuded area is calculated by measuring the perimeter of the scrape (**Figure 3.4.1**).

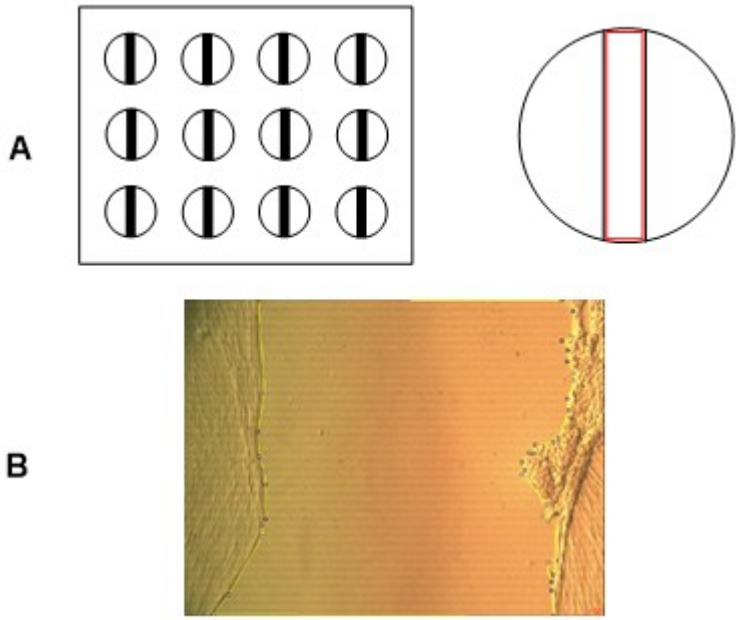


**Figure 3.4.1:** (**A**) Schematic of 12 Well Plate and Scrape Perimeter Measurement (red line); (**B**) An Example of Perimeter Measurement (yellow line) in Fibroblasts

This measurement is repeated after 24, 48 and 72 hours, with the perimeter taking into account any cells that have migrated into the denuded area (**Figure 3.4.2**). The percentage of wound area remaining, with respect to time 0, is calculated for each well. Thus, this is a model for wound healing that yields quantifiable results.

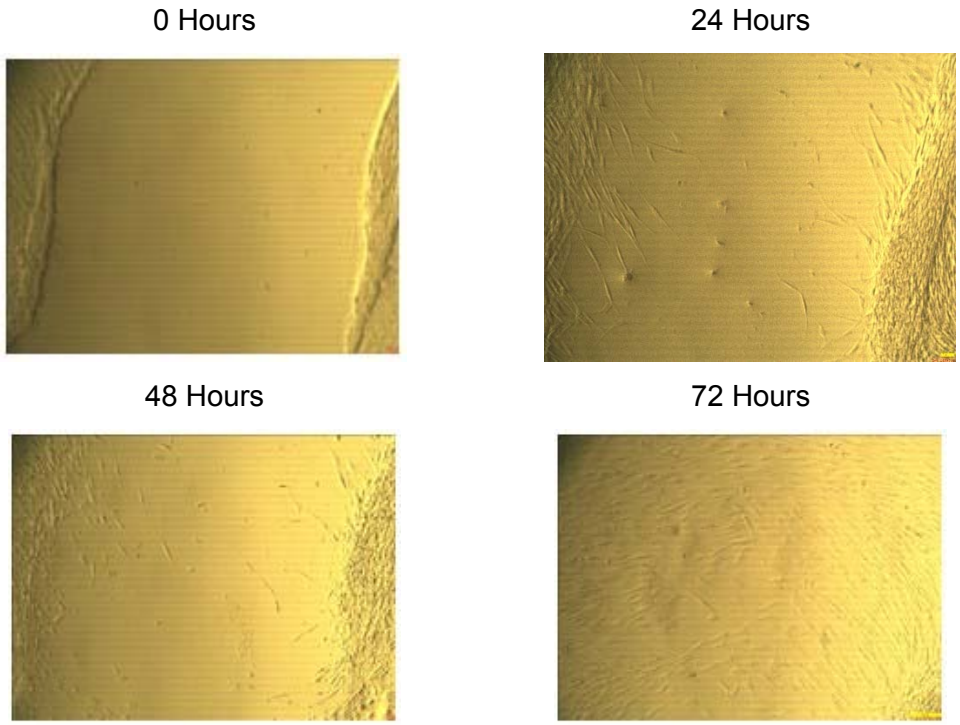


**Figure 3.4.2:** Scrape Wound Closure Over 72 Hours.

### 3.4.2 Serum Free vs. Complete Media Scratch Assay

In their experiments with Gap27, Wright and Martin used serum free media in order to ensure the availability of their mimetic in the cellular environment. With the concern that the lack of observed activity in our previous cell migration experiments could be, due to the use of complete media, efforts were concentrated on investigating this possibility. Thus, human dermal fibroblasts were plated in accordance with General HDFn Scrape Wounds Procedure (**Experimental 5.5**, **p178**) and wells were treated with one of four media solutions (**Table 3.4.1**).

**Table 3.4.1:** Composition of Serum Free and Complete Media Treatments.

| | Treatments | | | |
|---|---|---|---|---|
| Media Components | Serum Free Media + Compound | Serum Free Media Control | Complete Media + Compound | Complete Media Control |
| Media | sfDMEM | sfDMEM | cDMEM | cDMEM |
| DMSO | 1 µL/mL | 1 µL/mL | 1 µL/mL. | 1 µL/mL |
| [(*R*)-IGD peptidomimetic] | 0.1µg/mL | - | 0.1 µg/mL | - |

Analysis of scrape wounds results (please see **Appendix 6.1**, **p180** for data) with a two-tailed t-test between “serum free media control” and “serum free + compound” showed significance at 72 hours (p=0.0086), although no such significance was found between the complete media experiments (p=0.6789) (**Graph 3.4.1**).

**Graph 3.4.1**: HDFn Migration in Complete vs Serum Free Media With and Without (*R*)-Methyl IGD Peptidomimetic (**(*R*)-2**)

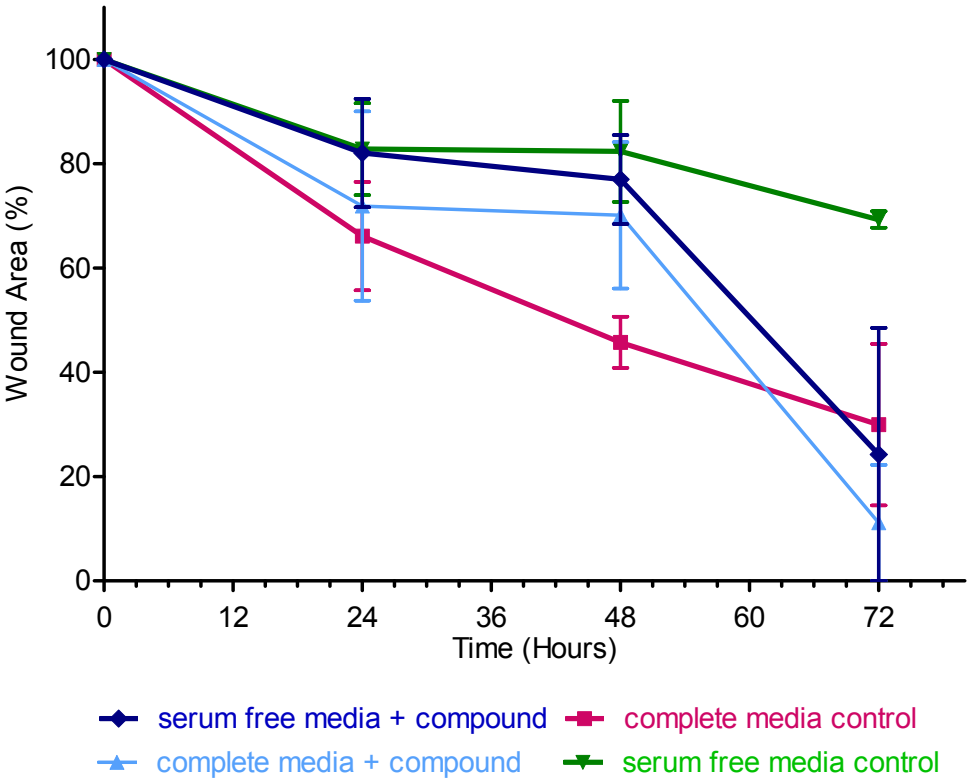


These results were highly encouraging. With an assay that could quantify the cell migratory properties of the IGD peptidomimetics in an efficient manner we were able to focus our attentions on establishing the optimal treatment dose.

3.4.3 Determination of Optimal Dose

With these promising initial results in hand, experiments to investigate the optimal dose for cellular migration were undertaken. Thus, cells were plated and scrape wounds were formed in according to General HDFn Scrape Wounds Procedure and wells were treated with 0, 0.1, 1, 10 µg/ mL of either (*S*)-methyl IGD peptidomimetic (**(*S*)-2**) or (*R*)-methyl IGD peptidomimetic (**(*R*)-2**).

To our surprise, initial plates experienced significant cell death. Although no contamination was observed in the plates, it was thought that this was a likely cause of the poor health of the cells. In order to minimise this issue, filter sterilisation of the peptidomimetic containing media was incorporated into the procedure. However, this precaution failed to improve the condition of the cells.

In subsequent plates, it was observed that the well centres were often dry upon removal from the incubator. It is believed that this was caused by the proximity of the plates to the incubator fan. Volume of media treatments per well was increased from 0.27 µL to 0.50 µL, and this issue was not encountered again.

The effect of each dose was measured 9 times (3 wells x 3 plates) for each enantiomer and the results were examined. The (*S*)-IGD peptidomimetic failed to show significant activity at any dose (**Graph 3.4.2**) (please see **Appendix 6.2**, **p181** for data). On the other hand, the (*R*)-methyl IGD peptidomimetic displayed significant activity at 0.1 µg/ mL ($3 \times 10^{-7}$ M) (**Graph 3.4.3**) (please see **Appendix 6.3**, **p182** for data).

**Graph 3.4.2**: Migration in HDF Cells Treated with Varying (*S*)-Methyl IGD Peptidomimetic Doses

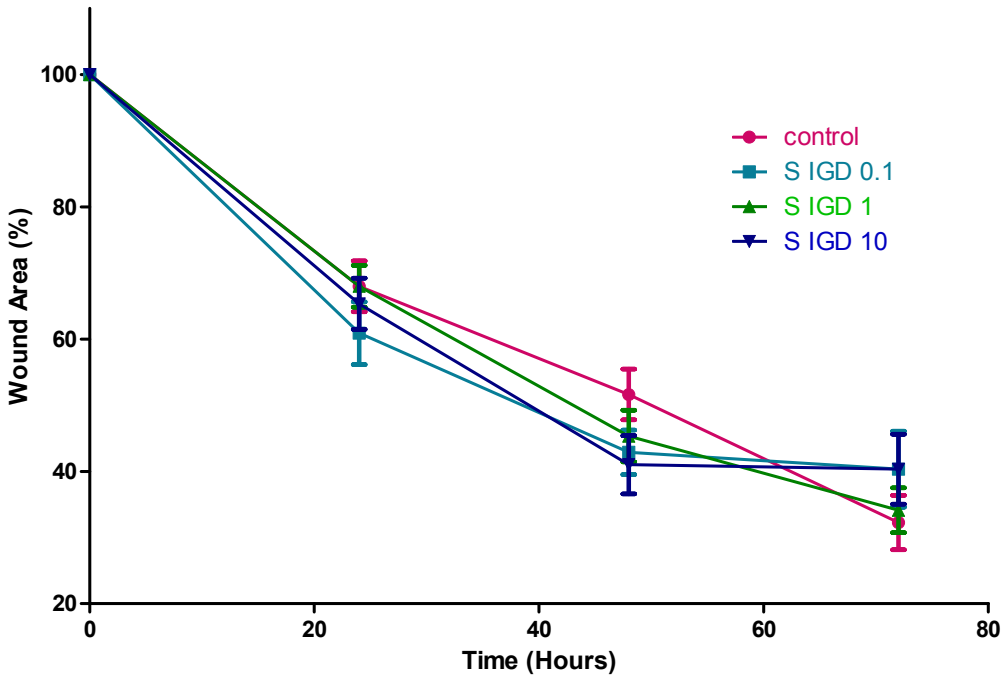


**Graph 3.4.3**: Migration in HDF Cells Treated with Varying (*R*)-Methyl IGD Peptidomimetic Doses

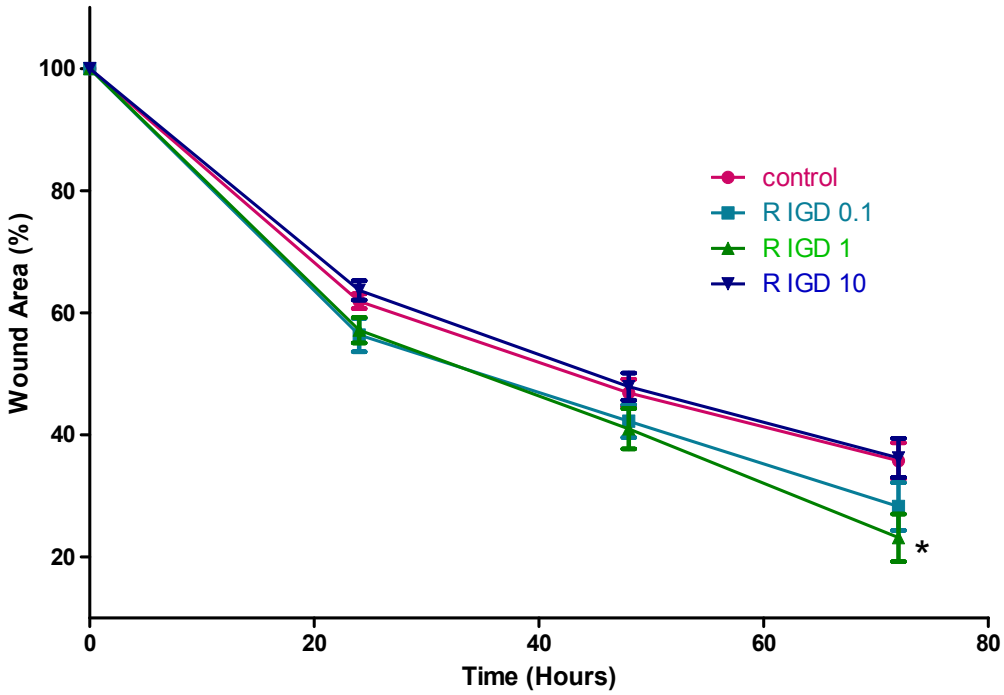

## 3.5 Polymerase Chain Reaction Experiments

### 3.5.1 Polymerase Chain Reaction

Polymerase Chain Reaction experiments transformed biological science when the technique was developed in 1983 by Kary Mullis.[38] This sensitive assay allows a piece of DNA to be amplified selectively in the presence of many others. This Nobel prize winning technique has many valuable applications including DNA cloning, genetic fingerprinting, diagnosis of hereditary diseases.[39]

To investigate a desired fragment of DNA first the sample is heated to 94-96 °C. This heating induces denaturation to give single stranded DNA (**Figure 3.5.1**). The subsequent annealing step allows short pieces of DNA with complimentary base pairs (primers) to bind to the fragment in question. The coordination of primers to the DNA single strand provides a 3'-OH onto which DNA polymerase can add nucleotides (elongation). Crucially, by selecting the primer in use we can amplify one desired piece of DNA and thus by exposing any DNA pool to a strategic range of primers we may see what DNA is present. These three steps are repeated many times, thereby amplifying the volume of our DNA of choice.[39]

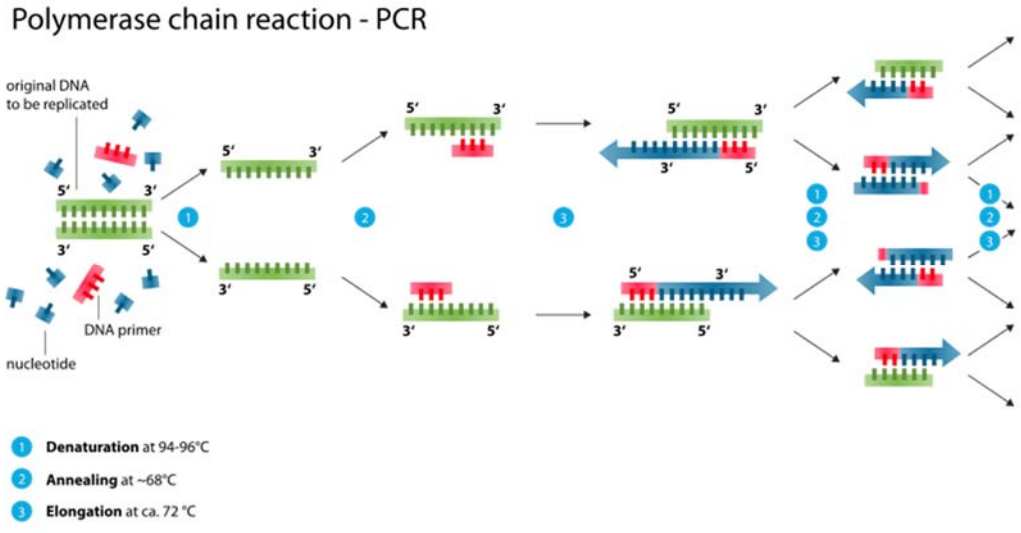


**Figure 3.5.1:** Polymerase Chain Reaction Increasing the Number of Copies of a Desired Piece of DNA. [39]

A modification of this technique Reverse Transcription PCR (RT-PCR) allows the detection of RNA, through the synthesis of cDNA. This technique is particularly

valuable for studying gene expression. Another variation is quantitative real time PCR (qPCR) where DNA is detected as it is formed through the release or activation of fluorophores.[40] Reverse transcriptase real time PCR (RT-qPCR) is the combination of both techniques and allows quantitative analysis of the RNA present in a sample, and thus, can be used to identify changes in gene regulation.[41]

Many companies offer RT-qPCR services, including the RT-qPCR experiments and data analysis (**Figure 3.5.2**). Qiagen's Human Cell Motility PCR Array includes 84 selected primers for the investigation of gene regulation in relation to cell motility (plus 12 quality control/ house keeping primers) (Please see **Appendix 6.4**, **p188** for a complete list of the genes investigated in this assay). Through these 84 primers many aspects of cell motility are investigated including chemotaxis, common receptors, growth factors, cell adhesion, integrin signalling and cellular projection. This assay would be particularly useful to give us information about the origin of activity of our peptidomimetics.

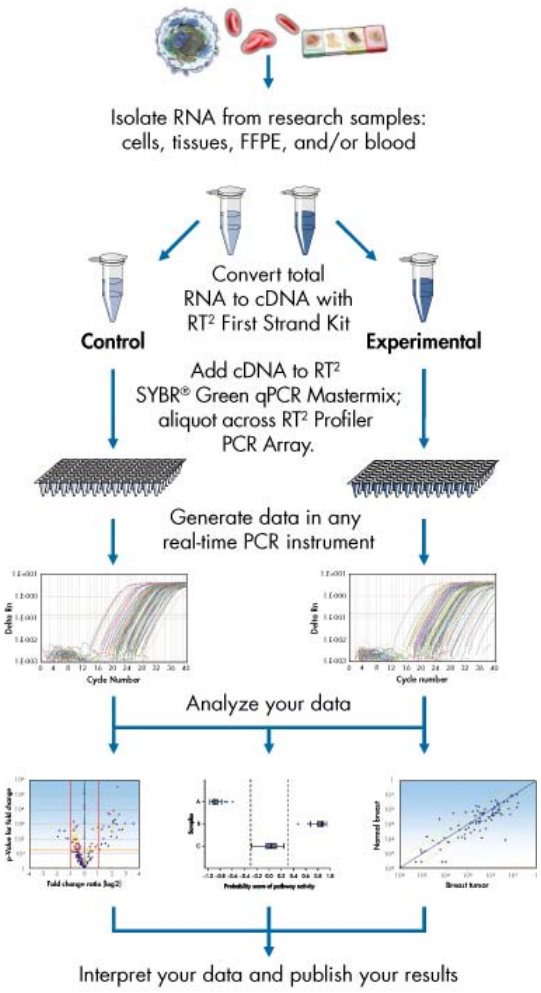


**Figure 3.5.2**: General RT2 Profiler PCR Array workflow from sample to result.[42]

## 3.5.2 RNA Extraction

Having confirmed that the (*R*)-IGD peptidomimetic (**(*R*)-2**) is the active enantiomer and having established our optimal dose, it was possible to focus our efforts towards obtaining RNA samples for RT-qPCR analysis.

The fibroblasts were treated with either (*R*)-methyl IGD peptidomimetic (**(*R*)-2**) or (*S*)-methyl IGD peptidomimetic (**(*S*)-2**) and the RNA was extracted from the cells and sent off for analysis. Using the (*S*)-IGD peptidomimetic as our control would allow us to highlight the differences in gene expression that are specifically implicated with the activity of the *R* enantiomer.

Cells were cultured as in General HDFn Scrape Wounds Procedure (**Experimental 5.5**, **p178**), with the exception that RNA was harvested after 24 h. RNA was harvested with Qiagen's RNeasy Mini Kit and RNase-Free DNase Set, following "Purification of Total RNA from Animal Cells using Spin Technology" and "Optional On-Column DNase Digestion with the RNase-Free DNase Set" protocols as outlined in Qiagen's RNeasy® Mini Handbook Fourth Edition June 2012. The steps followed from these protocols have been outlined in RNA Extraction Protocol (**Experimental 5.6**, **p179**).

The extracted RNA was analysed on a NanoDrop Spectrophotometer (**Table 3.5.1**). Experiments R4 and S4 were found to contain low quantites of RNA, possibly a result of incomplete aspiration of media during RNA extraction. Samples R1-3 and S1-3 were found to be of sufficient amounts and quality giving us the required number of replicates. The samples were sent to Qiagen to undergo RT-qPCR analysis.

**Table 3.5.1**: Analysis of Extracted RNA.

| Test Group | Volume | [RNA] ng/ µL | Control | Volume | [RNA] ng/ µL |
|---|---|---|---|---|---|
| R1 | 27 µL | 448.8 | S1 | 27 µL | 177.7 |
| R2 | 27 µL | 446.4 | S2 | 27 µL | 482.9 |
| R3 | 27 µL | 469.9 | S3 | 27 µL | 568.3 |
| R4 | 27 µL | 23.4 | S4 | 27 uL | 66.0 |

3.5.3 Human Cell Motility RT-qPCR Array Results

The scatter plot provided in the Qiagen report is a quick way to visualise up or down regulation of each studied gene (**Figure 3.5.3**). The central line indicates unchanged gene expression, genes above the line are upregulated, while those below are downregulated. From this plot we can see that two genes (highlighted in red) have been upregulated, Insulin Like Growth Factor 1 (IGF1) and Alpha Actinin 3 (ACTN3).

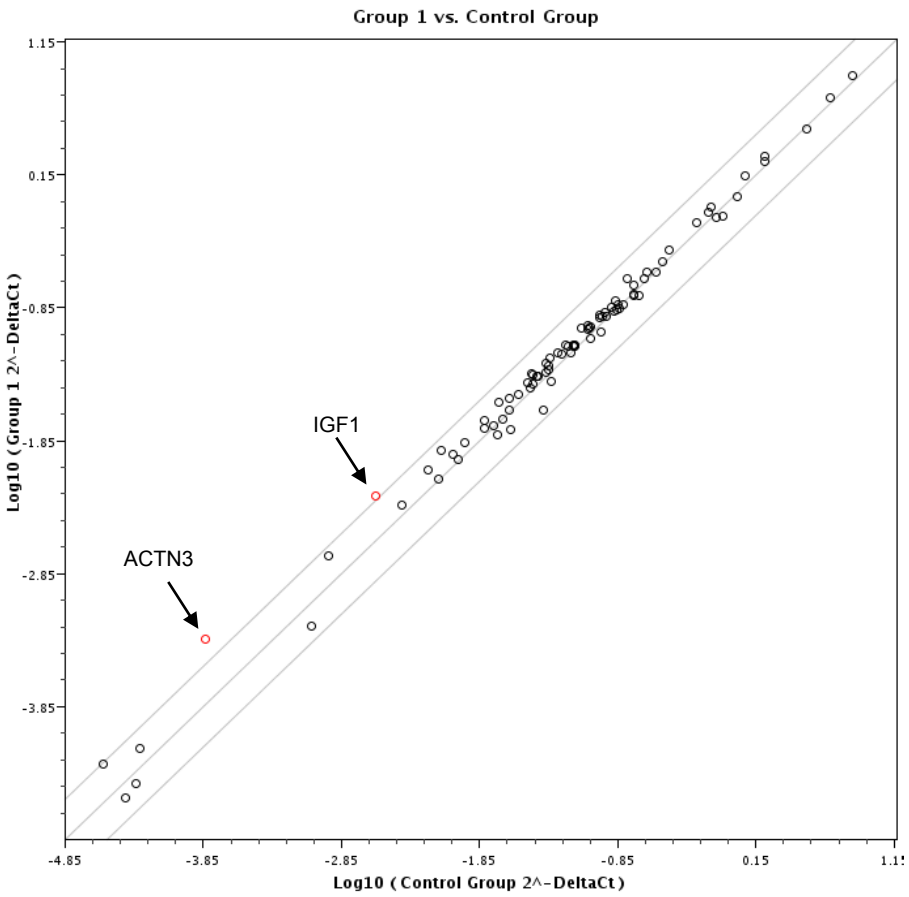


**Figure 3.5.3:** Scatter Plot of Gene Regulation.[42]

Representing the data as a volcano plot (**Figure 3.5.4**) allowed us to visualise the statistical significance of the observed gene expression and the fold regulation of the genes. Based on this analysis it can be determined that the two genes that have been upregulated (highlighted in red) vary in their statistical significance. IGF1 has an undesirable p value of 0.332608, whereas, ACTN3 has a very low value of p = 0.001347.

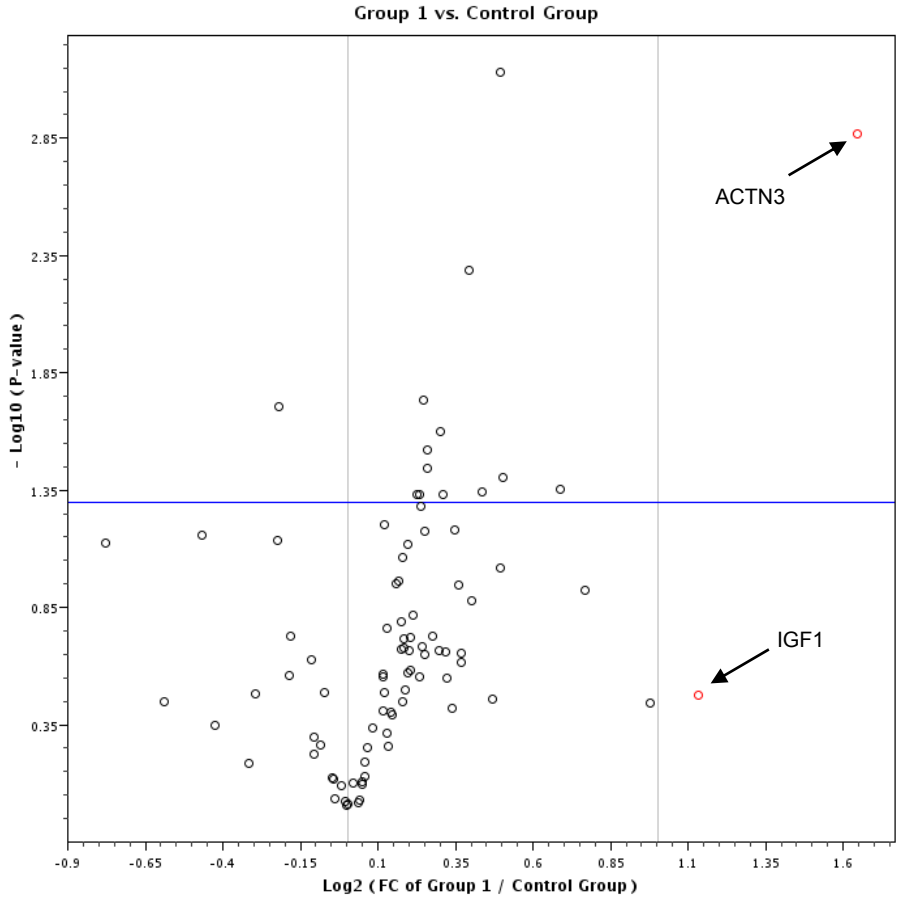


**Figure 3.5.4:** Volcano Plot of Statistical Significance vs Fold Gene Expression.[42]

In summary, the array shows the over expression of two genes in the samples treated with (*R*)-methyl IGD peptidomimetic (**(*R*)-2**) compared to (*S*)-methyl IGD peptidomimetic (**(*S*)-2**), no genes were under expressed. ACTN3 has been overexpressed by over three fold, and has a very low p value. IGF1 was upregulated by over two fold, however, the reliability of this result may be in question due to the high p value (**Table 3.5.2**).

**Table 3.5.2**: Summary of Upregulation of Gene Expression.

| Gene Over-Expressed | Fold Regulation | p-value |
|---|---|---|
| ACTN3 | 3.1246 | 0.001347 |
| IGF1 | 2.1865 | 0.332608 |

## 3.6 Implications of RT-qPCR Results

### 3.6.1 Insulin Like Growth Factor 1

The insulin like growth factor 1 gene (IGF1) encodes the homonymous protein Insulin Like Growth Factor 1 (**Figure 3.6.1**).[43] The biological activity of this protein is well documented, with involvement in childhood growth and, crucially for our purposes, tissue repair.

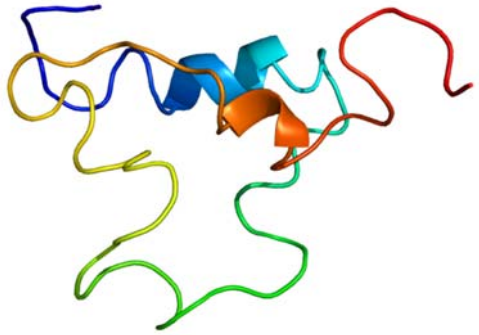

**Figure 3.6.1:** Insulin Like Growth Factor-1.[44]

During normal wound healing IGF1 is upregulated, and it plays a key role in reepithelialisation and the formation of granulation tissue, significantly, this activity is delayed or inhibited in diabetic patients.[45] Reduced levels of IGF1 are implicated in the microvascular complications of diabetic patients.[46] Further to this, *in ex-vivo* organ culture, healthy and diabetic tissues subjected to adenoviral overexpression of IGF-1 (Ad-IGF-1) show enhanced angiogenesis and wound healing in healthy and diabetic tissues.[47]

Further to this IGF-1 regulates the expression of other proteins implicated in wound healing. Vascular Endothelial Growth Factor (VEGF) and Hypoxia-Inducible Factor 1 (HIF-1) are regulated by IGF-1 and are particularly implicated in wound healing due to their effect on tissue repair, angiogenesis and cell proliferation.[48]

The high p value (0.332608) displayed with the upregulation of this gene casts doubt on the reliability of these results, and thus, it would be rash to conclude that the activity of the (*R*)-IGD peptidomimetic can be attributed to this observation. However, this is an important find and it would be wise to do further tests to investigate the impact of the regulation of this gene on our observed activity.

### 3.6.2 Alpha Actinin 3

The alpha actinin 3 gene (ACTN3) encodes Alpha Actinin 3 protein, also known as Alpha-Actinin skeletal muscle isoform 3 or F-actin cross-linking protein (**Figure 3.6.2**). As these names suggest, this protein is expressed by ACTN3 in skeletal muscle where its role is crosslinking actin containing filaments. The Alpha-Actinin-3 (ACTN3) gene has been most studied for its implications in athletic prowess, with different athletic abilities being linked to the normal expression or defunct nature of this gene.[49]

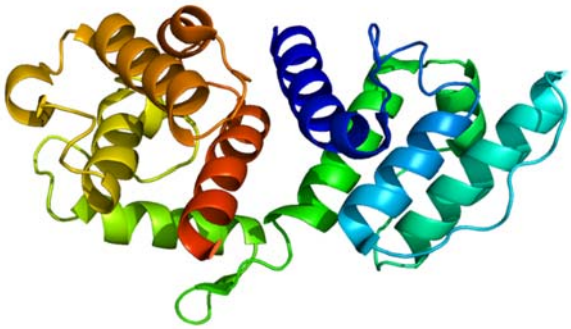

**Figure 3.6.2:** Alpha Actinin 3. [49]

For our purposes the role of ACTN3 are a little less defined, there are many implications of the alpha actinin family of genes in cellular migration but less specifically relating to ACTN3 alone.

The alpha actinin family are implicated in forming the cross linked actin cytoskeleton network that supports filopodia and lamellipodia (leading protrusions in migrating cells).[50] The alpha actinin family are also involved in binding other proteins, such as viniculin and titin which are involved in focal adhesions (links between the internal actin cytoskeleton and the ECM).[51] Alpha actinin links signalling proteins such as, phosphatidylinositol 3-kinase, PKN and Rho effector kinase to transmembrane receptors including *β*-integrins.[50] [52] It is possible that these interactions may responsible for the wound healing activity displayed by the (*R*)-IGD Peptidomimetic.

## 3.7 IGD Peptidomimetics with Synthetic Handles

### 3.7.1 Background of Functionalised IGD Peptidomimetics

Returning to the original modelling studies of the IGD tripeptide motif of MSF, we can see that the bicyclic ring system of the benzodiazepinone is essential to give our peptidomimetic the correct confirmation. It is also true that any alteration in the 1,2 or 3 positions of this bicyclic ring system would be likely to have significant implications for activity. However, looking at **Figure 3.7.1** we can see that it is possible that alteration of the *N*-methyl group may be possible without a loss of activity.[27]

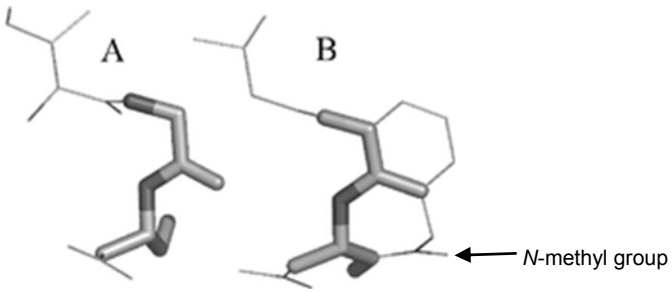


**Figure 3.7.1:** Model of the IGD Tripeptide Motif (**A**), Benzodiazepinone core (**B**).

Previously within the Marquez group Dr Phillip McGivern synthesised a small library of IGD peptidomimetics with a phenyl functionality attached to the benzodiazepinone core with varying alkyl chain lengths (**Figure 3.7.2**). Biological testing of these analogues by trans-membane assay showed no reduction in motogenic activity, thus, providing evidence to the suitability for modification of this position.

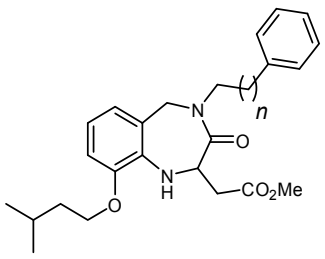


*n* = 1, **(±)-34**, *n* = 2 **(±)-35**, *n* = 3 **(±)-36**

**Figure 3.7.2:** IGD Peptidomimetics with *N*-Alkyl Phenyl.

Dr. McGivern's results, although preliminary, demonstrated that modification of the nitrogen substituents was indeed possible. Two classes of analogue were envisioned, one that could give information about the mode of action of the IGD

peptidomimetic core and one that could be used for drug delivery (**Figure 3.7.3**). With little information about the optimal length of any alkyl chain, *n* was designed to be one or three, to allow sufficient distance between the benzodiazepinone core and any new functionality whilst avoiding aggregation and coiling of the linker unit.

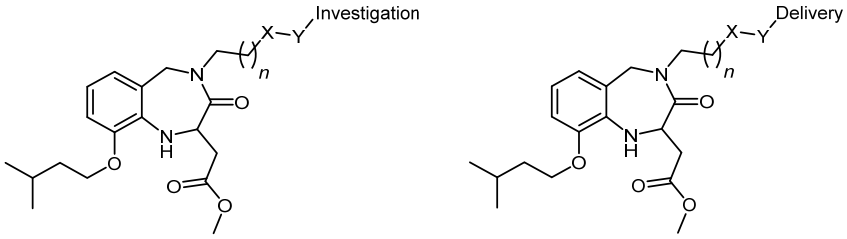


(*R*/*S*)-35 (*R*/*S*)-36

**Figure 3.7.3:** IGD Peptidomimetics Functionalised for Investigation (**35**) or Delivery (**36**).

In order to maximise the utility and versatility of the linker unit, it became desirable to synthesise a range of IGD peptidomimetics each containing a functionality that could be used in bond formation (**Figure 3.7.4**). Thus, it was envisioned that accessing acids **37**/**38** or amines **39**/**40** and alkynes **41**/**43** or azide **44**/**45** would allow further derivatisation *via* amide coupling or Huisgen cyclisation.[53]

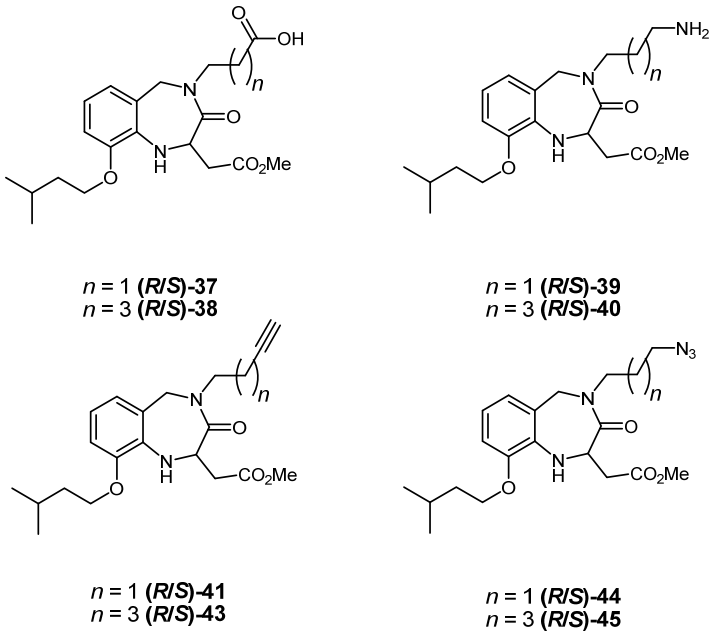

*n* = 1 (*R*/*S*)-37
*n* = 3 (*R*/*S*)-38

*n* = 1 (*R*/*S*)-39
*n* = 3 (*R*/*S*)-40

*n* = 1 (*R*/*S*)-41
*n* = 3 (*R*/*S*)-43

*n* = 1 (*R*/*S*)-44
*n* = 3 (*R*/*S*)-45

**Figure 3.7.4:** Desired Functionalised IGD peptidomimetics.

The generation of the desired analogues was envisioned to proceed through divergence from alcohols **24**/**26** (**Scheme 3.7.1**). It was hoped that oxidation of alcohols **24**/**26** would allow access to aldehyde **48/49** and acid **37/38**. An Ohira-

Bestmann olefination could be employed to access alkyne **41/43** from aldehyde **48/49**. Alkyne **41/43** could be used in Huisgen cyclisations, while the aldehyde unit **49/49** could potentially be used in reductive amination. Alternatively, tosylation of alcohol **24/26**, would provide a good leaving group which could then be used to generate azide **44/45** and subsequently amine **39/40**.

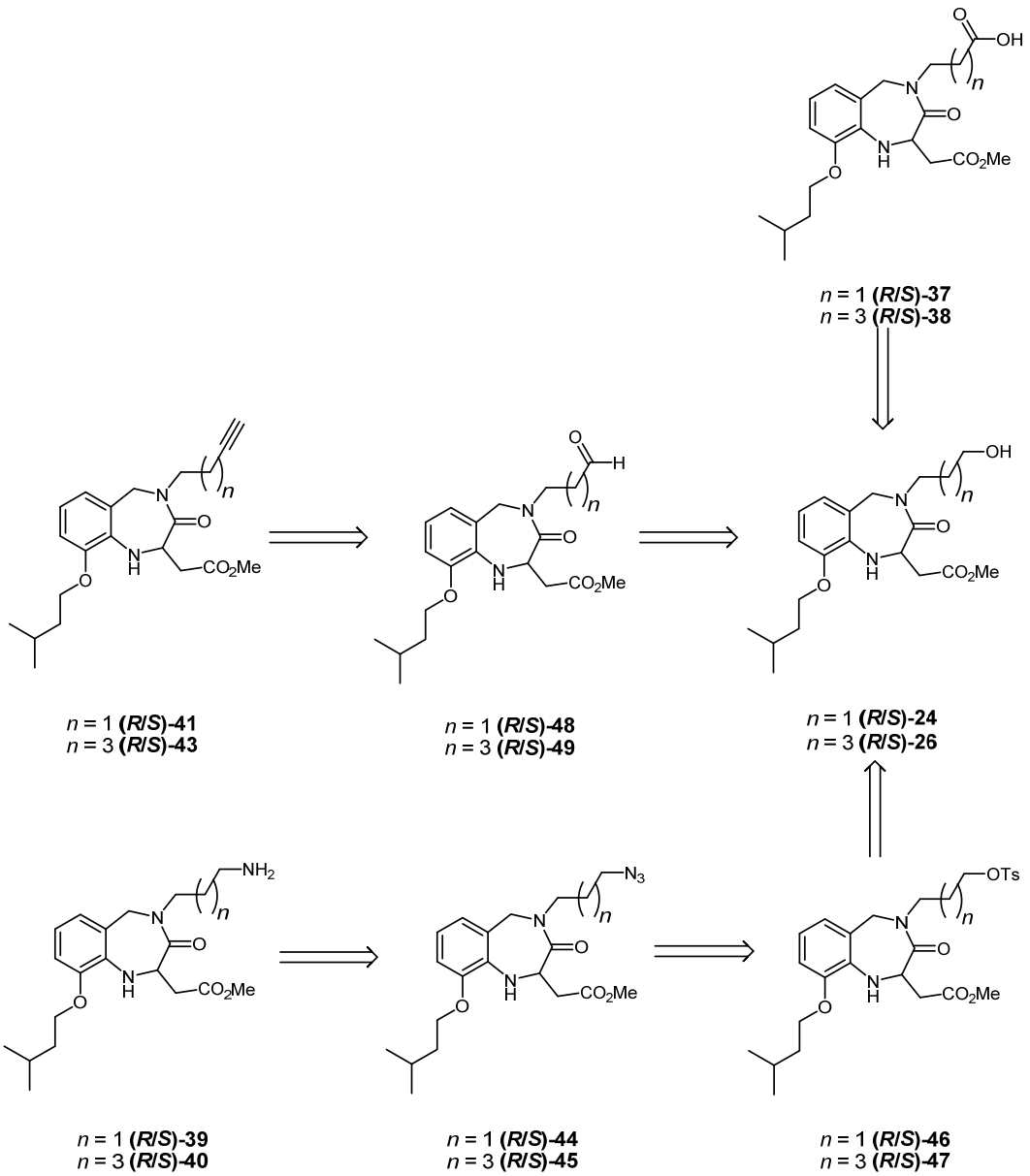


**Scheme 3.7.1:** Retrosynthetic Route of Functionalised IGD Peptidomimetics Diverging from Alcohols **24/26**.

Having established a reliable route to access multigram quantities of intermediate **18**, it was possible to adapt our efforts towards an efficient synthesis of alcohols **24/26**. The route was envisioned to proceed in an analogous manner to the synthesis of the

methyl IGD peptidomimetics ((***R***)-**2** and **(*S*)-2**, **Figure 2.1.1. p30**) (**Scheme 3.7.2**). Thus, the synthesis would require the introduction of the linker arm via the reductive amination of aldehyde **18**, followed by reduction and *N*-alkylation using triflate **20**.[27] The alcohol would be unmasked after cyclisation, allowing the desired diversification with the *n* carbon chain providing the required space between the IGD core and any desired functional group.

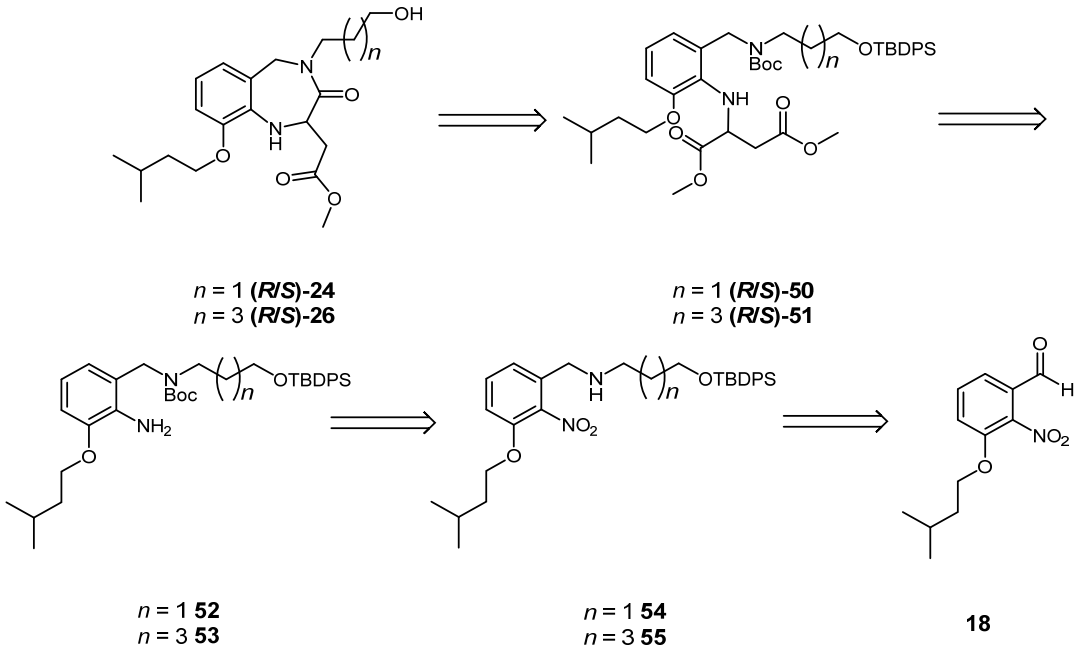


**Scheme 3.7.2**: Envisioned Route to IGD Peptidomimetics **24/26**.

3.7.2 Synthesis of Functionalised IGD Peptidomimetics

3-Aminopropanol and 5-aminopentanol were chosen as precursors for the reductive amination. The synthesis of amine **54** (**Scheme 3.7.3**) began with the protection of 3-aminopropanol, with *tert*-butyldiphenylmethylsilyl chloride to generate silyl ether **58** in good yield (85%).[54] 5-Aminopentanol was protected in an analogous manner giving silyl ether **59** in slightly lower yield (65%).

Nitrobenzaldehyde **18** underwent reductive amination with the free amine **58** giving benzylic amine **54** in excellent yield (94%). These conditions were reproduced for the reaction of the 5-amino-pentanol derived amine **59** and nitrobenzaldehyde **18** and gave the desired amine **55** in near quantitative yield (98%).

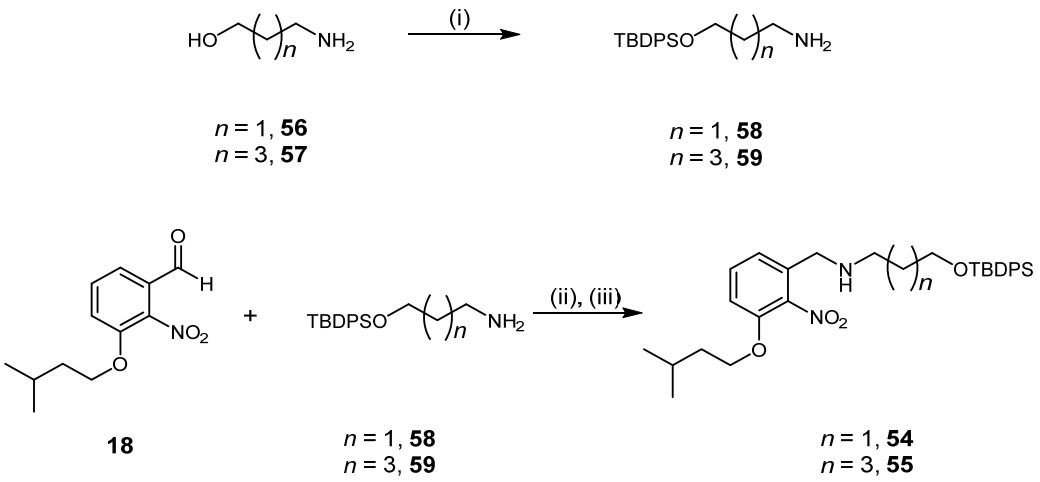


**Scheme 3.7.3**: Synthesis of Silyl Ethers **55** and **55**. *Reagents and Conditions*: (i) TBDPSCl, DCM, 0 ºC, *n* = 1, 85%, *n* = 3, 65%; (ii) Heptane, $CHCl_3$; (iii) MeOH, $NaBH_4$, *n* = 1, 94%, *n* = 3, 98%.

The newly formed benzylic amines **54** and **55** were protected as BOC carbamates **60** and **61** respectively in quantitative yields. With the protected amines in hand, the reduction of the nitro group to the corresponding aniline was initially attempted using 10% palladium on activated charcoal under a hydrogen atmosphere. The use of hydrogen gas was found to give incomplete conversion, and ammonium formate was used to drive the reaction to completion (**Scheme 3.7.4**).

Ammonium formate was found to be a slow but reliable method of hydrogenation, requiring increased time and higher temperatures than conditions reported for the generation of the corresponding methyl analogue, however, intermediates **52** and **53** can be accessed under these conditions in excellent yield without the need for purification. Attempts to improve rate of reaction, by changing the solvent to ethyl acetate proved to be counter productive, and methanol had to be added to the reaction mixture to drive the reaction to completion.

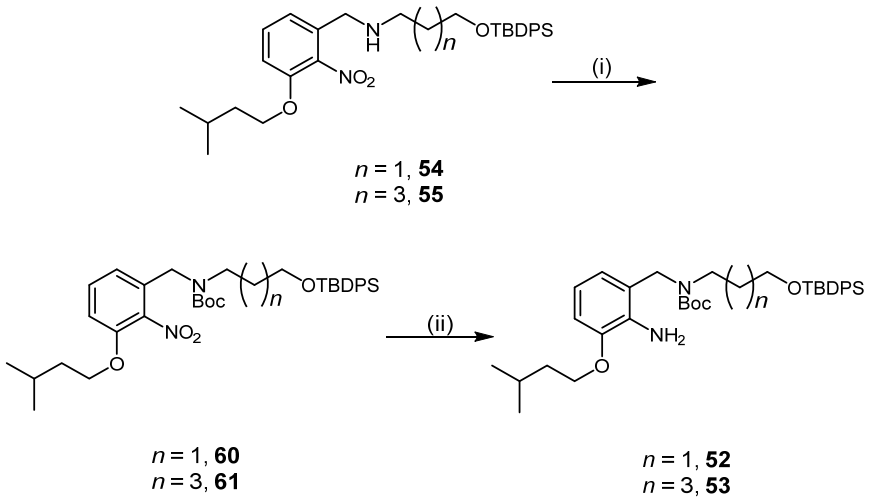


**Scheme 3.7.4**: Protection and Hydrogenation to give **52** and **53**. *Reagents and Conditions*: (i) Di-*t*-butyldicarbonate, $Et_3N$, DCM, *n* = 1, quantitative, *n* = 3, quantitative; (ii) $NH_4CO_2H$, Pd/C, methanol, *n* = 1, 78%, *n* = 3, 90%.

With the anilines in hand, the next step was the introduction of the chiral diester unit. Following a parallel approach to synthesis of the methyl IGD peptidomimetics, (S)-triflate (**(*S*)-20**), was generated by coupling (*S*)-(-)-dimethyl malate with trifluoromethylsulfonic anhydride in quantitative yield (**Scheme 3.7.5**).

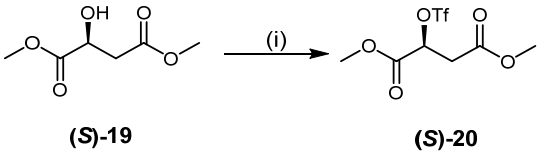


**Scheme 3.7.5**: Formation of Activated Malate **(*S*)-20**. *Reagents and Conditions*: (i) triflic anhydride, 2,6- lutidine, DCM, (quant).

The newly formed malate proved to be slightly moisture sensitive and had to be used promptly. Gratifyingly, immediate coupling of the chiral triflate (**(*S*)-20**) with anilines **52** and **53** gave the desired secondary amines **(*R*)-50** and **(*R*)-51** in excellent yields (**Scheme 3.7.6**).

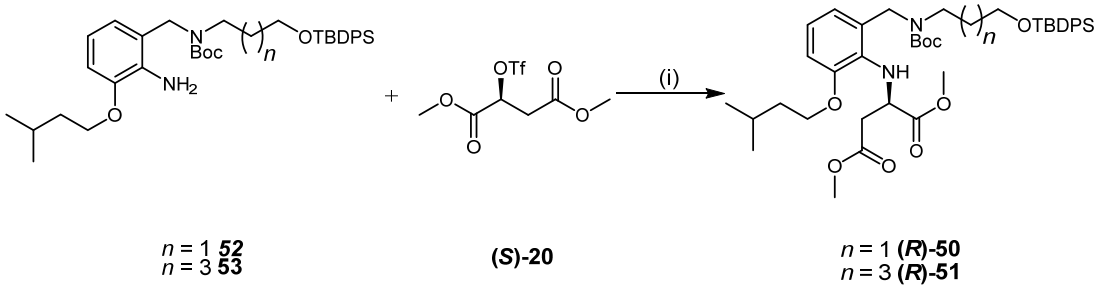


*n* = 1 ***52***
*n* = 3 **53**

**(*S*)-20**

*n* = 1 **(*R*)-50**
*n* = 3 **(*R*)-51**

**Scheme 3.7.6**: Formation of Chiral Intermediates **(*R*)-50** and **(*R*)-51**. *Reagents and Conditions*: (i) 2,6- lutidine, DCM, *n* = 1, 68%, *n* = 3, 73%.

The efficient coupling of triflate **(*S*)-20** with anilines **52/53** allowed us to get access to the precursor for the tetrahydrobenzodiazepinone cores for both chain lengths in excellent yields (*n* = 1, 50%, *n* = 3, 64%) over the five step sequence from nitrobenzaldehyde **18**. Significantly, this synthesis can be scaled up and requires minimal purification.

## 3.8 Benzodiazepinone Cyclisation

### 3.8.1 Examples of Benzodiazepinone Formation

Outwith work carried out in the Marquez group, there are several literature examples of formation of benzodiazepinones with a chiral centre at the 2-position.

Synthesis of fibrinogen receptor antagonist **3** took place via the cyclisation of intermediate **62**. This approach used sodium methoxide in methanol to afford the cyclisation, this is the method most frequently used in the literature for the synthesis of the benzodiazepine core of benzodiazepinone derived RGD mimetics (**Scheme 3.8.1**).[55]

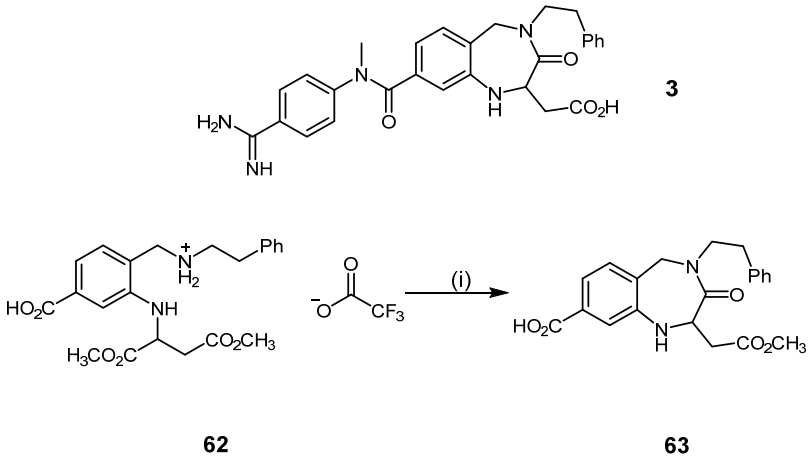


**Scheme 3.8.1:** Synthesis of **3**. *Reagents and Conditions*: (i) $NaOCH_3$, $CH_3OH$, reflux (70%).

A related example employed triethylamine and toluene to achieve the cyclisation of compound **65** en route to complete the synthesis of 2-benzazepine **64** (**Scheme 3.8.2**).[56]

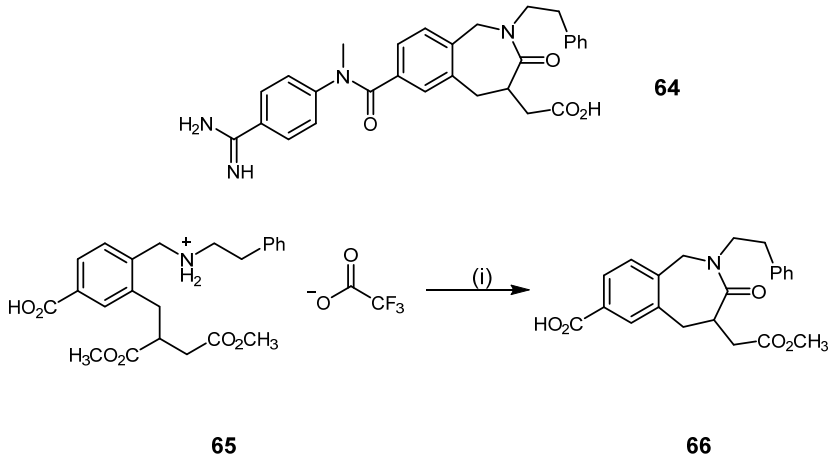


**Scheme 3.8.2:** Synthesis of **64**. *Reagents and Conditions*: (i) $Et_3N$, toluene, reflux (98%).

Miller reported the synthesis of enantiomerically pure SB214857 (**4**, **Scheme 3.8.3**) through the intramolecular displacement of an activated aryl fluoride.[56] The carboxylic ester **67** is sufficiently activated to allow this reaction to proceed giving **68** in moderate yield (47%) as a single enantiomer along with the elimination product **69** (27%).

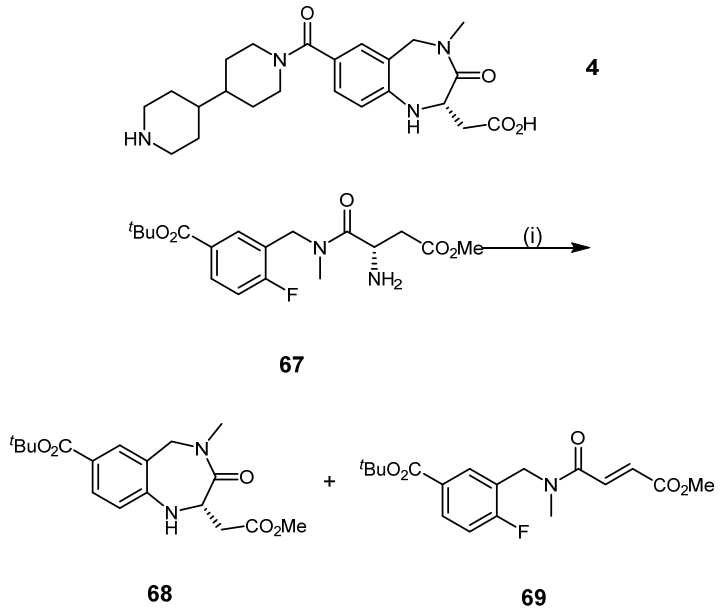


**Scheme 3.8.3**: Key Cyclisation in Route to SB214859 (**4**). *Reagents and Conditions*: (i) 0.1 M **67** in DMSO, 125 °C (47% of **68**, 28% of **69**).

3.8.2 Formation of the Benzodiazpinone Core: Propyl Analogues

With the synthesis of the IGD peptidomimetic framework complete, the key cyclisation step was attempted. Treatment of Boc amine **(*R*)-50** with trifluoroacetic acid cleanly removed the BOC group to yield the TFA salt **(*R*)-70**. Sodium methoxide was then used to try to induce cyclisation as in previous syntheses, however, no cyclisation occurred and the free amine (**(*R*)-72**) was isolated in reasonable yield (76%) (**Scheme 3.8.4**).

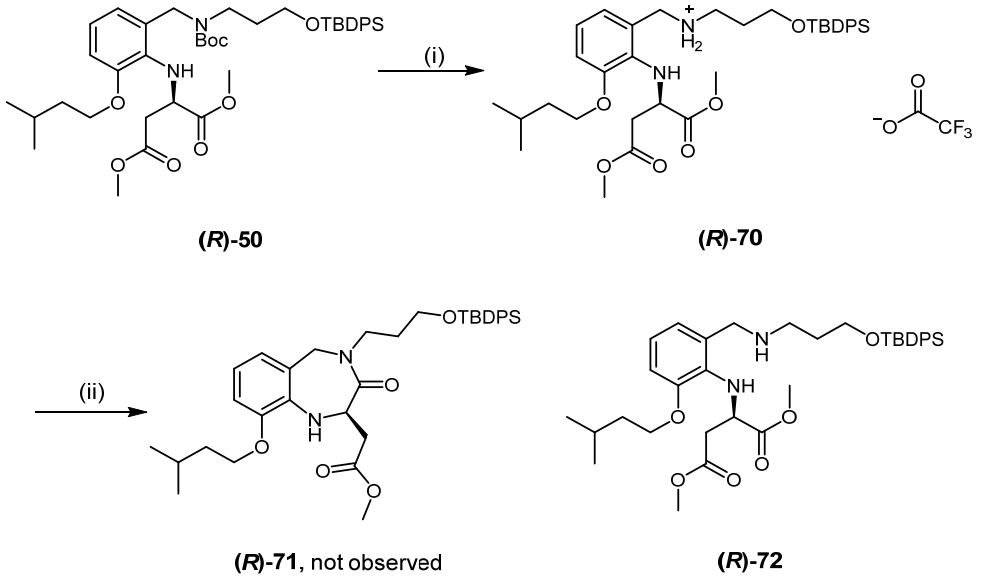


**(*R*)-50** **(*R*)-70**

**(*R*)-71**, not observed **(*R*)-72**

**Scheme 3.8.4**: Isolation of Amine **(*R*)-72**. *Reagents and Conditions*: (i) trifluoroacetic acid, DCM, (88%); (ii) NaOMe (2.0 eq.), MeOH, 70 ºC, 76%.

As discussed previously, the majority of benzodiazepine cyclisations are carried out with sodium methoxide in methanol.[55, 57-58] In an attempt to achieve cyclisation of salt **(*R*)-70**, the equivalents of sodium methoxide employed was increased.

Thus, the amount of sodium methoxide was increased from 2 to 5 equivalents, however, this lead to degradation of starting material. In subsequent attempts the number of equivalents was reduced to 3, with a short reaction time (5 minutes). Thin layer chromatography at this point indicated that the starting material had been consumed, however, flash column chromatography failed to isolate any product from a complex reaction mixture (**Scheme 3.8.5**).

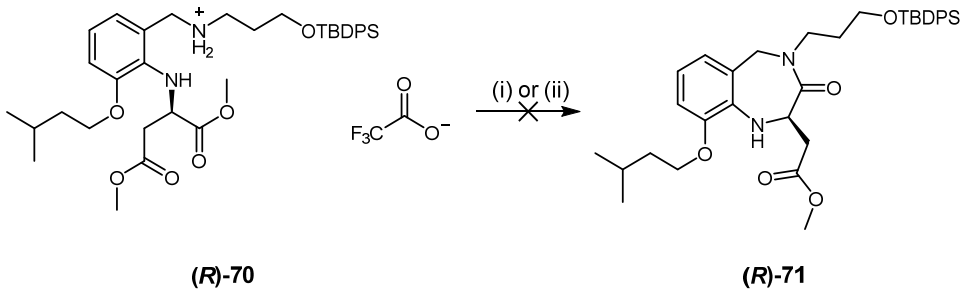


**(*R*)-70** **(*R*)-71**

**Scheme 3.8.5**: Attempted Synthesis of **(*R*)-71**. *Reagents and Conditions*: (i) NaOMe (5.0 eq.), MeOH, 70 ºC (degradation); (ii) NaOMe (3.0 eq.), MeOH, 22 ºC (degradation).

In order to gain further insight into these reactions it was decided to isolate the secondary amine **(*R*)-72** before subjecting it to further reactions. Hence, after treatment of **(*R*)-50** with trifluoroacetic acid, strong cation exchange silica was used

to in an attempt to generate the free amine **(*R*)-72**. The SCX silica was washed with methanol to remove non-amine impurities and then flushed with 7 M ammonia in methanol solution. However, unexpectedly and to our satisfaction, the major product isolated was the desired protected tetrahydrobenzodiazepinone **(*R*)-71** in reasonable yield (48%) (**Scheme 3.8.6**).

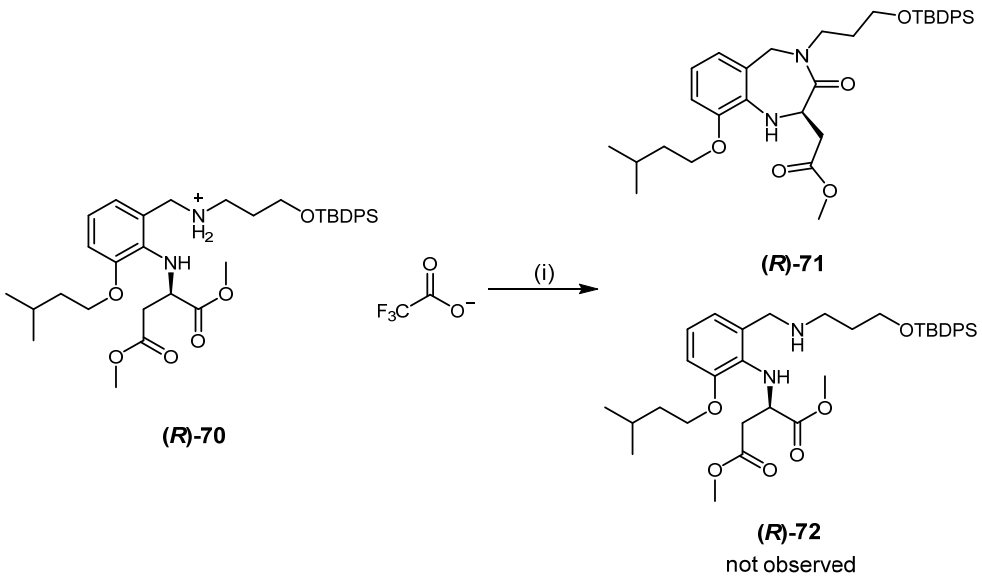


**Scheme 3.8.6**: Synthesis of Protected Tetrahydrobenzodiazepinone **(*R*)-71**. *Reagents and Conditions*: (i) SCX Column, 7 M $NH_3$/MeOH, **(*R*)-70** 48%.

Interestingly, a simultaneous reaction using one equivalent of sodium methoxide yielded amine **(*R*)-72** (30%) and cyclised alcohol **(*R*)-24** (18%). To our delight, solvation of the free amine **(*R*)-72** in 7 M ammonia in methanol solution gave the protected tetrahydrobenzodiazepinone **(*R*)-71** in quantitative yield (**Scheme 3.8.7**).

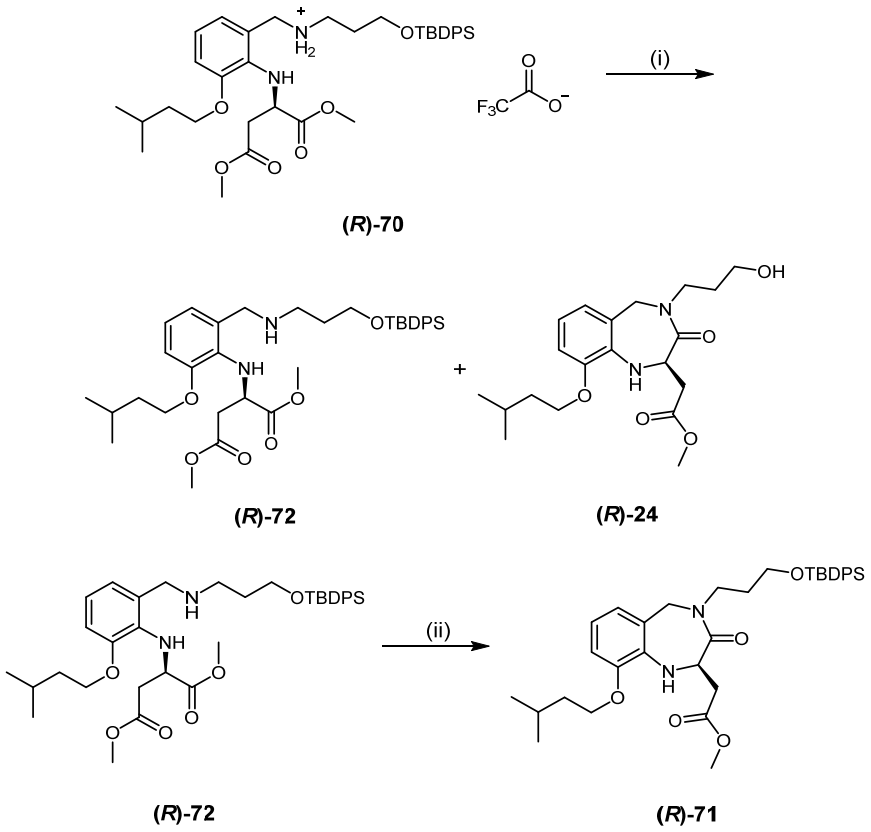


**Scheme 3.8.7**: Synthesis of Protected and Deprotected Tetrahydrobenzodiazepinones **(*R*)-24** and **(*R*)-71**. *Reagents and Conditions*: (i) NaOMe (1.0 eq.), MeOH, amine **(*R*)-72** 30%, alcohol **(*R*)-24** 18%; (ii) $NH_3$/MeOH, quantitative.

As summarised in **Table 3.8.1** after optimisation of the reaction conditions, it became possible to access the protected tetrahydrobenzodiazepinone **(*R*)-71**. Thus, it became possible to generate the desired benzodiazepinone alcohol **(*R*)-24** in 23% from amine **(*R*)-72** or 12% overall yield from **18**.

**Table 3.8.1**: Summary of Yields, Products and Reaction Conditions for Cyclisations and Deprotections.

| Starting Material | Reaction and Conditions | Yields and Products |
|---|---|---|
| Salt **(*R*)-70** | NaOMe (1.0 eq.), 22 ºC | **(*R*)-72** (30%), **(*R*)-24 (**18%) |
| Salt **(*R*)-70** | NaOMe (2.0 eq.), 70 ºC, | **(*R*)-72** (76%) |
| Salt **(*R*)-70** | NaOMe (5.0 eq.), 70 ºC | Degradation |
| Salt **(*R*)-70** | NaOMe (3.0 eq.), 22 ºC | Degradation |
| Salt **(*R*)-70** | SCX Column, 7 M $NH_3$/MeOH | **(*R*)-71** (48%). |
| Amine **(*R*)-72** | 7 M $NH_3$/MeOH | **(*R*)-71** (quant.) |

The protected tetrahydrobenzodiazepinone **(*R*)-71** was then taken on and deprotected using TBAF (**Scheme 3.8.8**). The reason for the low yield is not apparent, however, a number of low yields using TBAF were reported throughout the Marquez group at this time, thus, it is possible that the yield could be improved upon optimisation.

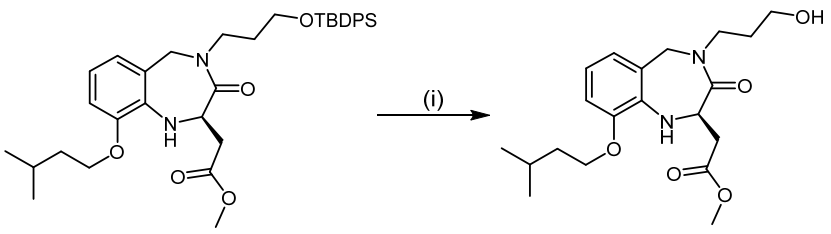


**(*R*)-71** **(*R*)-24**

**Scheme 3.8.8:** Deprotection of Benzodiazepinone **(*R*)-71**. *Reagents and Conditions*: (i) TBAF, THF (30%).

3.8.3 Formation of the Benzodiazpinone Core: Pentyl Analogues

Having successfully synthesised alcohol **(*R*)-24**, the ammonia/methanol and strong cation exchange conditions were applied to the synthesis of the five carbon chiral intermediate **(*R*)-26** (**Scheme 3.8.9**). Thus, trifluoroacetic acid deprotection, followed by purification with a SCX column and subsequent flash column chromatography provided us with benzodiazepinone **(*R*)-26** as the free alcohol (46%), with a small amount of uncyclised, deprotected amine **(*R*)-73** 9%.

Upon further optimisation of the deprotection cyclisation process, the ammonia methanol eluent from the SCX column was allowed to stand for an increased time (2 hours) before being concentrated *in vacuo*. This minor, yet important modification increased the yield of alcohol **(*R*)-26** to 56% with no side products being obtained.

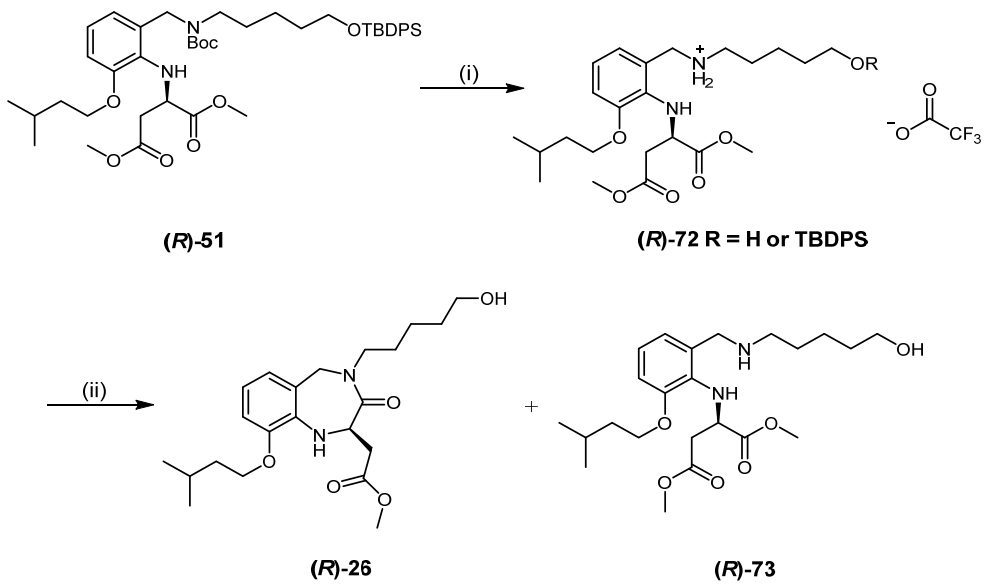


**Scheme 3.8.9**: Cyclisation and Deprotection. *Reagents and Conditions*: (i) trifluoroacetic acid, DCM; (ii) SCX, 7 M $NH_3$/MeOH, **(*R*)-26** (46%), **(*R*)-73** (9%).

It was clear that the use of trifluoroacetic acid for the carbamate deprotection was not an intuitive deprotection strategy when working with TBDPS protected compounds. In an attempt to improve yields, and avoid unwanted deprotections, the carbamate deprotection was carried out with 5% hydrochloric acid in ethyl acetate, and the resultant mixture was dissolved in ammonia methanol solution. This method yielded alcohol **(*R*)-26** (39%) and of acetate **(*R*)-74** (50%), suggesting that the labile nature of the TBDPS group under acidic conditions is responsible for the low yields rather than fluoride ions in the TFA (**Scheme 3.8.10**).

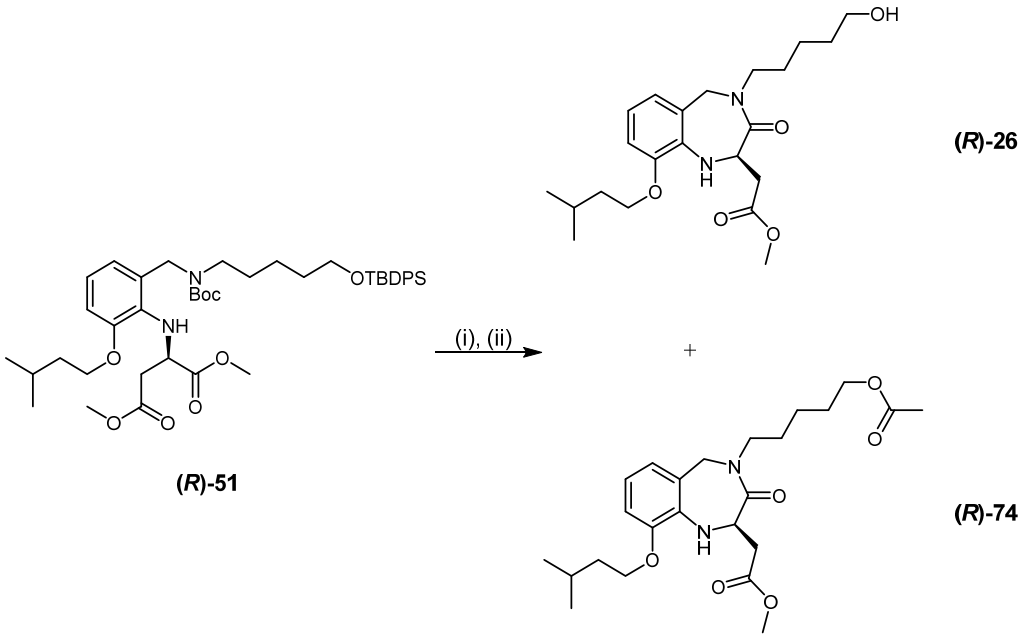


**Scheme 3.8.10**: Deprotection and Cyclisation of **(*R*)-51** Using Hydrochloric Acid. *Reagents and Conditions*: (i) 5% HCl in EtOAc; (ii) 7 M $NH_3$ in MeOH, **(*R*)-26** (39%), **(*R*)-74** (50%).

Since it was evident that a stepwise strategy would not be possible, it was decided to focus on a telescopic approach that would combine as many steps as possible. It was found that increasing the reaction time of the trifluoroacetic acid deprotection from 18 to 32 hours before purification with SCX silica and 2 hours in 7 M ammonia methanol solution yielded the desired alcohol **(*R*)-26** in 95% without the need for subsequent column chromatography (**Scheme 3.8.11**). This improved methodology allowed access to alcohol **(*R*)-26** in 61% yield from nitrobenzaldehyde **18**.

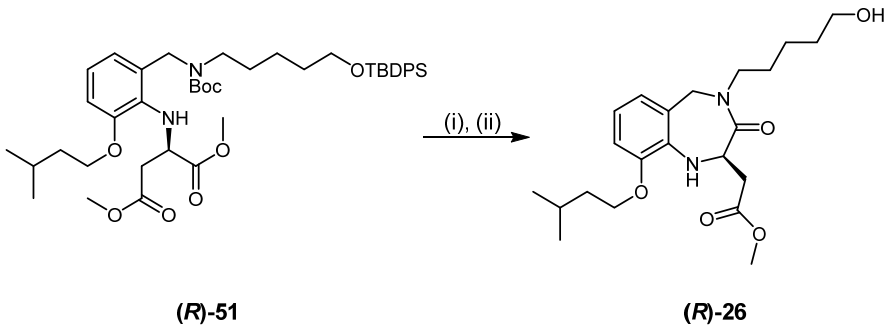


**Scheme 3.8.11**: Deprotection and Cyclisation of **(*R*)-51** Using Trifluoroacetic Acid. *Reagents and Conditions*: (i) TFA in $CH_2Cl_2$; (ii) SCX silica, 7 M $NH_3$ in MeOH (95%).

This improved and optimized synthetic route was then applied to the synthesis of the (*S*)-IGD peptidomimetic (**(*S*)-26**) (**Scheme 3.8.12**) giving the desired alcohol in 77% yield from aniline (**53**).

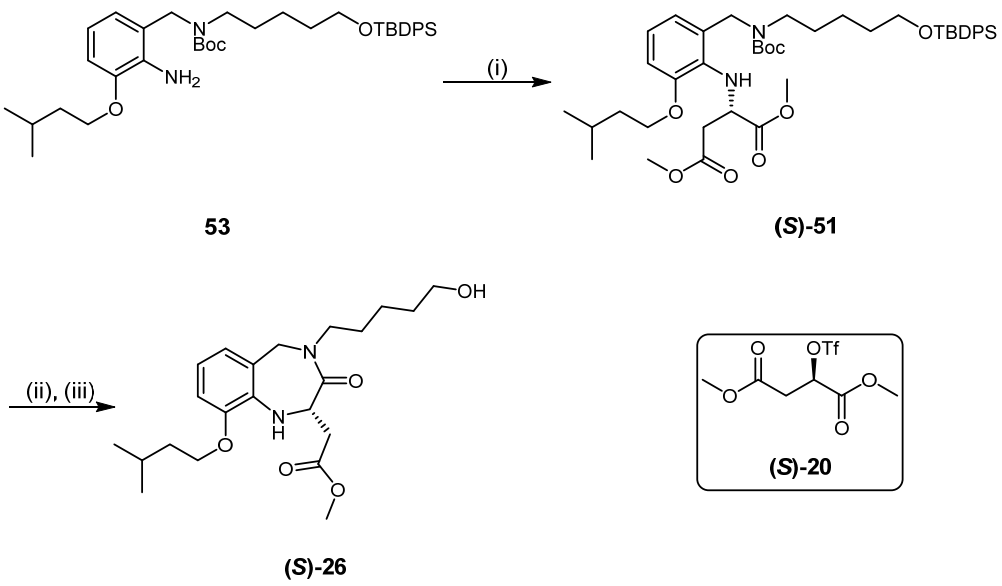


53 (*S*)-51 (*S*)-26

**Scheme 3.8.12:** Synthesis of (*S*)-IGD Peptidomimetic **(*S*)-26**. *Reagents and Conditions*: (i) **(*S*)-20**, 2,6-lutidine, $CH_2Cl_2$; (ii) TFA, $CH_2Cl_2$ ; (iii) SCX, 7 M $NH_3$/MeOH (77%).

The newly developed conditions for benzodiazepinone cyclisations were then also applied to the synthesis of methyl IGD peptidomimetic **(*R*)-2**. Deprotection of **(*R*)-14** proceeded with trifluoroacetic acid, and strong cation exchange conditions were employed to promote cyclisation giving the desired methyl IGD peptidomimetic (**(*R*)-2**) in 90% over the two steps, a slight improvement of the 85% yield previously seen upon deprotection and subsequent cyclisation with sodium methoxide (**Scheme 3.8.13**).

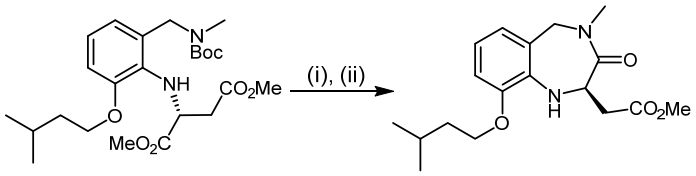


(*R*)-14 (*R*)-2

**Scheme 3.8.13:** Synthesis of (*R*)-Methyl IGD Peptidomimetic (**(*R*)-2**). *Reagents and Conditions*: (i) TFA, $CH_2Cl_2$; (ii) SCX, 7 M $NH_3$/MeOH (90%).

These synthetic conditions were applied to the synthesis of the (*S*)-methyl-enantiomer (**(*S*)-2**). *N*-Alkylation proceeded in good yield (86%) and deprotection and cyclisation occurred in yields analogous to the (*R*)-methyl IGD peptidomimetic (88%) (**Scheme 3.8.14**).

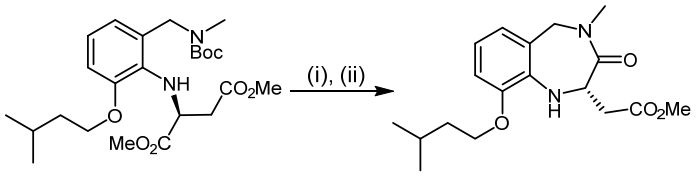


**(*S*)-14** **(*S*)-2**

**Scheme 3.8.14**: Synthesis of (*S*)-Methyl IGD Peptidomimetic (**(*S*)-2**). *Reagents and Conditions*: (i) TFA, $CH_2Cl_2$; (ii) SCX, 7 M $NH_3$/MeOH (88%).

## 3.9 Diverging from IGD Peptidomimetic Alcohols 24 and 26

Having successfully formed benzodiazepinone cores with both the 3 and 5 carbon chain handles, our efforts were focused on diverging from the primary alcohols **24** and **26**. Manipulation of the hydroxyl groups and the generation of other functional groups would allow us to tag our IGD peptidomimetic core with technologies which would be used to gain information about their mode of action or used for drug delivery.

### 3.9.1 Diverging from Propyl IGD Peptidomimetic Alcohol **24**

Thus, small amount of alcohol **(*R*)-24** gained through our synthetic approach was subjected to tosylation conditions. Tosylation of **(*R*)-24** (**Scheme 3.9.1**) gave poor conversion with only a small amount of impure tosylate **(*R*)-46** being isolated.

The lower yields in the synthesis of alcohol **(*R*)-24** compared to the longer chain analogue (**(*R*)-26**) and the difficulty in modifying the alcohol group encouraged efforts to be directed towards the synthesis of the five carbon chain analogues and thus, no further experimentation took place with the three carbon chain analogues.

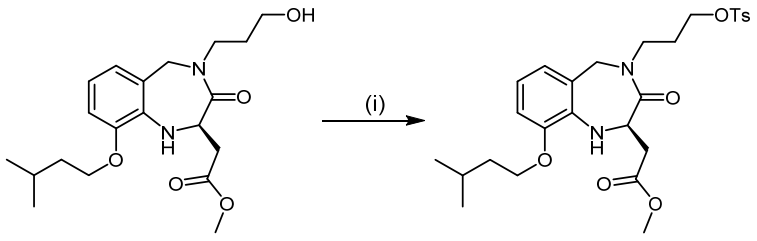


**(*R*)-24** **(*R*)-46**

**Scheme 3.9.1**: Attempted Tosylation of Alcohol **(*R*)-24**. *Reagents and Conditions*: (i) TsCl, $NEt_3$, $CH_2Cl_2$.

### 3.9.2 Diverging from Pentyl IGD Peptidomimetic Alcohol **26**

In contrast to the 3 carbon chain analogue, reaction of the 5 carbon chain analogue proved to be extremely reliable with tosylation of alcohol **(*R*)-26** proceeding to give tosylate **(*R*)-47** in excellent yield (quant.) (**Scheme 3.9.2**). Tosylate **(*R*)-47** was then reacted with sodium azide to give the desired azide **(*R*)-45** (78%). The corresponding amine (**(*R*)-40**) was then synthesised through hydrogenation using 10% palladium on activated charcoal and hydrogen gas in methanol (78%).

This efficient approach to the 5-carbon chain analogues allowed access to tosyl, azide and amine derived IGD peptidomimetics from commercially available 3-methoxy-2-

nitrobenzaldehyde (**18**) in reliable yields of 47, 47, 37% respectively over 10, 11 or 12 steps.

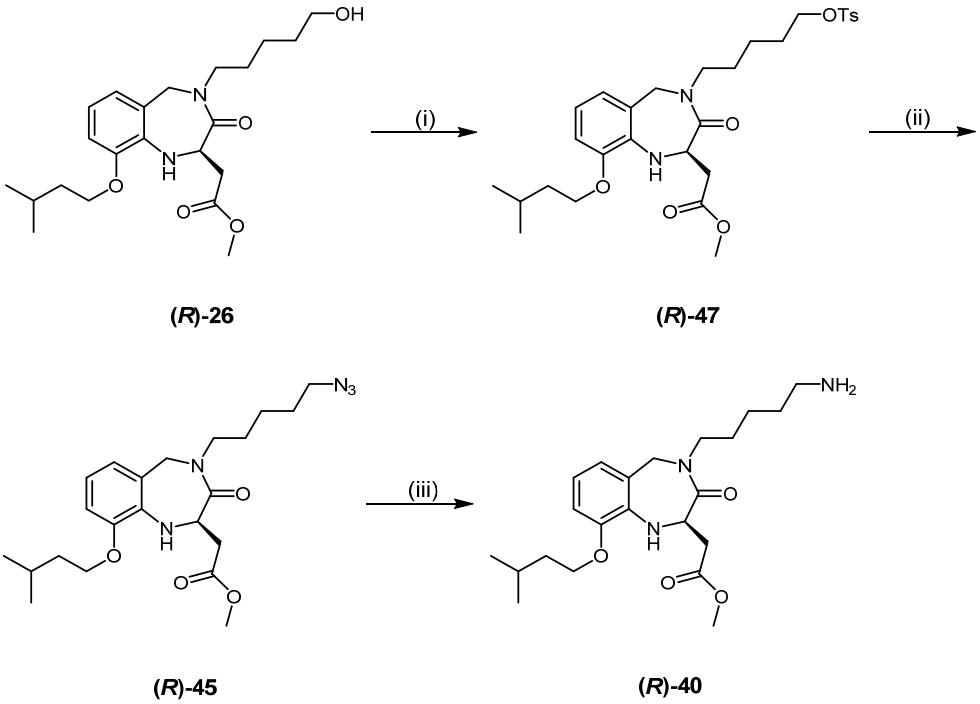


**Scheme 3.9.2**: Synthesis of Amine **(*R*)-40** from Alcohol **(*R*)-26**. *Reagents and Conditions*: (i) TsCl, $NEt_3$, $CH_2Cl_2$ (quant.); (ii) $NaN_3$, DMF (78%); (iii) $H_2$, Pd/C, MeOH (78%).

By comparison tosylation of (*S*)-alcohol (**(*S*)-26**) was achieved in good yield albeit lower than the (*R*)-counterpart (72%). Tosyl group displacement with sodium azide yielded the desired azido-derivative **(*S*)-45** in excellent yield (87%). Hydrogenation of azide **(*S*)-45** afforded the desired amine (**(*S*)-40**) in good yield (70%) giving (*S*)-IGD peptidomimetic amine **(*S*)-40** in 23% yield over twelve steps from commercially available materials (**Scheme 3.9.3**).

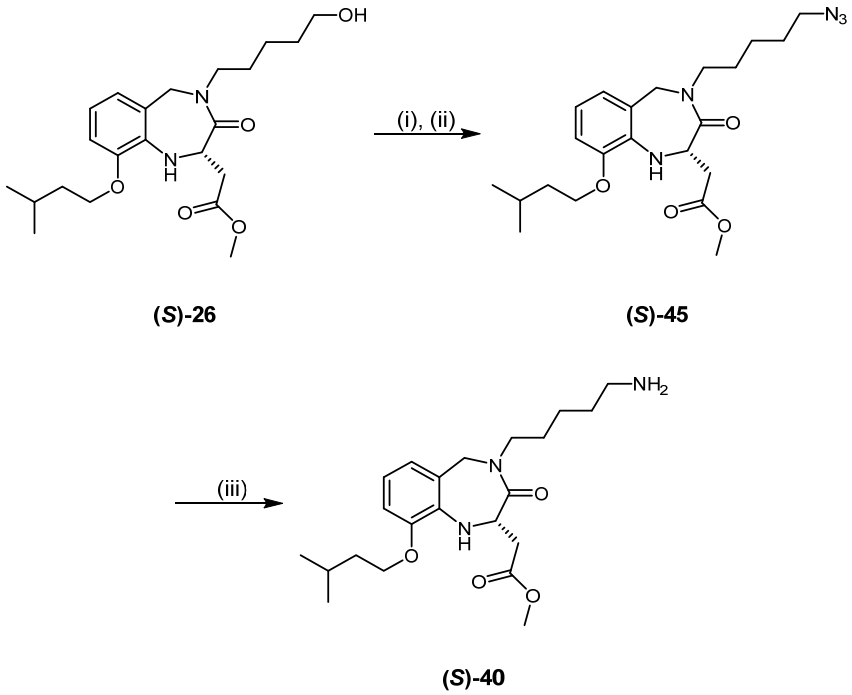


**Scheme 3.9.3**: Synthesis of (*S*)-IGD Mimetic (**(*S*)-40**). *Reagents and Conditions*: (i) TsCl, $NEt_3$, $CH_2Cl_2$ (72%); (ii) $NaN_3$, DMF (87%); (iii) $H_2$, Pd/C, MeOH (70%).

With access to tosyl (**(*S*)-47**), azido (**(*S*)-45**) and amine (**(*S*)-40**) analogues established, efforts were directed towards the synthesis of the carboxylate units. Thus, attempts were made towards achieving the oxidation of alcohol **(*S*)-26**.

Initial efforts towards the transformation of the alcohol **(*R*)-26** to acid **(*R*)-38** employed tetrapropylammonium perruthenate (TPAP) and *N*-methylmorpholine oxide. However, this was unsuccessful, with crude NMR analysis showing no trace of the desired aldehyde (**Scheme 3.9.4**).[59] It was observed that the TPAP used was dark in colour and thus, may not have been of sufficient quality to promote reaction. Time constraints allowed no further attempts towards the synthesis of **(*R*)-38**, however, it is possible that repetition of this experiment with fresh TPAP could have been successful.

Alcohol **(*R*)-26** was then subjected to Swern conditions, with the crude NMR analysis suggesting that a small amount of oxidation to the desired aldehyde may have occurred, however, significant degradation and multiple IGD peptidomimetic compounds were also detected.[60] TEMPO and BAIB were used in the hope of a more clean transformation, however, once again proton NMR analysis suggested that small amounts of **(*R*)-49** may have formed but were minimal compared to starting material and other undesired side products.[61]

It was thought that perhaps the lack of reaction observed may be a result of incompatible functionality between the secondary amine and the oxidants. Iwabuchi has recently discussed the "non-productive interaction" between the oxoammonium species present in nitroxyl radical catalysts and amine containing substrates (**Figure** 3.9.1).[62]

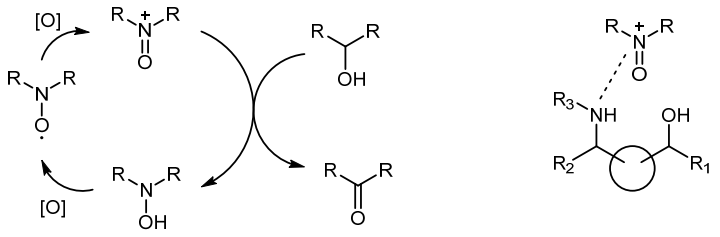


**Figure 3.9.1**: Oxoammonium Catalysis and Nonproductive Interaction between Oxoammonium and Amine.

Iwabuchi however, reports the use of AZADO and copper (I) to selectively oxidise alcohols in the presence of primary, secondary and tertiary amines (**Figure 3.9.2**). Iwabuchi suggests that the copper catalyst coordinates to the oxygen forming a copper alkoxide preferentially to a copper amide, and thus, effective oxidation can occur.

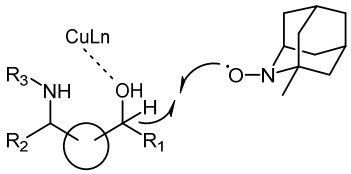


**Figure 3.9.2:** Coordination of Copper to Amino Alcohol Allowing Oxidation in the Presence of an Amine.

Unfortunately, upon treatment of primary alcohol **(*R*)-26** with AZADO, copper chloride and a seventy two hour reaction time, crude $^{1}$H NMR showed no desired aldehyde signal. It is possible that persistence and a comprehensive screen of conditions may allow access to either the aldehyde or the carboxylic acid in the future, but to date no oxidation product could be isolated.

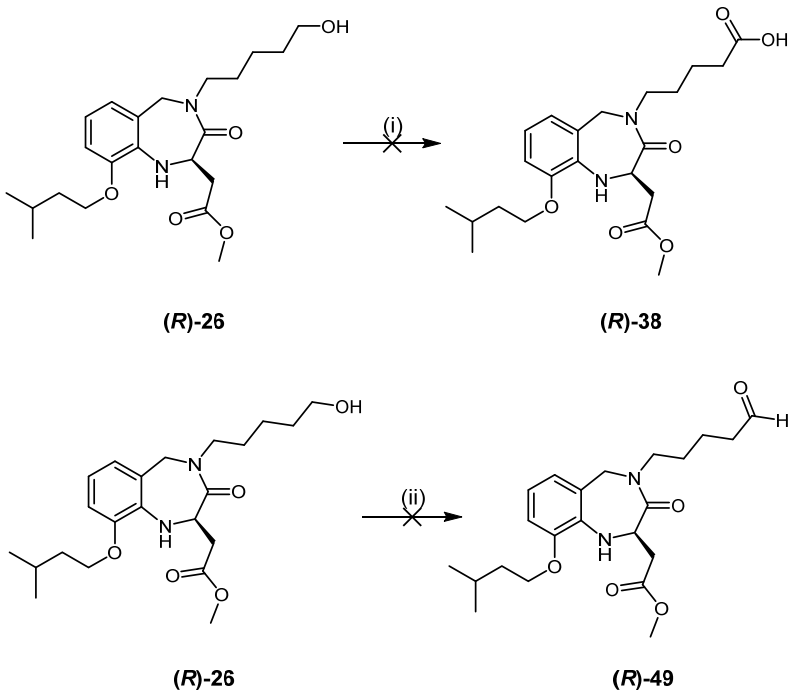


**Scheme 3.9.4**: Proposed Route to Aldehyde **(*R*)-49** and Acid **(*R*)-38**. *Reagents and conditions:* (i) TPAP, NMO, MeCN, $H_2O$ (failed). (i) DMSO, $SOCl_2$, $(OCCl)_2$, DCM, (failed); TEMPO, BAIB, DCM (failed); AZADO, CuCl, DMAP, Bipyridine, MeCN (failed).

The difficulty found in attempting to oxidise alcohol **(*R*)-26** prompted us to consider new approaches for its transformation. Attempts were made at introducing an alkyne functionality through alkylation of alcohol **(*R*)-26** (**Scheme 3.9.5**). Initially alkylation was attempted with propargyl bromide, however, despite the use of extensive experimentation no reaction was observed.[63]

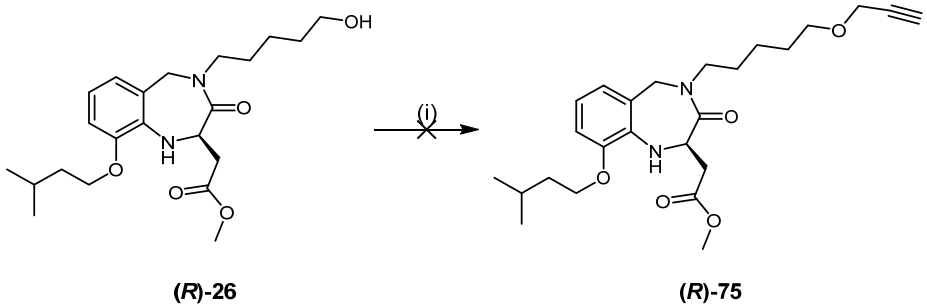


**Scheme 3.9.5**: Attempted Alkylation of Alcohol **(*R*)-26**. *Reagents and conditions:* (i) TBAI, NaI, $BrCH_2CCH$, 2,6- lutidine, THF (failed); TBAI, NaI, $BrCH_2CCH$, KOH, THF, 50 °C (failed); TBAI, NaI, $BrCH_2CCH$, $K_2CO_3$,THF (failed).

Propargyl alcohol was then deprotonated in an attempt to couple with tosylate **(*R*)-47** it through a displacement reaction. Disappointingly, $^1H$ NMR analysis indicated the

presence of the tosyl group in the product, while also showing the absence of the methyl ester (**Scheme 3.9.6**).

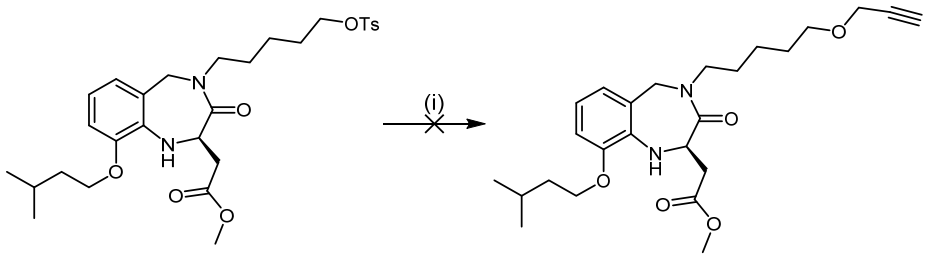


**(*R*)-47** **(*R*)-75**

**Scheme 3.9.6**: Attempted Displacement of Tosyl Group. *Reagents and conditions:* (i) NaH, $HCCCH_2OH$, THF (failed).

This prompted us to consider carrying out the reaction in the presence of the free carboxylic acid, in order to avoid side reactions. Saponification of ester **(*R*)-47** to the corresponding carboxylic acid **(*R*)-76** with potassium trimethylsilane occurred in 50% yield (**Scheme 3.9.7**). Subsequent displacement of the tosyl group of **(*R*)-76** was attempted with propargyl alcohol anion. $^{1}H$ NMR analysis suggested that the tosyl group had been removed, however, no product was isolated despite repeated attempts. Interestingly, characterisation of carboxylic acid **(*R*)-76** by $^{13}C$ NMR demonstrated the compound's poor stability, which could account for the difficulties encountered during the synthesis and isolation of **(*R*)-77**.

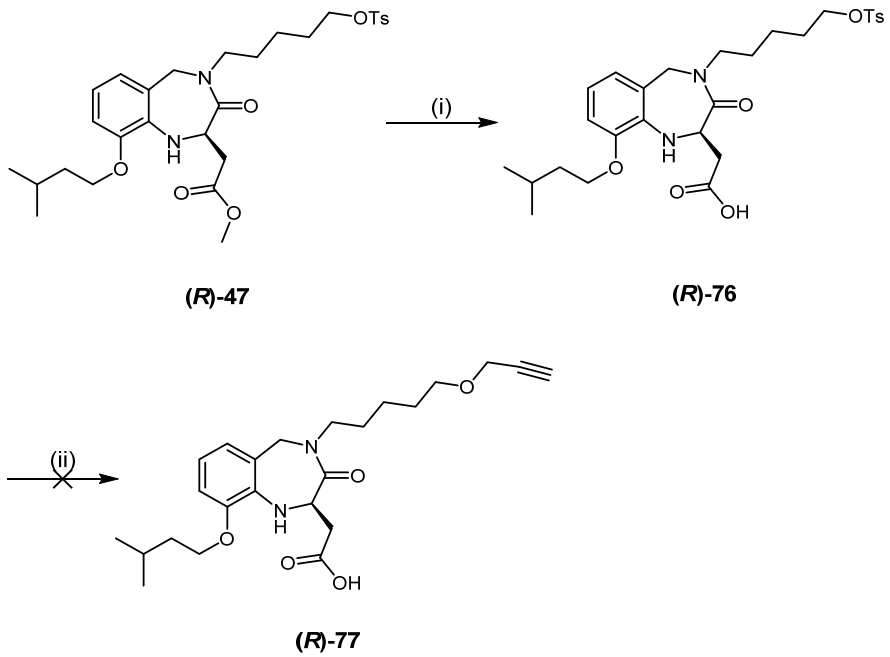


**(*R*)-47** **(*R*)-76**

**(*R*)-77**

**Scheme 3.9.7**: Saponification of **(*R*)-47** and Attempted Displacement. *Reagents and conditions:* (i) $KOSiMe_3$, $Et_2O$, then HCl (aq.) (50%); (ii) NaH, $HCCCH_2OH$, THF (failed).

In conclusion, tosyl, azide and amine-containing IGD peptidomimetics were synthesized efficiently and in good yields. Significantly, this approach allows the possibility of using these analogues in amide couplings and Huisgen cyclisations, opening up many potential coupling partners. At this point our efforts were directed towards applying these analogues alongside various technologies to gain further knowledge of the origin of the biological activity of IGD peptidomimetic, and to investigate potential modes of delivery.

## 3.10 IGD Peptidomimetic Immobilisation

The logical development of a drug with wound healing properties and topical application would be its incorporation into a medical device such as a bandage or other wound dressing. Ligand immobilisation could be a useful method for the future development of the IGD peptidomimetic. Further to this, the potential angiogenic properties of these mimetics may allow scope as part of a biologically active implant.

Furthermore, an immobilised ligand could be used to study binding to various cell types that overexpress (or do not express) particular cell surface receptors. Biological studies of this kind would be particularly interesting with cells that express different integrins.[64]

Foillard reported the immobilisation of a multivalent, RGD containing peptide on to a NovaSyn® TG resin in an effort to evaluate the effects of clustered vs individual RGD peptide ligands on integrin $\alpha_5\beta_3$ binding. [65] NovaSyn® TG carboxy resin is an appropriate choice of solid support as it has many features that would be desirable for any future biological testing. This resin is commercially available as 130 μM beads are comprised of a composite of low cross-linked polystyrene and 3000-4000 molecular weight polyethylene glycol, of which the ends are functionalised with carboxylic acid groups (**Figure 3.10.1**, **A**). The hydrophilic nature of the polyethylene glycol chains allow the immobilised ligand to sit at some distance from the core of the bead in aqueous solution, which is a necessary feature for any cell work. These beads are non toxic and non magnetic, allowing for *in vitro* work and NMR analysis. The loading of the carboxylic acid functionality is described as 0.20-0.30 mmole/g resin (**Figure 3.10.1**, **B**).

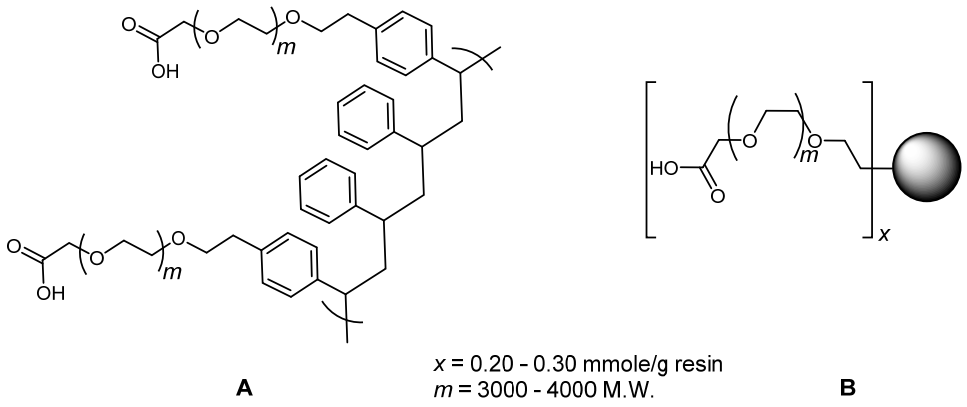


**Figure 3.10.1**: NovaSyn TG carboxy resin. A. Cross-linked hydroxyethylpolystyrene polyethylene glycol. B. Schematic of Bead.

Foillard decorated the beads in three ways (**Figure 3.10.2**), compounds **78** and **79** contained one and four recognition elements.[65] Compound **80** bore a nonsense R*β*AD peptide that served as a control for biological tests.

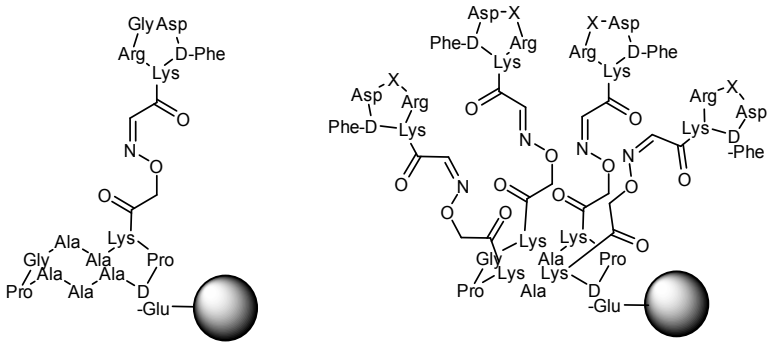

**78**

**79** X = Gly
**80** X = Beta-Ala

**Figure 3.10.2:** Synthesised Immobilised Ligands.

The ability of the cells to bind to the resin through RGD-$\alpha_5\beta_3$ was then assessed using Human Embryonic kidney cells (HEK 293) which express a high level of $\alpha_5\beta_3$ integrins (**Figure 3.10.3**). The cells were incubated with the three resins for thirty minutes at 37 °C. Both resins exhibiting the RGD functionality were found to bind to the cells, **80** did not. At very low densities (2 nmol/$g_{resin}$) only the clustered resin **79** was effective in binding to the cells. The resin beads were also found to be capable of capturing $\alpha_5\beta_3$ – expressing cells from a biological mixture.

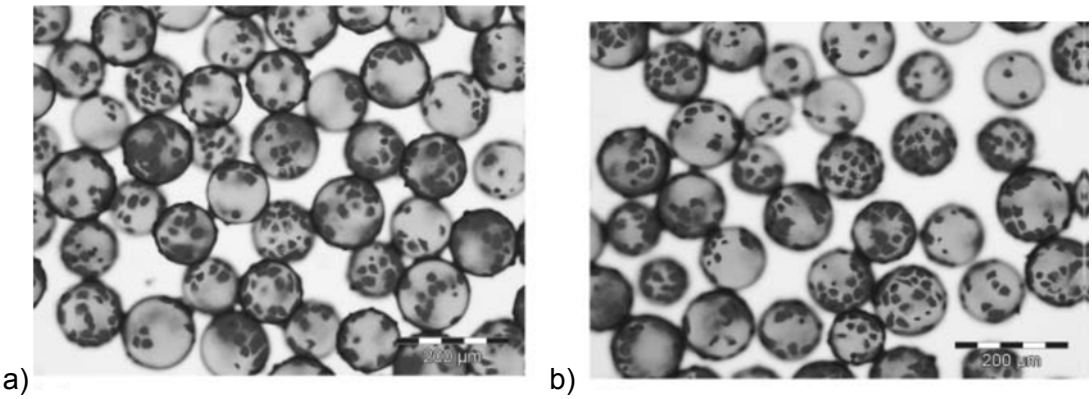


**Figure 3.10.3**: Optical Microscopy Images of Cell Adhesion to Resin Beads. HEK 293 were treated with 0.2 mmol/$g_{resin}$ a) Resin **78** b) Resin **79**, incubated for 30 mins at 37 °C and then fixed and stained with methylene blue.

Work of a similar nature would require the development of facile chemistry that could be carried out on a solid support. The robust synthesis of the amine IGD

peptidomimetic (**40**) provided us with an ideal platform from which to start, with an amide coupling as a natural choice for our preliminary work in this area.

Thus, the coupling of the IGD mimetic **(*R*)-40** and the carboxylic acid bead was attempted with HBTU and DIPEA (**Scheme 3.10.1**). Upon filtration it was observed that the beads were no longer free flowing. Microscopy showed that very few spherical beads remained, the majority having formed amalgams of damaged beads. It was hypothesised that this damage was the result of collisions caused by the internal stirrer bar. The experiment was repeated, this time with a source of external stirring. This approach was successful in allowing the beads to couple to the peptidomimetic and retain their integrity. Dr Michael Hansen (Max Planck Institute) was able to confirm the new amide bond by Magic angle spinning, liquid state, proton NMR (for $^{1}$H NMR spectrum please see **Appendix 6.4**, **p 183-184**).

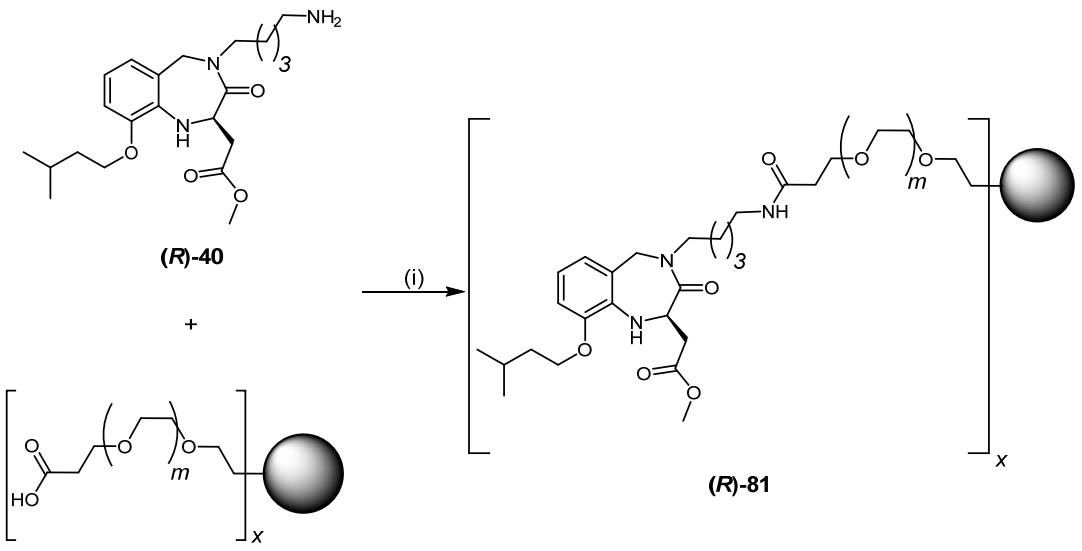


**Scheme 3.10.1:** Attachment of Amine **(*R*)-40** to Bead. *Reagents and Conditions*: (i) HBTU, DIPEA, $CH_2Cl_2$.

The polystyrene nature of these beads results in significant swelling upon treatment with solvent, leaving dichloromethane molecules within the bead.[66] This property was noted by Foillard as the beads were swollen in DCM before reaction, but it was not discussed any further. This particular property must be recognised as an area of concern in biological testing. It is entirely possible that solvent (or other small molecules from synthesis) could leach from the bead into any biological assay and interfere with results obtained.

While this approach remains a useful indication of cell-ligand interactions, but it would be sensible to exercise caution when attempting to quantify any results gained. It would also be important to ensure that all beads had been exposed to the same chemicals when comparing two or more functionalised beads. If we take the example of DMSO as a solvent or reagent, small amounts leaching from beads to cells could have a large impact on the health of treated cells.

Please see **p 81** for further discussion of this work.

## 3.11 Synthesis of BODIPY IGD Peptidomimetic *via* an Amide Coupling

### 3.11.1 BODIPY FL

Fluorescent molecules are extremely useful for the investigation of ligands and receptors. Their inherent properties are useful in showing the location of receptors present in low concentrations, as well as the reversibility of ligand binding, and binding affinity.[67]

The BODIPY family are a range of fluorophores that span the visible spectrum. Their versatility and desirable spectral characteristics affords their increasing use in the literature. The BODIPYs have a common 4,4-difluoro-4-bora-3a,4a-diaza-*s*-indacene chromophore (**82**, **Figure 3.11.1**), the electrical neutrality of this core allows increased cell permeability compared to charged fluorophores.[68]

BODIPY FL (**83**) is considered to be a replacement for fluorescein (**84**) due to its enhanced properties including, a red shift in fluorescence emission at high concentrations. This is particularly useful for example in *in vitro* studies, allowing easy detection of areas of high concentration of BODIPY FL-ligand conjugate within cells. Further to this, BODIPY FL has an increased photostability compared to fluorescein.[68]

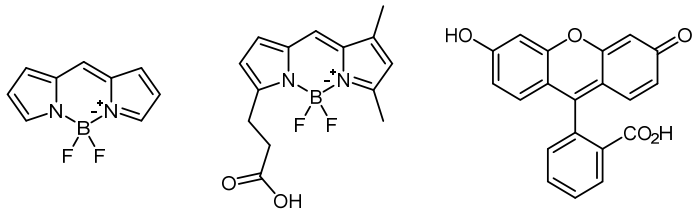


**82** **83** **84**

**Figure 3.11.1:** BODIPY Core **82**, BODIPY FL (**83**) and Fluorescein (**84**).

### 3.11.2 Synthesis of a BODIPY Tagged IGD Peptidomimetic

A fluorescent peptidomimetic analogue was designed with the intention to determine the peptidomimetic's cellular localisation, as it was hoped that this would give an insight into the mechanism of action. Retrosynthetically, the fluorescent IGD peptidomimetic (**Scheme 3.11.1**) was envisioned as originating from the IGD amine **(*R*)-40** and BODIPY FL (**83**) which is well known for its favourable properties in biological testing.

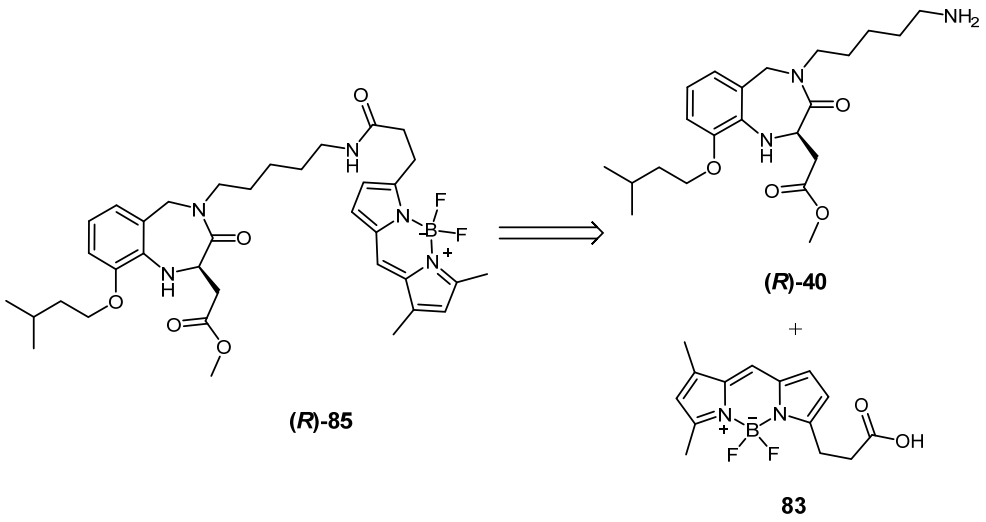


**Scheme 3.11.1**: Target Fluorescent IGD Peptidomimetic **(*R*)-85**.

The synthesis of BODIPY FL (**83**) was carried out following the route developed by Malan.[69] Thus, pyrrole-2-carboxaldehyde (**86**) was reacted with methyl (triphenylphosphoranylidene)acetate in a Wittig reaction to give the desired conjugated ester alkene **87** in moderate yield (49%), as a single geometric isomer. Hydrogenation of ester **87** proceeded in quantitative yield to afford the desired ester **88**. The coupling partner 3,5-dimethyl-pyrrole-2-carbaldehyde (**90**) was synthesised from 3,5-dimethyl-pyrrole (**89**), in excellent yield (83%) through Vilsmeier–Haack conditions.

Coupling of ester **88** with aldehyde **90** in the presence of phosphorous oxychloride gave a crude intermediate which upon treatment with boron trifluoride diethyl etherate and Hünig's base gave the BODIPY derivative **91** in 44% yield. Subsequent hydrolysis of ester **91** with hydrochloric acid gave the BODIPY FL free acid (**83**) in 50% yield (**Scheme 3.11.2**). The optimisation of this hydrolysis, was attempted by the Marquez group and other academic groups, however, yields remain moderate.[70]

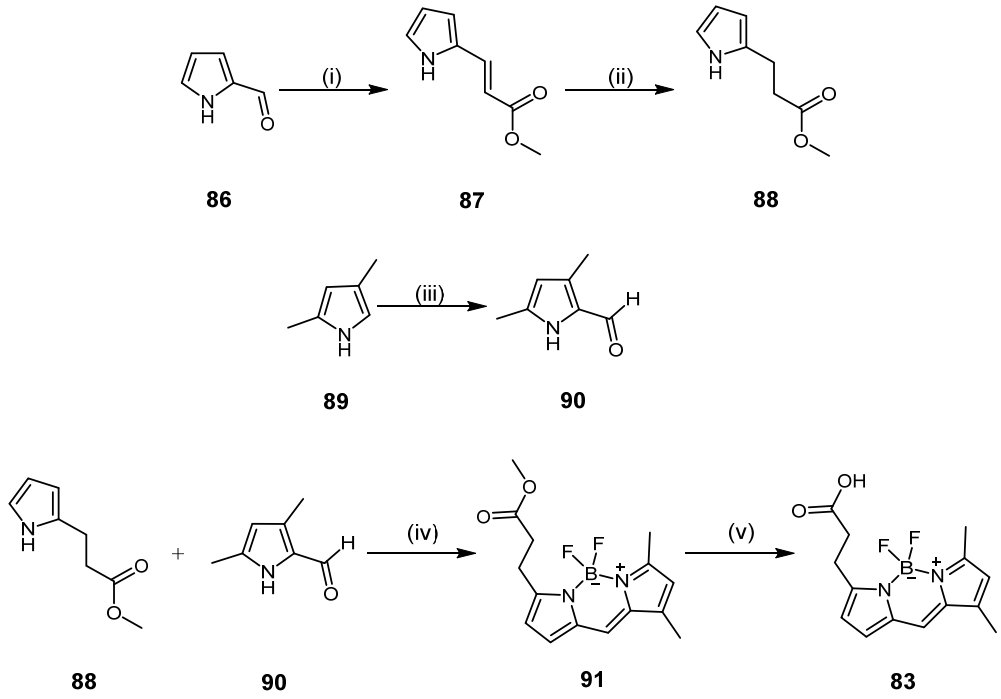


**Scheme 3.11.2:** Synthesis of BODIPY FL (**83**). *Reagents and Conditions*: (i) $Ph_3PCHCO_2Me$, $CH_2Cl_2$ (49%); (ii) Pd/C, MeOH, $H_2$, 40 °C (quant.); (iii) $POCl_3$, DMF (83%); (iv) $POCl_3$, $CH_2Cl_2$ then $BF_3{\cdot}OEt_2$ , DIPEA (44%); (v) THF, $H_2O$, HCl (50%).

With BODIPY FL (**83**) in hand, it was now possible to attempt the coupling to the IGD mimetic **(*R*)-40** (**Scheme 3.11.3**). Thus, coupling of acid **83** and amine **(*R*)-40** with HBTU and *N*,*N*-diisopropylethyldiamine yielded a one to one mixture (dark red) of the desired adduct **(*R*)-85** with the urea byproduct. Extensive, repeated purification by flash column chromatography yielded a clean sample of the key IGD-peptidomimetic BODIPY derivative **(*R*)-85**.

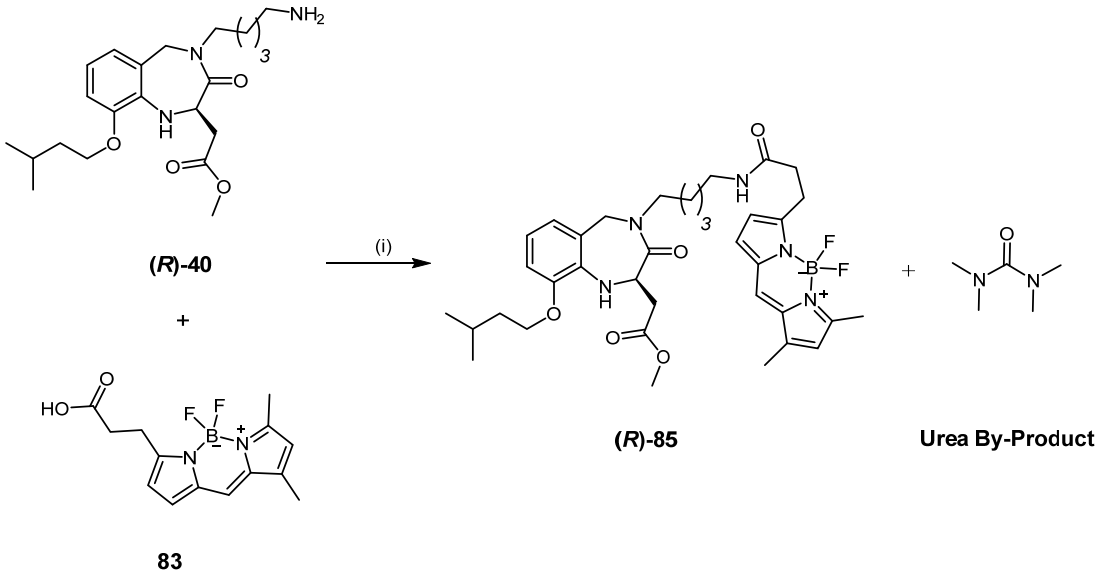


**Scheme 3.11.3**: Synthesis of Benzodiazepine **(*R*)-85**. *Reagents and Conditions*: (i) HBTU, DIPEA, $CH_2Cl_2$ (37%).

With the fluorescent IGD BODIPY derivative in hand visualisation studies were attempted using mouse embryoic fibroblasts (MEF) in collaboration with Dr Niall Fraser (MVLS, University of Glasgow).

Mouse embryonic fibroblasts were cultured in DMEM (Gibco) with 10% FBS, penicillin/streptomycin and L-glutamine (2mM) in a 5% $CO_2$ atmosphere at 37 $^oC$. Cells were seeded onto cover slips in 6 well plates (Corning) and incubated in serum free DMEM before treatment with 4 nM serum free media solution of BODIPY IGD peptidomimetic **(*R*)-85**. Pictures were taken with a Zeiss Axio Imager M1 fluorescence microscope at × 400 magnification (**Figure 3.11.2**).

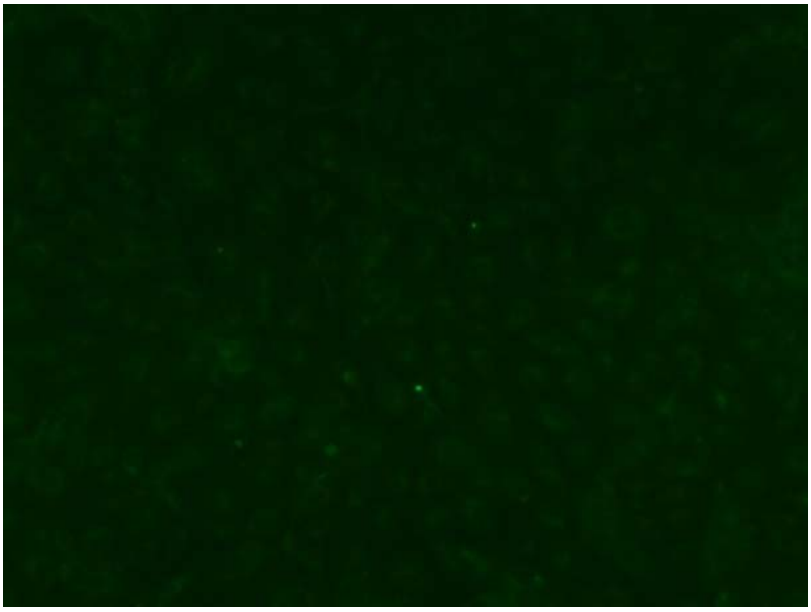

**Figure 3.11.2:** Poor Contrast in Mouse Embryonic Fibroblasts Treated with BODIPY IGD Peptidomimetic **(*R*)-85**.

Upon inspection of the confocal images, two main observations were made: firstly, the fluorophore had been internalised by the cells and secondly, that the contrast between the cells and the media was poor. Internalisation of the probe was not expected but not concerning, however, the internalisation coupled with the high concentrations of fluorophore remaining in the media suggested that hydrolysis of the amide functionality was taking place (**Scheme 3.11.4**). Previous work within the Marquez group has noted the indiscriminate distribution of free BODIPY tags in media and cellular environments.

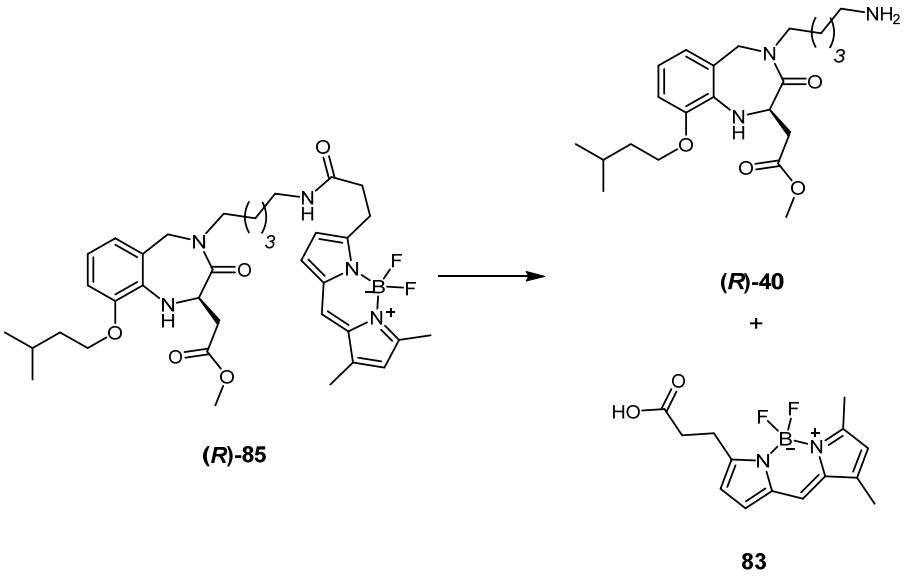


**Scheme 3.11.4:** Potential Hydrolysis of Fluorescent IGD peptidomimetic **(*R*)-85**.

The observed potential hydrolysis of the amide link under physiological conditions may also have serious implications for the immobilised IGD peptidomimetic ligand. Thus, it was reasoned that in order to rule out this possibility, a more biologically stable analogue must be generated before any further biological experiments take place.

## 3.12 Synthesis of BODIPY IGD Peptidomimetic *via* Meso Substitution

### 3.12.1 8-(Methyl-thio)-BODIPY

Thioether containing BODIPY **92** cores allow for the direct addition of alcohols and amines to the BODIPY unit under copper catalysed mild conditions, through an "$S_NAr$-like" reaction as reported by Cabrera (**Scheme 3.12.1**).[71] Mechanistically, the soft copper ion of copper(I)-thiophene-2-carboxylate coordinates to the sulfur, and weakens the C-S bond facilitating the attack of the alcohol. It was postulated by the authors that the strong (45-55 kcal/mol) S-CuTC bond is the driving force for this reaction.

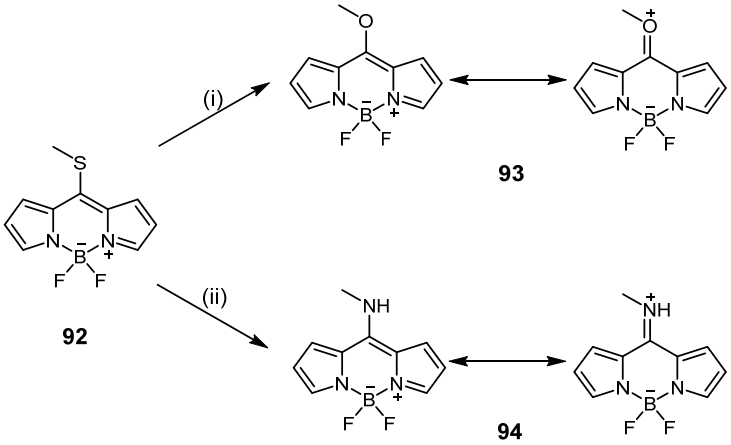


**Scheme 3.12.1**: Synthesis of Hemicyanine and Merocyanine. *Reported Reagents and Conditions*: (i) CuTc, $Na_2CO_3$, MeOH, MeCN, 55 °C (73%) (ii) CuTc, $Na_2CO_3$, $MeNH_2$, MeCN, 55 °C.

It was thought that a thioester substituted BODIPY **92** could be treated with either an IGD peptidomimetic amine or alcohol to give a suitable fluorescent analogue. Significantly, it was expected that an amine or ether linkage would prove to be more stable to hydrolysis than the previously developed amide **(*R*)-85** (**Scheme 3.12.2**).

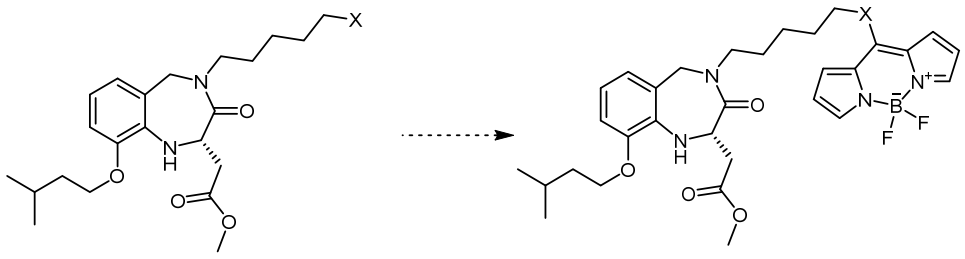


**Scheme 3.12.2**: Substitution Route to IGD Peptidomimetic Fluorophore.

The synthesis of thiomethyl BODIPY **92** proceeded as outlined by Biellmann starting from pyrrole (**Scheme 3.12.3**).[72] Coupling of pyrrole with thiophosgene afforded thioketone **97** in low yield (43%). Subsequent reaction of thioketone **97** with methyl iodide gave the interemediate salt which was treated with diisopropylethyl amine and boron trifluoride to give the desired thiomethyl BODIPY **92** in 6% yield.

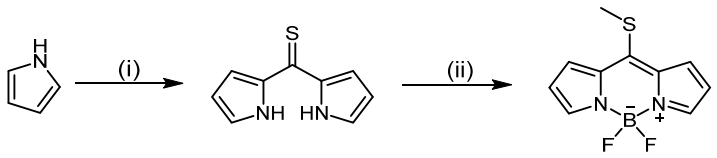


**96** **97** **92**

**Scheme 3.12.3**: Synthesis of BODIPY **92**. *Reagents and Conditions*: (i) PhMe, $SCCl_2$, $Et_2O$, 10% MeOH (aq.) (43%); (ii) DCM, MeI, then $Et_3N$, $BF_3.Et_2O$ (6%).

Unfortunately, treatment of **92** with copper thiophene-2-carboxylate, sodium carbonate and alcohol **(*S*)-26** showed little progress thermally at 55 °C. Microwave heating to 150 °C did show consumption of BODIPY **92**, however no fluorescent product could be isolated (**Scheme 3.12.4**).

Amine **(*S*)-40** was then used as the nucleophile in a subsequent reaction in the hope of achieving the desired coupling. Excitingly, mixing amine **(*S*)-40** with BODIPY **92** at room temperature saw spot to spot conversion (40%). Disappointingly, upon purification it was found that **(*S*)-95** was very weakly fluorescent compared to the parent BODIPY (**92**) and would not be suitable for biological testing. Although the poor fluorescence of compound **(*S*)-95** is disappointing, this result is not entirely unexpected, with examples of *meso* substituted BODIPYs with altered fluorescence being known in the literature. [55][71]

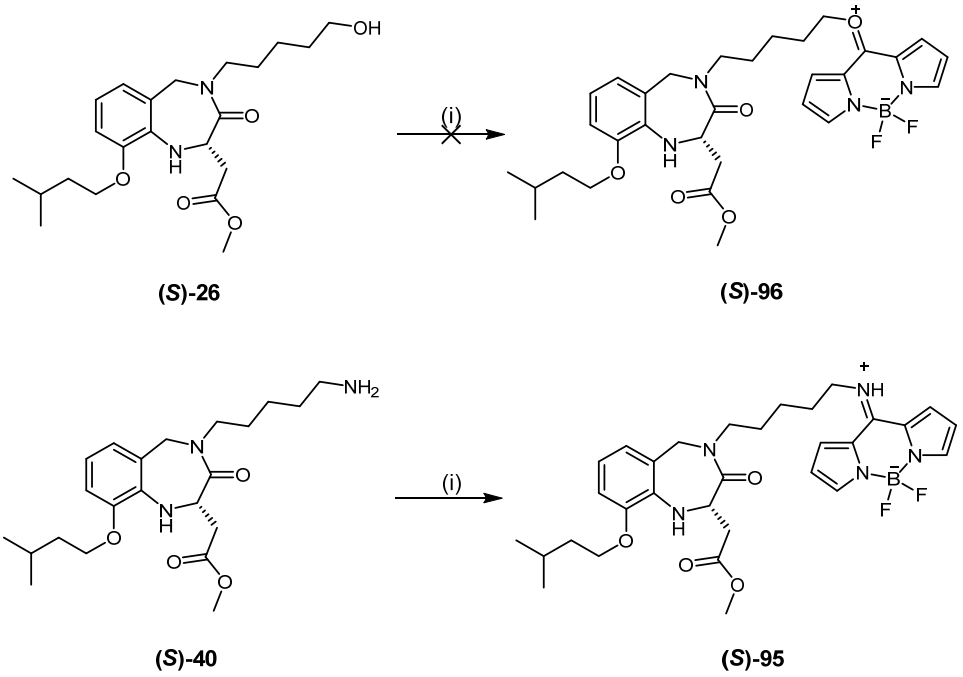


**Scheme 3.12.4**: Displacement of Methylthio Group. *Reagents and Conditions*: (i) BODIPY **92**, CuTC, $NaCO_3$, MeCN (40%).

The electron donating properties of an amine substituent will increase the LUMO energy of the system without affecting the HOMO. This increase is manifested as a larger Stokes shift. As expected, amine substituents display a more pronounced effect than their oxygen counterparts. In this case, we parallel this trend, we see a hypsochromic shift induced by *meso* position heteroatoms again with the amine compound being affected more than their oxygen counterparts. It is possible that this is the cause of our poor fluorescence. Another theory is that intramolecular charge-transfer (ICT) can be problematic for BODIPY groups conjugated with secondary or tertiary amines in polar solvents. With these points in mind it seemed likely that successful synthesis of a fluorescent IGD compatible with biological testing in aqueous solutions would have to follow a different pathway.

## 3.13 Synthesis of BODIPY IGD Peptidomimetic *via* Huisgen Cyclisation

### 3.13.1 Alkyne BODIPY

Having completed the synthesis of the azide IGD peptidomimetic (**(R/S)-45**), the coupling of our bioactive core to a BODIPY was envisioned to proceed via a Huisgen cyclisation (**Figure 3.13.1**). The structure of the alkyne BODIPY coupling partner was not defined at this point, but must have no labile bonds between the alkyne and the BODIPY core, and must not have diminished fluorescence.

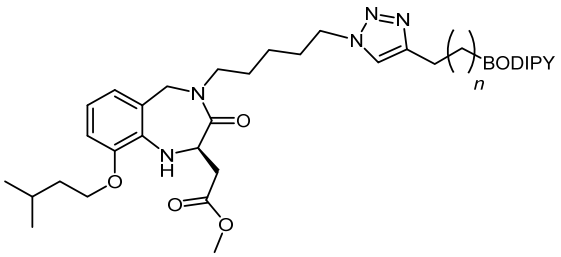


**(*R*)-97**

**Figure 3.13.1**: General structure of desired fluorescent labelled IGD mimetic.

BODIPY alkynes such as **98** made via *meso* substitution could potentially suffer from the reduced fluorescence issues as previously seen. Although there are several BODIPY alkynes known in the literature, many of these would not be suitable as the alkyne functionality is attached to the BODIPY core through a potentially labile bond such as an amide or ester (**99**) (**Figure 3.13.2**). Alkyne BODIPY **100** is a rarer example of a molecule with no labile bonds between the alkyne functionality and the BODIPY core, and consequently alkyne **100** was our chosen cyclisation partner.

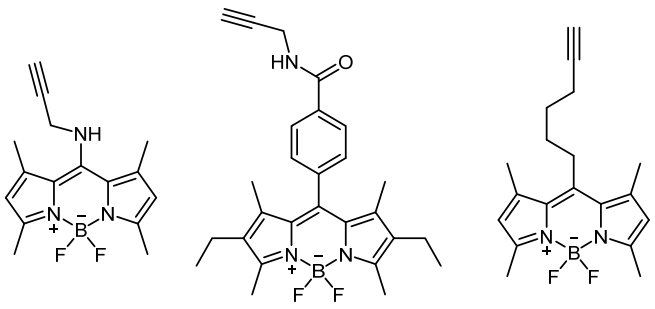


**98** **99** **100**

**Figure 3.13.2:** Examples of Alkyne Containing BODIPYs.

The synthesis of alkyne BODIPY **100** began with 6-heptynoic acid (**101**) in a one pot procedure following Overklefff's procedure.[73] The reaction of 6-heptanoic acid with

oxalyl chloride generated the desired acid chloride **102** (**Scheme 3.13.1**). Subsequent reaction of acid chloride **102** with 2,4-dimethylpyrrole and boron trifluoride generated alkyne BODIPY **100** as an impure red/green oil. Overkleff reports that flash column chromatography (10% acetone in petroleum ethers) and recrystallization (unspecified conditions) should afford alkyne **100**. However, in our hands multiple rounds of flash column chromatography failed to give clean alkyne.

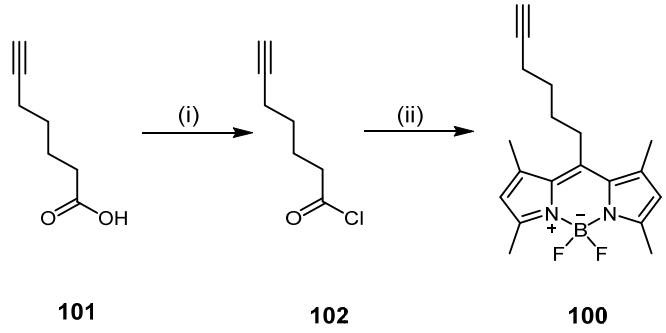


**101** **102** **100**

**Scheme 3.13.1**: Synthesis of Alkyne BODIPY **100**. *Reagents and conditions:* (i) $(OCCl)_2$, DMF, PhMe; (ii) 2,4-dimethyl pyrrole, DCE; (iii) $BF_3 \cdot Et_2O$, DIPEA.

The impure alkyne **100** was taken forwards to the cyclisation with the azido IGD peptidomimetic (**(*R*)-45**) (**Scheme 3.13.2**). $^1$H NMR studies suggest that it is possible that a click product formed (lack of alkyne peak and $CH_2$ alpha to $N_3$ shifted), however, due to low yields and impure alkyne starting material it was not possible to isolate any of the desired product.

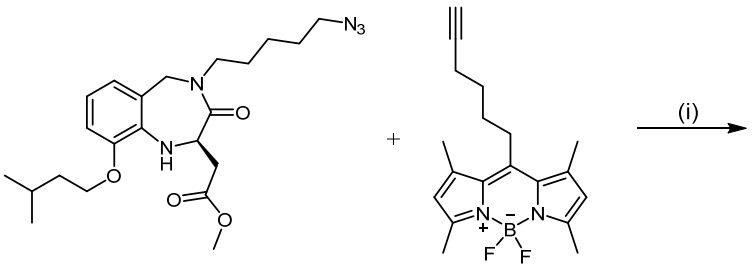

(*R*)-45 100

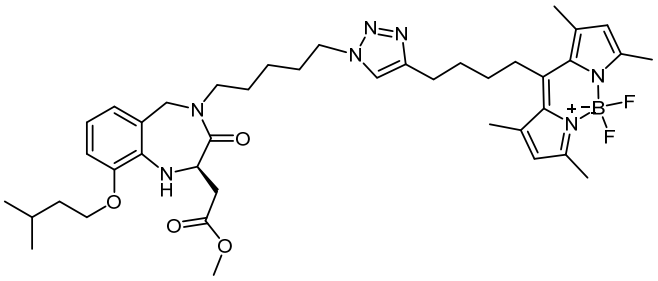

(R)-103

**Scheme 3.13.2**: Huisgen Cyclisation with Impure Alkyne **100**. *Reagents and conditions:* (i) DIPEA, CuI, PhMe.

3.13.2 Substitution Approach to Alkyne Synthesis

The difficulties in accessing an appropriate alkyne containing BODIPY, prompted us to attempt to design and develop a novel alkyne containing BODIPY (**104**) (**Figure 3.13.3**). It was reasoned that the incorporation of the alkyne at the C3 position would provide us with the desired emission wavelength.

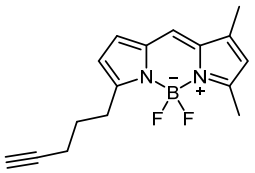

**104**

**Figure 3.13.3**: Desired Alkyne Containing BODIPY **104**.

Our synthesis began with the reduction of pyrrole **88**, with lithium aluminium hydride to give alcohol **105** in excellent yield (83%). Alcohol **105** was then tosylated in good yield (77%) to access novel tosylate **106** (**Scheme 3.13.3**). Treatment of tosylate **106** with lithium acetylide showed spot to spot conversion by TLC, however, no product was isolated. It was hypothesised that the likely high volatility of **107** could be the

cause of this lack of material, and the desired product may have been lost upon rotary evaporation during reaction work up.

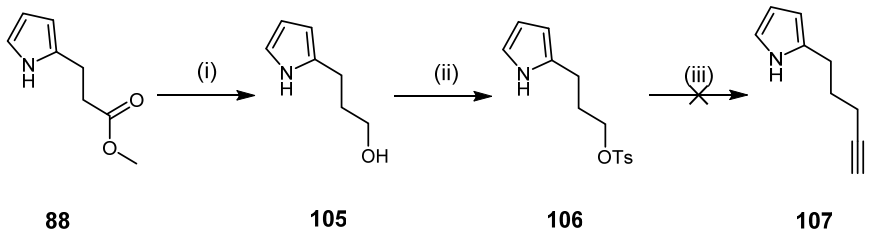


88 105 106 107

**Scheme 3.13.3**: Attempted Synthesis of Alkyne Pyrrole **107**. *Reagents and conditions*: (i) $LiAlH_4$, diethyl ether (83%); (ii) TsCl, $NEt_3$, DCM (77%); (iii) LiCCH, THF (0%).

In order to circumnavigate the potential volatility issue, tosyl pyrrole **106** was treated with pyrrole carbaldehyde **89** under BODIPY forming conditions. Gratifyingly, this generated the desired novel tosyl BODIPY **108** in good yield (67%) (**Scheme 3.13.4**).

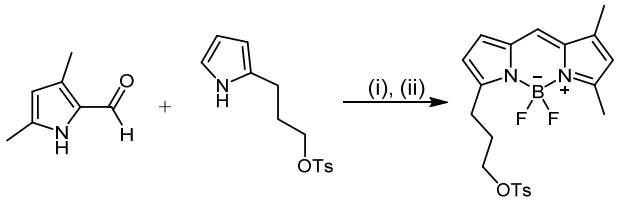


89 106 108

**Scheme 3.13.4**: Synthesis of Tosyl BODIPY **108**. *Reagents and conditions*: (i) $POCl_3$, DCM, then DIPEA, $BF_3{\cdot}Et_2O$ (67%).

Tosyl BODIPY **108** provided us with a shelf stable platform that could be used to provide late stage divergence in BODIPY synthesis (**Scheme 3.13.5**). To test the suitability of the tosylate BODIPY in displacement reactions, it was initially treated with sodium azide and DMF. Excitingly, this reaction was successful in producing the azide in a 50% yield without the need for optimisation.

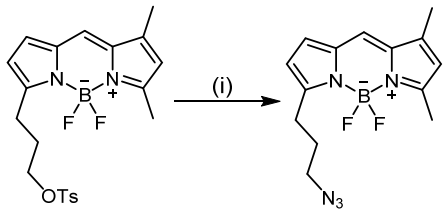


108 109

**Scheme 3.13.5**: Substitution of Tosyl Group. *Reagents and conditions*: (i) $NaN_3$, DMF (50%).

Unfortunately, the displacement of the tosyl functionality with an alkyne unit proved more challenging (**Scheme 3.13.6**). Displacement attempts with lithium acetylide (90% ethylene diamine complex), saw poor conversion of starting material to any new fluorescent spots (**Table 3.13.1**, entries 1-7). A degree of success was achieved by using 5 eq. of lithium acetylide at 40 ºC, which showed a new fluorescent spot, with a higher Rf than the starting material by TLC. This product was isolated by flash column chromatography, and was found to have no signals indicative of a tosyl group, however, the 4 mg of material was not pure enough to allow reliable characterisation. However, all other optimisation attempts failed to yield any of the desired adduct.

Switching to ethylnyl magnesium bromide in an effort to displace the tosyl group (**Table 3.13.1**, entries 8-12) gave very little conversion. Increasing the amounts of nucleophile to 10 and 15 eq. showed conversion of starting material into a new compound by thin layer chromatography. This new spot also had a higher Rf than the starting material, however, IR analysis indicated that this molecule did not contain an alkyne unit. The new spot was analysed by mass spectrometry, and was found to be a monobrominated derivative which was not investigated further.

Sodium hydride was then used to deprotonate trimethyl silyl acetylene to generate a stock solution which was then used to attempt to displace the tosyl group. Again a new high Rf fluorescent spot was seen by TLC, however, this was minimal compared to amounts of starting material in the reaction mixture. A wide range of reaction conditions (-78 °C - 45 °C) were also tested, however, none were found to give good results. Adding more than 2 eq. of the base above 0 °C caused degradation of the starting material.

**Table 3.13.1**: Reaction of Tosyl BODIPY with Alkyne Nucleophiles.

| Nucleophile | Entry | Solvent | Eq. | Condtions | Reaction |
|---|---|---|---|---|---|
| LiCCH (Ethylene diamine Complex) | 1 | MeCN | 2 | 22 ºC 18 h | Poor Conversion |
| | 2 | MeCN | 4 | 22 ºC 18 h | Degradation |
| | 3 | MeCN | 10 | 22 ºC 18 h | Degradation |
| | 4 | DMSO | 2 | 22 ºC 18 h | Degradation |
| | 5 | THF | 2 | 40 ºC 1.5 h | Poor Conversion |
| | 6 | THF | 5 | 40 ºC 3 h | 4 mg "product" isolated |
| | 7 | THF | 10 | 22 ºC 18 h | Poor Conversion |
| HCCMgBr | 8 | Et2O | 1.2 | 40 ºC 2 h | Poor Conversion |
| | 9 | THF | 1.2 | 40 ºC 18 h | Poor Conversion |
| | 10 | THF | 2 | 50 ºC 1 h | Poor Conversion |
| | 11 | THF | 10 | 50 ºC 1 h | Brominated BODIPY isolated |
| | 12 | THF | 15 | 50 ºC 18 h | Brominated BODIPY isolated |
| TMSCCNa | 13 | THF | 1.2 | 22 ºC 18 h | Poor Conversion |
| | 14 | THF | 1.2 | 45 ºC 18 h | Poor Conversion |
| | 15 | THF | 3 | 22 ºC 18 h | Degradation |
| | 16 | THF | 5 | -78 ºC 2 h | Degradation |

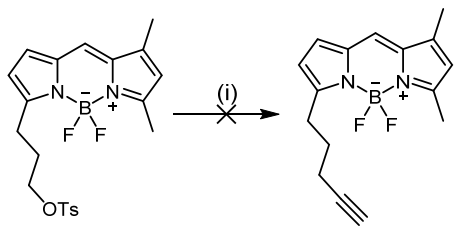


**108** **104**

**Scheme 3.13.6**: Reaction of Tosyl BODIPY with Alkyne Nucleophiles. *Reagents and conditions*: Please see **Table 3.13.1**.

Despite all efforts to access **104** via a nucleophilic displacement, no successful conditions were found. Thus, it was decided to investigate other methods of accessing an alkyne containing BODIPY.

3.13.3 Heptadiyne Bridge

The difficulty found in synthesising an alkyne containing BODIPY or IGD peptidomimetic lead to the idea that the simplest solution may be to exploit

functionalities already accessible. The reliable synthesis of IGD azide **45** and BODIPY azide **109** encouraged the development of a pragmatic, "double click", route. Thus, synthesis of an IGD containing fluorophore was envisioned to proceed with two successive click reactions, initially alkyne BODIPY **110** would be synthesised and then further reacted with IGD peptidomimetic **(*R*)-45** (**Scheme 3.13.7**). Azide BODIPY (**109**) has a shorter synthesis than azide IGD (**(*R*)-45**) (6 steps vs. 9 steps from commercially available materials), therefore **109** was chosen to undergo the initial click reaction in order keep the route as convergent as possible.

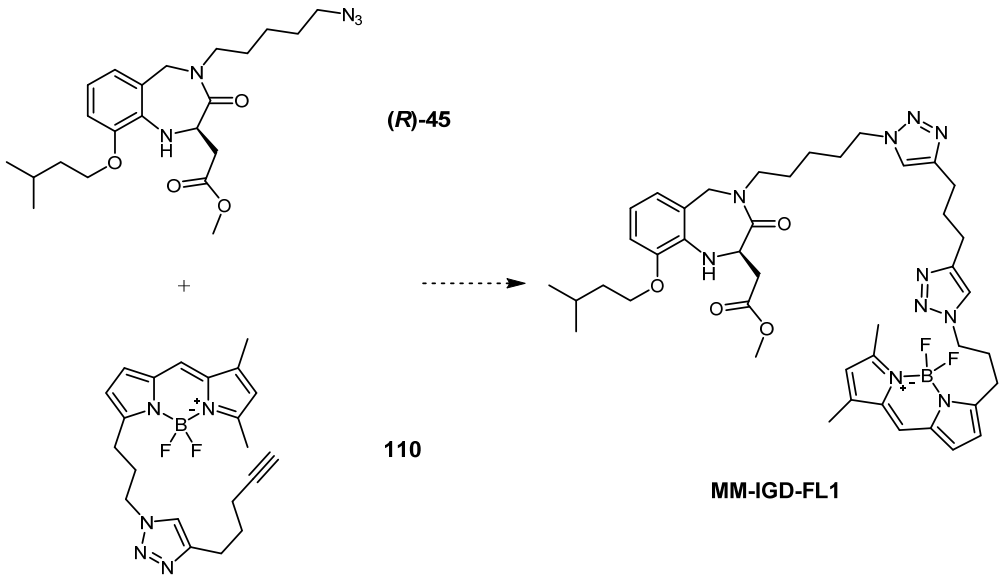


**Scheme 3.13.7**: Proposed Route to BODIPY tagged IGD mimetic **MM-IGD-FL1**.

Azide BODIPY **109** was synthesised as previously published by the Marquez group by converting alcohol **105** into the corresponding azide through mesylation and subsequent displacement with sodium azide (53%) (**Scheme 3.13.8**). Azide **111** was then treated with 3,5-dimethyl-pyrrole-2-carbaldehyde, phosphorous oxychloride and boron trifluoride to give azido BODIPY **109** in 43% yield.[74]

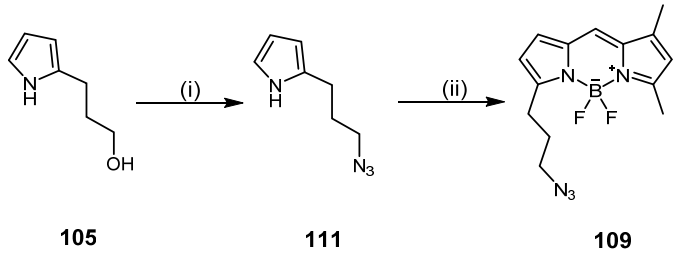


**Scheme 3.13.8**: Synthesis of Azide BODIPY **109**. Reagents and Conditions: (i) MsCl, $NEt_3$, THF then $NaN_3$, EtOH (53%); (ii) DCM, $POCl_3$, $BF_3.OEt_2$, DIPEA, 5-dimethyl-pyrrole-2-carbaldehyde (43%).

With azide BODIPY **109** in hand, the key reaction with 1,6-heptadiyne was attempted (**Scheme 3.13.9**). Initial attempts in dimethylformamide with copper iodide and triethylamine, showed no reaction after 18 h at 100 °C. Using bases other than triethylamine achieved more success, giving the desired alkyne (**110**) in 57% yield. This moderate yield of this reaction may be attributed to the incomplete conversion of starting material as well as the formation of the iodo triazole (**112**).

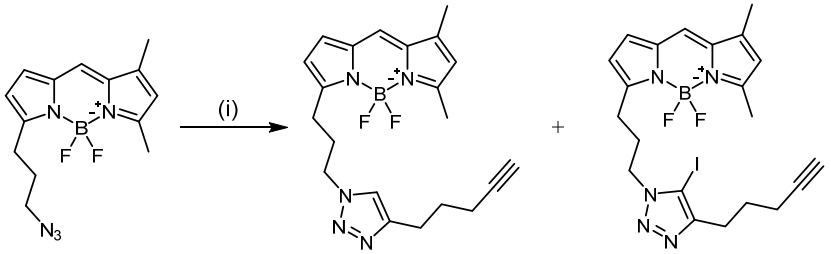


**Scheme 3.13.9**: Synthesis of an Alkyne Containing BODIPY **110** Via Click Conditions. *Reagents and Conditions*: (i) CuI, DIPEA, THF, 1,6 heptadiyne (57%).

Alternative copper sources were screened in an effort to avoid this iodine insertion product and promote complete conversion of starting material. Copper thiophene-2-carboxylate gave complete consumption of the BODIPY starting material, giving the desired product and the corresponding dimer, however, purification issues prohibited further work with this copper source (**Scheme 3.13.10**).[75]

Copper acetate monohydrate was successful in synthesising the desired product in moderate yield (54%) using a THF/water mixture.[76] Copper sulfate in the more polar solvent system of *t*-butanol and water gave the desired product in low yield (29%), together with a large amount of dimer **113**.[77] Unfortunately, the high polarity of dimer **113** proved a challenging issue which prevented the determination of the isolated yield. However, it is worth noting that these conditons the dimer seemed to form preferentially to the desired product, possibly due to the polar system used. Copper sulphate and sodium ascorbate in tetrahydofuran and water also promoted the complete consumption of starting material **109** giving alkyne **110** in low yield (5%) together with dimer **113** as the major product, but it is possible that this reaction would be improved through an increase in the equivalents of 1,6-heptadiyne used. These results are summarised in **Table 3.13.2**.

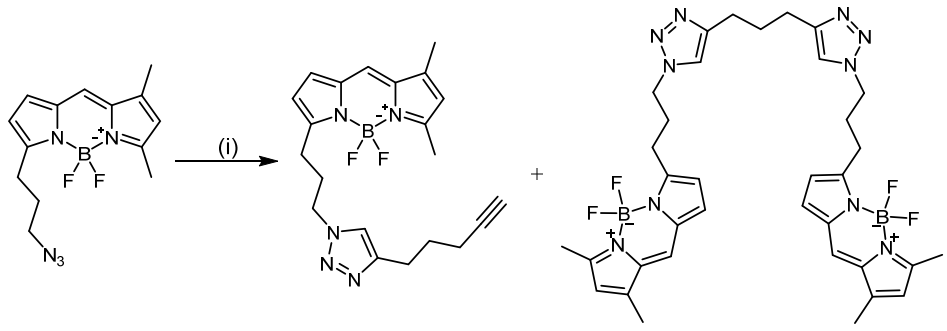


**Scheme 3.13.10**: Mono- and Di- Click Condensation Products. *Reagents and Conditions*: (i) CuTC, Toluene, 110 °C (**110** 60% (impure)); (i) $Cu(OAc)_2 \cdot H_2O$, NaAsc, THF, $H_2O$, (**110** 54% + **113**); (i) $Cu(SO_4) \cdot 5H_2O$, NaAsc, *t*BuOH, $H_2O$, (**110** 29% + **113** (major)); (i) $Cu(SO_4) \cdot 5H_2O$, NaAsc, THF, $H_2O$ (**110** 5% + **113** (major)).

**Table 3.13.2**: Summary of Reaction Conditions Screened in Alkyne **110** Synthesis.

| Eq of alkyne | Cu source | Base | Solvent, Temp (°C) | **109** Consumed | **110** | By prod |
|---|---|---|---|---|---|---|
| 5 | CuI | $NEt_3$ | DMF, 100 | No | 0% | - |
| 15 | CuI | DIPEA | THF, 55 | No | 57% | **112** |
| 3 | CuTC | - | Toluene, 110 | Yes | 60% (impure) | **113** |
| 6 | $Cu(OAc)_2 .H_2O$ | NaAsc | $THF/H_2O$, 50 | Yes | 54% | **113** |
| 6 | $CuSO_4$ | NaAsc | $tBuOH/H_2O$, 50 | Yes | 29% | **113** |
| 1.2 | $CuSO_4$ | NaAsc | $THF/H_2O$, 70 | Yes | 5% | **113** |

The small amounts of BODIPY alkyne **110** gained from the above reactions were taken forward to the final coupling step where copper iodide and diisopropylethylamine were employed (**Scheme 3.13.11**). The small scale of this reaction and the extensive purification required resulted in no clean product being isolated, however, two characteristic triazole protons were visible in $^1H$ NMR spectra. This partial evidence suggested that the desired product was being synthesised and it was a very encouraging result.

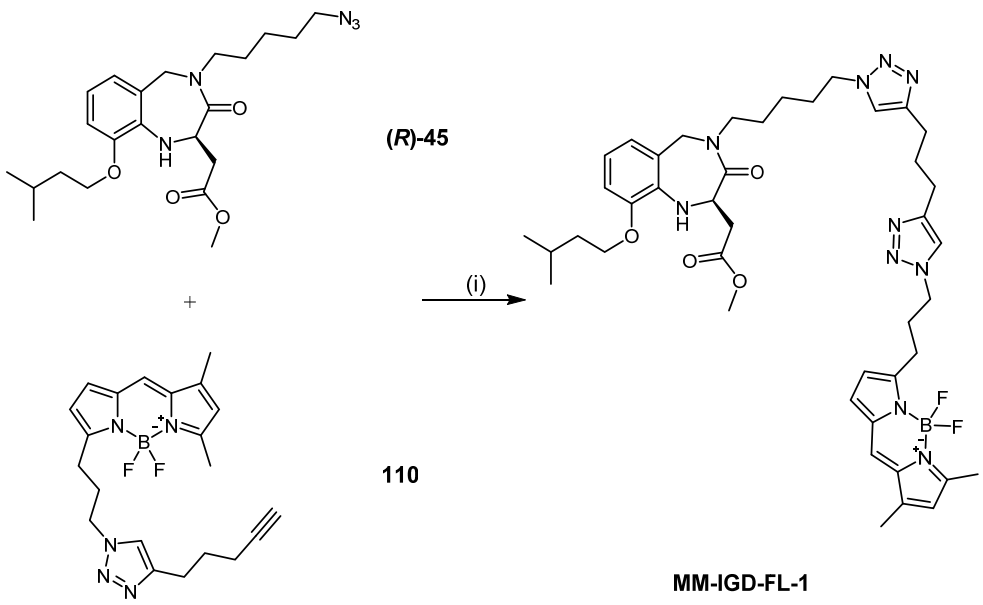


**Scheme 3.13.11**: Synthesis of **MM-IGD-FL-1** from BODIPY Alkyne **110**. *Reagents and Conditions*: (i) DIPEA (4.0 eq.), CuI (1.0 eq.), THF.

The variable yields, incomplete conversion, byproduct formation and purification difficulties in the synthesis of alkyne BODIPY **110** encouraged experimentation towards the synthesis of an IGD peptidomimetic alkyne derivative despite the potentially longer linear route. Thus, the synthesis of alkyne **(*R*)-114** was attempted with two different copper sources.

Reaction of azido-IGD peptidomimetic (***R*)-45** with 1,6-heptadiyne in the presence of copper iodide and DIPEA gave the desired alkyne **(*R*)-114** in good yield (57%), together with the residual starting material and dimer **(*R*)-115** (**Scheme 3.13.12**). Increasing the amount of 1,6-heptadiyne from 3 eq. to 10 eq. was unsuccessful in increasing yields of the desired alkyne **(*R*)-114** (51%).

Switching the catalyst to copper sulfate and sodium ascorbate successfully promoted the complete consumption of azide **(*R*)-45**, however, yield of desired **(*R*)-114** did not increase. Interestingly, significant amounts of dimer were still isolated despite the very large excesses of 1,6-heptadiyne being used (**Table 3.13.3**).

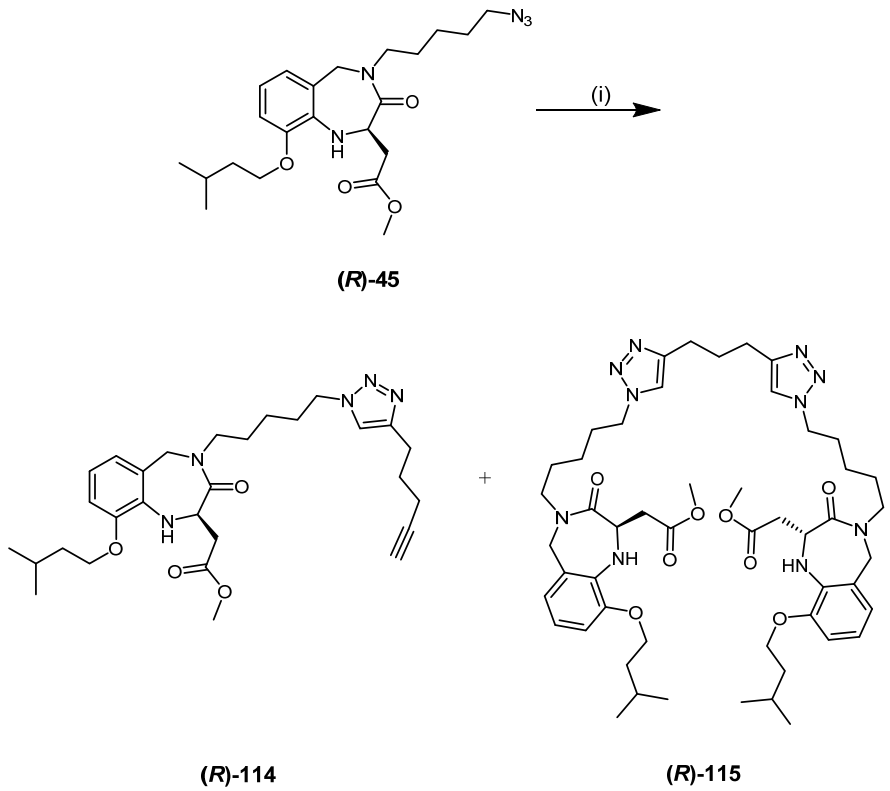


**Scheme 3.13.12**: Synthesis of Alkyne Containing IGD peptidomimetic **(*R*)-114**. *Reagents and Conditions*: (i) CuI, DIPEA, THF (51-57%); $Cu(SO_4)\cdot 5H_2O$, NaAsc, THF, $H_2O$ (46-61%).

**Table 3.13.3**: Synthesis of Alkyne Containing IGD **(*R*)-114**.

| Alkyne eq. | Cu Source | Base | Solvent | **(*R*)-45** present | **(*R*)-114** | Dimer Observ |
|---|---|---|---|---|---|---|
| 3 | CuI | DIPEA | THF | Yes | 57% | Yes |
| 10 | CuI | DIPEA | THF | Yes | 51% | Yes |
| 10 | $CuSO_4$ | NaAsc | THF/$H_2O$ | No | 46% | Yes |
| 13 | $CuSO_4$ | NaAsc | THF/$H_2O$ | No | 61% | Yes |
| 20 | $CuSO_4$ | NaAsc | THF/$H_2O$ | No | 46% | Yes |

Despite comparable yields to those seen in the synthesis of alkyne BODIPY **110**, the relative ease of purification of alkyne **(*R*)-114** encouraged the use this route in the synthesis of a fluorescent analogue (**Scheme 3.13.13**).

Thus, the synthesis of **MM-IGD-FL-1** was initially attempted in the presence of copper iodide. Unfortunately, despite complete consumption of alkyne **(*R*)-114**, and no observation of an iodine insertion product, extensive purification resulted in a low isolated yield of the desired compound (9%).

Subsequent cyclisation attempts using copper sulphate (1.2 eq.) and sodium ascorbate (2.4 eq.) were challenging, as significant degradation of starting materials was observed under the reaction conditions. Furthermore, the polarity of the cyclisation product meant that flash column chromatography and preparative thin layer chromatography were both required to access the clean product **MM-IGD-FL1** (30%). Optimisation however, was achieved by minimising the reaction time and by the inclusion of an aqueous work up, which significantly facilitated the product purification. Using these improvements, the desired compound **MM-IGD-FL1** was accessed through preparative thin layer chromatography (48%). This synthesis is the most successful effort to gain access to a BODIPY tagged IGD mimetic to date. The fluorescent probe was synthesised in 11% over 11 steps (longest linear sequence) from commercially available materials. The same route was followed to generate the matching (*S*)-IGD peptidomimetic derivative **MM-IGD-FL2** in reasonable yield from **(*S*)-45** (48%).

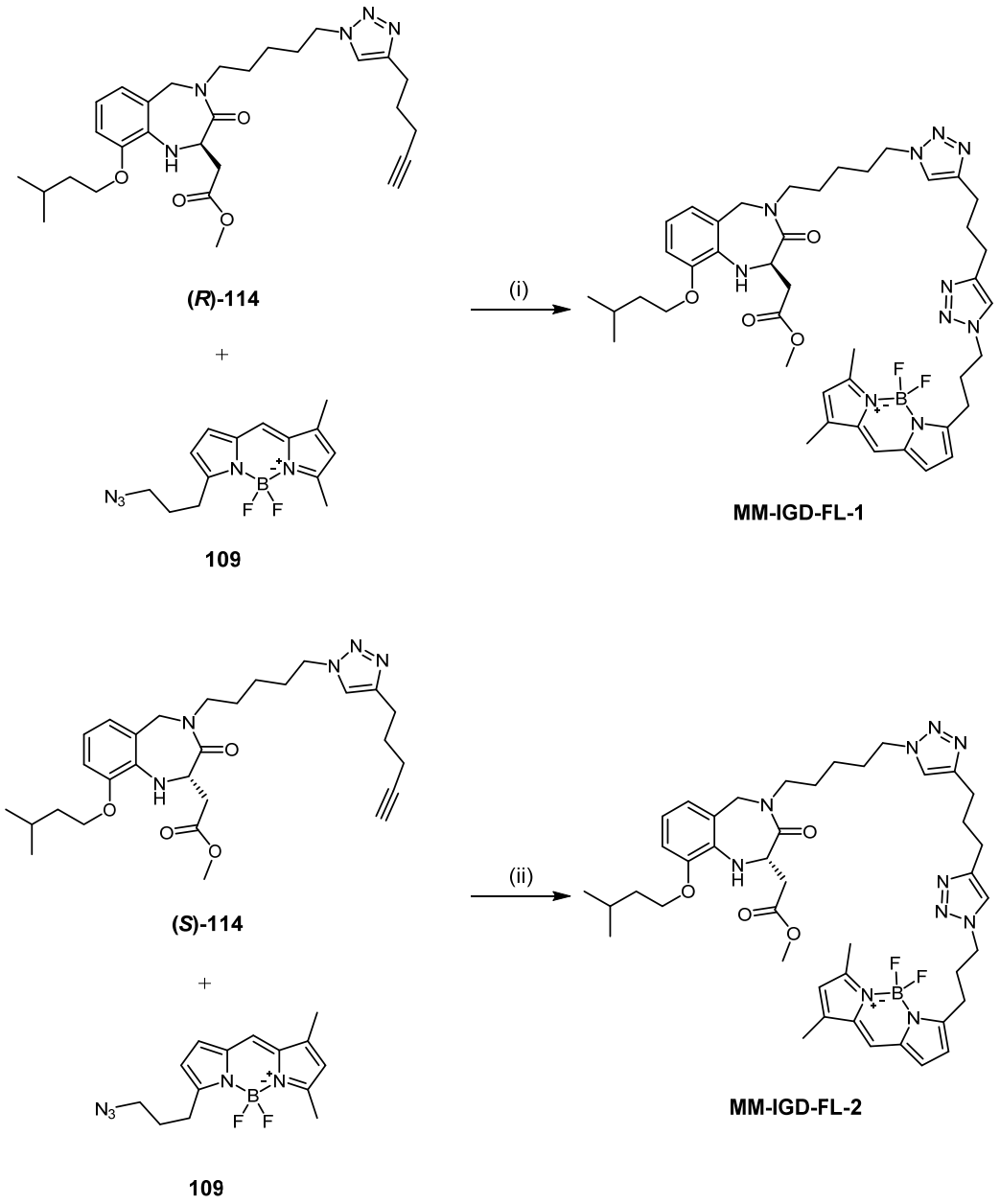


**Scheme 3.13.13**: Synthesis of **MM-IGD-FI-1** and **MM-IGD-FI-2**. *Reagents and Conditions*: (i) 1,6-heptadiyne, CuI, DIPEA, THF, (9%); $Cu(SO_4)\cdot 5H_2O$, NaAsc, DIPEA, THF, $H_2O$ (48%); (ii) $Cu(SO_4)\cdot 5H_2O$, NaAsc, DIPEA, THF, $H_2O$ (48%).

## 3.14 Confocal Microscopy with MM-IGD-FL1 and MM-IGD-FL2

With a reliable synthesis of the (*R*) and (*S*)- IGD peptidomimetic fluorophores in place, we were able to build upon our fruitful collaboration with Dr Catherine Wright by focusing our efforts on confocal microscopy.

Human Neonatal Fibroblasts were cultured as in General Protocols for Splitting and Maintaining Human Fibroblast Cultures (**Experimental 5.4**, **p 179**) onto 2 chamber Nunc™ Lab-Tek™ II cover slides. Cells were incubated with serum free media for one hour before treatment with 0.1 µg/mL solutions of **MM-IGD-FL1**, **MM-IGD-FL2** or a control, media only, solution. Images were then captured at 10 mins, 30 mins, 2 hours, 5 hours and 24 hours.

To our delight, microscopy at 10 minutes showed the internalisation of both (*R*) and (*S*)- fluorophores (**Figure 3.14.1**). Interestingly, although not quantitative, images consistently show higher concentrations of internalised **MM-IGD-FL1** than **MM-IGD-FL2**. This may be the result of increased uptake **MM-IGD-FL1** with respect to its enantiomer, however, it could also be due to increased efflux or greater metabolism of the (*S*)- enantiomer.

(A) (B)

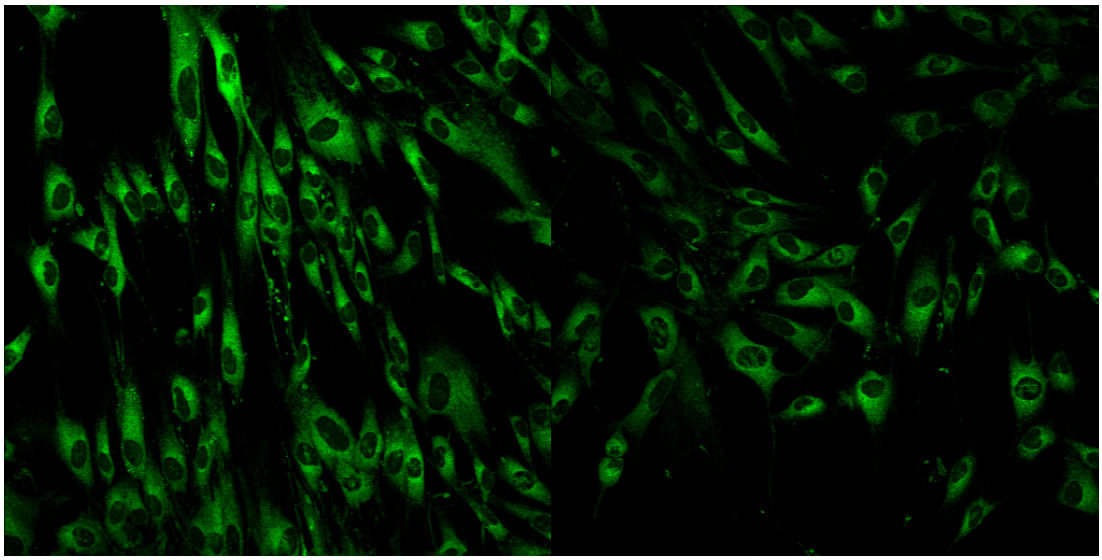

**Figure 3.14.1:** Fluorophores at ten minutes (460 x 460 µm) (A) Cells treated with **MM-IGD-FL-1**; (B) Cells treated with **MM-IGD-FL-2**.

Inspection of the images at a greater magnification highlights pin-pricks of more intense fluorescence on cell extremities (**Figure 3.14.2**). This is particularly interesting as it is indicative of a possible endocytic mechanism of uptake.

(A)

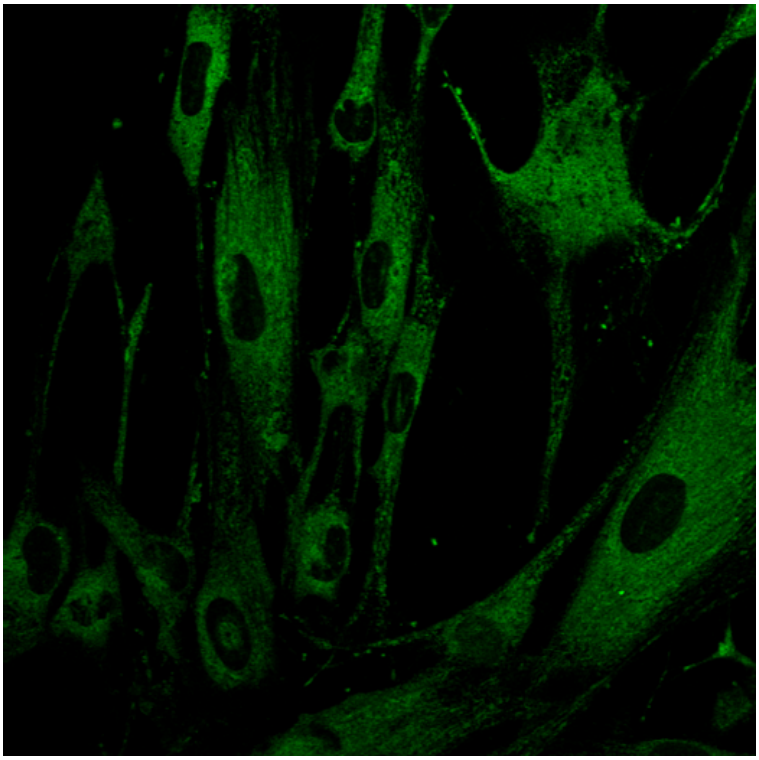

(B)

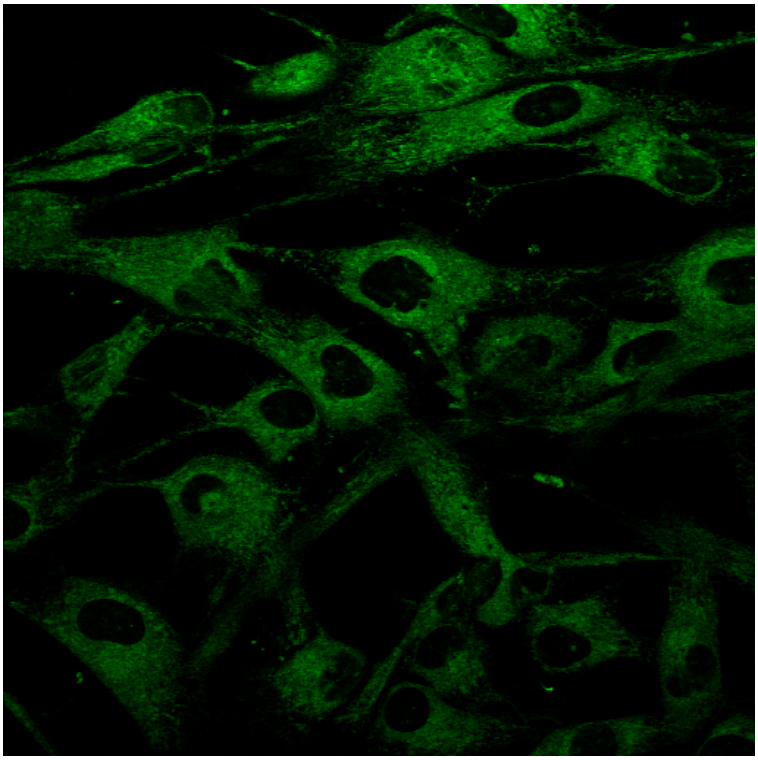

**Figure 3.14.2**: Fluorophores at ten minutes (230 x 230 μm). (A) Cells treated with **MM-IGD-FL-1**; (B) Cells treated with **MM-IGD-FL-2**.

Images at five hours showed particularly noticeable differences between the cellular levels of **MM-IGD-FL1** and **MM-IGD-FL2** (**Figure 3.14.3**).

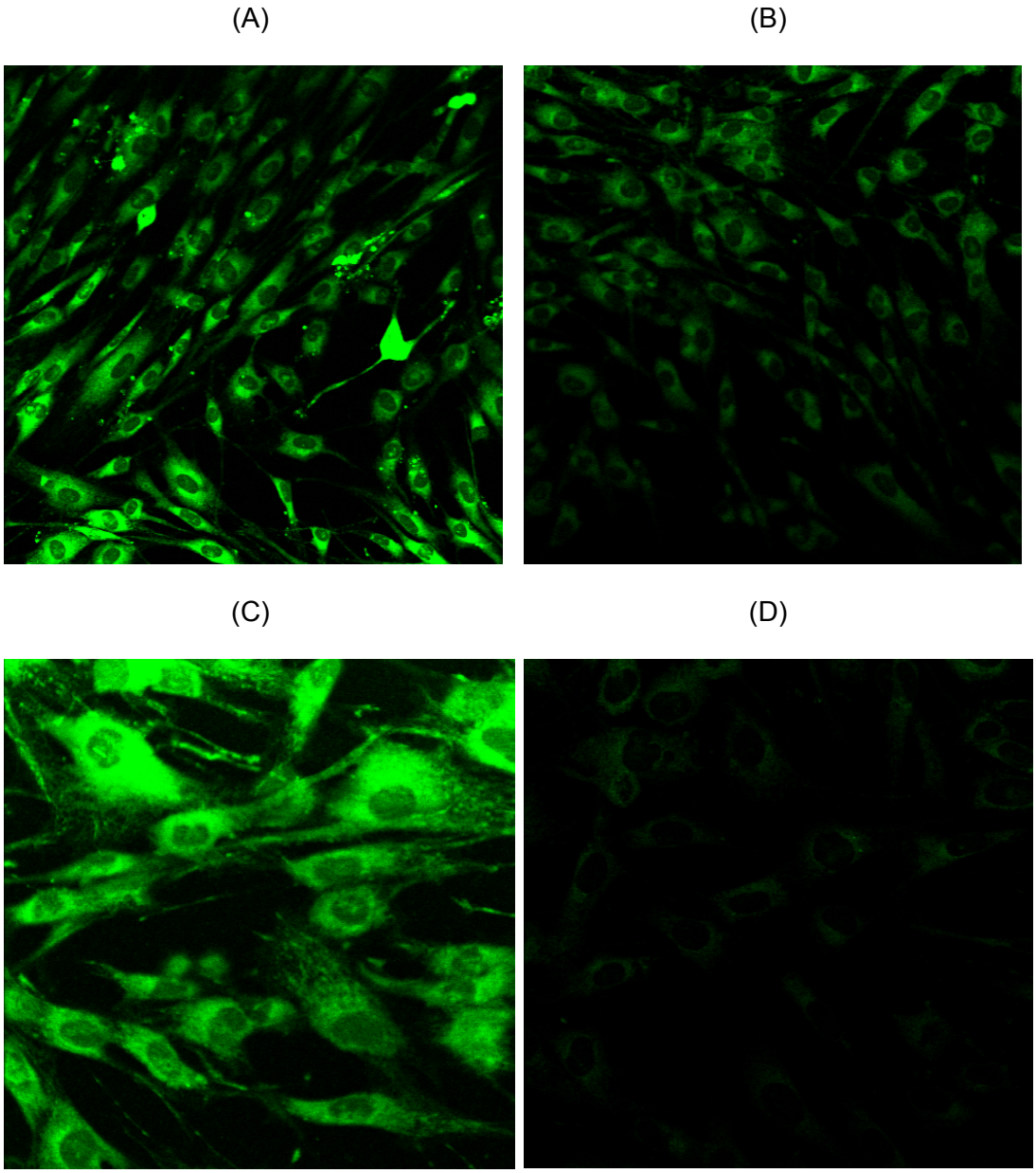


**Figure 3.14.3**: Cells Treated with IGD Peptidomimetic Fluorophores at Five Hours. (A) **MM-IGD-FL-1** (460 x 460 μm); (B) **MM-IGD-FL-2** (460 x 460 μm); (C) **MM-IGD-FL-1** (230 x 230 μm); (D) **MM-IGD-FL-2** (230 x 230 μm).

Fluorescence at 24 hours is diminished but we are still able to visualise the cells (**Figure 3.14.4**).

(A) (B)

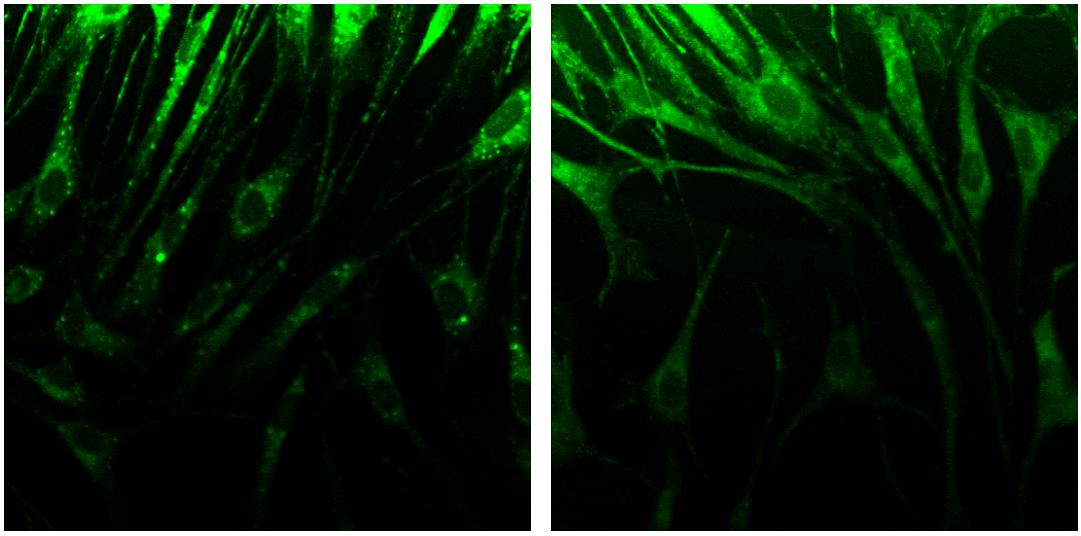

**Figure 3.14.4**: Cells Treated with IGD Peptidomimetic Fluorophores at Twenty Four Hours (230 x 230 μm). (A) **MM-IGD-FL1**; (B) **MM-IGD-FL2**.

Confocal microscopy with the IGD peptidomimetic fluorophores **MM-IGD-FL1** and **MM-IGD-FL2**, has been particularly valuable. We can now say with confidence that the compounds are rapidly internalised, most likely through endocytosis. It is known that fibroblasts take up fibronectin coated collagen *via* phagocytosis during remodelling of granulation tissue, which may be relevant to our observations.[78-79] This in turn may support an intergrin based interaction.[80-81] We can also conclude that cellular concentration of the active enantiomer, **MM-IGD-FL1** is higher than **MM-IGD-FL2**.

## 3.15 Iodine Containing IGD Peptidomimetic

Based on the success of our click reaction, we became interested in the application of a similar approach for the development of potential new PET imaging agents. A PET imaging agent could be used when carrying out *in vivo* studies allowing visualisation of areas of high uptake and metabolism of our IGD peptidomimetics.

In 2013 Arstad outlined the use of an electrophilic iodine source to give 5-iodo-1,2,3-triazoles in a one-pot synthesis of $^{125}$iodine containing molecular probes.[82] This functionality is advantageous in radioactive tracers as it lends high *in vivo* stability to deiodination. Arstad also reported the generation of a radioactive species using $^{125}$I labelled sodium iodide and copper chloride as an alternative to copper iodide and *N*-iodosuccinimide (**Scheme 3.15.1**).

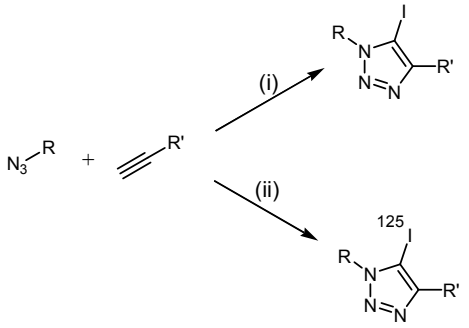


**Scheme 3.15.1**: (i) CuI, NIS, TEA, DMF; (ii) [$^{125}$I]NaI, $CuCl_2$, TEA, $CH_3CN/H_2O$.

In our hands treatment of (**(*S*)-45**) with copper iodide and *N*-iodosuccinimide successfully generated the desired iodo-derivative (**(*S*)-117**) in 30% yield. Sodium iodide and copper chloride on the other hand, only afforded the dehalogenated analogue **(*S*)-116** in 41% yield (**Scheme 3.15.2**).

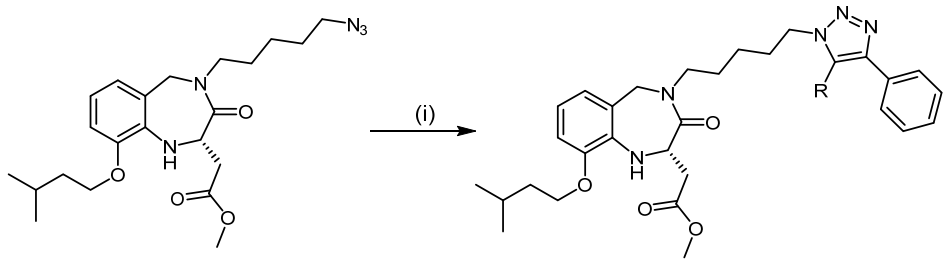


**(*S*)-45**

R = H **(*S*)-116**
R = I **(*S*)-117**

**Scheme 3.15.2**: (i) CuI, $NEt_3$, DMF, NIS, phenylacetylene (**(*S*)-117**, 30%); (ii) NaI, $CuCl_2$, TEA, $MeCN/H_2O$, Phenylacetylene (**(*S*)-116**, 41%).

Despite the promising results obtained with copper iodide and NIS which showed that it was possible to incorporate an iodine atom into the triazole via click reaction, time constraints together with the difficult logistics associated with the incorporation of a $^{125}I$ unit meant that this work could not be taken any further at this point.

## 3.16 Difunctionalised BODIPY Tagged IGD Peptidomimetic

The development of a BODIPY group containing two synthetic handles has been a goal of the Marquez group for some time. A bisfunctional fluorescent tag could be used in solid support work to circumnavigate the need for specialist NMR studies, as the presence of fluorescence would indicate successful binding (**Scheme 3.16.1**).

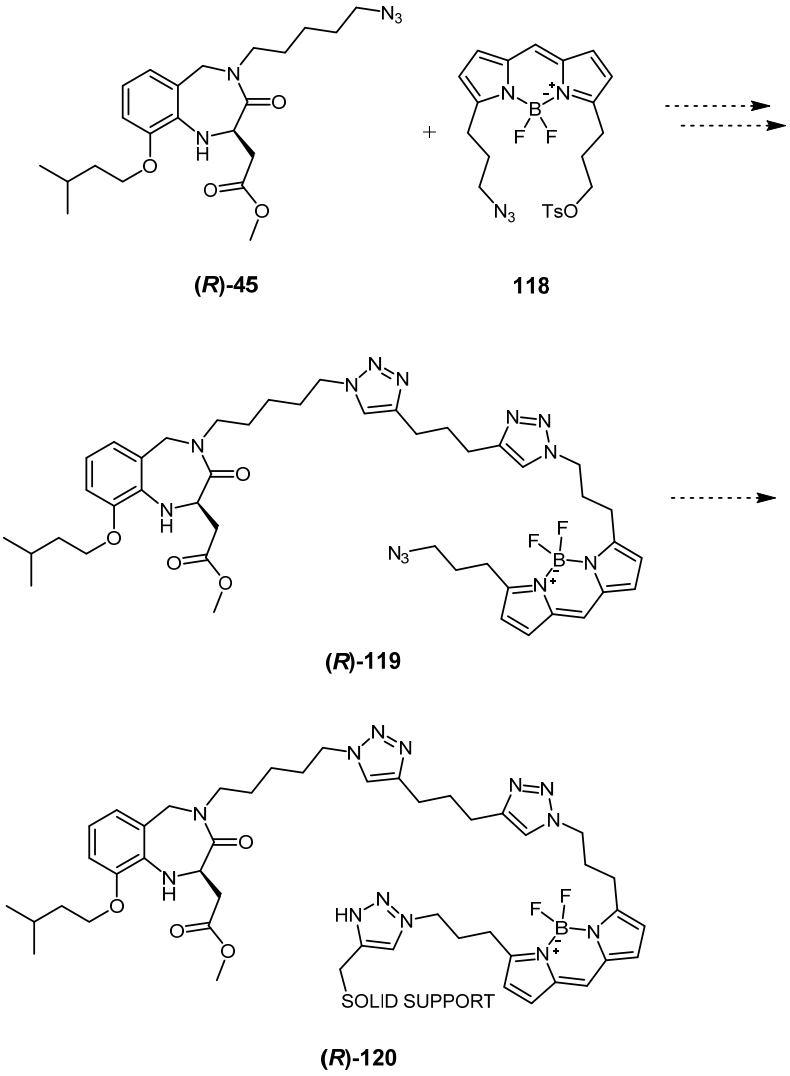


**Scheme 3.16.1:** Proposed Incorporation of a difunctionalised BODIPY **118** onto a Solid Support.

To maximise the utility of the fluorescent unit, it would be beneficial if the two functional groups had orthogonal reactivity. Thus, our new BODIPY target **118** was designed with these parameters in mind (**Scheme 3.16.2**).

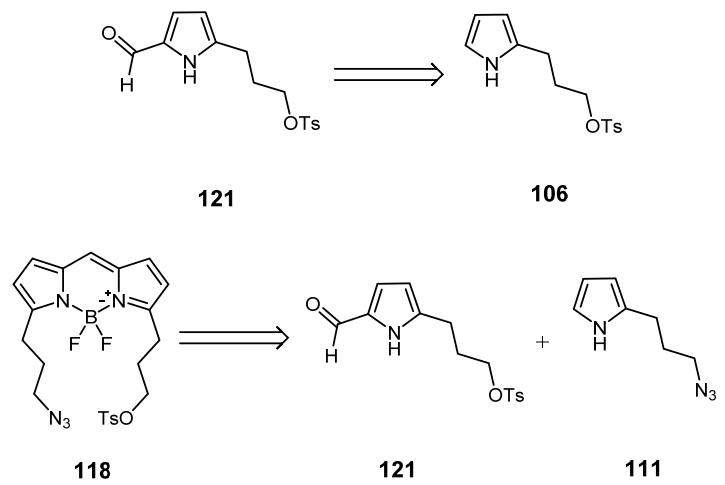


**Scheme 3.16.2**: Proposed Route to Difunctionalised BODIPY **118**.

Our initial approach towards the synthesis of the difunctionalised BODIPY **118** proceeded via our previously synthesised tosyl pyrrole **106**. Synthesis of formylated tosylate **121** was attempted by treatment of pyrrole **106** with phosphorous oxychloride and DMF, however, upon treatment no tosyl peaks were visible by $^{1}$H NMR. Mass spectrometry confirmed the formation of chloro-pyrrole **122** (**Scheme 3.16.3**).

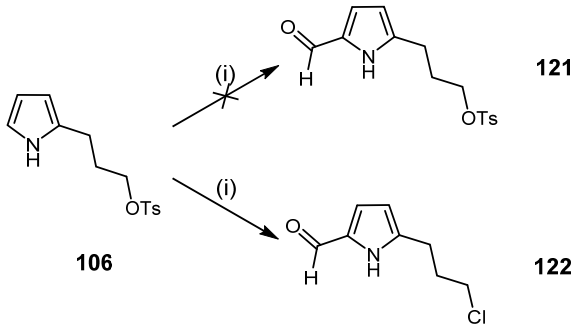


**Scheme 3.16.3**: Synthesis of Undesired Chloride **122**. *Reagents and Conditions*: (i) DMF, $POCl_3$, 50 °C (67%).

In an alternative approach to the synthesis of the bis-functionalised BODIPY, it was decided to proceed via formylated azido pyrrole **111** (**Scheme 3.16.4**). Formylation of azido-pyrrole was initially attempted with standard 1.1 equivalents of phosphorous oxychloride, however, no reaction was observed. Increasing the phosphorous oxychloride to 15 equivalents successfully afforded formylated pyrole **123** in good yield.

Gratifyingly, coupling of formylated azido-pyrrole **123** with tosyl-pyrrole **106** under standard BODIPY forming conditions proceeded to generate the desired target

BODIPY **118** in good yield. Interestingly, the azido tosyl BODIPY was not the sole BODIPY product from the reaction, both diazide and ditosyl species were also observed as minor products.

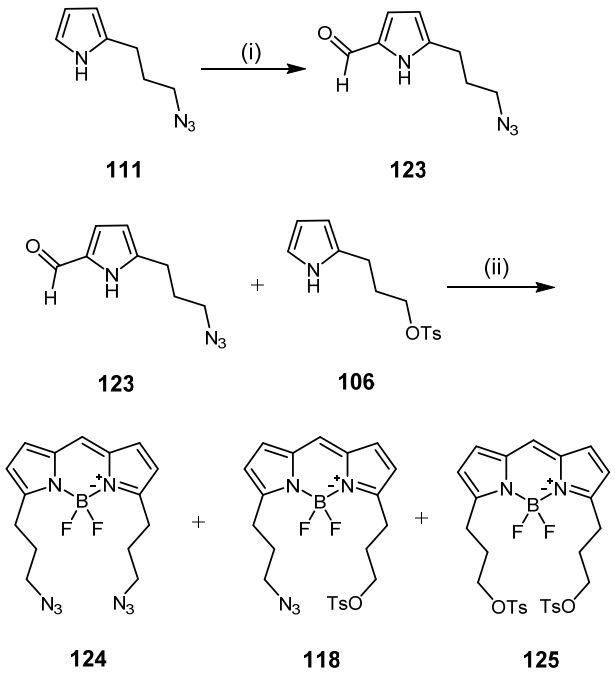


**Scheme 3.16.4**: Synthesis of Difunctionalised BODIPYs **124**, **118** and **125**. *Reagents and Conditions*: (i) DMF, $POCl_3$, 40 °C (70%); (ii) DCM, DIPEA, $BF_3{\cdot}OEt_2$ **124** (16%), **118** (54%), **125** (29%).

The formation of BODIPYs **124** and **125** raises an interesting mechanistic feature of the synthesis of the dipyrromethane scaffold. Wu and Burgess describe a condensation–decarbonylation mechanism of pyrrole-2-carbaldehydes to yield dipyrrins and subsequently BODIPY dyes.[83] It is possible that the formation of diazide BODIPY **124** could be explained though an analogous mechanism, as shown below (**Scheme 3.16.5**). In the proposed Burgess mechanism, azafulvene **126** is synthesised by reaction of **89** with phosphorous oxychloride. Sequential attack from a second equivalent of **126** and then a chloride ion results in loss of carbon monoxide and 2 equivalents of hydrochloric acid giving dipyrrinium **129**.

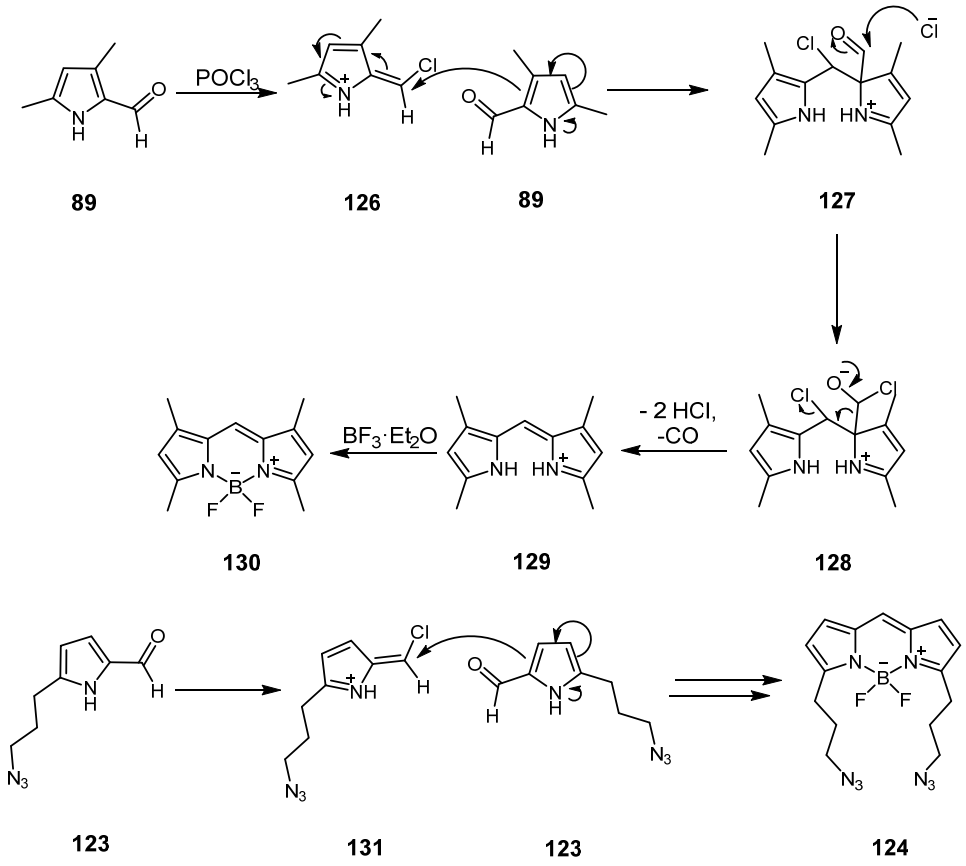


**Scheme 3.16.5**: Dimerisation of Azido pyrrole **124**.

It is possible that this mechanism accounts for the (at least partial) synthesis of diazide **124**, however, it does not account for the formation of ditosyl BODIPY **125**. The synthesis of this product implies that the transfer of the *meso* carbon is occurring. This "scrambling" of dipyrromethane scaffolds is well documented, particularly in the syntheses of porphyrins. Smith discusses the origin of this scrambling in "Porphyrins and Metalloporphyrins": under acidic conditions. In the presence of acid, the protonation takes place (**Scheme 3.16.6**), subsequent electron donation by the most electron rich nitrogen results in fragmentation. The new species which can then recombine to give three different products.[84]

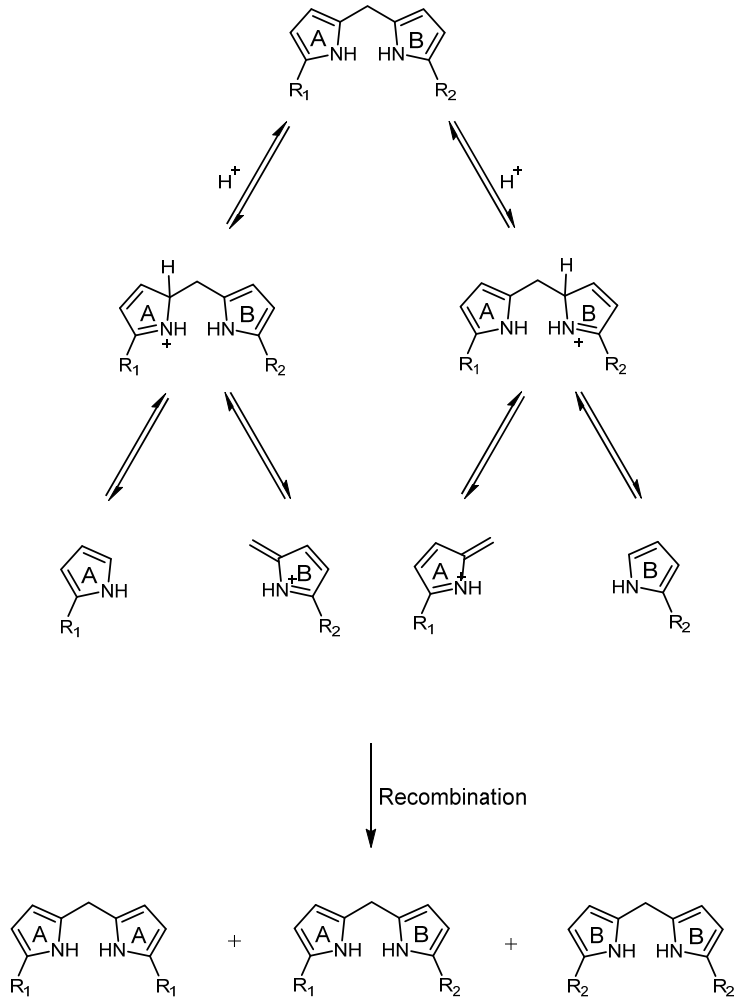


**Scheme 3.16.6:** The Origin of "Scrambled" Fragments in Porphyrin Synthesis.

This mechanism rationalises the synthesis of difunctionalised BODIPYs **118**, **124** and **125**, the acidic environment provided by phosphorous oxychloride generates fragments **131** and **136** which can combine with **106** and **123** (**Scheme 3.16.7**) to give the three observed novel BODIPYs.

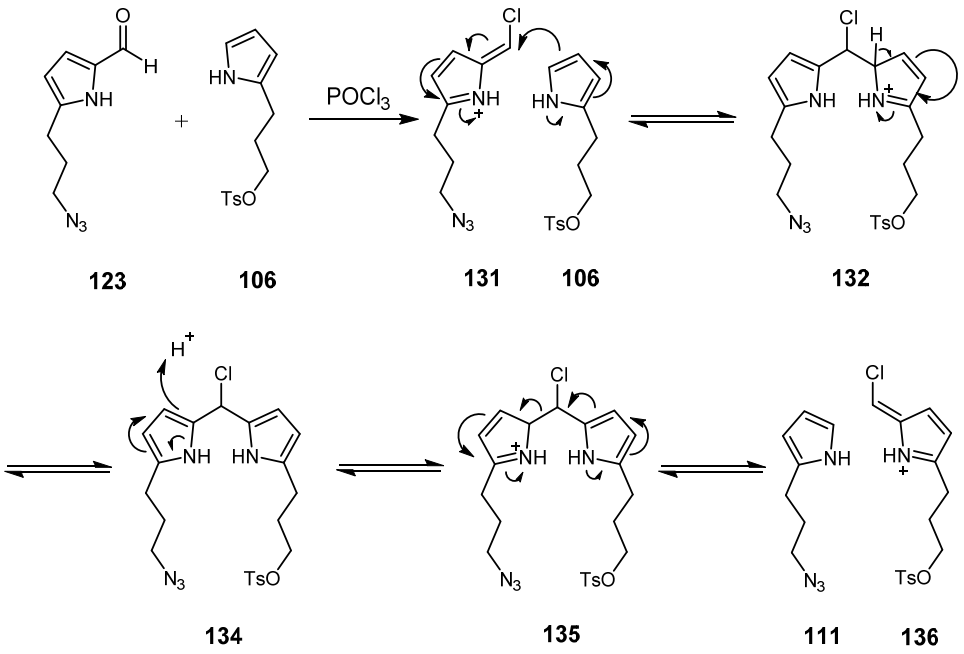


**Scheme 3.16.7**: Suggested Mechanism of *Meso* Substitent Scrambling in Disubstituted BODIPYs.

In an attempt to desymmetrise the homo-dimer generated, ditosyl BODIPY **125** was treated with sodium azide to increase the amount of desired product accessible through this route (**Scheme 3.16.8**). Initially ditosyl BODIPY **124** was used in excess, however, poor conversion prompted the addition of higher equivalents of sodium azide resulting in the formation of **124** and **118**. The small amounts of desired **124** in the reaction mixture discouraged further attempts at this transformation.

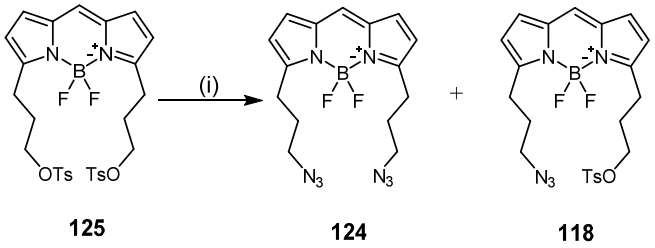


**Scheme 3.16.8**: Ditosyl BODIPY **125** as *Reagents and Conditions*: (i) $NaN_3$, EtOH.

With a small amount of **118** in hand synthesis of click product **137** was attempted with copper iodide. Good conversion of IGD peptidomimetic was seen by TLC, however, the small scale of the reaction and lengthy purification required did not allow full characterisation of **(*R*)-119**, however, mass spectroscopy indicates a successful coupling (HRMS (ESI) calcd for $C_{51}H_{65}F_2N_{10}NaO_7SB$ [$(M+Na)^+$]: *m*/*z* 1032.4748,

found *m*/*z*, 1032.4698) (**Scheme 3.16.9**). Time constraints did not allow for completion of this potentially very useful tool, however, the groundwork has been laid for future development.

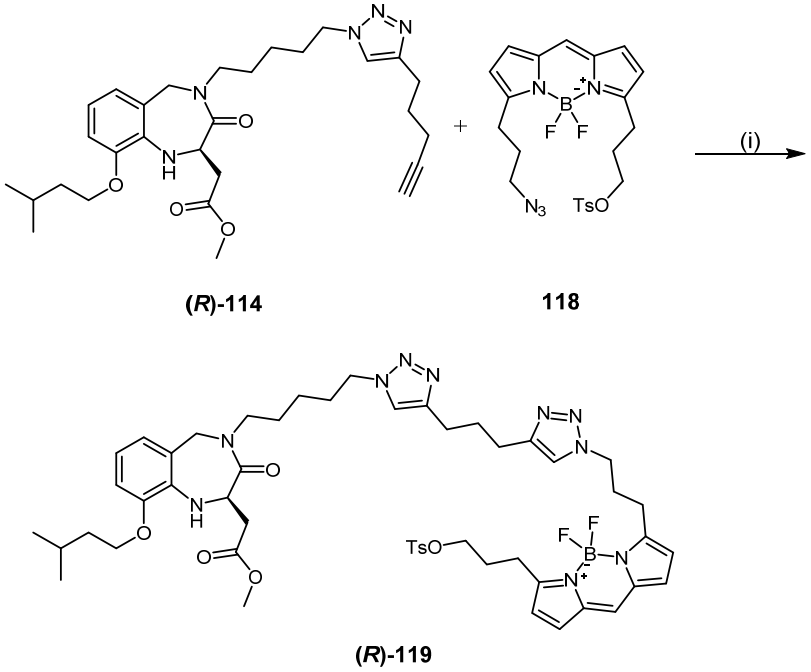


**Scheme 3.16.9**: Synthesis of a Difunctionalised BODIPY Tagged IGD Peptidomimetic
*Reagents and Conditions*: (i) CuI, DIPEA, THF (36%).

## 3.17 Triethylene Glycol IGD Peptidomimetic

### 3.17.1 Tripeptide Containing Hydrogels

The intuitive delivery route for our IGD peptidomimetics as wound healing agents is topical application. Topical delivery would allow the drug to be placed in close proximity to the site of action while minimising required dosages, premature metabolism and unwanted distribution and side effects within the body.[85]

A topical delivery method would require the IGD peptidomimetic to be incorporated into some form of interactive dressing. There are several forms of dressing that are widely used to interact with wound beds including, collagen gels, hydrofoams, and most importantly, hydrogels.[86]

Recently, Ulijn reported the formation of nanofibrous hydrogel comprised of Fmoc - RGD **137** (**Figure 3.17.1**).[87] Arene-arene interactions allow the individual molecules to arrange into cylindrical nanofibres composed of interlocking beta-sheets.

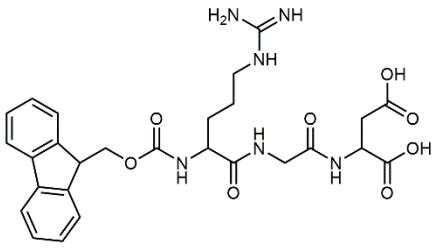


**137**

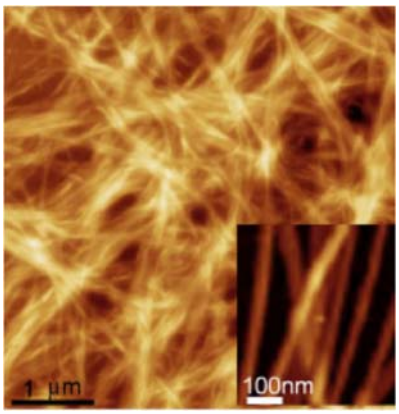


**Figure 3.17.1**: Fmoc-RGD **137** and AFM image of hydrogel shows an overlapping mesh of nanofibres. [87]

Crucially, the twisted nature of these sheets presents the RGD functionality to the surface of the cylinder (**Figure 3.17.2**).[87] This feature of the hydrogel is particularly desirable as it may allow easier interaction between the active moiety and the relevant cellular receptors. The importance of this feature can be further emphasized by considering the case of Regranex® in which poor bioavailability of the PDGF growth factor in the carboxymethylcellulose gel may be, at least partially, to blame for its lack of activity outside of clinical trials.[16]

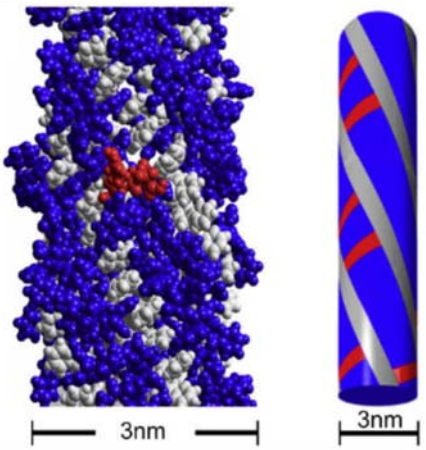


**Figure 3.17.2:** RGD moieties (in red) on the surface of fibrils within the hydrogel.[87]

Work carried out by Dr Anna Mette Hansen within the Marquez group found that analogous hydrogels can also be formed from the Fmoc-IGD molecule **138**. Studies of these novel gels are on-going, however, early results are encouraging as transmission electron microscopy has shown them to have the desired fibrous nature (**Figure 3.17.3**).

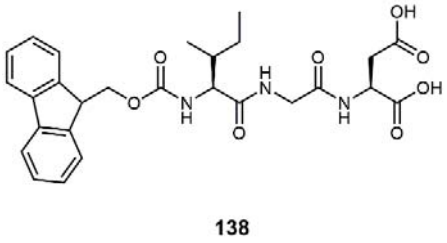


**138**

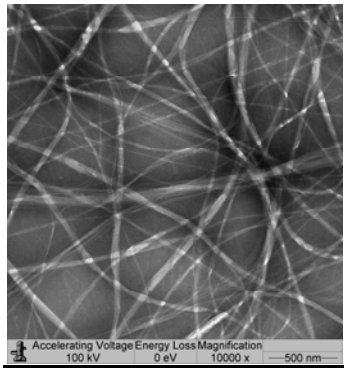


**Figure 3.17.3**: Structure of Fmoc- IGD **138** and TEM image of Fmoc-IGD hydrogel.

We hypothesised that an analogous hydrogel with the IGD peptidomimetic could be a valuable drug delivery method. As previously discussed, the nature and length of the alkyl chain used in our IGD peptidomimetic has not been optimised. It is possible that the all carbon alkyl chain, designed to put distance between IGD core and immobilised technologies, will be less effective than a hydrophilic equivalent due to the potential of hydrophobic coiling. With this in mind, an ethylene glycol based synthetic handle was designed in order to enable the synthesis of a molecule with significant distance between the active IGD peptidomimetic core and any introduced functionality while reducing the hydrophobicity of an all carbon chain (**Scheme**

**3.17.1**). The synthesis of this compound was envisioned to follow a similar route to the alkyl chain analogues.

Alcohol **(*R*)-145/(*R*)-146** would be derived from the aniline **147/148** and would be followed by the synthesis of the corresponding amine. Focus would then be directed towards the synthesis of carbamate **(*R*)-140/(*R*)-142** which is envisioned to be the hydrogel building block.

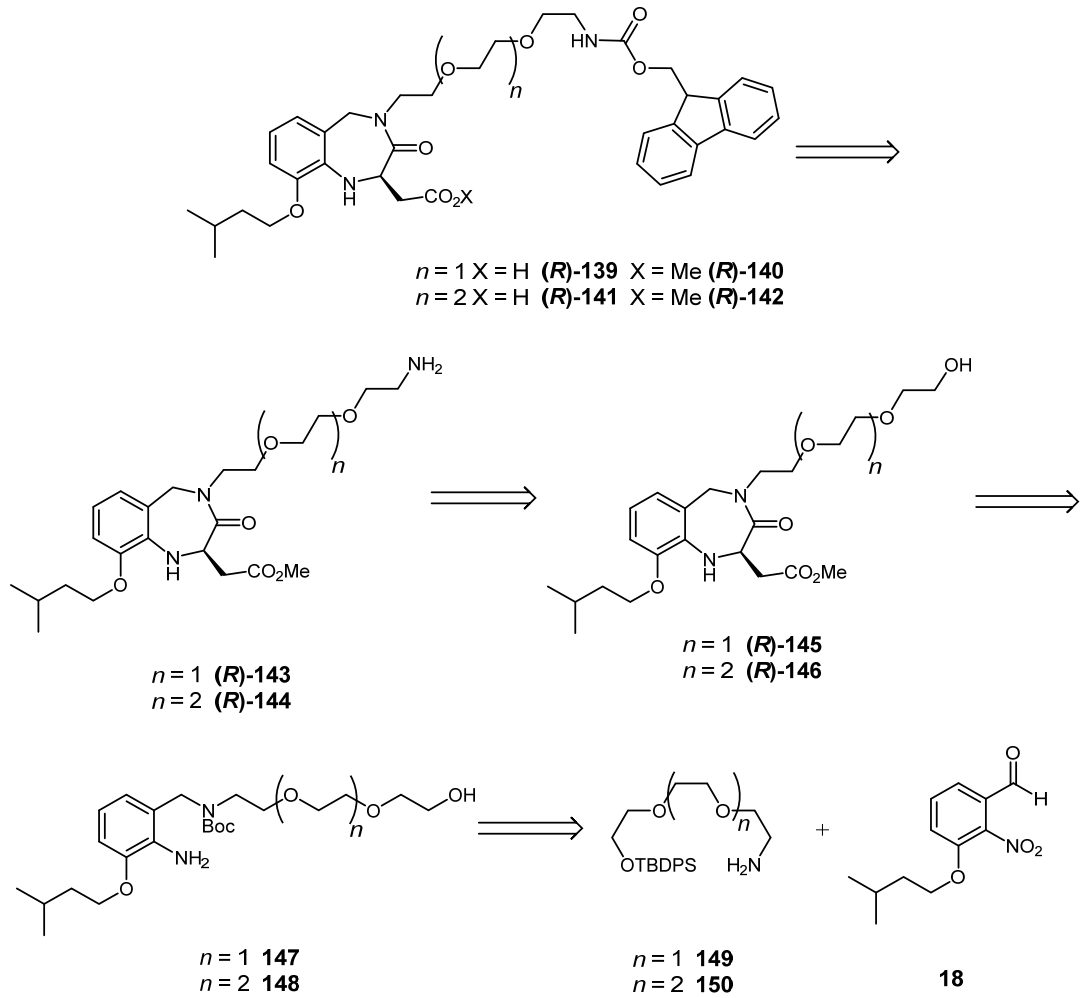


**Scheme 3.17.1:** : Retrosynthesis of Fmoc-(*R*)-IGD mimetic hydrogel building block

With this in mind, efforts were focused on the synthesis of the polyethylene glycol linker. Initial attempts were carried out with tetraethylene glycol (**151**) (**Scheme 3.17.2**). Mesylation of glycol **151** proceeded at room temperature with methanesulfonyl chloride and triethylamine. Unfortunately, reaction of the crude mesylate with sodium azide gave no trace of the desired product. It was hypothesised

that the lack of success in this reaction could be attributed to the quality of the methanesulfonyl chloride used. This procedure was repeated with fresh methanesulfonylchloride, to give the crude mesylate, but again, no product could be detected.

In an attempt to synthesise the more stable intermediate, tetraethylene glycol (**151**) was reacted with *para*-toluenesulfonyl chloride and sodium hydroxide (**Scheme 3.17.2**).[88] Disappointingly, this reaction also failed to generate any of the desired product.

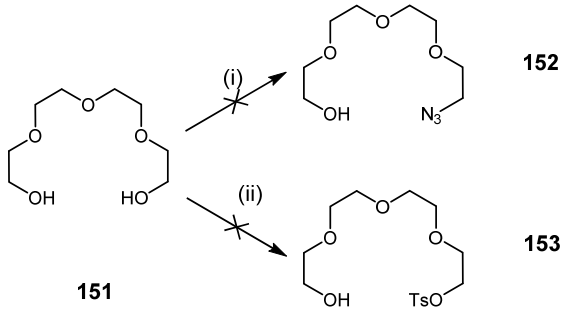


**Scheme 3.17.2**: Attempted Synthesis of Azide **152** and Tosylate **153**. *Reagents and Conditions*: (i) MsCl, $Et_3N$, THF; $NaN_3$, EtOH (ii) TsCl, $NEt_3$, DCM.

Faced with a lack of success using tetraethylene glycol, it was decided to switch to triethylene glycol based on the work of Jeong and O'Brien. Thus, triethylene glycol was treated with methanesulfonyl chloride and triethylamine, for eighteen hours followed by addition of sodium azide and ethanol (**Scheme 3.17.3**).[89] Thin layer chromatography highlighted one product with a higher Rf than the starting alcohol **154**, which was then found to be the cyclisation product **156**.

To reduce the possibility of self cyclisation of intermediate (**155**) the reaction was repeated, allowing mesylate **155** only ten minutes to form before the reaction mixture was concentrated and taken onto the azide formation. This approach was successful in forming the desired azide albeit in low yield (17%). The aqueous work up used to remove the sodium azide residues was believed to be responsible for the low yield of this reaction. Indeed, the removal of the aqueous work up step resulted in a vastly improved yield (81%). Flash column chromatography was time consuming due to close running impurities, however, this was circumnavigated by carrying the crude product onto the subsequent protection (61%). The reduction of the protected azide proceeded with ammonium formate. Purification of amine **149** also required significant optimisation, however, it was possible to isolate **149** in 45% yield from alcohol **154**.

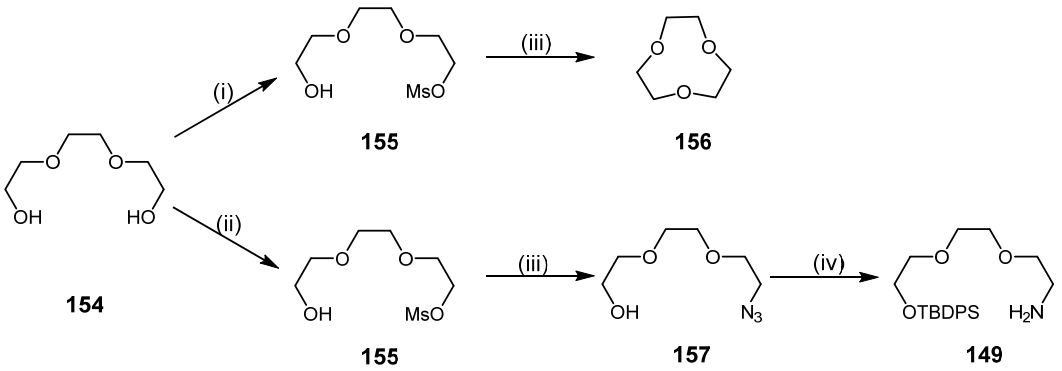


**Scheme 3.17.3:** Synthesis of Amine **149**. *Reagents and Conditions*: (i) MsCl, $Et_3N$, THF, overnight; (ii) MsCl, $Et_3N$, THF (10 mins); (iii) $NaN_3$, EtOH 70 °C (**157**, 81%); (iv) TBDPSCl, DCM, $NEt_3$ (61%) then Pd/C, $NH_4CO_2$, MeOH (91%).

Reductive amination of aldehyde **18** with the amine **149** proceeded cleanly and in good yield with sodium cyanoborohydride (70%) (**Scheme 3.17.4**). Subsequent protection of benzylic amine **158** proceeded in 80% yield, this relatively average protection yield could be explained by the instability of the reductive amination product. Hydrogenation and subsequent *N*-alkylation proceeded in 36% yield over two steps. Finally, deprotection and cyclisation of **(*S*)-159** were effective in synthesising the desired IGD peptidomimetic **(*S*)-145** in 62% yield over two steps, thus, completing the synthesis of the IGD peptidomimetic with a ethylene glycol based synthetic handle. Unfortunately, handling error led to the loss of this compound before full characterisation could take place, however, mass spectrometry showed the desired mass.

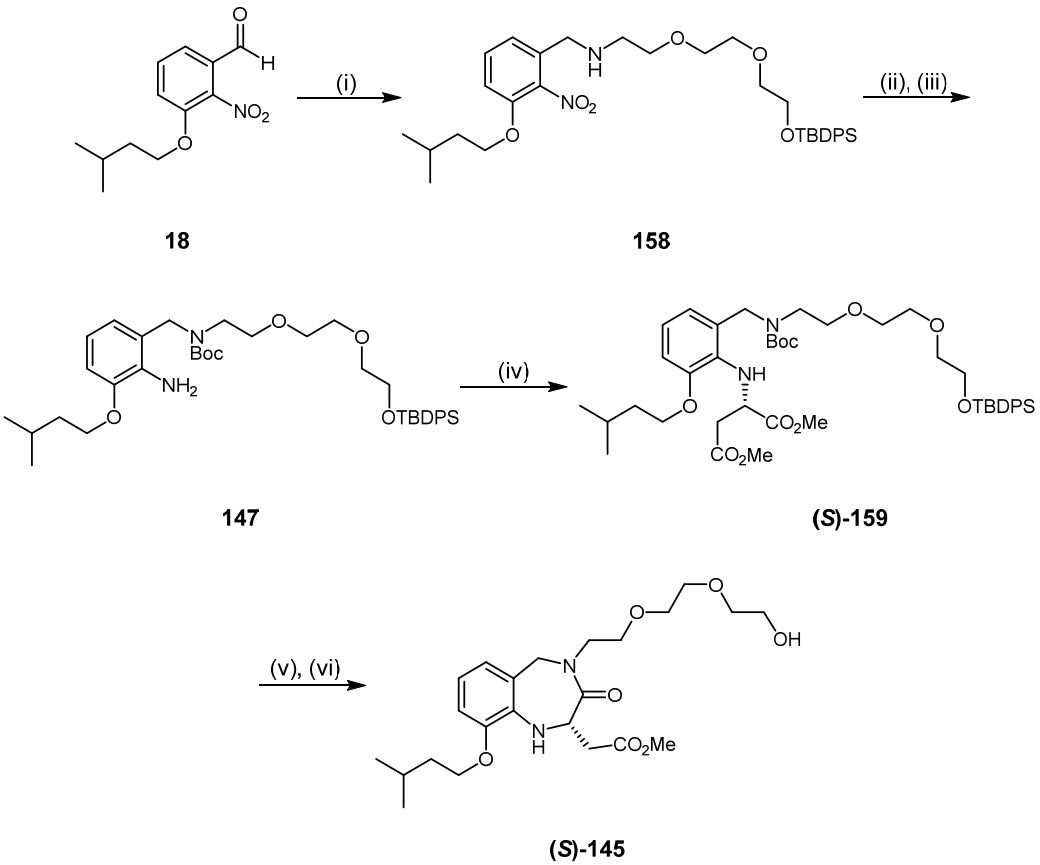


**Scheme 3.17.4**: Synthesis of IGD Peptidomimetic with Ethylene Glycol Chain. *Reagents and conditions*: (i) **149**, heptane, $NaBH_3CN$, 80 °C; (ii) $Boc_2O$, DCM, $NEt_3$; (iii) Pd/C, $NH_4CO_2$, MeOH; (iv) **(*R*)-20**, 2,6-lutidine, DCM; (v) TFA, DCM; (vi·) SCX, 7 M $NH_3$/MeOH, MeOH (62%).

## 4.0 Future Directions and Conclusions

### 4.1 Methyl IGD Peptidomimetics

In conclusion, the synthesis of the methyl IGD peptidomimetics has been optimised with the development of a novel route to key intermediate **18**. This new route is able to generate multigram amounts of material quicky and efficiently with minimal purification (**Scheme 4.1.1**).

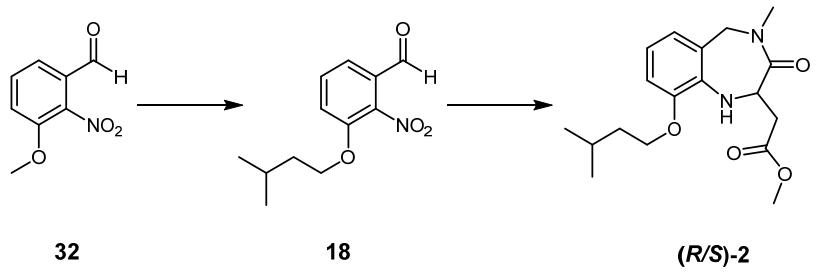


**32** **18** **(*R/S*)-2**

**Scheme 4.1.1**: Route to Methyl IGD peptidomimetic via intermediate **18.**

The biological activity of (*R*)-methyl IGD peptidomimetic has been corroborated *via* scratch assays. Work will continue to build upon the knowledge gained from the qRT-PCR experiments carried out. The results gained showed the upregulation of ACTN3 and IGF1 in human dermal neonatal fibroblasts treated with (*R*)-methyl IGD peptidomimetic compared to those treated with the (*S*)-enantiomer.

Further qRT-PCR work would be valuable for this project. The repetition of the Human Cell Motility microarray with cells treated with the (*R*)-Methyl IGD peptidomimetic and (*S*)-Methyl IGD peptidomimetic could allow more confidence to be given to the displayed upregulation of the IGF1 gene. Arrays could be undertaken with cells treated with (*R*)-Methyl IGD peptidomimetic vs media only treatments, which may show more dramatic results. A particularly interesting future direction may be the analysis of gene regulation in diabetic fibroblasts treated with the (*R*)-Methyl IGD peptidomimetic. Further to this, arrays carried out with keratinocytes or endothelial cells may be valuable. This work could form the basis of a further collaboration with the Wright group.

Both (*R*) and (*S*)-Methyl IGD peptidomimetics have also been submitted to the Fraunhofer Institute for *in vitro* toxicology studies. Efforts are also under way to assess the blood clearance of the compounds in mice.

## 4.2 Pentyl IGD Peptidomimetics

The development of our optimised synthetic route also allowed the synthesis of alcohols **(R/S)-24** (*n* = 1) and **(R/S)-26** (*n* = 3) from intermediate **18** (**Scheme 4.2.1**). Yields were particularly good with **(R)-26** being synthesized in 61% from intermediate **18**. The synthesis of tosylate **(R/S)-47**, azide **(R/S)-45**, amine **(R/S)-40** and alkyne **(R/S)-114** were also achieved starting from the hydroxyl derivative..

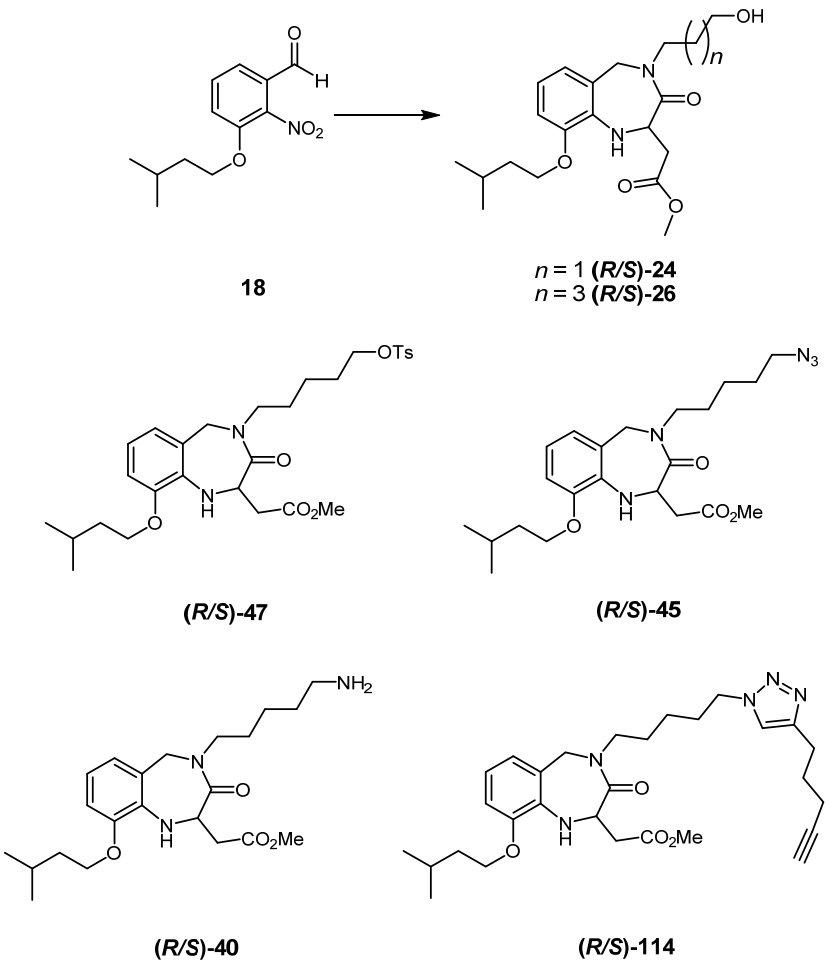


**Scheme 4.2.1:** Synthesis of Alcohol Alkyl Chain Containing IGD Peptidomimetics and Analogues.

## 4.3 BODIPY Tagged IGD Peptidomimetics

Functionalised IGD peptidomimetics were used to synthesise fluorescent tagged analogues (**Figure 4.3.1**). Amide **(*R*)-85** showed internalisation of the IGD peptidomimetic into mouse embryonic fibroblast, however, in order to have confidence in this result synthesis and testing of **MM-IGD-FL1** and **MM-IGD-FL2** was

undertaken. Testing of **MM-IGD-FL1** confirmed the internalisation of the molecule in human dermal neonatal fibroblasts, and indicated a possible endocytosis mechanism.

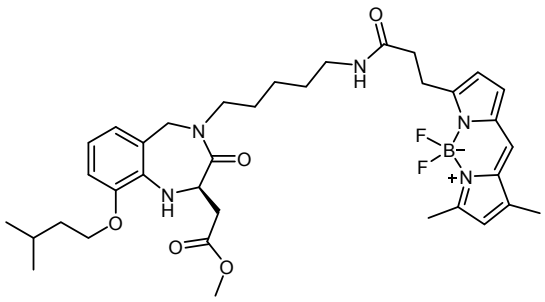

(*R*)-85

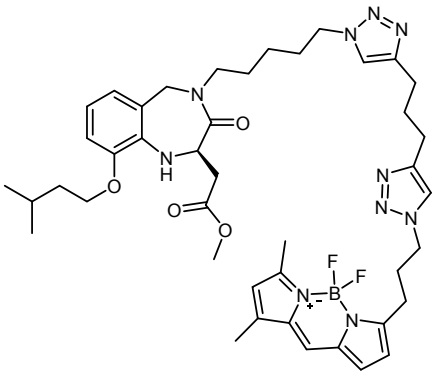

MM-IGD-FL-1

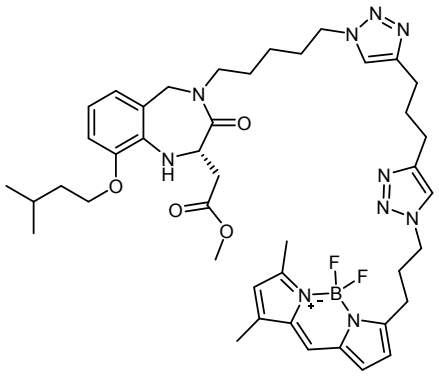

MM-IGD-FL-2

**Figure 4.3.1:** BODIPY tagged IGD Peptidomimetics.

## 4.4 Difunctionalised BODIPY Tagged IGD Peptidomimetics

In order to obtain stable and useful molecular probes, several novel BODIPY species were synthesised (**Figure 4.4.1**) during these investigations. It is likely that difunctionalised species **118** will be the most valuable in synthesising a fluorescent IGD peptidomimetic that can be further tagged onto a solid supports or other delivery vehicles.

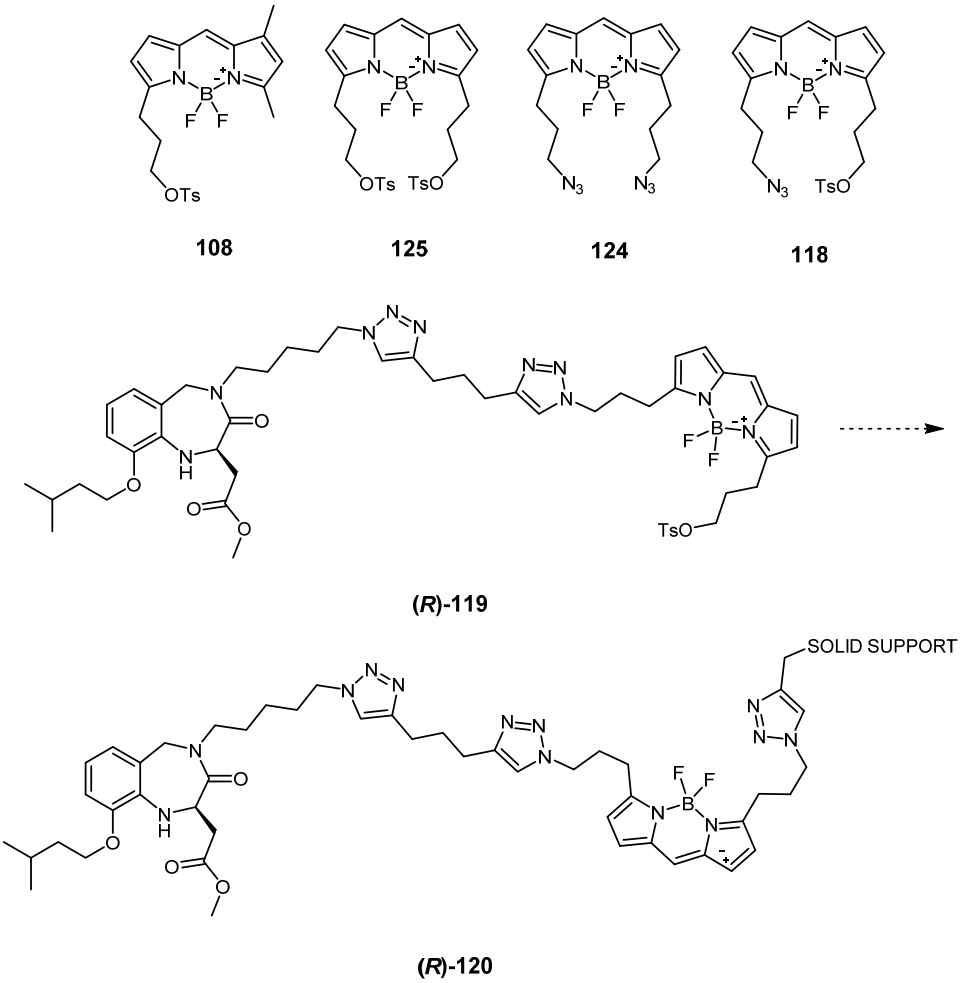


**Figure 4.4.1: Novel BODIPYs and Incorporation of (R)-45 onto a Solid Support**

## 4.5 Triethylene Glycol IGD Peptidomimetic

Having established a reliable synthesis of an IGD peptidomimetic with increased hydrophilicity **(*S*)-145** (**Scheme 4.5.1**) work should proceed towards the synthesis of the corresponding amine **(*S*)-143**. Focus would then be directed towards the synthesis of the desired hydrogel building block **(*S*)-140**.

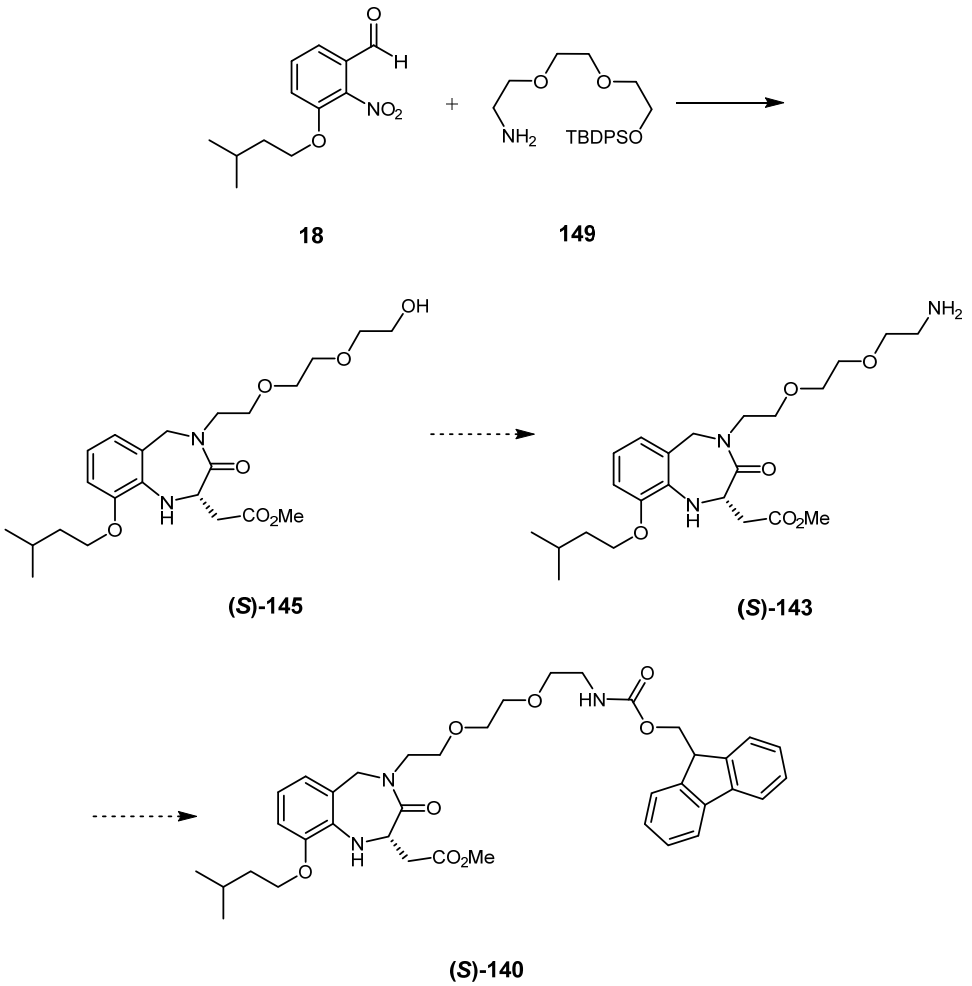


**Scheme 4.5.1**: Further Development of Alcohol **(*S*)-145**.

4.6 Biotinylated IGD Peptidomimetic

The biotinylation of small molecules, used in conjunction with avidin/streptavidin pull down and SDS-PAGE experiments, is an incredibly useful tool for the indentification relevant cellular binding sites.[90] In future work, efforts should be directed towards the biotinylation of azide **(R/S)-45** as a priority (**Scheme 4.5.1**).[91] Biotinylated IGD peptidomimetic **(R/S)-160** would be a very exciting compound and could be instrumental in helping to elucidate the biological target of the peptidomimetics.

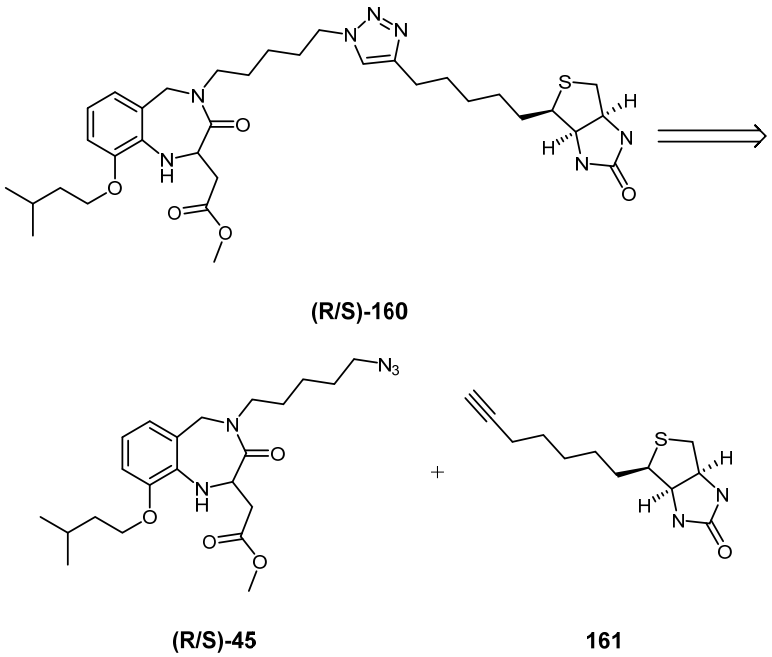


**Scheme 4.5.1:** Retrosynthetic Analysis of Biotinylated IGD Peptidomimetic.

.

# 5.0 EXPERIMENTAL

## 5.1. Chemistry General Information

Reactions involving air sensitive reagents and anhydrous solvents were performed in glassware dried in an oven (130 °C). These reactions were carried out with the exclusion of air using an argon atmosphere. Tetrahydrofuran, diethyl ether, and dichloromethane were purified through a Pure Solv 400-5 MD solvent purification system. Solvents were evaporated under reduced pressure at 40 °C using a Büchi Rotavapor.Column chromatography was performed under pressure using silica gel (Fluoro Chem Silica LC 60A) as the stationary phase and HPLC grade solvents as eluent. Reactions were monitored by thin layer chromatography. TLC was performed on aluminium sheets pre-coated with silica gel (Merck Silica Gel 60 $F_{254}$). The plates were visualised by the quenching of UV fluorescence ($\lambda_{max}$254 nm) and/ or by staining with anisaldehyde.

Proton magnetic resonance ($^{1}$H-NMR) spectra were recorded on a Bruker DPX Avance400 instrument at 400 MHz or at 500 MHz using Bruker DPX Avance500. Chemical shifts (δ) are recorded as parts per million and are referenced to the appropriate residual solvent peak. Signals in NMR spectra are described as singlet (s), doublet (d), triplet (t), quartet (q), multiplet (m), broad (br) or a combination of these terms which refer to the spin-spin coupling pattern observed. $^{13}$C NMR were recorded at 100 MHz or at 125 MHz using Bruker DPX Avance500. DEPT 135, DEPT 90 and two-dimensional (COSY, HSQC) NMR spectroscopy were used in novel compounds to assist in the assignment of signals in the $^{1}$H and $^{13}$C NMR spectra. Structures have been given an arbitrary numbering system to enable $^{1}$H and $^{13}$C NMR assignment.

IR spectra were obtained employing a Golden Gate™ attachment that uses a type IIa diamond as a single reflection element so that the IR spectrum of the compound (solid or liquid) could be detected directly (thin layer) without any sample preparation (Shimadzu FTIR-8400). Only significant absorptions are reported in wavenumbers with the following terms to describe intensity: w (weak), m (medium) or s (strong). High resolution mass spectra were recorded by the analytical services at the University of Glasgow on a JEOL JMS-700 mass spectrometer by electrospray and chemical ionisation operating at a resolution of 15000 full widths at half height. Melting points were recorded on a Stuart Scientific Melting Point SMPI apparatus and are uncorrected.

5.2 Reaction Procedures and Compound Analysis

2-Methyl-6-(3-Methylbutoxy)nitrobenzene

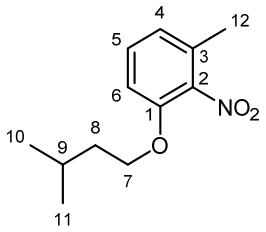


**27**

3-Methyl-2-nitrophenol (2.00 g, 13.1 mmol, 1.0 eq.) was dissolved in dimethylformamide (50 mL) giving a light yellow solution. Potassium carbonate (3.62 g, 26.2 mmol, 2.0 eq.) and 1-bromo-3-methyl butane (4.70 mL, 39.3 mmol, 3.0 eq.) were added to the solution which was allowed to stir at room temperature for 48 h. The reaction mixture was quenched with water (50 mL), diluted with ethyl acetate (100 mL) and allowed to stir for 20 min. The phases were separated and the aqueous layer was extracted with ethyl acetate (3 × 50 mL). The combined organic layers were washed with water (50 mL), brine (50 mL), dried ($Na_2SO_4$), filtered and evaporated *in vacuo* giving the title compound as a brown oil (2.59 g, 11.6 mmol, 89%).

$^1$H NMR ($CDCl_3$, 400 MHz) δ: 7.29 (1H, t, *J* = 8.1 Hz, $C_{(5)}$**H**), 6.88 (1H, d, *J* = 8.4 Hz, $C_{(4)}$**H**), 6.83 (1H, *J* = 7.7 Hz, $C_{(6)}$**H**), 4.08 (2H, t, *J* = 6.6 Hz, $C_{(7)}$**H$_2$**), 2.30 (3H, s, $C_{(12)}$**H$_3$**), 1.80 (1H, apparent septet, *J* = 6.7 Hz, $C_{(9)}$**H**), 1.66 (2H, q, *J* = 6.7 Hz, $C_{(8)}$**H$_2$**), 0.95 (6H, d, *J* = 6.7 Hz $C_{(10)}$**H$_3$** + $C_{(11)}$**H$_3$**). $^{13}$C NMR ($CDCl_3$, 100 MHz) δ: 150.3 (**C**$_{(1)}$), 142.3 (**C**$_{(2)}$), 130.8 (**C**$_{(3)}$), 130.6 (**C**$_{(5)}$), 122.3 (**C**$_{(4)}$), 110.9 (**C**$_{(6)}$), 67.8 (**C**$_{(7)}$), 37.5 (**C**$_{(8)}$), 24.9 (**C**$_{(9)}$), 22.4 (**C**$_{(10)}$ + **C**$_{(11)}$), 16.9 (**C**$_{(12)}$). HRMS (EI+) calcd for $C_{12}H_{17}NO_3$ [$M^+$]: *m*/*z* 223.2719, found *m*/*z* 223.2727. $\nu_{max}$ ($CDCl_3$)/$cm^{-1}$: 2957.0 (m), 1612 (w), 1583 (m), 1529.6 (s), 1086 (s).

2-Methyl-6-(3-Methylbutoxy)aniline

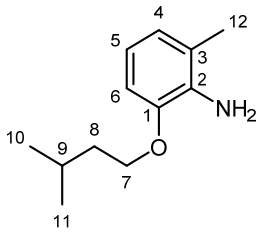


**29**

Nitro-benzene **27** (1.00 g, 4.48 mmol, 1.0 eq.), was dissolved in methanol (30 mL). Ammonium formate (2.83 g, 44.8 mmol, 10 eq.) and 10% palladium on activated charcoal (30 mg) were added to the mixture which was allowed to stir at 50 ºC for 16

h. The reaction mixture was filtered through celite, and washed with methanol (60 mL). The combined organics were evaporated *in vacuo* giving the title compound (0.73 g, 3.81 mmol, 85%).

$^1$H NMR ($CDCl_3$, 400 MHz): 6.70-6.62 (3H, m, $C_{(4)}$**H** + $C_{(5)}$**H** + $C_{(6)}$**H**), 4.01 (2H, t, *J* = 6.6 Hz, $C_{(7)}$**H**$_2$), 3.75 (2H, br. s, N**H**$_2$), 2.18 (3H, s, $C_{(12)}$**H**$_3$), 1.85 (1H, apparent septet, $C_{(9)}$**H**), 1.70 (2H, q, *J* = 6.7 Hz, $C_{(8)}$**H**$_2$), 0.96 (6H, d, *J* = 6.6 Hz, $C_{(10)}$**H**$_3$ + $C_{(11)}$**H**$_3$). $^{13}$C NMR ($CDCl_3$, 100 MHz): 146.4 (**C**$_{(1)}$), 134.3 (**C**$_{(2)}$), 122.6 (**C**$_{(3)}$), 122.4 (**C**$_{(4)}$), 117.6 (**C**$_{(5)}$), 109.0 (**C**$_{(6)}$), 66.7 (**C**$_{(7)}$), 38.2 (**C**$_{(8)}$), 25.2 (**C**$_{(9)}$), 22.7 (**C**$_{(10)}$ + **C**$_{(11)}$), 17.2 (**C**$_{(12)}$). HRMS (CI) calcd for $C_{12}H_{20}NO$ [M+H$^+$]: *m*/*z* 194.2969, found *m*/*z* 194.2980. $\nu_{max}$ ($CDCl_3$)/cm$^{-1}$: 3475 (w), 3381 (w), 2955 (s), 1616 (m), 1489 (s).

3-(3'-Methylbutoxy)benzaldehyde

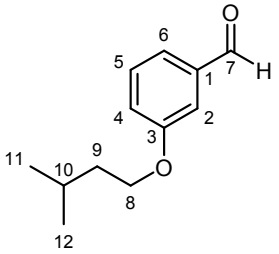


**17**

3-Hydroxybenzaldehyde (15.0 g, 123 mmol, 1.0 eq.) was dissolved in anhydrous dimethylformamide (600 mL) under argon giving a light yellow solution. Potassium carbonate (33.9 g, 246 mmol, 2.0 eq.) was added to the solution and the resulting mixture was allowed to stir for 25 min giving a yellow cloudy mixture. 1-Bromo-3-methyl butane (44.1 mL, 368 mmol, 3.0 eq.) was added to the mixture which was allowed to stir for 24 h giving a cream cloudy mixture. The reaction mixture was slowly added to water (600 mL) (Caution: exotherm). Ethyl acetate (400 mL) was added and the biphasic mixture was allowed to stir for 20 min. The phases were separated and the aqueous layer was extracted with ethyl acetate (2 × 400 mL). The combined organic layers were washed with water (400 mL), brine (400 mL), dried ($Na_2SO_4$) and concentrated *in vacuo* giving the title compound as a light coloured oil (19.6 g, 102 mmol, 83%).

$^1$H NMR ($CDCl_3$, 400 MHz): 9.89 (1H, s, $C_{(7)}$**H**O), 7.38-7.36 (2H, m, $C_{(5)}$**H** + $C_{(6)}$**H**), 7.31 (1H, m, $C_{(2)}$**H**), 7.11-7.09 (1H, m, $C_{(4)}$**H**), 3.97 (2H, t, *J* = 6.8 Hz, $C_{(8)}$**H**$_2$), 1.80-1.74 (1H, apparent sept., *J* = 6.8 Hz, $C_{(10)}$**H**), 1.65-1.60 (2H, apparent q, *J* = 6.6 Hz, $C_{(9)}$**H**$_2$), 0.89 (6H, d, *J* = 6.9 Hz, $C_{(11)}$**H**$_3$ + $C_{(12)}$**H**$_3$). $^{13}$C NMR ($CDCl_3$, 125 MHz): 192.3 (**C**$_{(7)}$), 159.7 (**C**$_{(1)}$), 137.7 (**C**$_{(3)}$), 130.0 (**C**$_{(5)}$), 123.4 (**C**$_{(4/6)}$), 122.0 (**C**$_{(4/6)}$)), 112.7 (**C**$_{(2)}$), 66.7 (**C**$_{(8)}$), 37.8 (**C**$_{(9)}$), 24.7 (**C**$_{(10)}$), 22.9 (**C**$_{(11)}$ + **C**$_{(12)}$ ). LRMS (EI+) calcd for $C_{12}H_{16}O_2$

[$M^+$]: *m*/*z* 192.12, found *m*/*z* 192.16. $\nu_{max}$ ($CDCl_3$)/$cm^{-1}$: 2956 (m), 1696 (s), 1260 (s), 909 (m), 751 (s).

3-Hydroxy-2-nitrobenzaldehyde[32]

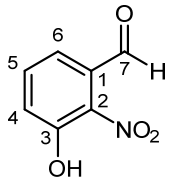


**5**

3-Methoxy-2-nitrobenzaldehyde (0.50 g, 2.76 mmol, 1.0 eq.) was dissolved in anhydrous dichloromethane (10 mL) and cooled to 0 ºC. A solution of boron tribromide (1 M in dichloromethane, 8.4 mL, 8.4 mmol, 3.0 eq.) was added dropwise to the solution, the reaction mixture was allowed to warm to room temperature and stirred for 1 h. The reaction mixture was syringed into ice water (100 mL). The phases were separated and the aqueous phase was extracted with chloroform (3 × 25 mL). The combined organic layer was dried ($Na_2SO_4$), filtered and concentrated *in vacuo* giving the title compound as a dark brown solid (0.42 g, 2.5 mmol, 89%).

$^1$H NMR ($CDCl_3$, 400 MHz) δ: 10.35 (1H, s, $C_{(7)}$**H**), 10.25 (1H, s, O**H**), 7.60 (1H, t, *J* = 7.6 Hz, $C_{(5)}$**H**), 7.31 (1H, dd, *J* = 8.5, 1.4 Hz, $C_{(6)}$**H**), 7.25 (1H, dd, *J* = 7.4, 1.4, $C_{(4)}$**H**). $^{13}$C NMR ($CDCl_3$, 125 MHz) δ: 187.9 (**C**$_{(7)}$), 155.0 (**C**$_{(3)}$), 136.6 (**C**$_{(5)}$), 136.6 (**C**$_{(2)}$), 135.0 (**C**$_{(1)}$), 124.3 (**C**$_{(6)}$), 121.5 (**C**$_{(4)}$). HRMS (CI+) calcd for $C_7H_6NO_4$ [$M+H^+$]: *m*/*z* 168.1289, found *m*/*z* 168.1291. $\nu_{max}$ ($CDCl_3$)/$cm^{-1}$: 3218 (s), 1678 (s), 1529 (s), 1313 (s). M.P. 156-158 ºC.[92]

3-(3-Methylbutoxy)-2-nitrobenzaldehyde

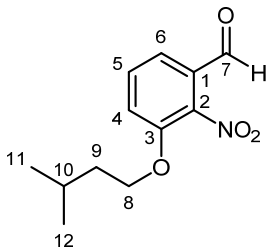


**18**

From 3-Hydroxy-2-nitrobenzaldehyde:

3-Hydroxy-2-nitrobenzaldehyde (3.40 g, 20.0 mmol, 1.0 eq.) was dissolved in anhydrous dimethylformamide (100 mL) under argon giving a light brown solution. Potassium carbonate (5.52 g, 40.0 mmol, 2.0 eq.) was added to the solution and the resulting mixture was allowed to stir for 25 min giving a yellow cloudy mixture. 1-Bromo-3-methyl butane (7.20 mL, 60.0 mmol, 3.0 eq.) was added to the mixture which

was allowed to stir for 24 h. The reaction mixture was slowly added to water (600 mL) (Caution: exotherm). Ethyl acetate (400 mL) was added and the biphasic mixture was allowed to stir for 20 min. The phases were separated and the aqueous layer was extracted with ethyl acetate (2 × 400 mL). The combined organic layer was washed with water (400 mL), brine (400 mL), dried ($Na_2SO_4$) and concentrated *in vacuo* giving the title compound as a light yellow oil (3.90 g, 16.5 mmol, 82%).

From 3-(3-Methylbutoxy)benzaldehyde:

3-(3-Methylbutoxy)-benzaldehyde (4.82 g, 25.1 mmol, 1.0 eq.) was dissolved in anhydrous dichloromethane (150 mL) under argon and the mixture was cooled to -25 ºC. Nitronium tetrafluoroborate (5.00 g, 37.6 mmol, 1.5 eq.) was added in one portion and the light yellow solution was allowed to stir at -25 ºC for 5 h. The reaction mixture was quenched with water (100 mL), the phases were separated and the aqueous layer was extracted with ethyl acetate (3 × 60 mL). The combined organic layer was washed with brine (60 mL), dried ($Na_2SO_4$) and concentrated *in vacuo*. The crude mixture was purified by column chromatography (0-15% ethyl acetate in petroleum ether) giving the title compound as a yellow, oily solid (1.54 g, 6.5 mmol, 26%).

$^1$H NMR ($CDCl_3$, 400 MHz): 9.85 (1H, s, $C_{(7)}$**H**O), 7.30 (1H, t, *J* = 8.2 Hz, $C_{(5)}$**H**), 7.40 (1H, dd, *J* = 7.7, 1.0 Hz, $C_{(6)}$**H**), 7.27 (1H, dd, *J* = 8.3, 1.0 Hz, $C_{(4)}$**H**), 4.06 (2H, t, *J* = 6.5 Hz, $C_{(8)}$**H$_2$**), 1.82 (1H, apparent septet, *J* = 6.87 Hz, $C_{(10)}$**H**), 1.62 (2H, apparent q, *J* = 6.47 Hz, $C_{(9)}$**H$_2$**), 0.86 (6H, d, *J* = 6.92 Hz, $C_{(11)}$**H$_3$** + $C_{(12)}$**H$_3$**). $^{13}$C NMR ($CDCl_3$, 125 MHz): 187.0 (**C**$_{(7)}$), 150.6 (**C**$_{(3)}$), 140.3 (**C**$_{(2)}$), 131.3 (**C**$_{(5)}$), 128.0 (**C**$_{(1)}$), 122.0 (**C**$_{(6)}$), 119.7 (**C**$_{(4)}$), 68.5 (**C**$_{(8)}$), 37.3 (**C**$_{(9)}$), 24.8 (**C**$_{(10)}$), 22.5 (**C**$_{(11)}$ + **C**$_{(12)}$). HRMS (EI+) calcd for $C_{12}H_{15}O_4N$ [$M^+$]: *m*/*z* 237.2554, found *m*/*z* 237.2560. $\nu_{max}$ ($CDCl_3$)/cm$^{-1}$: 2958 (m), 1770 (m), 1546 (s), 1286(s), 908 (s).

(*S*)-2-Trifluoromethanesulfonyloxy-succinic acid dimethyl ester[27]

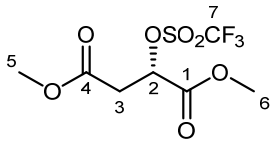


**(*S*)-20**

Dimethyl-(*S*)-(-)-malate (1.70 mL, 11.8 mmol, 1.0 eq) was dissolved in anhydrous dichloromethane (25 mL). 2,6-Lutidine (2.60 mL, 22.4 mmol, 1.9 eq.) was added and the solution was allowed to stir at -78 ºC for 20 min. Trifluoromethanesulfonic anhydride (5.90 g, 17.7 mmol, 1.5 eq.) was dissolved in dichloromethane (25 mL) and added dropwise to the solution which was allowed to stir at -78 ºC for 1 hour. The reaction mixture was quenched with water (50 mL) and was allowed to warm to room

temperature. The phases were separated and the organic phase was washed with copper sulfate (aq. sat.) (3 × 50 mL), dried ($Na_2SO_4$) and concentrated *in vacuo* giving the title compound as a light coloured oil (3.66 g, 11.8 mmol, quantitative).

$^1$H NMR ($CDCl_3$, 400 MHz) δ: 5.50 (1H, t, *J* = 5.9 Hz, $C_{(2)}$**H**), 3.88 (3H, s, $C_{(6)}$**H**$_3$), 3.77 (3H, s, $C_{(5)}$**H**$_3$), 3.07 (2H, d, *J* = 5.9 Hz, $C_{(3)}$**H**$_3$) $^{13}$C NMR ($CDCl_3$, 125 MHz) δ: 167.9 (**C**$_{(1)}$), 166.5 (**C**$_{(3)}$), 118.6 (**C**$_{(7)}$), 78.5 (**C**$_{(2)}$), 53.7 (**C**$_{(5/6)}$), 52.6 (**C**$_{(5/6)}$), 36.6 (**C**$_{(3)}$). $\nu_{max}$ ($CDCl_3$)/cm$^{-1}$: 1743.7 (s), 1419.7 (s), 1203.6 (s), 1141.9 (s).

(*R*)-2-Trifluoromethanesulfonyloxy-succinic acid dimethyl ester[27]

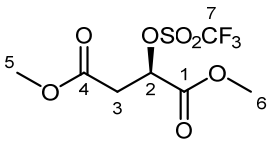


**(*R*)-20**

**(*R*)-20** was synthesised *via* the method described above in quantitative yield.

3-(*tert*-Butyldiphenyl silanyloxy)-propylamine [54]

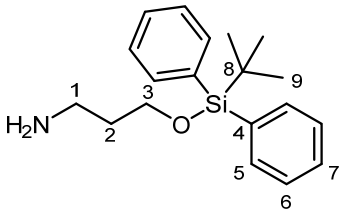


**68**

3-Aminopropanol (1.50 mL, 19.6 mmol, 2.5 eq.) was dissolved in dichloromethane (30 mL) and the mixtue was cooled to 0 ºC. *t*-Butyldiphenylsilyl chloride (2.00 mL, 7.80 mmol, 1.0 eq.) was dissolved in dichloromethane (5 mL) and slowly added to the solution. Triethylamine (1.20 mL, 11.8 mmol, 1.5 eq.) was added, and the reaction mixture was allowed to warm to room temperature and stir for 3 h. The reaction mixture was then acidified with 1 M hydrochloric acid (aq.) solution (25 mL) and the phases were separated. The organic layer was washed with sodium bicarbonate (aq. sat.) (25 mL), brine (25 mL), dried ($Na_2SO_4$), and concentrated *in vacuo* giving the title compound (2.08 g, 6.62 mmol, 85%).

$^1$H NMR ($CDCl_3$, 400 MHz): 7.60-7.57 (4H, m, **4** × $C_{(5)}$**H**), 7.34-7.26 (6H, m, **4** × $C_{(6)}$**H** + **2** × $C_{(7)}$**H**), 3.65 (2H, t, *J* = 6.0 Hz, $C_{(3)}$**H**$_2$), 2.75 (2H, t, *J* = 6.8 Hz, $C_{(1)}$**H**$_2$), 1.74 (2H, broad singlet, N**H**$_2$), 1.64-1.58 (2H, apparent quintet, *J* = 6.5 Hz, $C_{(2)}$**H**$_2$), 0.97 (9H, s, **3** × $C_{(9)}$**H**$_3$). $^{13}$C NMR ($CDCl_3$, 100 MHz): 135.7 (**4** × **C**$_{(5)}$), 133.8 (**2** × **C**$_{(4)}$), 129.6 (**2** × **C**$_{(7)}$), 127.7 (**4** × **C**$_{(6)}$), 61.9 (**C**$_{(3)}$), 39.3, (**C**$_{(1)}$), 36.0 (**C**$_{(2)}$), 26.9 (**3** × **C**$_{(9)}$), 19.2 (**C**$_{(8)}$). LRMS (FAB+) calcd for $C_{19}H_{27}NOSi$ [$(M+H)^+$]: *m*/*z* 314.5, found *m*/*z* 314.2. $\nu_{max}$ ($CDCl_3$)/cm$^{-1}$: 3071 (w), 2930 (m), 1589 (m), 1105 (s), 730 (s), 699 (s).

3-(*tert*-Butyldiphenyl silanyloxy)propyl-[3-(3-methylbutoxy)-2-nitrobenzyl]-amine

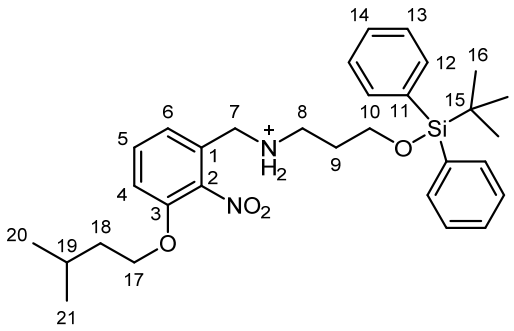


**64**

Nitrobenzaldehyde **18** (0.85 g, 3.60 mmol, 1.0 eq.) was dissolved in heptane (20 mL) and amine **68** (1.68 g, 5.40 mmol, 1.5 eq.) was added. The reaction mixture was allowed to stir for 48 h, concentrated *in vacuo* and dissolved in methanol (20 mL). Sodium borohydride (0.20 g, 5.40 mmol, 1.5 eq.) was added and the solution was allowed to stir for 12 h. The reaction mixture was quenched by the addition of water (20 mL), ethyl acetate (20 mL) was added and the phases separated. The aqueous layer was extracted with ethyl acetate (2 × 20 mL). The combined organic layer was washed with brine (20 mL), dried ($Na_2SO_4$), and concentrated *in vacuo*. The resulting mixture was purified by flash column chromatography (0-20% ethyl acetate in petroleum ether) giving the title compound as a yellow oil (1.76 g, 3.40 mmol, 94%).

$^1$H NMR ($CDCl_3$, 400 MHz) δ: 7.59-7.57 (4H, m, **4** × $C_{(12)}$**H**), 7.36-7.26 (7H, m, **4** × $C_{(13)}$**H** + **2** × $C_{(14)}$**H** + $C_{(5)}$**H**), 6.95 (1H, d, *J* = 8.0 Hz, $C_{(6)}$**H**), 6.84 (1H, d, *J* = 8.6 Hz, $C_{(4)}$**H**), 3.99 (2H, t, *J* = 6.8 Hz, $C_{(17)}$**H$_2$**), 3.66-3.63 (4H, apparent t, *J* = 4.9 Hz, $C_{(10)}$**H$_2$** + $C_{(7)}$**H$_2$**), 2.64 (2H, t, *J* = 7.4 Hz, $C_{(8)}$**H$_2$**), 1.74-1.57 (6H, m, N**H** + $C_{(18)}$**H$_2$** + $C_{(19)}$**H** + $C_{(9)}$**H$_2$**), 0.95 (9H, s, **3** × $C_{(16)}$**H$_3$**), 0.87 (6H, d, *J* = 6.8 Hz, $C_{(20)}$**H$_3$** + $C_{(21)}$**H$_3$**). $^{13}$C NMR ($CDCl_3$, 125 MHz) δ: 150.3 (**C**$_{(3)}$), 141.5 (**C**$_{(2)}$), 135.6 (**4** × **C**$_{(12)}$), 133.8 (**2** × **C**$_{(11)}$), 133.7 (**C**$_{(1)}$), 130.8 (**C**$_{(5)}$), 129.6 (**2** × **C**$_{(14)}$), 127.6 (**4**× **C**$_{(13)}$), 121.1 (**C**$_{(6)}$), 112.0 (**C**$_{(4)}$), 67.9 (**C**$_{(17)}$), 62.3 (**C**$_{(10)}$), 49.2 (**C**$_{(7)}$), 46.5 (**C**$_{(8)}$), 37.6 (**C**$_{(18)}$), 32.6 (**C**$_{(9)}$), 26.9 (**C**$_{(19)}$), 24.9 (**C**$_{(20)}$ + **C**$_{(21)}$), 22.5 (**3** × **C**$_{(16)}$), 19.2 (**C**$_{(15)}$). LRMS (FAB+) calcd for $C_{19}H_{27}NOSi$ [$(M+H)^+$]: *m*/*z* 535.3, found *m*/*z* 535.1. $\nu_{max}$ ($CDCl_3$)/cm$^{-1}$: 2962 (s), 1684 (m), 1533 (m), 1112 (m), 907 (s), 730 (s).

3-[(*tert*-butyldiphenylsilyl)oxy]propyl -[3-(3-methyl-butoxy)-2-nitro-benzyl]-carbamic acid *tert*-butyl ester

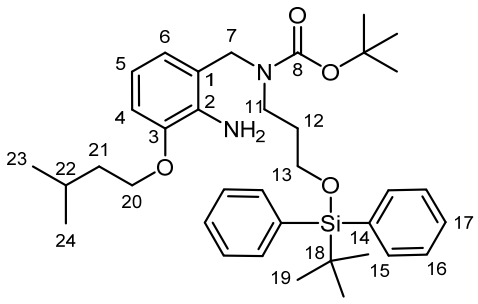

**80**

Amine **64** (2.10 g, 3.93 mmol, 1.0 eq.) was dissolved in anhydrous dichloromethane (100 mL), triethylamine (1.10 mL, 7.86 mmol, 2.0 eq.) was added and the solution was allowed to stir for 25 min. Di-*tert*-butyl dicarbonate (1.11 g, 5.09 mmol, 1.3 eq.) was added to the reaction mixture which was then allowed to stir for 16 h. The reaction mixture was quenched with water (75 mL), and diluted with dichloromethane (75 mL). The phases were separated and the aqueous layer was extracted with ethyl acetate (2 × 75 mL). The combined organic layer was then washed with brine (75 mL), dried ($Na_2SO_4$) and concentrated *in vacuo*. The crude mixture was purified by flash column chromatography (0-10% ethyl acetate in petroleum ether) giving the title compound as a light coloured oil (2.59 g, 3.93 mmol, quantitative).

$^1$H NMR ($CDCl_3$, 400 MHz) δ: 7.66-7.65 (4H, m, **4** × $C_{(15)}$**H**), 7.36-7.26 (7H, m, $C_{(5)}$**H** + **4** × $C_{(16)}$**H** + **2** × $C_{(17)}$**H**), 6.96-6.93 (2H, m, $C_{(4)}$**H** + $C_{(6)}$**H**), 3.99 (2H, $CH_2$, t, *J* = 6.8 Hz, $C_{(20)}$**H**$_2$), 3.66-3.63 (4H, apparent t, *J* = 4.9 Hz, $C_{(13)}$**H**$_2$ + $C_{(7)}$**H**$_2$), 2.63 (2H, t, *J* = 7.4 Hz, $C_{(11)}$**H**$_2$), 1.74-1.57 (5H, m, $C_{(12)}$**H**$_2$ + $C_{(21)}$**H**$_2$ + $C_{(22)}$**H**), 1.37 (9H, s, **3** × $C_{(10)}$**H**$_3$) 0.95 (9H, s, **3** × $C_{(19)}$**H**$_3$), 0.86 (6H, d, *J* = 6.8 Hz, $C_{(23)}$**H**$_3$ + $C_{(24)}$**H**$_3$). $^1$H NMR ($CDCl_3$, 400 MHz, 55 ºC) δ: 7.60-7.58 (4H, m, **4** × $C_{(15)}$**H**), 7.37-7.25 (7H, m, $C_{(5)}$**H** + **4** × $C_{(16)}$**H** + **2** × $C_{(17)}$**H**), 6.85 (2H, dd, *J* = 16.1, 8.4 Hz, $C_{(4)}$**H** + $C_{(6)}$**H**), 4.36 (2H, s, $C_{(7)}$**H**$_2$), 4.03 (2H, t, *J* = 6.4 Hz, $C_{(20)}$**H**$_2$), 3.63 (2H, t, *J* = 6.4 Hz, $C_{(13)}$**H**$_2$), 3.27 (2H, m, $C_{(11)}$**H**$_2$), 1.80 - 1.68 (3H, m, $C_{(12)}$**H**$_2$ + $C_{(22)}$**H**), 1.61 (2H, q, *J* = 6.8 Hz, $C_{(21)}$**H**$_2$), 1.37 (9H, s, **3** × $C_{(10)}$**H**$_3$), 1.00 (9H, s, **3** × $C_{(19)}$**H**$_3$), 0.89 (6H, d, *J* = 6.8 Hz, $C_{(23)}$**H**$_3$ + $C_{(24)}$**H**$_3$).$^{13}$C NMR ($CDCl_3$, 100 MHz, 55 ºC) δ: 155.5 (**C**$_{(3)}$), 150.5 (**C**$_{(8)}$), 141.4 (**C**$_{(2)}$), 135.5 (**4** × **C**$_{(15)}$), 133.9 (**2** × **C**$_{(14)}$), 132.1 (**C**$_{(1)}$), 130.7 (**C**$_{(5)}$), 129.5 (**2** × **C**$_{(17)}$), 127.6 (**4** × **C**$_{(16)}$), 119.6 (**C**$_{(6)}$), 112.4 (**C**$_{(4)}$), 80.0 (**C**$_{(9)}$), 68.2 (**C**$_{(20)}$), 61.9 (**C**$_{(13)}$), 46.0 (**C**$_{(7)}$), 44.8 (**C**$_{(11)}$) 37.7 (**C**$_{(21)}$), 31.1 (**C**$_{(12)}$), 28.3 (**3** × **C**$_{(10)}$), 27.4 (**3** × **C**$_{(19)}$), 26.9 (**C**$_{(23/24)}$), 26.9 (**C**$_{(23/24)}$), 24.9 (**C**$_{(22)}$), 19.1 (**C**$_{(18)}$). $\nu_{max}$ ($CDCl_3$)/cm$^{-1}$: 2956 (m), 1740 (s), 1691 (s), 1534 (s), 1112 (m), 909 (s).

[2-Amino-3-(3-methyl-butoxy)-benzyl]-[3-[(*tert*-butyldiphenylsilyl)oxy]propyl]-carbamic acid *tert*-butyl ester

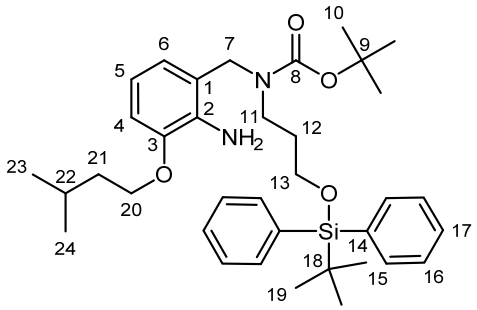

**62**

Nitrophenol **80** (0.45 g, 0.71 mmol, 1.0 eq.) was dissolved in anhydrous methanol (20 mL). Ammonium formate (0.45 g, 7.1 mmol, 10 eq.) was added to the solution. Palladium on activated charcoal (30 mg) was added and the mixture was heated to 35 ºC. After 48 h, the reaction mixture was filtered through celite and washed with ethyl acetate (150 mL). The filtrate was washed with water (150 mL) and the phases were separated. The aqueous phase was extracted with ethyl acetate (2 × 50 mL), the combined organic layer was then washed with brine, dried ($Na_2SO_4$) and filtered giving the title compound as a light red oil (0.32 g, 0.55 mmol, 76 %).

$^1$H NMR ($CDCl_3$, 400 MHz, 55 ºC) δ: 7.64-7.62 (4H, m, **4** × $C_{(15)}$**H**), 7.40-7.32 (6H, m, **4** × $C_{(16)}$**H** + **2** × $C_{(17)}$**H**), 6.71 (1H, apparent d, *J* = 8.0 Hz, $C_{(5)}$**H**), 6.62 (1H, apparent d, *J* = 7.5 Hz, $C_{(6)}$**H**), 6.52 (1H, t, *J* = 7.8 Hz, $C_{(4)}$**H**), 4.51 (2H, broad s, N**H**$_2$), 4.36 (2H, s, $C_{(7)}$**H**$_2$), 3.99 (2H, t, *J* = 6.6 Hz, $C_{(20)}$**H**$_2$), 3.63 (2H, t, *J* = 6.2 Hz, $C_{(13)}$**H**$_2$), 3.25-3.21 (2H, m, $C_{(11)}$**H**$_2$), 1.84 (1H, n, *J* = 6.8 Hz, $C_{(22)}$**H**), 1.76-1.67 (4H, m, $C_{(21)}$**H**$_2$ + $C_{(12)}$**H**$_2$), 1.43 (9H, s, **3** × $C_{(10)}$**H**$_3$), 1.05 (9H, s, **3** × $C_{(19)}$**H**$_3$), 0.96 (6H, d, *J* = 6.6 Hz, $C_{(23)}$**H**$_3$ + $C_{(23)}$**H**$_3$ ). $^{13}$C NMR ($CDCl_3$, 100 MHz) δ: 156.3 (**C**$_{(8)}$), 146.3 (**C**$_{(3)}$), 136.2 (**C**$_{(2)}$), 135.5 (**4** × **C**$_{(15)}$), 133.7 (**2** × **C**$_{(14)}$), 129.6 (**2** × **C**$_{(17)}$), 127.6 (**4** × **C**$_{(16)}$), 123.4 (**C**$_{(1)}$), 120.8 (**C**$_{(6)}$), 115.8 (**C**$_{(5)}$), 110.6 (**C**$_{(4)}$), 79.8 (**C**$_{(9)}$), 66.6 (**C**$_{(20)}$), 61.9 (**C**$_{(13)}$), 47.4 (**C**$_{(7)}$), 42.9 (**C**$_{(11)}$), 38.2 (**C**$_{(21)}$), 30.7 (**C**$_{(12)}$), 28.4 (**3** × **C**$_{(10)}$), 26.9 (**C**$_{(22)}$), 25.1 (**C**$_{(23)}$ + **C**$_{(24)}$), 22.6 (**C**$_{(18)}$), 19.2 (**3** × **C**$_{(19)}$). LRMS (CI+) calcd for $C_{36}H_{53}N_2O_4Si$ [M+H$^+$]: *m*/*z* 605.9, found *m*/*z* 605.7. $\nu_{max}$ ($CDCl_3$)/cm$^{-1}$: 2959 (m), 1668 (m), 1472 (m), 1106 (m).

(*R*)-Dimethyl 2-(2-((*tert*-butoxycarbonyl(3-(*tert*-butyldiphenyl silanyloxy)propyl)amino)methyl)-6-(isopentoxy)phenylamino)succinate

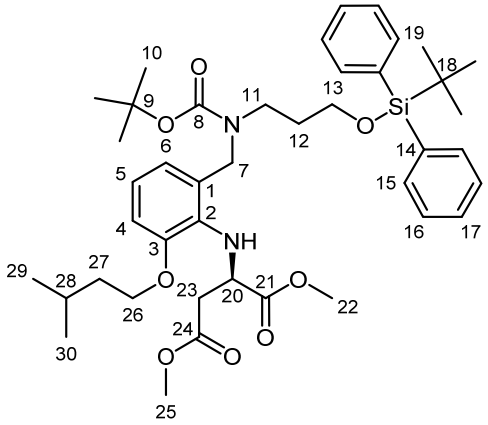

**(*R*)-60**

Aniline **62** (0.85 g, 1.40 mmol, 1.0 eq.) was dissolved in anhydrous dichloromethane (20 mL), 2,6-lutidine (0.32 mL, 2.80 mmol, 2.0 eq.) was added and the solution was allowed to stir at room temperature for twenty minutes. Triflate **(*S*)-20** (0.70 g, 2.38 mmol, 1.7 eq.) was dissolved in anhydrous dichloromethane (20 mL) and was added dropwise to the solution. The reaction mixture was heated to 45 ºC and stirred for 16 hours. The reaction mixture was then quenched with water (40 mL) and the phases were separated. The aqueous phase was extracted with dichloromethane (40 mL), and the combined organic layer was then washed with copper sulfate solution (aq. sat.) (3 × 40 mL), dried ($Na_2SO_4$), filtered and concentrated *in vacuo*. The crude mixture was purified by flash column chromatography (0-10% ethyl acetate in petroleum ether) giving the title compound as a clear oil (0.72 g, 0.96 mmol, 69%).

$^1$H NMR ($CDCl_3$, 400 MHz, 55 ºC) δ: 7.62-7.60 (4H, m, **4** × $C_{(15)}$**H**), 7.40-7.31 (6H, m, **4** × $C_{(16)}$**H** + **2** × $C_{(17)}$**H**), 6.81-6.74 (2H, m, $C_{(4)}$**H** + $C_{(5)}$**H**), 6.70-6.68 (1H, dd, *J* = 7.0, 1.6 Hz, $C_{(6)}$**H**), 4.65-4.61 (3H, m, $C_{(7)}$**H**$_2$ + $C_{(20)}$**H**), 4.33 (1H, d, *J* = 15.4 Hz, N**H**), 3.98 (2H, t, *J* = 6.9 Hz, $C_{(26)}$**H**$_2$), 3.63 (8H, $C_{(29)}$**H**$_3$ + $C_{(30)}$**H**$_3$+ $C_{(13)}$**H**$_2$), 3.20 (2H, m, $C_{(11)}$**H**$_2$), 2.82-2.79 (2H, m, $C_{(23)}$**H**$_2$), 1.83 (1H, nonet, *J* = 6.7 Hz, $C_{(28)}$**H**), 1.75-1.69 (4H, m, $C_{(27)}$**H**$_2$ + $C_{(12)}$**H**$_2$), 1.42 (9H, s, **3** × $C_{(10)}$**H**$_3$), 1.02 (9H, s, **3** × $C_{(19)}$**H**$_3$), 0.96 (6H, d, *J* = 6.6 Hz, $C_{(29)}$**H**$_3$ + $C_{(30)}$**H**$_3$ ).$^{13}$C NMR ($CDCl_3$, 100 MHz, 55 ºC) δ: 173.2 (**C**$_{(21)}$), 171.0 (**C**$_{(24)}$), 155.9 (**C**$_{(8)}$), 151.0 (**C**$_{(3)}$), 135.5 (**4** × **C**$_{(15)}$), 134.0 (**2** × **C**$_{(14)}$), 129.5 (**2** × **C**$_{(17)}$), 129.2 (**C**$_{(2)}$), 127.5 (**4** × **C**$_{(16)}$), 122.0 (**C**$_{(6)}$), 121.9 (**C**$_{(1)}$), 121.3 (**C**$_{(5)}$), 111.7 (**C**$_{(4)}$), 79.6 (**C**$_{(9)}$), 67.1 (**C**$_{(26)}$), 62.1 (**C**$_{(13)}$), 56.4 (**C**$_{(21)}$), 51.7 (**C**$_{(22)}$), 51.4 (**C**$_{(25)}$), 46.8 (**C**$_{(7)}$), 43.5 (**C**$_{(27)}$), 38.2 (**C**$_{(23)}$), 38.1 (**C**$_{(11)}$), 31.0 (**C**$_{(12)}$), 28.4 (**3** × **C**$_{(10)}$), 26.9 (**C**$_{(29)}$ + **C**$_{(30)}$), 25.2 (**C**$_{(28)}$), 22.5 (**C**$_{(18)}$), 19.1 (**3** × **C**$_{(19)}$). $[\alpha]_D$:1.41 (*c* = 1.0, $CHCl_3$, 25.8 ºC). HRMS (CI+) calcd for $C_{42}H_{61}N_2O_8Si$ [M+H$^+$]: *m*/*z* 749.4197, found *m*/*z* 749.4202. $\nu_{max}$ ($CDCl_3$)/cm$^{-1}$: 2930.9 (m), 1739.9 (s), 1674.3 (s), 1472.7 (s), 1167.0 (s).

(*R*)-Methyl 2-(9-(3-methylbutoxy)-4-(3-(tert-Butyl-diphenyl-silanyloxy)propyl)-3-oxo-2,3,4,5-tetraydro-1*H*-benzo-1,4-diazepin-2-yl)acetate

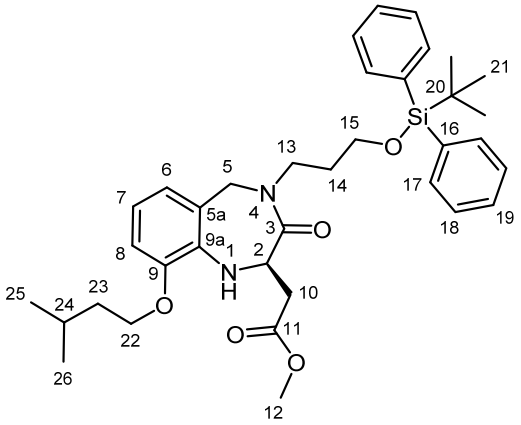


**(*R*)-71**

Amine **(*R*)-60** (0.20 g, 0.27 mmol, 1.0 eq.) was dissolved in anhydrous dichloromethane (2 mL) and trifluoroacetic acid (2 mL) and the solution was allowed to stir for 16 h. Analysis by thin layer chromatography indicated that the salt had formed. The reaction mixture was concentrated *in vacuo*, the reaction mixture was loaded onto a strong cation exchange silica column which was washed with methanol (20 mL), and flushed with 7 M ammonia in methanol solution (20 mL). The ammonia in methanol fraction was concentrated *in vacuo* giving the title compound as a light yellow oil (0.08 g, 0.13 mmol, 48%).

$^1$H NMR ($CDCl_3$, 500 MHz) δ: 7.52 (4H, apparent t, *J* = 6.8 Hz, **4** × $C_{(17)}$**H**), 7.33-7.25 (6H, m, **4** × $C_{(18)}$**H** + **2** × $C_{(19)}$**H**), 6.59 (1H, d, *J* = 6.6 Hz, $C_{(9)}$**H**), 6.46 (1H, app. t, *J* = 7.9 Hz, $C_{(7)}$**H**), 6.40 (1H, d, *J* = 7.4 Hz, $C_{(8)}$**H**), 5.27 (1H, d, *J* = 16.3 Hz, $C_{(5)}$**H**), 4.93-4.90 (1H, m, $C_{(2)}$**H**), 4.32 (1H, d, *J* = 4.3 Hz, N**H**), 3.88-3.84 (2H, m, $C_{(22)}$**H**$_2$), 3.71 (1H, d, *J* = 16.5 Hz, $C_{(5)}$**H**), 3.60 (3H, s, $C_{(12)}$**H**$_3$), 3.57-3.47 (4H, m, $C_{(13)}$**H**$_2$ + $C_{(15)}$**H**$_2$), 2.91 (1H, dd, *J* = 15.9, 6.9 Hz, $C_{(10)}$**H**), 2.56 (1H, dd, *J* = 15.9, 6.9 Hz, $C_{(10)}$**H**), 1.70 (1H, apparent septet, *J* = 6.7 Hz, ($C_{(24)}$**H**), 1.66-1.60 (2H, m, $C_{(14)}$**H**$_2$), 1.58 (2H, app. q, *J* = 6.5 Hz, $C_{(23)}$**H**$_2$), 0.94 (9H, s, **3** × $C_{(21)}$**H**$_3$), 0.85 (6H, apparent dd, *J* = 6.7, 1.3 Hz, $C_{(25)}$**H**$_3$ + $C_{(26)}$**H**$_3$). $^{13}$C NMR ($CDCl_3$, 125 MHz) δ: 171.8 (**C**$_{(3)}$), 169.3 (**C**$_{(11)}$), 146.6 (**C**$_{(9)}$), 135.6 (**4** × **C**$_{(17)}$), 135.0 (**C**$_{(9a)}$), 133.8 (**2** × **C**$_{(16)}$), 129.7 (**2** × **C**$_{(19)}$), 127.7 (**4** × **C**$_{(18)}$), 121.2 (**C**$_{(6)}$), 119.9 (**C**$_{(5a)}$), 116.9 (**C**$_{(7)}$), 110.5 (**C**$_{(8)}$), 66.8 (**C**$_{(22)}$), 61.3 (**2** × **C**$_{(15)}$), 52.0 (**C**$_{(5)}$), 51.9 (**C**$_{(2)}$), 51.6 (**C**$_{(12)}$), 45.2 (**C**$_{(13)}$), 38.0 (**C**$_{(23)}$), 36.2 (**C**$_{(10)}$), 31.2 (**C**$_{(14)}$, 26.9 (**3** × **C**$_{(21)}$), 25.2 (**C**$_{(24)}$), 22.7 (**C**$_{(25)}$), 22.6 (**C**$_{(26)}$), 19.2 (**C**$_{(20)}$). HRMS (CI+) calcd for $C_{36}H_{49}N_2O_5Si$ [$(M+H)^+$]: *m*/*z* 617.3411, found *m*/*z* 617.3406. $\nu_{max}$ ($CDCl_3$)/cm$^{-1}$: 2955 (m), 2929 (s), 1738 (s), 1658 (s), 1105 (s), 1089 (s), 701 (s).

(*R*)-Methyl 2-(9-(3-methylbutoxy)-4-(3-hydroxypropyl)-3-oxo-2,3,4,5-tetraydro-1*H*-benzo-1,4-diazepin-2-yl)acetate

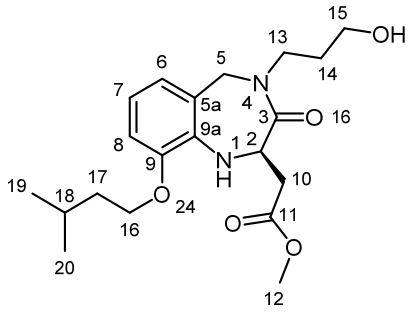

**(*R*)-24**

Silyl ether **(*R*)-71** (80 mg, 0.13 mmol, 1.0 eq.), was dissolved in tetrahydrofuran (2 mL). Tetrabutylammonium fluoride (1 M THF, 0.16 mL, 0.16 mmol, 1.2 eq.) was added to the reaction mixture which was allowed to stir for 16 h. The reaction mixture was concentrated *in vacuo* and purified by flash column chromatography (0-1% methanol in ethyl acetate) giving the title compound as an oil (15 mg, 0.04 mmol, 30%).

$^{1}$H NMR ($CDCl_3$, 400 MHz) δ: 6.73 (1H, dd, *J* = 7.9, 1.3 Hz, $C_{(6)}$**H**), 6.61 (1H, apparent t, *J* = 7.8 Hz, $C_{(7)}$**H**), 6.56 (1H, dd, *J* = 7.5, 1.1 Hz, $C_{(8)}$**H**), 5.50 (1H, d, *J* = 16.3 Hz, $C_{(5)}$**H**), 5.13 (1H, dt, *J* = 10.9, 5.8 Hz, $C_{(2)}$**H**), 4.40 (1H, d, *J* = 4.7 Hz, N**H**),4.00 (2H, t, *J* = 6.7 Hz, $C_{(16)}$**H$_2$**), 3.79 (1H, d, *J* = 16.5 Hz, $C_{(5)}$**H**), 3.76 (3H, s, $C_{(12)}$**H$_3$**), 3.72 (1H, m, $C_{(13)}$**H**), 3.64 (1H, m, $C_{(13)}$**H**), 3.39 (2H, m, $C_{(15)}$**H$_2$**), 3.09 (1H, dd, *J* = 16.0, 8.1 Hz, $C_{(10)}$**H**), 2.71 (1H, dd, *J* = 16.0, 6.0 Hz, $C_{(10)}$**H**), 1.83 (1H, apparent septet, $C_{(18)}$**H**), 1.69 (5H, m, O**H** + $C_{(14)}$**H$_2$** + $C_{(17)}$**H$_2$**), 0.99 (6H, dd, *J* = 6.6, 2.4 Hz, $C_{(19)}$**H$_3$** + $C_{(20)}$**H$_3$**). $^{13}$C NMR ($CDCl_3$, 100 MHz) δ: 171.5 (**C**$_{(3)}$), 170.9 (**C**$_{(11)}$), 146.6 (**C**$_{(9)}$), 134.7 (**C**$_{(9a)}$), 121.1 (**C**$_{(6)}$), 119.3 (**C**$_{(5a)}$), 116.9 (**C**$_{(7a)}$), 110.5 (**C**$_{(8a)}$), 67.0 (**C**$_{(16)}$), 57.8 (**C**$_{(15)}$), 52.0 (**C**$_{(12)}$), 51.9 (**C**$_{(5)}$), 51.5 (**C**$_{(12)}$), 44.1 (**C**$_{(13)}$), 37.8 (**C**$_{(17)}$), 36.1 (**C**$_{(10)}$), 30.5 (**C**$_{(14)}$), 25.2 (**C**$_{(18)}$), 22.7 (**C**$_{(19/20)}$), 22.6 (**C**$_{(19/20)}$). HRMS (CI+) calcd for $C_{20}H_{31}N_2O_5$ [$(M+H)^+$]: *m*/*z* 379.2233, found *m*/*z* 379.2236. $\nu_{max}$ ($CDCl_3$)/cm$^{-1}$: 2951 (m), 1734 (s), 1647 (s), 1486 (m), 905 (s), (728). $[\alpha]_D$: 6.88 (*c* = 1.0, $CHCl_3$, 25.9 ºC).

5-(*tert*-Butyldiphenyl silanyloxy)-pentylamine [54]

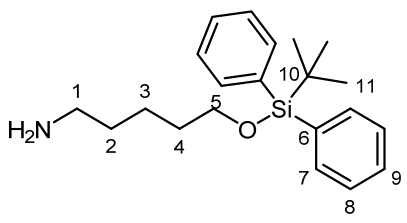

**69**

5-Aminopentanol (2.57 g, 25.0 mmol, 2.5 eq.) was dissolved in anhydrous dichloromethane (50 mL) and the solution was cooled to 0 ºC. *t*-Butyldiphenylsilyl chloride (2.60 mL, 10.0 mmol, 1.0 eq.) was dissolved in anhydrous dichloromethane (10 mL) and slowly added to the solution. Triethylamine (2.10 mL, 15.0 mmol, 1.5 eq.) was added, the reaction mixture was allowed to warm to room temperature and stir for 3 h. The reaction mixture was then acidified with 1 M hydrochloric acid (aq.) solution (25 mL) and the phases were separated. The organic layer was washed with sodium bicarbonate (aq. sat) (25 mL), brine (50 mL), dried ($Na_2SO_4$), and concentrated *in vacuo* giving the title compound as a clear oil (2.20 g, 6.47 mmol, 65%).

$^1$H NMR ($CDCl_3$, 400 MHz) δ: 7.67-7.65 (4H, m, **4** × $C_{(7)}$**H**), 7.43-7.35 (6H, m, **4** × $C_{(8)}$**H** + **2** × $C_{(9)}$**H**), 3.66 (2H, t, *J* = 7.0 Hz, $C_{(5)}$**H$_2$**), 2.68 (2H, t, *J* = 7.0 Hz, $C_{(1)}$**H$_2$**), 1.88 (2H, broad s, N**H$_2$**), 1.59-1.54 (2H, m, $C_{(2)}$**H$_2$**), 1.45-1.35 (4H, m, $C_{(3)}$**H$_2$** + $C_{(4)}$**H$_2$**), 1.05 (9H, s, **3** × $C_{(11)}$**H$_3$**). $^{13}$C NMR ($CDCl_3$, 125 MHz) δ: 135.6 (**4** × **C**$_{(7)}$), 134.0 (**2** × **C**$_{(6)}$), 129.5 (**2** × **C**$_{(9)}$), 127.6 (**4** × **C**$_{(8)}$), 63.8 (**C**$_{(5)}$), 42.0 (**C**$_{(1)}$), 33.7 (**C**$_{(2)}$), 32.3 (**C**$_{(4)}$), 26.9 (**3** × **C**$_{(11)}$), 23.1 (**C**$_{(3)}$), 19.2 (**C**$_{(10)}$). HRMS (CI+) calcd for $C_{21}H_{32}NOSi$ [$(M+H)^+$]: *m*/*z* 342.2253, found *m*/*z* 342.2249. $\nu_{max}$ ($CDCl_3$)/cm$^{-1}$: 3050 (w), 1605 (m), 1472 (m), 1427 (m), 1105 (s), 1092 (s), 699 (s).

5-(*tert*-Butyldiphenyl silanyloxy)pentyl-[3-(3-methylbutoxy)-2-nitro-benzyl]-amine

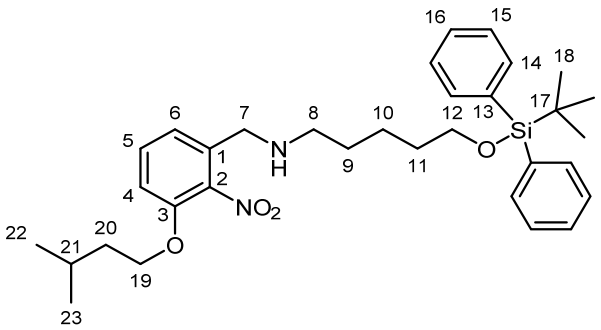


**55**

Nitrobenzaldehyde **18** (0.97 g, 4.08 mmol, 1.0 eq.) was dissolved in heptane (60 mL) and amine **69** (2.10 g, 6.16 mmol, 1.5 eq.) was added. The reaction mixture was allowed to stir for 48 h, concentrated *in vacuo* and dissolved in methanol (60 mL). Sodium borohydride (0.23 g, 6.16 mmol, 1.5 eq.) was added and the solution was allowed to stir for 12 h. The reaction mixture was quenched by the addition of water (20 mL), ethyl acetate (20 mL) was added and the phases separated. The aqueous layer was extracted with ethyl acetate (2 × 60 mL). The combined organic layers were washed with brine (20 mL), dried ($Na_2SO_4$), and concentrated *in vacuo*. The

resulting mixture was purified by flash column chromatography (0-20% ethyl acetate in petroleum ether) giving the title compound as a yellow oil (2.29 g, 4.07 mmol, 98%).

$^{1}$H NMR ($CDCl_3$, 400 MHz) δ: 7.70-7.68 (4H, m, **4** × $C_{(14)}$**H**), 7.47-7.35 (7H, m, **4** × $C_{(15)}$**H** + **2** × $C_{(16)}$**H** + $C_{(5)}$**H**), 7.07 (1H, d, *J* = 7.6 Hz, $C_{(6)}$**H**), 6.85 (1H, d, *J* = 8.2 Hz, $C_{(4)}$**H**), 4.10 (2H, t, *J* = 6.4 Hz, $C_{(19)}$**H**$_2$), 3.76 (2H, s, $C_{(7)}$**H**$_2$), 3.68 (2H, t, *J* = 6.4 Hz, $C_{(12)}$**H**$_2$), 2.58 (2H, t, *J* = 6.9 Hz, $C_{(8)}$**H**$_2$), 1.82 (1H, apparent septet, *J* = 6.9 Hz, $C_{(21)}$**H**), 1.62-1.55 (4H, m, $C_{(9)}$**H**$_2$ + $C_{(11)}$**H**$_2$), 1.50-1.37 (5H, m, N**H** + $C_{(10)}$**H**$_2$ + $C_{(20)}$**H**$_2$), 1.07 (9H, s, **3** × $C_{(18)}$**H**$_3$), 0.97 (6H, d, *J* = 6.5 Hz, $C_{(22)}$**H**$_3$ + $C_{(23)}$**H**$_3$). $^{13}$C NMR ($CDCl_3$, 125 MHz) δ: 150.8 (**C**$_{(3)}$), 142.0 (**C**$_{(2)}$), 135.6 (**4** × **C**$_{(14)}$), 134.1 (**2** × **C**$_{(13)}$), 133.6 (**C**$_{(1)}$), 130.8 (**C**$_{(5)}$), 129.5 (**2** × **C**$_{(16)}$), 127.6 (**4** × **C**$_{(15)}$), 121.2 (**C**$_{(6)}$), 112.1 (**C**$_{(4)}$), 67.9 (**C**$_{(19)}$), 63.82 (**C**$_{(12)}$), 49.4 (**C**$_{(7)}$), 49.3 (**C**$_{(8)}$), 37.5 (**C**$_{(20)}$), 32.4 (**C**$_{(11)}$), 29.7 (**C**$_{(9)}$), 26.9 (**3** × **C**$_{(18)}$), 24.9 (**C**$_{(21)}$) 23.4 (**C**$_{(10)}$), 22.5 (**C**$_{(22)}$ + **C**$_{(23)}$),19.2 (**C**$_{(17)}$). HRMS (CI+) calcd for $C_{33}H_{47}O_4N_2Si$ [(M+H)$^+$]: *m*/*z* 563.3305, found *m*/*z* 563.3304. $\nu_{max}$ ($CDCl_3$)/cm$^{-1}$: 2930 (m), 1589 (m), 1389 (m), 1105 (s), 727 (s), 907 (s), 702 (s).

[2-Amino-3-(3-methyl-butoxy)-benzyl]-{5-[(*tert*-butyldiphenylsilyl)oxy]pentyl}-carbamic acid *tert*-butyl ester

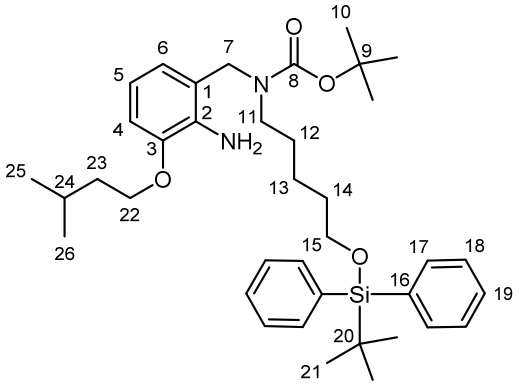


**53**

Nitobenzene **55** (2.58 g, 4.58 mmol, 1.0 eq.) was dissolved in anhydrous dichloromethane (100 mL), triethylamine (1.08 mL, 7.78 mmol, 1.7 eq.) was added and the solution was allowed to stir for 25 min. Di-*t*-butyl dicarbonate (1.11 g, 5.33 mmol, 1.2 eq.) was added to the reaction mixture which was then allowed to stir for 16 h. The reaction mixture was quenched with water (75 mL), and diluted with ethyl acetate (75 mL). The phases were separated and the aqueous layer was extracted with ethyl acetate (2 × 75 mL). The combined organic layer was then washed with brine (75 mL), dried ($Na_2SO_4$) and concentrated *in vacuo*. The crude mixture was purified by flash column chromatography (0-10% ethyl acetate in petroleum ether) giving the intermediate carbamate as a light yellow oil. This oil was dissolved in anhydrous methanol (60 mL). Ammonium formate (2.58 g, 41.0 mmol, 9.0 eq.) and

10% palladium on activated charcoal (200 mg) were added to the solution and heated to 35 ºC. The reaction mixture was allowed to stir for 48 h. The reaction mixture was filtered through celite and washed with ethyl acetate (400 mL). The filtrate was washed with water (400 mL) and the phases were separated. The aqueous phase was extracted with ethyl acetate (2 × 200 mL), the combined organic layer was then washed with brine, dried ($Na_2SO_4$) and filtered giving the title compound as a light red oil (2.19 g, 3.50 mmol, 76%).

$^1$H NMR ($CDCl_3$, 500 MHz) δ: 7.59-7.57 (4H, m, **4** × $C_{(17)}$**H**), 7.35-7.28 (6H, m, **4** × $C_{(18)}$**H** + **2** × $C_{(19)}$**H**), 6.64 (1H, d, *J* = 7.9 Hz, $C_{(5)}$**H**), 6.53 (1H, d, *J* = 7.4 Hz, $C_{(6)}$**H**), 6.50-6.48 (1H, m, $C_{(4)}$**H**), 4.59 (2H, broad s, N**H**$_2$), 4.29 (2H, s, $C_{(7)}$**H**$_2$), 3.91 (2H, t, *J* = 6.7 Hz, $C_{(22)}$**H**$_2$), 3.55 (2H, t, *J* = 6.2 Hz, $C_{(15)}$**H**$_2$), 2.98 (2H, broad s, $C_{(11)}$**H**$_2$), 1.77 (1H, apparent septet, *J* = 6.7 Hz, $C_{(24)}$**H**), 1.62 (2H, q, *J* = 6.7 Hz, $C_{(23)}$**H**$_2$), 1.48-1.43 (2H, m, $C_{(12)}$**H**$_2$), 1.40-1.35 (11H, m, $C_{(14)}$**H**$_2$ + **3** × $C_{(10)}$**H**$_3$), 1.25-1.19 (2H, m, $C_{(13)}$**H**$_2$), 0.97 (9H, s, **3** × $C_{(21)}$**H**$_3$), 0.88 (6H, d, *J* = 6.6 Hz, $C_{(25)}$**H**$_3$ + $C_{(26)}$**H**$_3$). $^{13}$C NMR ($CDCl_3$, 125 MHz) δ: 156.4 (**C**$_{(8)}$), 146.4 (**C**$_{(3)}$), 136.2 (**C**$_{(2)}$), 135.6 (**4** × **C**$_{(17)}$), 133.8 (**2** × **C**$_{(16)}$), 129.5 (**2** × **C**$_{(19)}$), 127.6 (**4** × **C**$_{(18)}$), 123.3 (**C**$_{(1)}$), 120.8 (**C**$_{(6)}$), 115.8 (**C**$_{(5)}$), 110.6 (**C**$_{(4)}$), 79.8 (**C**$_{(9)}$), 66.7 (**C**$_{(22)}$), 63.8 (**C**$_{(15)}$), 47.1(**C**$_{(7)}$), 45.2 (**C**$_{(11)}$), 38.2 (**C**$_{(23)}$), 32.3 (**C**$_{(12)}$), 28.5 (**3** × **C**$_{(10)}$), 27.3 (**C**$_{(14)}$), 26.9 (**3** × **C**$_{(21)}$), 25.2 (**C**$_{(24)}$), 23.1 (**C**$_{(13)}$), 22.7 (**C**$_{(25)}$ + **C**$_{(26)}$), 19.2. (**C**$_{(20)}$). HRMS (CI+) calcd for $C_{38}H_{57}O_4N_2Si$ [$(M+H)^+$]: *m*/*z* 633.4088, found *m*/*z* 633.4082. $\nu_{max}$ ($CDCl_3$)/cm$^{-1}$: 2929.5 (m), 1670.0 (s), 1472.7 (m), 1237.9 (m).

(*R*)-Dimethyl 2-(2-((*tert*-butoxycarbonyl(5-(*tert*-butyldiphenyl silanyloxy)pentyl)amino)methyl)-6-(isopentoxy)phenylamino)succinate

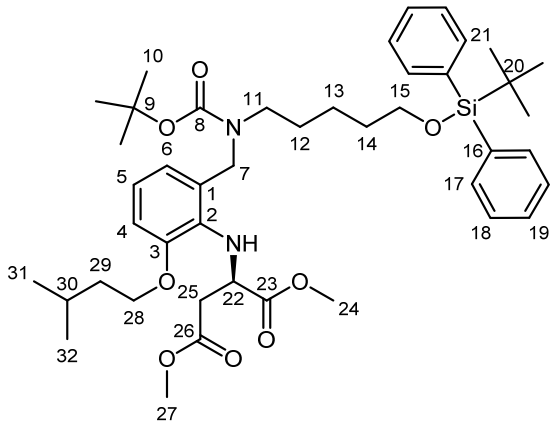


**(*R*)-51**

Aniline **53** (1.90 g, 3.01 mmol. 1.0 eq.) was dissolved in anhydrous dichloromethane (30 mL), 2,6- lutidine (0.70 mL, 6.02 mmol, 2.0 eq.) was added and the solution was allowed to stir at room temperature for 20 min. Triflate **(*S*)-20** (1.50 g, 5.10 mmol, 1.7 eq.) was dissolved in anhydrous dichloromethane (30 mL) and was added dropwise

to the solution. The reaction mixture was heated to 45 ºC and stirred for 48 h. The reaction mixture was then quenched with water (60 mL) and the phases were separated. The aqueous phase was extracted with dichloromethane (60 mL), and the combined organic layer was then washed with copper sulfate solution (aq. sat.) (3 × 60 mL), dried ($Na_2SO_4$), filtered and concentrated *in vacuo*. The resulting mixture was purified by flash column chromatography (0-10% ethyl acetate in 40-60 petroleum ethers) giving the desired compound as a clear oil (1.65 g, 2.10 mmol, 70%).

$^1$H NMR ($CDCl_3$, 400 MHz, 55 ºC) δ: 7.66-7.64 (4H, m, **4** × $C_{(17)}$**H**), 7.42-7.34 (6H, m, **4** × $C_{(18)}$**H** + **2** × $C_{(19)}$**H**), 6.84-6.81 (1H, m, $C_{(4)}$**H**), 6.77-6.75 (1H, m, $C_{(5)}$**H**), 6.68 (1H, d, *J* = 1.6 Hz, $C_{(6)}$**H**), 4.62-4.59 (3H, m, $C_{(7)}$**H$_2$** + $C_{(22)}$**H**), 4.35 (1H, d, *J* = 15.4 Hz, N**H**), 3.98 (2H, t, *J* = 6.9 Hz, $C_{(28)}$**H$_2$**), 3.65-3.62 (8H, m, $C_{(24)}$**H$_3$** + $C_{(27)}$**H$_3$** + $C_{(15)}$**H$_2$**), 3.09-3.04 (2H, m, $C_{(11)}$**H$_2$**), 2.80 (2H, dd, *J* = 6.6, 3.6 Hz, $C_{(25)}$**H$_2$**), 1.83 (1H, n, *J* = 6.9 Hz, $C_{(30)}$**H**), 1.71 (2H, q, *J* = 6.7 Hz, $C_{(29)}$**H$_2$**), 1.57-1.45 (13H, m, **3** × $C_{(10)}$**H$_3$** + $C_{(12)}$**H$_2$** + $C_{(14)}$**H$_2$**), 1.33-1.26 (2H, m, $C_{(13)}$**H$_2$**), 1.04 (9H, s, **3** × $C_{(21)}$**H$_3$**), 0.97 (6H, d, *J* = 6.6 Hz, $C_{(31)}$**H$_3$** + $C_{(32)}$**H$_3$**). $^{13}$C NMR ($CDCl_3$, 100 MHz, 55 ºC) δ: 173.2 (**C**$_{(23)}$), 171.0 (**C**$_{(26)}$), 156.0 (**C**$_{(8)}$), 151.1 (**C**$_{(3)}$), 135.5 (**4** × **C**$_{(17)}$), 134.3 (**2** × **C**$_{(16)}$), 129.4 (**2** × **C**$_{(19)}$), 127.5 (**4** × **C**$_{(18)}$), 121.4 (**C**$_{(4)}$ + **C**$_{(5)}$), 111.6 (**C**$_{(6)}$), 79.5 (**C**$_{(9)}$), 67.2 (**C**$_{(28)}$), 63.9 (**C**$_{(15)}$), 56.5 (**C**$_{(22)}$), 51.7 (**C**$_{(24)}$), 51.4 (**C**$_{(27)}$), 46.6 (**C**$_{(7)}$), 46.0 (**C**$_{(11)}$), 38.2 (**C**$_{(25)}$), 38.1 (**C**$_{(14)}$), 32.3 (**C**$_{(29)}$), 28.4 (**3** × **C**$_{(10)}$), 27.6 (**C**$_{(12)}$), 26.9 (**C**$_{(31)}$ + **C**$_{(32)}$) , 25.2 (**C**$_{(30)}$), 23.2 (**C**$_{(13)}$), 22.5 (**C**$_{(20)}$), 19.2 (**3** × **C**$_{(21)}$), (**C**$_{(1)}$) unresolved, (**C**$_{(2)}$) unresolved. HRMS (CI+) calcd for $C_{44}H_{65}N_2O_8Si$ [M+H$^+$]: *m*/*z* 777.4510, found *m*/*z* 777.4505. $\nu_{max}$ ($CDCl_3$)/cm$^{-1}$: 2953 (m), 1741 (s), 1672 (s), 1471 (s), 1163 (s). [α]$_D$: 1.33 (*c* = 1.0, $CHCl_3$, 25.8 ºC).

(*S*)-Dimethyl 2-(2-((*tert*-butoxycarbonyl(5-(*tert*-butyldiphenyl silanyloxy)pentyl)amino)methyl)-6-(isopentoxy)phenylamino)succinate

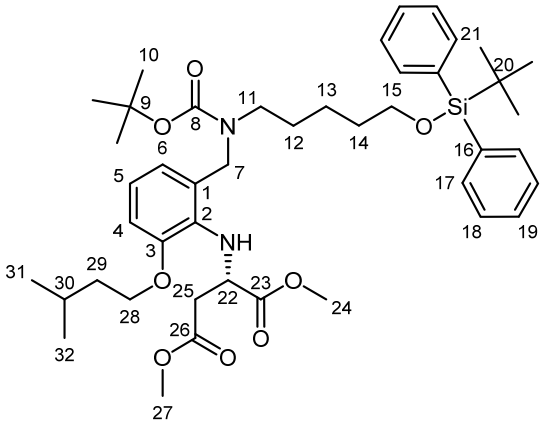


**(*S*)-51**

**(*S*)-51** was synthesised *via* the method described above (73%). $[\alpha]_D$: -2.64 (*c* = 1.0, $CHCl_3$, 28.7 ºC)

(*R*)-Methyl 2-(9-(isopentyloxy)-4-(5-hydroxypentyl)-3-oxo-2,3,4,5-tetraydro-1*H*-benzo-1,4-diazepin-2-yl)acetate

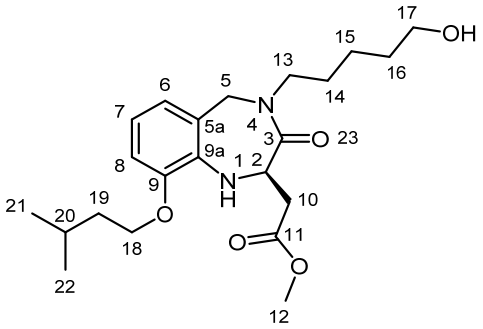

**(*R*)-26**

Amine **(*R*)-51** (0.24 g, 0.30 mmol, 1.0 eq.) was dissolved in anhydrous dichloromethane (2 mL) and trifluoroacetic acid (2 mL) and the solution was allowed to stir for 16 h. Analysis by thin layer chromatography indicated that the salt had formed. The reaction mixture was concentrated *in vacuo*, and loaded onto a strong cation exchange silica column which was washed with methanol (20 mL) and flushed with 7 M ammonia in methanol solution (20 mL). The ammonia in methanol fraction was allowed to stand for two hours before concentration *in vacuo*, giving the title compound as a white solid (0.12 g, 0.28 mmol, 95%).

$^1$H NMR ($CDCl_3$, 400 MHz) δ: 6.70 (1H, dd, *J* = 7.4, 1.9 Hz, $C_{(6)}$**H**), 6.60-6.54 (2H, m, $C_{(7)}$**H** + $C_{(8)}$**H**), 5.44 (1H, d, *J* = 16.4 Hz, $C_{(5)}$**H**), 5.07 (1H, m, $C_{(2)}$**H**), 4.40 (1H, *J* = 4.6 Hz, N**H**), 3.97 (2H, *J* = 6.5 Hz, $C_{(18)}$**H**$_2$), 3.77 (1H, *J* = 16.6 Hz, $C_{(5)}$**H**), 3.72 (3H, s, $C_{(12)}$**H**$_3$), 3.50 (4H, m, $C_{(17)}$**H**$_2$ + $C_{(13)}$**H**$_2$), 3.05 (1H, *J* = 16.1, 7.6 Hz, $C_{(10)}$**H**), 2.67 (1H, dd, *J* = 15.9, 6.3 Hz, $C_{(10)}$**H**), 1.81 (1H, apparent septet, *J* = 6.8 Hz, $C_{(20)}$**H**), 1.70-1.64 (3H, m, $C_{(19)}$**H**$_2$ + O**H**), 1.58-1.44 (4H, m, $C_{(14)}$**H**$_2$ + $C_{(16)}$**H**$_2$), 1.34-1.22 (2H, m, $C_{(15)}$**H**$_2$), 0.96 (6H, dd, *J* = 6.6, 1.0 Hz, $C_{(21)}$**H**$_3$ + $C_{(22)}$**H**$_3$). $^{13}$C NMR ($CDCl_3$, 125 MHz) δ: 171.8 (**C**$_{(3)}$), 169.5 (**C**$_{(11)}$), 146.6 (**C**$_{(9)}$), 135.0 (**C**$_{(9a)}$), 121.1 (**C**$_{(6)}$), 119.8 (**C**$_{(5a)}$), 116.9 (**C**$_{(7)}$), 110.5 (**C**$_{(8)}$), 66.9 (**C**$_{(18)}$), 62.6 (**C**$_{(17)}$), 52.0 (**C**$_{(12)}$), 51.5 (**C**$_{(2)}$), 51.4 (**C**$_{(13)}$), 47.3 (**C**$_{(5)}$), 38.0 (**C**$_{(19)}$), 36.2 (**C**$_{(10)}$), 32.2 (**C**$_{(16)}$), 27.9 (**C**$_{(14)}$), 25.2 (**C**$_{(20)}$), 22.7 (**C**$_{(15)}$), 22.6 (**C**$_{(21)}$ + **C**$_{(22)}$). HRMS (CI+) calcd for $C_{22}H_{35}O_5N_2$ [M+H$^+$]: *m*/*z* 407.2546, found *m*/*z* 407.2541. M.P. 62-64 ºC. $\nu_{max}$ ($CDCl_3$)/cm$^{-1}$: 3410.3 (m), 2931.9 (m), 1736.0 (s), 1643.4 (s), 1373.4 (m). $[\alpha]_D$: 6.79 (*c* = 1.0, $CHCl_3$, 25.8 ºC).

(*S*)-Methyl 2-(9-(isopentyloxy)-4-(5-hydroxypentyl)-3-oxo-2,3,4,5-tetraydro-1*H*-benzo-1,4-diazepin-2-yl)acetate

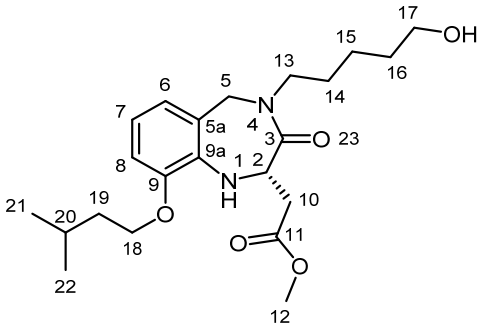

**(*S*)-26**

Alcohol **(*S*)-26** was synthesised *via* the method described above. $[\alpha]_D$: -13.97 (*c* = 1.0, $CHCl_3$, 24.7 ºC).

(*R*)-Methyl 2-(9-(3-methylbutoxy)-4-(5-{[(4-methylbenzene)sulfonyl]oxy}pentyl)-1H-1,2,3-triazol-1-yl] pentyl)-3-oxo-2,3,4,5-tetraydro-1H-benzo-1,4-diazepin-2-yl)acetate

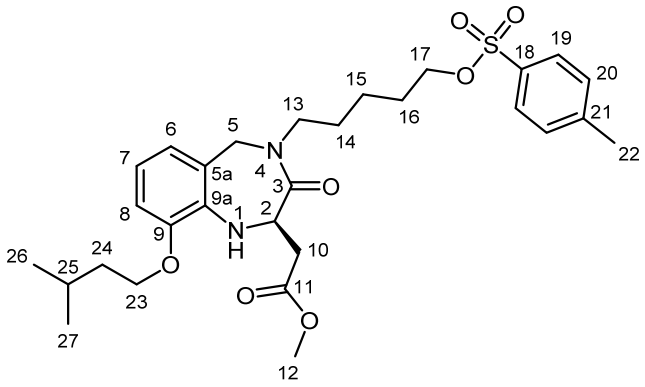

**(*R*)-47**

Alcohol **(*R*)-20** (0.10 g, 0.25 mmol, 1.0 eq.) was dissolved in dichloromethane (10 mL). Triethylamine (0.26 mL, 1.85 mmol, 7.5 eq.) was added to the solution and the reaction mixture was allowed to stir for 10 min. *p*-Toluenesulfonyl chloride (0.12 g, 0.63 mmol, 2.5 eq.) was added to reaction mixture which was allowed to stir at room temperature for 18 h. Water (10 mL) was added to the reaction mixture and the phases were separated. The organic layer was dried ($Na_2SO_4$), filtered and concentrated *in vacuo.* The resulting residue was purified by flash column chromatography (10-50% ethyl acetate in petroleum ether) giving the title compound as a colourless oil (0.93 g, 0.17 mmol, 68%).

$^1$H NMR ($CDCl_3$, 400 MHz) δ: 7.78 (2H, d, *J* = 8.3 Hz, **2** × $C_{(19)}$**H**), 7.35 (2H, d, *J* = 8.0 Hz, **2** × $C_{(20)}$**H**), 6.71 (1H, dd, *J* = 8.0, 1.5 Hz, $C_{(6)}$**H**), 6.61-6.54 (2H, m, $C_{(7)}$**H** + $C_{(8)}$**H**), 5.42 (1H, d, *J* = 16.4 Hz, $C_{(5)}$**H**), 5.09-5.04 (1H, m, $C_{(2)}$**H**), 4.44 (1H, d, *J* = 4.4 Hz, N**H**),

3.99 (2H, t, *J* = 6.7 Hz, $C_{(23)}\mathbf{H_2}$), 3.93 (2H, t, *J* = 6.5 Hz, $C_{(17)}\mathbf{H_2}$), 3.77-3.74 (1H, m, $C_{(5)}\mathbf{H}$), 3.74 (3H, s, $C_{(12)}\mathbf{H_3}$), 3.55-3.48 (1H, m, $C_{(13)}\mathbf{H}$), 3.44-3.37 (1H, m, $C_{(13)}\mathbf{H}$), 3.05 (1H, dd, *J* = 15.8, 7.4 Hz, $C_{(10)}\mathbf{H}$), 2.68 (1H, dd, *J* = 15.8, 6.4 Hz, $C_{(10)}\mathbf{H}$), 2.46 (3H, s, $C_{(22)}\mathbf{H_3}$), 1.83 (1H, apparent septet, *J* = 6.8 Hz, $C_{(25)}\mathbf{H}$), 1.68 (2H, q, *J* = 6.5 Hz, $C_{(24)}\mathbf{H_2}$), 1.58 (2H, apparent quintet, *J* = 7.5 Hz, $C_{(14)}\mathbf{H_2}$), 1.48 (2H, apparent quintet, *J* = 7.5 Hz, $C_{(16)}\mathbf{H_2}$), 1.35-1.12 (2H, m, $C_{(15)}\mathbf{H_2}$), 0.98 (6H, dd, *J* = 6.6, 0.4 Hz, $C_{(26)}\mathbf{H_3}$ + $C_{(27)}\mathbf{H_3}$). $^{13}$C NMR ($CDCl_3$, 125 MHz) δ:171.7 (**C**$_{(3)}$), 169.4 (**C**$_{(11)}$), 146.6 (**C**$_{(21)}$), 144.7 (**C**$_{(9)}$), 134.9 (**C**$_{(18)}$), 133.2 (**C**$_{(9a)}$), 129.8 (**2 × C**$_{(20)}$), 127.9 (**2 × C**$_{(19)}$), 121.1 (**C**$_{(6)}$), 119.8 (**C**$_{(5a)}$), 117.0 (**C**$_{(7)}$), 110.5 (**C**$_{(8)}$), 70.4 (**C**$_{(17)}$), 66.9 (**C**$_{(23)}$), 52.0 (**C**$_{(2)}$), 51.5 (**C**$_{(5)}$), 51.5 (**C**$_{(12)}$), 47.2 (**C**$_{(13)}$), 38.0 (**C**$_{(24)}$), 36.2 (**C**$_{(10)}$), 28.4 (**C**$_{(14)}$), 27.6 (**C**$_{(16)}$), 25.2 (**C**$_{(25)}$), 22.7 (**C**$_{(26)}$), 22.6 (**C**$_{(27)}$), 22.5 (**C**$_{(15)}$), 21.6 (**C**$_{(22)}$). $[\alpha]_D$: 3.11 (*c* =0.8, $CHCl_3$, 24.8 ºC). LRMS (EI+) calcd for $C_{29}H_{41}O_7N_2S$ [$(M+H)^+$]: *m*/*z* 561.3, found *m*/*z* 561.2. $\nu_{max}$ ($CDCl_3$)/$cm^{-1}$: 1736.0 (s), 1658.8 (s), 1589.4 (m), 1450.5 (s), 1172.8 (s).

(*S*)-Methyl 2-(9-(3-methylbutoxy)-4-(5-{[(4-methylbenzene)sulfonyl]oxy}pentyl)-1*H*-1,2,3-triazol-1-yl] pentyl)-3-oxo-2,3,4,5-tetraydro-1H-benzo-1,4-diazepin-2-yl)acetate

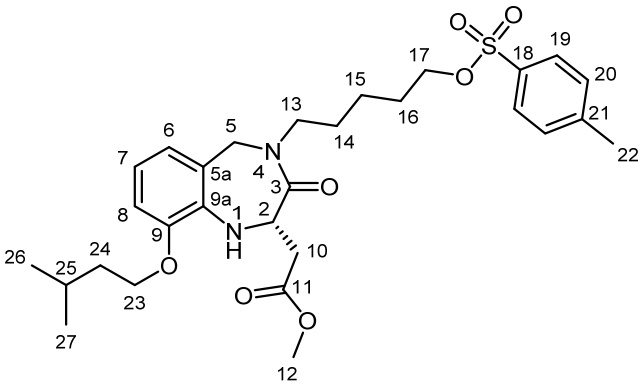

**(*S*)-47**

**(*S*)-47** was synthesised *via* the method described above. $[\alpha]_D$: -4.36 (*c* =1.0, $CHCl_3$, 26.1 ºC).

(*R*)-Methyl 2-(9-(3-methylbutoxy)-4-(5-azidopentyl)-3-oxo-2,3,4,5-tetraydro-1*H*-benzo-1,4-diazepin-2-yl)acetate

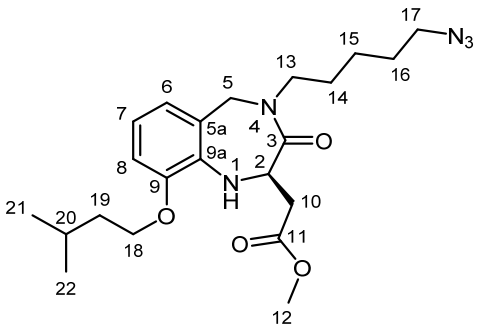

**(*R*)-45**

Tosylate **(*R*)-47** (30 mg, 0.05 mmol, 1.0 eq.) was dissolved in dimethylformamide (2 mL). Sodium azide (30 mg, 0.50 mmol, 10 eq.) was added to the solution which was heated to 70 ºC and stirred for 24 h. The reaction mixture was diluted with water (10 mL) and ethyl acetate (15 mL), the phases were separated and the organic layer was washed with water (4 × 10 mL). The organic layer was then dried ($Na_2SO_4$), filtered and concentrated *in vacuo*. The crude mixture was purified by flash column chromatography (0-30% EtOAc in petroleum ether) giving the title compound as a yellow oil (20 mg, 0.04 mmol, 80 %).

$^1$H NMR ($CDCl_3$, 500 MHz) δ: 6.63 (1H, dd, *J* = 7.6, 1.3 Hz, $C_{(6)}$**H**), 6.53-6.47 (2H, m, $C_{(7)}$**H** + $C_{(8)}$**H**), 5.37 (1H, d, *J* = 16.4 Hz, $C_{(5)}$**H**), 5.00 (1H, t, *J* = 6.9 Hz, $C_{(2)}$**H**), 4.36 (1H, broad singlet, N**H**), 3.91 (2H, t, *J* = 6.6 Hz, $C_{(18)}$**H**$_2$), 3.68 (1H, d, *J* = 16.6 Hz, $C_{(5)}$**H**), 3.66 (3H, s, $C_{(12)}$**H**$_3$), 3.56-3.50 (1H, m, $C_{(13)}$**H**), 3.36-3.31 (1H, m, $C_{(13)}$**H**), 3.06 (2H, t, *J* = 7.0 Hz, $C_{(17)}$**H**$_2$), 2.98 (1H, dd, *J* = 15.9, 7.4 Hz, $C_{(10)}$**H**), 2.60 (1H, dd, *J* = 15.8, 6.4 Hz, $C_{(10)}$**H**), 1.74 (1H, nonet, *J* = 6.7 Hz, $C_{(20)}$**H**), 1.63-1.58 (2H, m, $C_{(19)}$**H**$_2$), 1.50-1.36 (4H, m, $C_{(14)}$**H**$_2$ + $C_{(16)}$**H**$_2$), 1.26-1.13 (2H, m, $C_{(15)}$**H**$_2$), 0.90 (6H, dd, *J* = 6.6, 1.2 Hz, $C_{(21)}$**H**$_3$ + $C_{(22)}$**H**$_3$). $^{13}$C NMR ($CDCl_3$, 125 MHz) δ:171.7 (**C**$_{(3)}$), 169.5 (**C**$_{(11)}$), 146.6 (**C**$_{(9)}$), 135.0 (**C**$_{(9a)}$), 121.1 (**C**$_{(8)}$), 119.8 (**C**$_{(5a)}$), 116.9 (**C**$_{(7)}$), 110.5 (**C**$_{(6)}$), 66.9 (**C**$_{(18)}$), 51.9 (**C**$_{(12)}$), 51.5 (**C**$_{(17)}$), 51.5 (**C**$_{(2)}$), 51.2 (**C**$_{(13)}$), 47.4 (**C**$_{(5)}$), 38.0 (**C**$_{(19)}$), 36.2 (**C**$_{(10)}$), 28.4 (**C**$_{(16)}$), 21.8 (**C**$_{(14)}$), 25.2 (**C**$_{(20)}$), 23.8 (**C**$_{(15)}$), 22.7 (**C**$_{(21)}$), 22.6 (**C**$_{(22)}$). LRMS (CI+) calcd for $C_{22}H_{34}N_5O_4$ [M+H$^+$]: *m*/*z* 432.3, found *m*/*z* 432.3. $\nu_{max}$ ($CDCl_3$)/cm$^{-1}$: 3421 (w), 2860 (m), 2092 (s), 1735 (s), 1659 (s), 1249 (s). $[\alpha]_D$: 4.38 (*c* = 1.0, $CHCl_3$, 25.1 ºC).

(*S*)-Methyl 2-(9-(3-methylbutoxy)-4-(5-azidopentyl)-3-oxo-2,3,4,5-tetraydro-1*H*-benzo-1,4-diazepin-2-yl)acetate

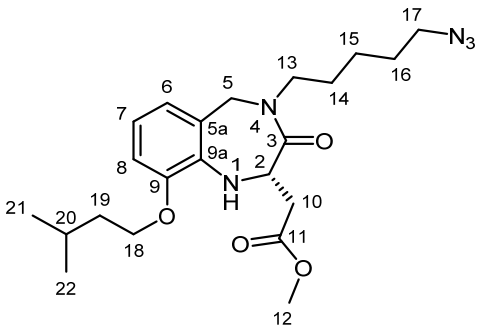


**(*S*)-45**

**(*S*)-45** was synthesised via the method described above (87%). $[\alpha]_D$: -.5.59 (*c* =1.0 , 26.2 ºC).

(*R*)-Methyl 2-(9-(3-methylbutoxy)-4-(5-[4-(pent-4-yn-1-yl)-1H-1,2,3-triazol-1-yl] pentyl)-3-oxo-2,3,4,5-tetraydro-1H-benzo-1,4-diazepin-2-yl)acetate

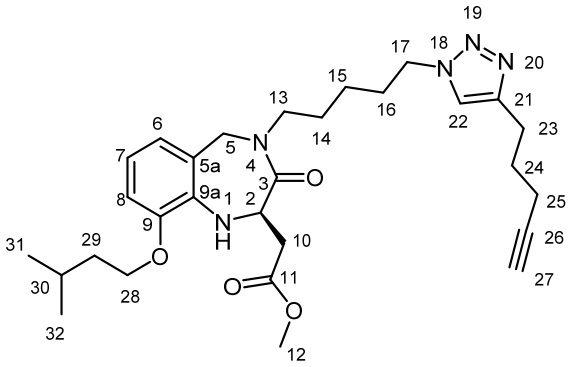

**(*R*)-114**

Azide **(*R*)-45** (44 mg, 0.10 mmol, 1.0 eq.) was dissolved in THF (0.75 mL) and water (0.25 mL). Copper (II) sulfate (30 mg, 0.12 mmol, 10.0 eq.), sodium ascorbate (48 mg, 0.24 mmol, 2.4 eq.) and 1,6-heptadiyne (0.12 mL, 1.00 mmol, 10.0 eq.) were added to the solution which was heated to 70 °C for 18 h. The reaction mixture was diluted with water (5 mL) and ethyl acetate (5 mL) and the phases were separated. The aqueous phase was extracted with ethyl acetate (2 × 5 mL) and the combined organic layer was dried ($Na_2SO_4$), filtered and concentrated *in vacuo* onto silica gel. Flash column chromatography (50-100% ethyl acetate in petroleum ether) gave the title compound as a light yellow oil (40 mg, 0.76 mmol, 76%).

$^1$H NMR ($CDCl_3$, 500 MHz) δ: 7.22 (1H, s, $C_{(22)}$**H**), 6.63 (1H, dd, *J* = 7.7, 1.4 Hz, $C_{(6)}$**H**), 6.53-6.47 (2H, m, $C_{(7)}$**H** + $C_{(8)}$**H**), 5.37 (1H, d, *J* = 16.5 Hz, $C_{(5)}$**H**), 5.02-4.98 (1H, m, $C_{(2)}$**H**), 4.37 (1H, d, *J* = 4.4 Hz, N**H**), 4.09 (2H, td, *J* = 7.1, 3.1 Hz, $C_{(17)}$**H$_2$**), 3.91 (2H, t, *J* = 6.5 Hz, $C_{(28)}$**H$_2$**), 3.68 (1H, d, *J* = 16.7 Hz, $C_{(5)}$**H**), 3.65 (3H, s, $C_{(12)}$**H$_3$**), 3.50 (1H, dt, *J* = 14.0, 7.1 Hz, $C_{(13)}$**H**), 3.34 (1H, dt, *J* = 14.0, 7.2 Hz, $C_{(13)}$**H**), 2.97 (1H, dd, *J* = 15.9, 7.5 Hz, $C_{(10)}$**H**), 2.75 (2H, t, *J* = 7.4 Hz, $C_{(23)}$**H$_2$**), 2.60 (1H, dd, *J* = 15.7, 6.2 Hz, $C_{(10)}$**H**), 2.17 (1H, td, *J* = 6.9, 2.4 Hz, $C_{(25)}$**H$_2$**), 1.91 (1H, t, *J* = 2.6 Hz, $C_{(27)}$**H**), 1.83 (2H, tt, *J* = 7.4, 7.2 Hz, $C_{(16)}$**H$_2$**), 1.77-1.68 (3H, m, $C_{(30)}$**H** + $C_{(24)}$**H$_2$**), 1.63-1.58 (2H, m, $C_{(29)}$**H$_2$**), 1.50-1.44 (2H, m, $C_{(14)}$**H$_2$**), 1.21-1.09 (2H, m, $C_{(15)}$**H$_2$**), 0.88 (6H, d, *J* = 6.6 Hz, $C_{(31)}$**H$_3$** + $C_{(32)}$**H$_3$**). $^{13}$C NMR ($CDCl_3$, 125 MHz) δ:171.7 (**C**$_{(3)}$), 169.5 (**C**$_{(11)}$), 146.6 (**C**$_{(9)}$ + **C**$_{(21)}$), 135.0 (**C**$_{(9a)}$), 121.1 (**C**$_{(8)}$), 120.8 (**C**$_{(22)}$), 119.8 (**C**$_{(5a)}$), 116.9 (**C**$_{(7)}$), 110.5 (**C**$_{(6)}$), 83.8 (**C**$_{(26)}$), 68.9 ($C_{(27)}$), 66.9 (**C**$_{(28)}$), 51.9 (**C**$_{(12)}$), 51.5 (**C**$_{(17)}$), 51.5 (**C**$_{(2)}$), 49.9 (**C**$_{(13)}$), 47.1 (**C**$_{(5)}$), 38.0 (**C**$_{(19)}$), 36.1 (**C**$_{(10)}$), 29.8 (**C**$_{(23)}$), 28.0 (**C**$_{(16)}$), 27.5 (**C**$_{(14)}$), 25.2 (**C**$_{(30)}$), 24.4 (**C**$_{(24)}$), 23.4 (**C**$_{(15)}$), 22.7 (**C**$_{(31)}$), 22.7 (**C**$_{(32)}$), 17.8 (**C**$_{(25)}$). HRMS (ESI) calcd for $C_{29}H_{41}O_4N_5Na$ [M+Na$^+$]: *m*/*z* 546.3031, found *m*/*z* 546.3031. $\nu_{max}$ ($CDCl_3$)/cm$^{-1}$: 3291 (m), 2950 (s), 2358 (m), 1617 (s), 1274 (s). $[\alpha]_D$: 4.19 (*c* = 1.0, $CHCl_3$, 23.3 ºC).

(*S*)-Methyl 2-(9-(3-methylbutoxy)-4-(5-[4-(pent-4-yn-1-yl)-1H-1,2,3-triazol-1-yl] pentyl)-3-oxo-2,3,4,5-tetraydro-1H-benzo-1,4-diazepin-2-yl)acetate

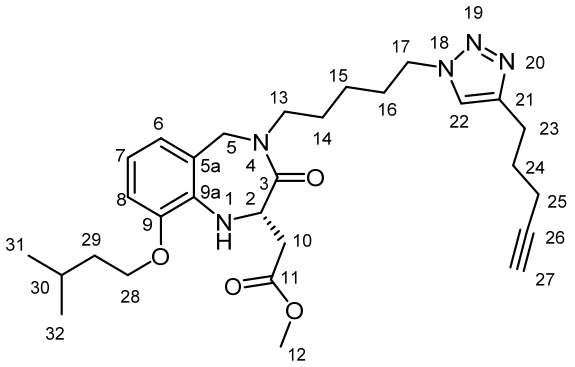

**(*S*)-114**

**(S)-114** was synthesised via the method described above (46%).

(*R*)-Methyl 2-(9-(3-methylbutoxy)-4-(5-[4-(prop-3-{1-[(*R*)-Methyl 2-(9-(3-methylbutoxy)-4-(pentyl)-3-oxo-2,3,4,5-tetraydro-1*H*-benzo-1,4-diazepin-2-yl)acetate]-1*H*-1,2,3-triazol-4-yl }-1-yl)-1H-1,2,3-triazol-1-yl] pentyl)-3-oxo-2,3,4,5-tetraydro-1*H*-benzo-1,4-diazepin-2-yl)acetate

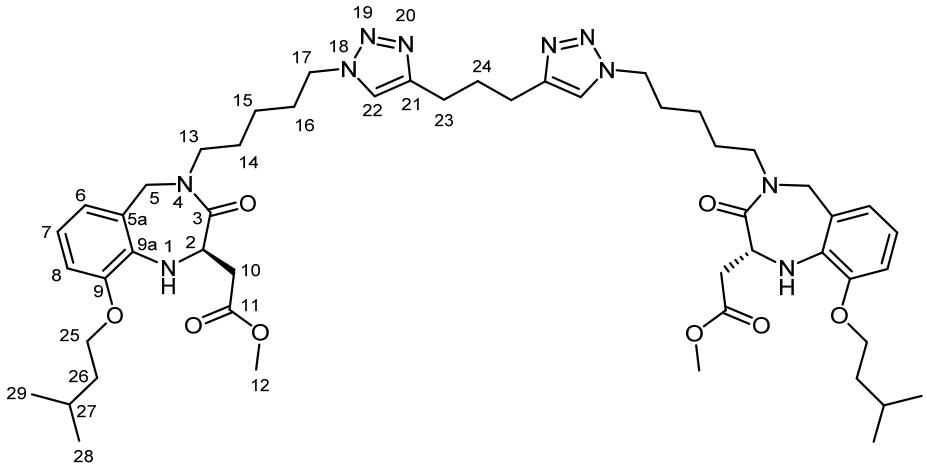

**(*R*)-115**

This compound was isolated as a by-product in the synthesis of **(*R*)-114**.

$^1$H NMR ($CDCl_3$, 500 MHz) δ: 7.22 (2H, s, **2** × $C_{(22)}$**H**), 6.63 (2H, dd, *J* = 7.7, 1.1 Hz, **2** × $C_{(6)}$**H**), 6.53-6.47 (4H, m, **2** × $C_{(7)}$**H** + **2** × $C_{(8)}$**H**), 5.37 (2H, d, *J* = 16.5 Hz, **2** × $C_{(5)}$**H**), 5.02-4.98 (2H, m, **2** × $C_{(2)}$**H**), 4.36 (2H, d, *J* = 4.4 Hz, **2** × N**H**), 4.10 (4H, t, *J* = 7.1 Hz, **2** × $C_{(17)}$**H**$_2$), 3.91 (4H, t, *J* = 6.7 Hz, **2** × $C_{(25)}$**H**$_2$), 3.68 (2H, d, *J* = 16.7 Hz, **2** × $C_{(5)}$**H**), 3.65 (6H, s, **2** × $C_{(12)}$**H**$_3$), 3.50 (2H, dt, *J* = 7.1, 13.7 Hz, **2** × $C_{(13)}$**H**), 3.35 (2H, dt, *J* = 6.7,13.7 Hz, **2** × $C_{(13)}$**H**), 2.97 (2H, dd, *J* = 7.4, 15.8 Hz, **2** × $C_{(10)}$**H**), 2.69 (4H, br s, **2** × $C_{(23)}$**H**$_2$), 2.60 (2H, dd, *J* = 15.8, 6.2 Hz, **2** × $C_{(10)}$**H**), 1.99-1.96 (2H, m, $C_{(24)}$**H**$_2$), 1.76-1.71 (6H, m, **2** × $C_{(27)}$**H** + **2** × $C_{(16)}$**H**$_2$), 1.61 (4H, qd, *J* = 6.5, 1.2 Hz, **2** × $C_{(26)}$**H**$_2$), 1.50-

1.44 (4H, m, **2** × $C_{(14)}\mathbf{H_2}$), 1.23-1.10 (4H, m, **2** × $C_{(15)}\mathbf{H_2}$), 0.89 (12H, dd, *J* = 6.6, 1.3 Hz, **2** × $C_{(28)}\mathbf{H_3}$ + **2** × $C_{(29)}\mathbf{H_3}$). $^{13}$C NMR ($CDCl_3$, 125 MHz) δ: 171.7 (**2** × $\mathbf{C}_{(3)}$), 169.5 (**2** × $\mathbf{C}_{(11)}$), 146.6 (**2** × $\mathbf{C}_{(9)}$ + **2** × $\mathbf{C}_{(21)}$), 135.0 (**2** × $\mathbf{C}_{(9a)}$), 121.1 (**2** × $\mathbf{C}_{(6)}$ + **2** × $\mathbf{C}_{(22)}$), 119.8 (**2** × $\mathbf{C}_{(5a)}$), 117.0 (**2** × $\mathbf{C}_{(7)}$), 110.6 (**2** × $\mathbf{C}_{(8)}$), 67.0 (**2** × $\mathbf{C}_{(25)}$), 51.9 (**2** × $\mathbf{C}_{(12)}$), 51.5 (**2** × $\mathbf{C}_{(2)}$),51.5 (**2** × $\mathbf{C}_{(5)}$),49.9 (**2** × $\mathbf{C}_{(17)}$), 47.2 (**2** × $\mathbf{C}_{(13)}$), 38.0 (**2** × $\mathbf{C}_{(26)}$), 36.2 (**2** × $\mathbf{C}_{(10)}$), 29.8 (**2** × $\mathbf{C}_{(16)}$), 29.2 ($\mathbf{C}_{(24)}$), 27.6 (**2** × $\mathbf{C}_{(14)}$), 25.2 (**2** × $\mathbf{C}_{(27)}$), 25.0 (**2** × $\mathbf{C}_{(23)}$),23.5 (**2** × $\mathbf{C}_{(15)}$), 22.7 (**2** × $\mathbf{C}_{(28/29)}$), 22.6 (**2** × $\mathbf{C}_{(28/29)}$). HRMS (ESI) calcd for $C_{51}H_{70}O_8N_{10}Na$ [$(M+Na)^+$]: *m*/*z* 973.5270, found *m*/*z* 973.5234. $\nu_{max}$ ($CDCl_3$)/$cm^{-1}$: 2928 (s), 2360 (m), 1647 (s), 1616 (s). $[\alpha]_D$: -3.29 (*c* = 1.0, $CHCl_3$, 24.7 ºC).

(*S*)-Methyl 2-(9-(3-methylbutoxy)-4-(5-[4-phenyl-1*H*-1,2,3-triazol-1-yl]pentyl)-3-oxo-2,3,4,5-tetraydro-1*H*-benzo-1,4-diazepin-2-yl)acetate

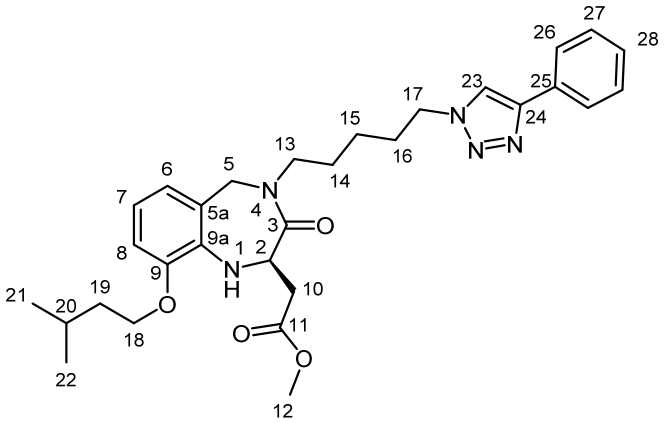


**(*S*)-116**

Copper (II) chloride (7.0 mg, 0.05 mmol, 1.0 eq.) was suspended in acetonitrile (0.2 mL), triethylamine (11 µL, 0.08 mmol, 1.5 eq.) was added and the suspension was sonicated for 1 min. Phenylacetylene (5 µL, 0.05 mmol, 1.0 eq.) was added to the solution and allowed to stir for 10 min. Sodium iodide (9 mg, 0.06 mmol, 1.2 eq.) was dissolved in water (0.1 mL). Azide **(*S*)-45** (20 mg, 0.05 mmol, 1.0 eq.) was dissolved in acetonitrile (0.2 mL). The solutions were combined and allowed to stir at room temperature for 16 h. The reaction mixture was concentrated *in vacuo* onto silica gel and purified by flash column chromatography (20-60% EtOAc in petroleum ether) giving the title compound as a light brown oil (10 mg, 0.19 mmol, 41%).

$^1$H NMR ($CDCl_3$, 500 MHz) δ: 7.76 (2H, d, *J* = 8.5 Hz, **2** × $C_{(26)}\mathbf{H}$), 7.65 (1H, s, $C_{(23)}\mathbf{H}$), 7.35 (2H, apparent t, *J* = 7.9 Hz, **2** × $C_{(27)}\mathbf{H}$), 7.25 (1H, t, *J* = 7.5 Hz, $C_{(28)}\mathbf{H}$), 6.62 (1H, dd, *J* = 7.6, 1.4 Hz, $C_{(6)}\mathbf{H}$), 6.52-6.46 (2H, m, $C_{(7)}\mathbf{H}$ + $C_{(8)}\mathbf{H}$), 5.37 (1H, d, *J* = 16.4 Hz, $C_{(5)}\mathbf{H}$), 5.01 (1H, m, $C_{(2)}\mathbf{H}$), 4.36 (1H, d, *J* = 4.1 Hz, N**H**), 4.18 (2H, td, *J* = 7.0, 4.5 Hz, $C_{(17)}\mathbf{H_2}$), 3.89 (2H, t, *J* = 6.6 Hz, $C_{(18)}\mathbf{H_2}$), 3.68 (1H, d, *J* = 16.6 Hz, $C_{(5)}\mathbf{H}$), 3.64 (3H, s, $C_{(12)}\mathbf{H_3}$), 3.53 (1H, dt, *J* = 13.6, 7.0 Hz, $C_{(13)}\mathbf{H}$), 3.35 (1H, dt, *J* = 13.7, 6.9 Hz, $C_{(13)}\mathbf{H}$),

2.97 (1H, dd, *J* = 15.8, 7.4 Hz, $C_{(10)}\mathbf{H}$), 2.60 (1H, dd, *J* = 15.9, 6.3 Hz, $C_{(10)}\mathbf{H}$), 1.84-1.77 (2H, m, $C_{(16)}\mathbf{H_2}$), 1.73 (1H, apparent septet, *J* = 6.8 Hz, $C_{(20)}\mathbf{H}$), 1.60 (2H, qd, *J* = 6.5, 1.6 Hz, $C_{(19)}\mathbf{H_2}$), 1.53-1.46 (2H, m, $C_{(14)}\mathbf{H_2}$), 1.27-1.18 (2H, m, $C_{(15)}\mathbf{H_2}$), 0.88 (6H, dd, *J* = 5.0, 1.7 Hz, $C_{(21)}\mathbf{H_3}$ + $C_{(22)}\mathbf{H_3}$). $^{13}$C NMR ($CDCl_3$, 125 MHz) δ: 171.7 ($\mathbf{C}_{(11)}$), 169.6 ($\mathbf{C}_{(3)}$), 147.7 ($\mathbf{C}_{(24)}$), 146.6 ($\mathbf{C}_{(9)}$), 135.0 ($\mathbf{C}_{(9a)}$), 130.8 ($\mathbf{C}_{(25)}$), 128.8 (**2** × $\mathbf{C}_{(26)}$), 128.1 ($\mathbf{C}_{(28)}$), 125.7 (**2** × $\mathbf{C}_{(27)}$), 121.1 ($\mathbf{C}_{(23)}$), 119.8 ($\mathbf{C}_{(5a)}$), 119.5 ($\mathbf{C}_{(6)}$), 117.0 ($\mathbf{C}_{(7)}$), 110.6 ($\mathbf{C}_{(8)}$), 67.0 ($\mathbf{C}_{(18)}$), 51.9 ($\mathbf{C}_{(12)}$), 51.5 ($\mathbf{C}_{(2)}$), 51.5 ($\mathbf{C}_{(5)}$), 50.2 ($\mathbf{C}_{(17)}$), 47.1 ($\mathbf{C}_{(13)}$), 38.0 ($\mathbf{C}_{(10/19)}$), 36.1 ($\mathbf{C}_{(10/19)}$), 29.7 ($\mathbf{C}_{(14/16)}$), 27.5 ($\mathbf{C}_{(14/16)}$), 25.2 ($\mathbf{C}_{(20)}$), 23.4 ($\mathbf{C}_{(15)}$), 22.7 ($\mathbf{C}_{(21)}$), 22.6 ($\mathbf{C}_{(22)}$). HRMS (ESI) calcd for $C_{30}H_{39}N_5NaO_4$ [$(M+Na)^+$]: *m*/*z* 556.2894, found *m*/*z* 556.2879. $\nu_{max}$ ($CDCl_3$)/$cm^{-1}$: 2926 (s), 2359 (m), 1734 (s), 1653 (s), 1250 (s). $[\alpha]_D$: + 18.4 (c = 1.0, $CHCl_3$, 22.7 ºC).

(*S*)-Methyl 2-(9-(3-methylbutoxy)-4-(5-[5-iodo-4-phenyl-1*H*-1,2,3-triazol-1-yl]pentyl)-3-oxo-2,3,4,5-tetraydro-1*H*-benzo-1,4-diazepin-2-yl)acetate

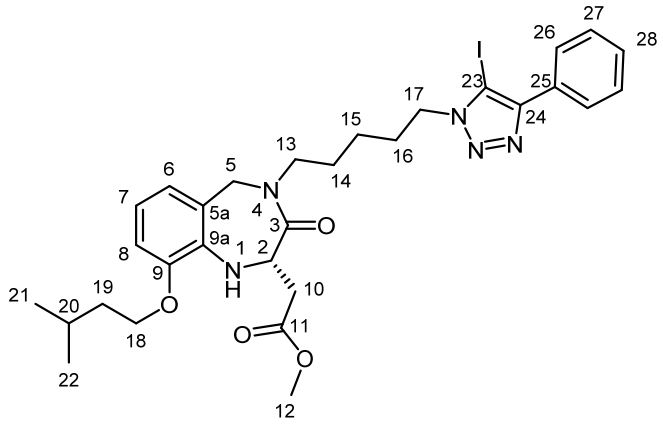


**(*S*)-117**

Copper (I) iodide (14 mg, 0.07 mmol, 1.0 eq.), *N*-iodosuccinimide (0.017 g, 0.08 mmol, 1.1 eq.) and triethylamine (0.01 mL, 0.07 mmol, 1.0 eq.) were added to a solution of azide **(*S*)-45** (30 mg, 0.07 mmol, 1.0 eq.) in dimethylformamide (1 mL). The reaction mixture was allowed to stir at room temperature for 2.5 h at which point thin layer chromatography indicated complete consumption of starting material. The reaction mixture was diluted with water (5 mL) and dichloromethane (5 mL) and the phases were separated. The organic layer was washed with water (5 × 10 mL), brine (5 mL), dried ($Na_2SO_4$) and concentrated *in vacuo*. The resulting mixture was purified by flash column chromatography giving the title compound as a colourless oil (0.014 g, 0.02 mmol, 30 %).

$^1$H NMR ($CDCl_3$, 500 MHz) δ: 7.85 (2H, d, *J* = 8.5 Hz, **2** × $C_{(26)}\mathbf{H}$ ), 7.35 (2H, apparent t, *J* = 7.7 Hz, **2** × $C_{(27)}\mathbf{H}$), 7.32 (1H, t, *J* = 7.4 Hz, $C_{(28)}\mathbf{H}$), 6.62 (1H, dd, *J* = 6.7, 2.7 Hz, $C_{(6)}\mathbf{H}$), 6.52-6.49 (2H, m, $C_{(7)}\mathbf{H}$ + $C_{(8)}\mathbf{H}$), 5.39 (1H, d, *J* = 16.4 Hz, $C_{(5)}\mathbf{H}$), 5.01 (1H, m,

$C_{(2)}$**H**), 4.38 (1H, d, *J* = 4.1 Hz, N**H**), 4.23 (2H, t, *J* = 7.5 Hz, $C_{(17)}$**H**$_2$), 3.90 (2H, t, *J* = 6.6 Hz, $C_{(18)}$**H**$_2$), 3.70 (1H, d, *J* = 16.6 Hz, $C_{(5)}$**H**), 3.66 (3H, s, $C_{(12)}$**H**$_3$), 3.56 (1H, dt, *J* = 13.6, 7.0 Hz, $C_{(13)}$**H**), 3.35 (1H, dt, *J* = 13.7, 6.9 Hz, $C_{(13)}$**H**), 2.98 (1H, dd, *J* = 16.0, 7.5 Hz, $C_{(10)}$**H**), 2.61 (1H, dd, *J* = 15.8, 6.4 Hz, $C_{(10)}$**H**), 1.78 (2H, apparent septet, *J* = 6.5 Hz, $C_{(16)}$**H**$_2$), 1.74 (1H, apparent septet, *J* = 6.7 Hz, $C_{(20)}$**H**), 1.61 (2H, qd, *J* = 6.6, 1.3 Hz, $C_{(19)}$**H**$_2$), 1.52 (2H, dq, *J* = 7.5, 7.3 Hz, $C_{(14)}$**H**$_2$), 1.30-1.19 (2H, m, $C_{(15)}$**H**$_2$),0.89 (6H, dd, *J* = 6.6, 1.7 Hz, $C_{(21)}$**H**$_3$ + $C_{(22)}$**H**$_3$). $^{13}$C NMR ($CDCl_3$, 125 MHz) δ: 171.7 (**C**$_{(11)}$), 169.5 (**C**$_{(3)}$), 149.7 (**C**$_{(24)}$), 146.6 (**C**$_{(9)}$), 135.0 (**C**$_{(9a)}$), 131.6 (**C**$_{(23)}$), 130.4 (**C**$_{(25)}$), 128.7 (**2** × **C**$_{(26)}$ + **C**$_{(28)}$), 127.5 (**2** × **C**$_{(27)}$), 121.1 (**C**$_{(6)}$), 119.8 (**C**$_{(5a)}$), 117.0 (**C**$_{(7)}$), 110.6 (**C**$_{(8)}$), 66.9 (**C**$_{(18)}$), 52.0 (**C**$_{(12)}$), 51.5 (**C**$_{(2)}$), 51.5 (**C**$_{(5)}$), 50.5 (**C**$_{(17)}$), 47.3 (**C**$_{(13)}$), 38.0 (**C**$_{(10/19)}$), 36.2 (**C**$_{(10/19)}$), 29.5 (**C**$_{(14/16)}$), 27.7 (**C**$_{(14/16)}$), 25.2 (**C**$_{(20)}$), 23.5 (**C**$_{(15)}$), 22.7 (**C**$_{(21)}$), 22.6 (**C**$_{(22)}$). HRMS (ESI) calcd for $C_{30}H_{38}IN_5NaO_4$ [$(M+Na)^+$]: *m*/*z* 682.1861, found *m*/*z* 682.1847. $\nu_{max}$ ($CDCl_3$)/$cm^{-1}$: 3405 (m), 2951 (m), 1735 (m), 1658 (s), 1249 (s).

(*S*)-Methyl 2-(9-(3-methylbutoxy)-4-[5-(4-{3-[1-(3-{4,4-difluoro-5,7-dimethyl-4-bora-3a,4a-diaza-*s*-indacene-3-yl}propyl)-1*H*-1,2,3-triazol-4-yl]propyl}-1H-1,2,3-triazol-1-yl)pentyl]-3-oxo-2,3,4,5-tetraydro-1*H*-benzo-1,4-diazepin-2-yl)acetate

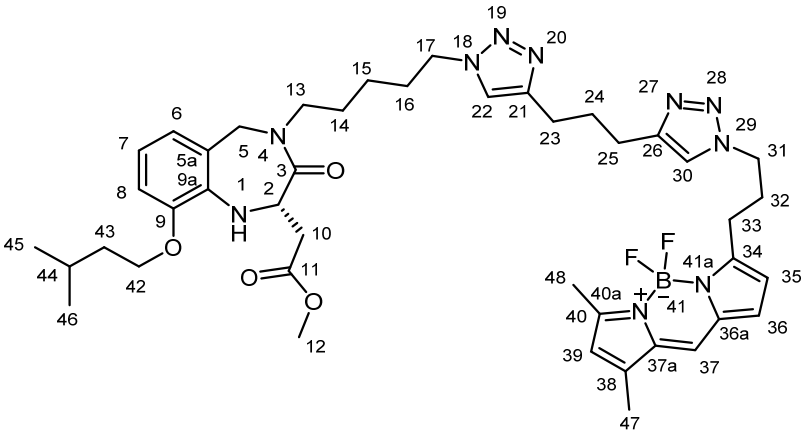

**MM-IGD-FL2**

Alkyne **(*S*)-114** (72 mg, 0.14 mmol, 1.0 eq.) was dissolved in THF (3 mL) and water (1 mL). Azide **109** (46 mg, 0.15 mmol, 1.1 eq.), copper (II) sulfate pentahydrate (27 mg, 0.17 mmol, 1.2 eq.) and sodium ascorbate (67 mg, 0.34 mmol, 2.4 eq.) were added to the solution and the resulting mixture was allowed to stir at 70 °C for 2 h. The reaction mixture was concentrated *in vacuo* and diluted in ethyl acetate (15 mL) and water (15 mL) and the phases were separated. The aqueous phase was extracted with EtOAc (10 mL x 2). The combined organic phases were dried ($Na_2SO_4$), filtered and concentrated *in vacuo*. Preparative thin layer chromatography (10% MeOH in EtOAc) gave the title compound as a red/green solid (55 mg, 0.07 mmol, 48%)

$^{1}$H NMR ($CDCl_3$, 500 MHz) δ: 7.29 (1H, s, $C_{(30)}$**H**), 7.20 (1H, s, $C_{(22)}$**H**),7.02 (1H, s, $C_{(37)}$**H**), 6.80 (1H, d, *J* = 4.1 Hz, $C_{(36)}$**H**),6.62 (1H, dd, *J* = 7.6, 1.8 Hz, $C_{(6)}$**H**), 6.52-6.46 (2H, m, $C_{(7)}$**H** + $C_{(8)}$**H**), 6.18 (1H, d, *J* = 4.0 Hz, $C_{(35)}$**H**), 6.05 (1H, s, $C_{(39)}$**H**), 5.35 (1H, d, *J* = 16.6 Hz, $C_{(5)}$**H**), 4.99 (1H, dt, *J* = 4.9, 6.5 Hz, $C_{(2)}$**H**), 4.35 (1H, d, *J* = 4.4 Hz, N**H**), 4.33 (2H, t, *J* = 4.4 Hz, C$\mathbf{H_2}$), 4.09 (2H, t, *J* = 7.3 Hz, C$\mathbf{H_2}$), 3.90 (2H, t, *J* = 6.6 Hz, C$\mathbf{H_2}$), 3.67 (1H, d, *J* = 16.7 Hz, $C_{(5)}$**H**), 3.65 (3H, s, $C_{(12)}\mathbf{H_3}$), 3.49 (1H, dt, *J* = 13.7, 6.9 Hz, $C_{(13)}$**H**), 3.33 (1H, dt, *J* = 13.7, 6.9 Hz, $C_{(13)}$**H**), 3.00-2.92 (3H, m, $C_{(10)}$**H** + C$\mathbf{H_2}$), 2.68 (2H, t, *J* = 7.5 Hz, C$\mathbf{H_2}$), 2.60 (1H, dd, *J* = 15.9, 6.3 Hz, $C_{(10)}$**H**), 2.47 (3H, s, $C_{(47/48)}\mathbf{H_3}$), 2.29 (2H, tt, *J* = 7.5, 7.3, C$\mathbf{H_2}$), 2.18 (3H, s, $C_{(47/48)}\mathbf{H_3}$), 1.97 (2H, tt, *J* = 7.6, 6.5, C$\mathbf{H_2}$), 1.78-1.68 (4H, m, 2 × C$\mathbf{H_2}$), 1.63-1.58 (2H, m, C$\mathbf{H_2}$), 1.46 (2H, tt, *J* = 7.3, 7.2, C$\mathbf{H_2}$), 1.22-1.13 (3H, m, C$\mathbf{H_2}$ + $C_{(44)}$**H**), 0.88 (6H, dd, *J* = 6.6, 1.0, $C_{(45)}\mathbf{H_3}$ + $C_{(46)}\mathbf{H_3}$). $^{13}$C NMR ($CDCl_3$, 125 MHz): 171.7 ($\mathbf{C}_{(11/3)}$), 169.5 ($\mathbf{C}_{(11/3)}$), 160.4 (Ar$\mathbf{C}_q$), 156.9 (Ar$\mathbf{C}_q$), 147.5 ($\mathbf{C}_{(21)}$ + $\mathbf{C}_{(26)}$), 146.6 (Ar$\mathbf{C}_q$), 144.0 (Ar$\mathbf{C}_q$), 135.2 (Ar$\mathbf{C}_q$), 135.0 (Ar$\mathbf{C}_q$), 133.2 (Ar$\mathbf{C}_q$), 128.2 (Ar**C**H), 123.8 (Ar**C**H), 121.1 (Ar**C**H), 120.8 (Ar**C**H), 120.5 (Ar**C**H), 119.8 ($\mathbf{C}_{(5a)}$), 117.0 (Ar**C**H), 116.7 (Ar**C**H), 110.6 (Ar**C**H), 67.0 ($\mathbf{C}_{(42)}$), 51.9 ($\mathbf{C}_{(12)}$), 51.5 ($\mathbf{C}_{(2)}$), 51.5 ($\mathbf{C}_{(5)}$), 49.9 (**C**$H_2$), 49.6 (**C**$H_2$), 47.2 (**C**$H_2$), 38.0 (**C**$H_2$), 36.2 (**C**$H_2$), 29.8 (**C**$H_2$), 29.7 (**C**$H_2$), 29.6 (**C**$H_2$), 29.5 (**C**$H_2$), 29.1 (**C**$H_2$), 27.5 (**C**$H_2$), 25.7 (**C**$H_2$), 25.2 ($\mathbf{C}_{(44)}$), 24.9 (**C**$H_2$), 23.5 (**C**$H_2$), 22.7 ($\mathbf{C}_{(45/46)}$), 22.6 ($\mathbf{C}_{(45/46)}$), 14.9 ($\mathbf{C}_{(47/48)}$), 11.3 ($\mathbf{C}_{(47/48)}$). HRMS (ESI) calcd for $BC_{43}F_2H_{57}N_{10}NaO_4$ [M+Na$^+$]: *m/z* 849.4523, found *m/z* 849.4465. $\nu_{max}$ ($CDCl_3$)/cm$^{-1}$: 2925 (m), 2361 (w), 1602 (s), 1437 (m), 1138 (s). $[\alpha]_D$: -18.4 (*c* = 1.0, 23.1 ºC). λabs,max (MeCN): 503 nm, λem,max (MeCN): 513 nm.

(*R*)-Methyl 2-(9-(3-methylbutoxy)-4-[5-(4-{3-[1-(3-{4,4-difluoro-5,7-dimethyl-4-bora-3a,4a-diaza-*s*-indacene-3-yl}propyl)-1*H*-1,2,3-triazol-4-yl]propyl}-1*H*-1,2,3-triazol-1-yl)pentyl]-3-oxo-2,3,4,5-tetraydro-1*H*-benzo-1,4-diazepin-2-yl)acetate

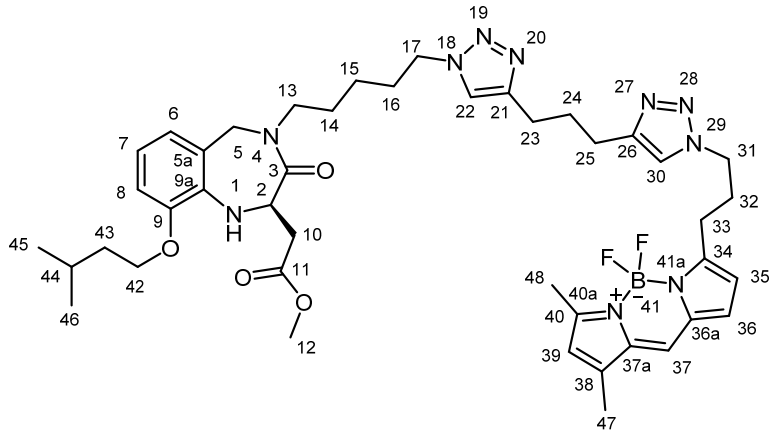

**MM-IGD-FL1**

**MM-IGD-FL1** was synthesised via the method described above. $[\alpha]_D$: 16.6 (*c* = 1.0, 23.2 ºC).

(*R*)-Methyl 2-(9-(3-methylbutoxy)-4-(5-aminopentyl)-3-oxo-2,3,4,5-tetraydro-1*H*-benzo-1,4-diazepin-2-yl)acetate

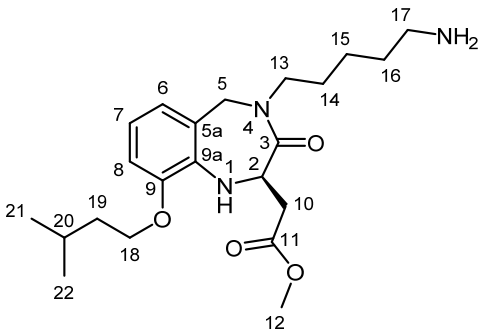


**(*R*)-40**

Azide **(*R*)-45** (0.15 g, 0.36 mmol, 1.0 eq.), was dissolved in methanol (10 mL) and 10 % palladium on activated charcoal (20 mg) was added and the reaction mixture was stirred at 40 ºC. Hydrogen gas was allowed to bubble through the reaction mixture for 3 h. The reaction mixture was filtered through celite, washed with methanol (3 × 10 mL) and the filtrate was concentrated *in vacuo* giving the title compound as a yellow oil (0.14 g, 0.36 mmol, 100%).

$^1$H NMR ($CDCl_3$, 400 MHz) δ: 6.62 (1H, dd, *J* = 7.4, 2.0 Hz, $C_{(6)}$**H**), 6.53-6.47 (2H, m, $C_{(7)}$**H** + $C_{(8)}$**H**), 5.37 (1H, d, *J* = 16.4 Hz, $C_{(5)}$**H**), 5.03-4.98 (1H, m, $C_{(2)}$**H**), 4.35 (1H, d, *J* = 4.5 Hz, N**H**), 3.90 (2H, t, *J* = 6.6 Hz, $C_{(18)}$**H**$_2$), 3.70 (1H, d, *J* = 16.6 Hz, $C_{(5)}$**H**), 3.66 (3H, s, $C_{(12)}$**H**$_3$), 3.53-3.43 (1H, m, $C_{(13)}$**H**), 3.39-3.33 (1H, m, $C_{(13)}$**H**), 2.97 (1H, dd, *J* = 16.0, 7.4 Hz, $C_{(10)}$**H**), 2.60 (1H, dd, *J* = 15.9, 6.5 Hz, $C_{(10)}$**H**), 2.50 (2H, t, *J* = 6.8 Hz, $C_{(17)}$**H**$_2$), 1.74 (1H, apparent septet, *J* = 6.7 Hz, $C_{(20)}$**H**), 1.61 (2H, q, *J* = 6.5 Hz, $C_{(19)}$**H**$_2$), 1.45 (2H, tt, *J* = 15.0, 7.5 Hz, $C_{(14)}$**H**$_2$), 1.35-1.23 (4H, m, $C_{(16)}$**H**$_2$ + N**H**$_2$), 1.20-1.11 (2H, m, $C_{(15)}$**H**$_2$), 0.89 (6H, dd, *J* = 6.5, 0.8 Hz, $C_{(21)}$**H**$_3$ + $C_{(22)}$**H**$_3$). $^{13}$C NMR ($CDCl_3$, 100 MHz) δ: 171.8 (**C**$_{(3)}$), 169.4 (**C**$_{(11)}$), 146.6 (**C**$_{(9)}$), 135.1 (**C**$_{(9a)}$), 121.1 (**C**$_{(6)}$), 119.9 (**C**$_{(5a)}$), 116.9 (**C**$_{(7)}$), 110.5 (**C**$_{(8)}$), 66.9 (**C**$_{(18)}$), 51.9 (**C**$_{(12)}$), 51.6 (**C**$_{(2)}$), 51.5 (**C**$_{(5)}$), 47.6 (**C**$_{(13)}$), 42.0 (**C**$_{(17)}$), 38.0 (**C**$_{(19)}$), 36.2 (**C**$_{(10)}$), 33.5 (**C**$_{(16)}$), 28.1 (**C**$_{(14)}$), 25.2 (**C**$_{(20)}$), 23.9 (**C**$_{(15)}$), 22.7 (**C**$_{(21)}$), 22.6 (**C**$_{(22)}$). HRMS (EI+) calcd for $C_{22}H_{35}N_3O_4$ [$M^+$]: *m/z* 405.2628, found *m/z* 405.2630. $\nu_{max}$ ($CDCl_3$)/$cm^{-1}$: 3410 (m), 1736 (s), 1658 (s), 1435 (s), 748 (s). $[\alpha]_D$: 4.32 (*c* = 1.0, $CHCl_3$, 28.8 ºC).

(*S*)-Methyl 2-(9-(3-methylbutoxy)-4-(5-aminopentyl)-3-oxo-2,3,4,5-tetraydro-1*H*-benzo-1,4-diazepin-2-yl)acetate

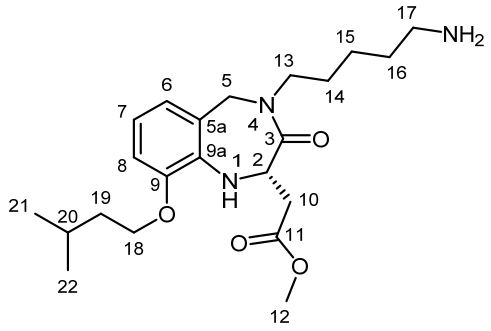

**(*S*)-45**

**(*S*)-45** was synthesised via the method described above (70%). $[\alpha]_D$: - 4.82 (*c* = 1.0, $CHCl_3$, 28.8 ºC).

(*R*)-Methyl 2-(9-(3-methylbutoxy)-4-(pentyl-5-[carbamoylethyl-2-{4,4-difluoro-5,7-dimethyl-4-bora-3a,4a-diaza-*s*-indacene-3-yl}])-3-oxo-2,3,4,5-tetraydro-1*H*-benzo-1,4-diazepin-2-yl)acetate

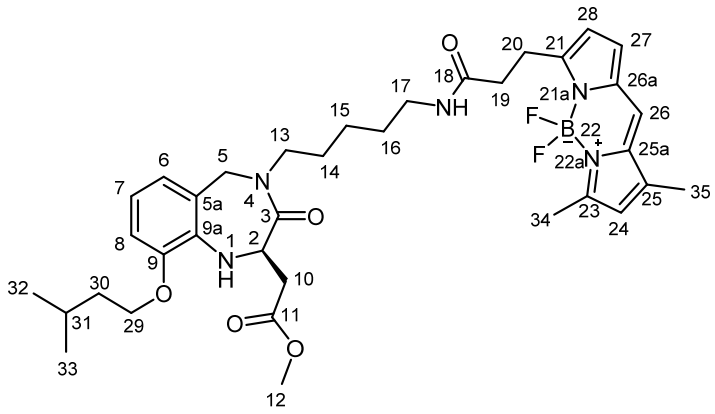

**(*R*)-85**

BODIPY FL (18 mg, 0.06 mmol, 1.2 eq.) was dissolved in dichloromethane (5 mL). *O*-(Benzotriazol-1-yl)-*N*,*N*,*N*′,*N*′-tetramethyluronium hexafluorophosphate (23 mg, 0.06 mmol, 1.2 eq.) and *N*,*N*-di*iso*propylethylamine (22 µL, 0.125 mmol, 2.5 eq.), were added to the mixture which was allowed to stir at room temperature for 20 min. Amine **(*R*)-40** (20 mg, 0.05 mmol, 1.0 eq.) was added and the reaction mixture was allowed to stir for 16 h. The reaction mixture was concentrated onto silica gel *in vacuo* and purified by flash column chromatography (0-1% methanol in ethyl acetate) giving the title compound as a red/green oil (15 mg, 0.02 mmol, 37%).

$^1$H NMR ($CD_3OD$, 500 MHz) δ: 7.30 (1H, s, Ar**H**), 6.90-6.89 (1H, m, Ar**H**), 6.59 (1H, dd, *J* = 7.8, 1.2 Hz, $C_{(6)}$**H**), 6.52-6.46 (2H, m, $C_{(7)}$**H** + $C_{(8)}$**H**), 6.20 (1H, d, *J* = 4.0 Hz,

Ar**H**), 6.09 (1H, br s, Ar**H**), 5.33 (1H, d, *J* = 16.5 Hz, $C_{(5)}$**H**), 4.99 (1H, t, *J* = 6.8 Hz, $C_{(2)}$**H**), 3.88 (2H, t, *J* = 6.5 Hz, $C_{(29)}$**H**$_2$), 3.80 (1H, d, *J* = 16.8 Hz, $C_{(5)}$**H**), 3.59 (3H, s, $C_{(12)}$**H**$_3$), 3.46 (1H, dt, *J* = 13.5, 6.7 Hz, $C_{(13)}$**H**), 3.26 (1H, dt, *J* = 13.7, 6.7 Hz, $C_{(13)}$**H**), 3.10 (2H, t, *J* = 7.5 Hz, $C_{(19)}$**H**$_2$), 3.00-2.88 (2H, m, $C_{(17)}$**H**$_2$), 2.81 (1H, dd, *J* = 16.2, 7.6 Hz, $C_{(10)}$**H**), 2.58 (1H, dd, *J* = 16.2, 6.3 Hz, $C_{(10)}$**H**), 2.47 (2H, td, *J* = 7.2, 1.9 Hz, $C_{(20)}$**H**$_2$), 2.39 (3H, s, $C_{(34/35)}$**H**$_3$), 2.16 (3H, s, $C_{(34/35)}$**H**$_3$), 1.72 (1H, apparent septet, *J* = 6.7 Hz, $C_{(31)}$**H**), 1.58-1.54 (2H, m, $C_{(30)}$**H**$_2$), 1.43- 1.37 (2H, m, $C_{(14)}$**H**$_2$), 1.31-1.19 (2H, m, $C_{(16)}$**H**$_2$), 1.09-0.97 (2H, m, $C_{(15)}$**H**$_2$), 0.86 (6H, d, *J* = 6.6 Hz, $C_{(32)}$**H**$_3$ + $C_{(33)}$**H**$_3$). $^{13}$C NMR ($CD_3OD$, 125 MHz) δ: 174.5 (**C**O), 173.4 (**C**O), 172.0 (**C**O), 161.3 (Ar**C**), 158.5 (Ar**C**), 148.0 (Ar**C**), 145.8 (Ar**C**), 136.5 (Ar**C**), 136.4 (Ar**C**), 134.9 (Ar**C**), 129.6 (Ar**C**H), 125.8 (Ar**C**H), 122.5 (Ar**C**H), 121.6 (Ar**C**), 121.3 (Ar**C**H), 118.4 (Ar**C**H), 117.8 (Ar**C**H), 112.1 (Ar**C**H), 68.1 ($\mathbf{C}_{(29)}$), 52.5 ($\mathbf{C}_{(12)}$), 52.4 ($\mathbf{C}_{(2)}$), 52.2 ($\mathbf{C}_{(5)}$), 40.2 (**C**H$_2$), 39.2 (**C**H$_2$), 36.7 (**C**H$_2$), 36.0 (**C**H$_2$), 30.8 (**C**H$_2$), 29.7 (**C**H$_2$), 28.8 (**C**H$_2$), 26.4 ($\mathbf{C}_{(31)}$), 25.7 (**C**H$_2$), 24.8 (**C**H$_2$), 23.1 ($\mathbf{C}_{(32/33)}$), 23.0 ($\mathbf{C}_{(32/33)}$), 14.9 ($\mathbf{C}_{(34/35)}$), 11.2 ($\mathbf{C}_{(34/35)}$). HRMS (ESI) calcd for $BC_{36}F_2H_{48}N_5NaO_5$ [(M+Na)$^+$]: 702.3645, found: 702.3611. $\nu_{max}$ ($CDCl_3$)/cm$^{-1}$:2929.0 (w), 2358.1 (w), 1734.1 (m), 1603.9 (s), 1136.1 (s). $[\alpha]_D$: +0.120 (*c* = 1.0, $CHCl_3$, 28.4 ºC). λabs,max (MeCN): 504 nm, λem,max (MeCN): 513 nm.

((*S*)-Methyl 2-(9-(3-methylbutoxy)-4-(5-amino-(4,4-difluoro-4-bora-3a,4a-diaza-*s*-indacene-8-yl)-pentyl)-3-oxo-2,3,4,5-tetraydro-1*H*-benzo-1,4-diazepin-2-yl)acetate)

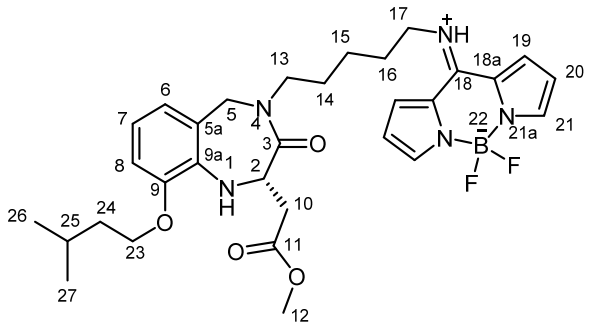

**(*S*)-95**

Amine **(*S*)-40** (0.02 g, 0.05 mmol, 1.0 eq.) was added to BODIPY **92** (0.011 g, 0.05 mmol, 1.0 eq.) in dichloromethane (1 mL) and the reaction mixture was allowed to stir at room temperature for 18 h. The reaction mixture was concentrated onto silica gel *in vacuo* and purified by flash column chromatography (0-60% ethyl acetate in petroleum ether). The desired fractions were concentrated *in vacuo* and dissolved in ethyl acetate (10 mL). The ethyl acetate solution was washed with water (10 mL), brine (10 mL), dried ($Na_2SO_4$), filtered and concentrated *in vacuo* giving the title compound (10 mg, 0.02 mmol, 40%).

$^{1}$H NMR ($CDCl_3$, 500 MHz) δ: 7.62 (1H, br s, BODIPY**H**), 7.43-7.38 (3H, m, **3** x BODIPY**H**), 7.05 (1H, br s, BODIPY**H**), 6.62 (1H, dd, *J* = 7.6, 1.6 Hz, $C_{(6)}$**H**), 6.53-6.48 (2H, m, $C_{(7)}$**H** + $C_{(8)}$**H**), 6.44 (1H, br s, BODIPY**H**), 6.34 (1H, br s, BODIPY**H**), 5.43 (1H, d, *J* = 16.3 Hz, $C_{(5)}$**H**), 5.06-5.02 (1H, m, $C_{(2)}$**H**), 4.29 (1H, d, *J* = 4.3 Hz, N**H**), 3.88 (2H, t, *J* = 6.6 Hz, $C_{(23)}$**H**$_2$), 3.74 (1H, *J* = 16.7 Hz, $C_{(5)}$**H**), 3.61-3.47 (5H, m, $C_{(12)}$**H**$_3$ + $C_{(13)}$**H**$_2$), 3.04 (1H, dd, *J* = 16.4, 8.6 Hz, $C_{(10)}$**H**), 2.60 (1H, dd, *J* = 16.4, 5.6 Hz, $C_{(10)}$**H**), 1.82-1.75 (2H, m, $C_{(17)}$**H**$_2$), 1.70 (1H, apparent septet, $C_{(25)}$**H**$_2$), 1.62-1.57 (6H, m, $C_{(14)}$**H**$_2$ + $C_{(16)}$**H**$_2$ + $C_{(19)}$**H**$_2$), 1.41-1.34 (2H, m, $C_{(15)}$**H**$_2$), 0.88 (3H, d, *J* = 3.8 Hz, $C_{(26/27)}$**H**$_3$), 0.86 (3H, d, *J* = 3.8 Hz, $C_{(26/27)}$**H**$_3$). $^{13}$C NMR ($CDCl_3$, 125 MHz) δ: 171.7 (**C**$_{(3/11)}$), 170.8 (**C**$_{(3/11)}$), 149.0 (**C**$_{(9)}$), 146.6 (**C**$_{(9a)}$), 134.9 (**C**$_{(18)}$), 132.3 (**2** × **C**$_{(18a)}$), 121.1 (**C**$_{(6)}$), 119.4 (**C**$_{(5a)}$), 117.2 (**C**$_{(7)}$), 116.3 (**2** × Ar**C**), 114.3 (**2** × Ar**C**), 113.2 (**2** × Ar**C**), 110.7 (**C**$_{(8)}$), 67.0 (**C**$_{(23)}$), 51.9 (**C**$_{(12)}$), 51.7 (**C**$_{(2)}$), 51.3 (**C**$H_2$), 47.7 (**C**$H_2$), 46.5 (**C**$H_2$), 37.8 (**C**$H_2$), 36.1 (**C**$H_2$), 29.7 (**C**$H_2$), 27.6 (**C**$H_2$), 25.3 (**C**$_{(25)}$), 24.1 (**C**$H_2$), 22.7 (**C**$_{(26/27)}$), 22.6 (**C**$_{(26/27)}$). HRMS (ESI) calcd for $BC_{31}F_2H_{40}N_5NaO_5$ [$(M+Na)^+$]: 617.3070, found: 617.3047. $\nu_{max}$ ($CDCl_3$)/$cm^{-1}$: 2924 (s), 1735 (s), 1643 (s), 1395 (s), 1083 (s).

3,5-Dimethyl-1*H*-pyrrole-2-carboxaldehyde[70, 93]

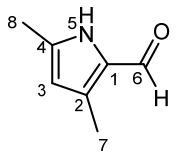


**90**

Phosphorous oxychloride (1.02 mL, 11.0 mmol, 1.1 eq.) was added dropwise to dimethylformamide (20 mL) at 0 °C and allowed to stir for 10 min and warm to room temperature for 30 min. The reaction mixture was cooled to 0 °C and 2,4-dimethylpyrrole (1.02 mL, 10.0 mmol, 1.0 eq.) was added. The reaction mixture was heated to 40 °C and allowed to stir for 18 h. Sodium hydroxide (1 M aq.) was added dropwise increasing to pH 11. The reaction mixture was diluted with ethyl acetate (20 mL) and brine (20 mL) and the phases were separated. The organic layer was washed with brine (5 × 20 mL), dried ($Na_2SO_4$), filtered and concentrated *in vacuo* onto silica gel. Flash column chromatography (0-20% ethyl acetate in petroleum ether) gave the title compound as a colourless oil (1.04 g, 8.3 mmol, 83%).

$^{1}$H NMR ($CDCl_3$, 500 MHz) δ: 9.72 (1H, br s, N**H**), 9.32 (1H, s, $C_{(6)}$**H**), 5.76 (1H, br s, $C_{(3)}$**H**), 2.23 (3H, s, $C_{(7/8)}$**H**$_3$), 2.21 (3H, s, $C_{(7/8)}$**H**$_3$). $^{13}$C NMR ($CDCl_3$, 125 MHz) $\delta_C$: 176.0 (**C**$_{(6)}$), 138.1 (**C**$_{(ArQ)}$), 134.5 (**C**$_{(ArQ)}$), 128.8 (**C**$_{(ArQ)}$), 112.0 (**C**$_{(3)}$), 13.2 (**C**$_{(7/8)}$), 10.6 (**C**$_{(7/8)}$).

(*E*)-Methyl 3-(1*H*-pyrrol-2-yl)acrylate[70, 93]

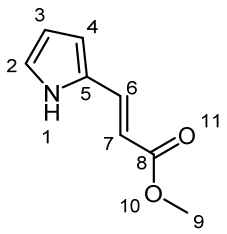


**87**

Methyl (triphenylphosphoranylidene) acetate (35.1 g, 105 mmol, 2.0 eq.), was dissolved in anhydrous dichloromethane (50 mL). Pyrrole-2-carbaldehyde (**90**) (5.00 g, 52.6 mmol, 1.0 eq) was dissolved in dichloromethane (50 mL) and added to the solution. The reaction mixture was allowed to stir for 24 hours before dilution with diethyl ether (100 mL) and water (100 mL). The phases were separated and the aqueous layer was extracted with diethyl ether (2 × 50 mL), the combined organic layer was washed with brine (100 mL), dried ($Na_2SO_4$), and concentrated *in vacuo*. The crude residue was purified by flash column chromatography (20 % ethyl acetate in petroleum ether) giving the title compound (5.79 g, 38.3 mmol, 73%).

$^1$H NMR ($CDCl_3$, 400 MHz): 8.57 (1H, br s, N**H**), 7.58 (1H, d, *J* = 16.0 Hz, $C_{(6)}$**H**), 6.96-6.95 (1H, m, Ar**H**), 6.60-6.58 (1H, m, Ar**H**), 6.32-6.30 (1H, m, Ar**H**), 6.00 (1H, d, *J* = 16.0 Hz, $C_{(7)}$**H**), 3.80 (3H, s, $C_{(9)}$**H**$_3$). $^{13}$C NMR ($CDCl_3$, 125 MHz): 174.5 (**C**$_{(8)}$), 130.9 (**C**$_{(5)}$), 116.8 (**C**$_{(2)}$), 108.0 (**C**$_{(4)}$), 105.5(**C**$_{(3)}$), 51.8 (**C**$_{(9)}$), 34.4 (**C**$_{(6)}$), 22.6 (**C**$_{(7)}$).

Methyl 3-(1*H*-pyrrol-2-yl) propanoate[70, 93]

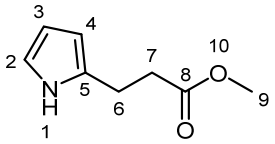


**88**

Alkene **87** (0.40 g, 2.60 mmol, 1.0 eq.) was dissolved in anhydrous methanol (15 mL), 10% palladium on activated charcoal (40 mg) was added. Hydrogen gas was bubbled through the slurry for 5 min and reaction mixture was heated to 40 ºC under a hydrogen atmosphere for 2 h. The mixture was filtered through celite which was then washed with methanol (2 × 30 mL). The methanol portions were then combined and concentrated *in vacuo* giving the title compound (0.40 g, 2.6 mmol, quantitative).

$^1$H NMR ($CDCl_3$, 400 MHz): 8.57 (1H, br s, N**H**), 6.71-6.69 (1H, m, Ar**H**), 6.13 (1H, q, *J* = 2.9 Hz, Ar**H**), 5.95-5.93 (1H, m, Ar**H**), 3.72 (3H, s, $OC_{(9)}$**H**$_3$), 2.94 (1H, t, *J* = 6.7 Hz, $C_{(7)}$**H**$_2$CO), 2.67 (1H, t, *J* = 6.5 Hz, $C_{(6)}$**H**$_2$). $^{13}$C NMR ($CDCl_3$, 125 MHz):174.5 (**C**$_{(8)}$), 130.9 (**C**$_{(5)}$), 116.8 (Ar**C**), 108.0 (Ar**C**), 105.5 (Ar**C**), 51.8 (**C**$_{(7)}$), 34.3 (**C**$_{(9)}$), 22.6 (**C**$_{(6)}$).

Methyl 3-[4,4-Difluoro-5,7-dimethyl-4-bora-3a,4a-diaza-*s*-indacene-3-yl]propionate[70]

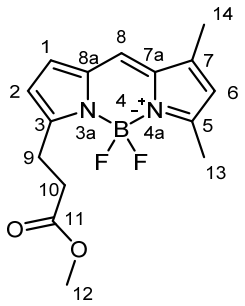


**91**

Pyrrole **88** (0.15 g, 1.0 mmol, 1.0 eq.) and aldehyde **90** were dissolved in dichloromethane (6 mL) and cooled to 0 ºC. Phosphorous oxychloride (0.16 g, 1.10 mmol, 1.1 eq.) was dissolved in dichloromethane (4 mL) and added to the solution. The black reaction mixture was allowed to warm to room temperature and stir for 16 h. The reaction mixture was cooled to 0 °C and boron trifluoride diethyl etherate (0.50 mL, 4.00 mmol, 4.2 eq.) and *N*,*N*-diisopropylethylamine (0.73 mL, 3.20 mmol, 4.0 eq.) were added. The reaction mixture was allowed to warm to room temperature and stir for 16 hours. The reaction mixture was diluted with water (20 mL) and then filtered through celite and washed with dichloromethane (2 × 20 mL). The filtrate was concentrated *in vacuo* and purified by flash column chromatography (20% ethyl acetate in petroleum ether) giving the title compound as a red solid (0.13 g, 0.42 mmol, 44%).

$^{1}$H NMR ($CDCl_3$, 400 MHz): 7.09 (1H, s, $C_{(8)}$**H**), 6.88 (1H, d, *J* = 4.0 Hz, $C_{(1)}$**H**), 6.27 (1H, d, *J* = 4.0 Hz, $C_{(2)}$**H**), 6.12 (1H, s, $C_{(6)}$**H**), 3.71 (3H, s, $C_{(12)}$**H**$_3$), 3.30 (2H, t, *J* = 7.7 Hz, $C_{(10)}$**H**$_2$), 2.79 (2H, t, *J* = 7.9 Hz, $C_{(9)}$**H**$_2$), 2.57 (3H, s, $C_{(13/14)}$**H**$_3$), 2.25 (3H, s, $C_{(13/14)}$**H**$_3$). $^{13}$C NMR ($CDCl_3$, 125 MHz):173.0 (**C**$_{(11)}$), 160.5 (Ar**C**), 157.0 (Ar**C**), 143.9 (Ar**C**), 135.2 (Ar**C**), 133.3 (Ar**C**), 128.0 (Ar**C**), 123.8 (Ar**C**), 120.4 (Ar**C**), 116.7 (Ar**C**), 51.7 (**C**$_{(12)}$), 33.3 (**C**$_{(10)}$), 24.0 (**C**$_{(9)}$), 15.0 (**C**$_{(13/14)}$), 11.3 (**C**$_{(13/14)}$).

3-[4,4-Difluoro-5,7-dimethyl-4-bora-3a,4a-diaza-*s*-indacene-3-yl]propionic acid[70]

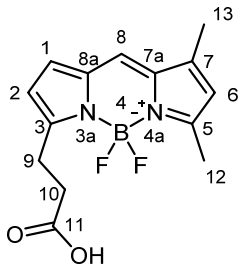


**83**

BODIPY **91** (0.10 g, 0.33 mmol, 1.0 eq.) was dissolved in tetrahydrofuran (15 mL). Water (10 mL) and 1 M hydrochloric acid (5 mL) were added to the solution and the reaction mixture was allowed to stir for 48 h. The reaction mixture was diluted with dichloromethane (20 mL) and the layers were separated. The aqueous layer was extracted with dichloromethane (2 × 20 mL) and the combined organic layer was washed with brine (30 mL), dried ($Na_2SO_4$), filtered and concentrated *in vacuo* onto silica gel. The crude mixture was purified by flash column chromatography (2 % methanol in dichloromethane) giving the title compound as a dark red/green oil (50 mg, 0.16 mmol, 50%).

$^1$H NMR ($CD_3CN$, 500 MHz): 7.40 (1H, s, $C_{(8)}$**H**), 7.02 (1H, d, *J* = 3.8 Hz, $C_{(1)}$**H**), 6.35 (1H, d, *J* = 3.9 Hz, $C_{(2)}$**H**), 6.25 (1H, s, $C_{(6)}$**H**), 3.18 (2H, t, *J* = 7.6 Hz, $C_{(10)}$**H$_2$**), 2.73 (2H, t, *J* = 7.5 Hz, $C_{(9)}$**H$_2$**), 2.53 (3H, s, $C_{(12/13)}$**H$_3$**), 2.28 (3H, s, $C_{(12/13)}$**H$_3$**). $^{13}$C NMR ($CDCl_3$, 125 MHz):172.7 (**C**$_{(11)}$), 160.3 (Ar**C**), 156.5 (Ar**C**), 144.8 (Ar**C**), 134.8 (Ar**C**), 132.9 (Ar**C**), 128.1 (Ar**C**H), 124.6 (Ar**C**H), 120.2 (Ar**C**H), 116.0 (Ar**C**H), 31.6 (**C**$_{(10)}$), 23.2 (**C**$_{(9)}$), 13.8 (**C**$_{(12/13)}$), 10.1 (**C**$_{(12/13)}$).

1*H*-Pyrrole-2-propanol[74]

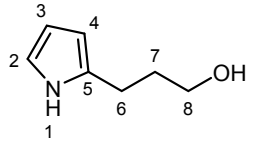


**105**

Ester **88** (1.20 g, 7.80 mmol, 1.0 eq.) was dissolved in anhydrous diethyl ether (50 mL), and the solution was cooled to 0 °C. Lithium aluminium hydride (1 M solution in diethyl ether, 12.0 mL, 12.0 mmol, 1.5 eq.) was added dropwise and the resulting mixture was allowed to come to room temperature and stir for 16 h giving a thick yellow mixture. The reaction mixture was quenched with 15% sodium hydroxide (aq.) (0.5 mL, solution to pH 10). Water (50 mL) was added to the solution and the phases were separated. The aqueous layer was washed with diethyl ether (2 × 50 mL) and

the combined organic layer was dried ($Na_2SO_4$), filtered and concentrated *in vacuo* giving the title compound as a colourless oil (0.81 g, 6.5 mmol, 83%).

$^1$H NMR ($CDCl_3$, 500 MHz) δ: 8.26 (1H, br s, N**H**), 6.71-6.69 (1H, m, $C_{(2/3/4)}$**H**), 6.17-6.15 (1H, m, $C_{(2/3/4)}$**H**), 5.97-5.96 (1H, m, $C_{(2/3/4)}$**H**), 3.74 (2H, m, $C_{(8)}$**H$_2$**), 2.76 (2H, t, *J* = 7.4 Hz, $C_{(6)}$**H$_2$**), 1.91 (2H, tt, *J* = 7.3, 6.2 Hz, $C_{(7)}$**H$_2$**), 1.54 (1H, br s, O**H**) . $^{13}$C NMR ($CDCl_3$, 125 MHz) δ: 131.8 (**C**$_{(5)}$), 116.4 (**C**$_{(2/3/4)}$), 108.3 (**C**$_{(2/3/4)}$), 105.2 (**C**$_{(2/3/4)}$), 62.3 (**C**$_{(8)}$), 32.2 (**C**$_{(6)}$), 24.2 (**C**$_{(7)}$).

2-(3-Tosylpropyl)-1*H*-pyrrole

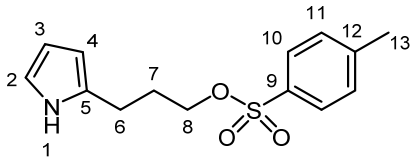


**106**

Alcohol **105** (0.81 g, 6.5 mmol, 1.0 eq.) was dissolved in anhydrous dichloromethane (50 mL). *p*-Toluenesulfonyl chloride (3.10 g, 16.2 mmol, 2.5 eq.) and triethylamine (6.70 mL, 48.6 mmol, 7.5 eq.) were added to the solution and the reaction mixture was allowed to stir for 48 h. Water (50 mL) was added to the reaction mixture and the phases were separated, the organic phase was washed with brine (50 mL), dried ($Na_2SO_4$), filtered and concentrated *in vacuo* onto silica gel. Flash column chromatography was used to purify the crude mixture (0-25% EtOAc in petroleum ether) giving the title compound in good yield (1.38 g, 5.0 mmol, 77%).

$^1$H NMR ($CDCl_3$, 500 MHz): 7.95 (1 H, br s, N**H**), 7.72-7.71 (2H, d, *J* = 8.4 Hz, **2** × $C_{(10)}$**H**), 7.39-7.37 (2H, d, *J* = 8.4 Hz, **2** × $C_{(11)}$**H**), 6.68-6.66 (1H, m, $C_{(2)}$**H**), 6.12 (1H, apparent quartet, *J* = 3.0 Hz, $C_{(3)}$**H**), 5.86 (1H, br s, $C_{(4)}$**H**), 4.08 (2H, t, *J* = 5.8 Hz, $C_{(8)}$**H$_2$**), 2.71 (2H, t, *J* = 7.2 Hz, $C_{(6)}$**H$_2$**), 2.49 (3H, s, $C_{(13)}$**H$_3$**), 1.97 (2H, tt, *J* = 7.2, 6.0 Hz, $C_{(7)}$**H$_2$**).$^{13}$C NMR ($CDCl_3$, 125 MHz): 144.9 (**C**$_{(12)}$), 133.1 (**C**$_{(9)}$), 130.3 (**C**$_{(5)}$), 129.9 (**2 × C**$_{(11)}$), 127.9 (**2 × C**$_{(10)}$), 116.6 (**C**$_{(2)}$), 108.5 (**C**$_{(4)}$), 105.5 (**C**$_{(3)}$), 66.6 (**C**$_{(8)}$), 29.3 (**C**$_{(6)}$), 23.4 (**C**$_{(7)}$), 21.7 (**C**$_{(13)}$). HRMS (ESI) calcd for $C_{14}H_{17}NO_3S$ [$M^+$]: 279.0929, found: 279.0930. $\nu_{max}$ ($CDCl_3$)/cm$^{-1}$: 3406 (m), 2960 (m), 2359 (w), 1350 (s), 1173 (s).

5-(3-chloropropyl)-1*H*-pyrrole-2-carbaldehyde

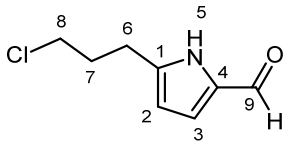


**112**

Dimethylformamide (1.0 mL) was cooled to 0 °C and phosphorous oxychloride(0.01 mL, 0.08 mmol, 1.1 eq.) was added dropwise. The reaction mixture was allowed to stir for 20 min. The reaction mixture was warmed to room temperature and allowed to stir for a further 20 min. The reaction mixture was cooled to 0 °C. Tosylate **106** (20.0 mg, 0.07 mmol, 1.0 eq.) was dissolved in dimethylformamide and added to the reaction mixture which was heated to 50 °C for 18 h. Water (5 mL) and ethyl acetate (5 mL) were added to the reaction mixture and the phases were separated. The pH of the aqueous phase was increased from pH 1 to pH 14 with 15% NaOH (aq.). The aqueous layer was extracted with ethyl acetate (2 × 5 mL) and the combined organic layer was washed with brine (5 × 5mL), dried ($Na_2SO_4$), filtered, and concentrated *in vacuo* giving the title compound as a waxy oil (8.0 mg, 4.7 mmol, 67%).

$^1$H NMR ($CDCl_3$, 500 MHz) δ: 9.84 (1H, br s, (N**H**), 9.32 (1H, s, ($C_{(9)}$**H**), 6.85 (1H, dd, J = 2.4, 3.8, ($C_{(3)}$**H**), 6.06–6.05 (1H, m, ($C_{(2)}$**H**), 3.49 (2H, t, J = 6.3 Hz, ($C_{(8)}$**H₂**), 2.81 (2H, t, J = 7.4 Hz, ($C_{(6)}$**H₂**), 2.07 (2H, tt, J = 7.6, 6.4 Hz, ($C_{(7)}$**H₂**). $^{13}$C NMR ($CDCl_3$, 125 MHz) δ: 178.4 (**C**$_{(9)}$), 140.9 (**C**$_{(1)}$), 132.2 (**C**$_{(4)}$), 122.6 (**C**$_{(3)}$), 109.8 (**C**$_{(2)}$), 43.8 (**C**$_{(8)}$), 31.7 (**C**$_{(6)}$), 24.9 (**C**$_{(7)}$). HRMS (ESI) calcd for $C_8ClH_{10}NO$ [$M^+$]: 171.0451, found: 171.0456. $\nu_{max}$ ($CDCl_3$)/$cm^{-1}$: 3253.1 (m), 1638.6 (s), 1495.9 (m), 1187.2 (m), 1042.6 (m).

3-Tosyl[4,4-difluoro-5,7-dimethyl-4-bora-3a,4a-diaza-*s*-indacene-3-yl]propane

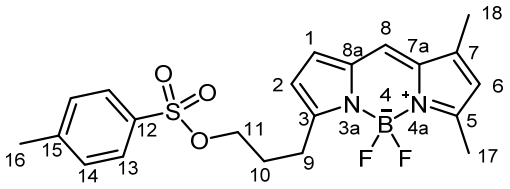


**108**

Pyrrole **106** (0.67 g, 2.40 mmol, 1.0 eq) was dissolved in dichloromethane (20 mL). Aldehyde **90** (0.25 g, 2.60 mmol, 1.1 eq) was added and the solution was cooled to 0 °C and phosphorous oxychloride (0.24 g, 2.60 mmol, 1.1 eq.) was added (light brown to greenish brown). The reaction mixture was allowed to warm to room temperature and stir for 4 hours. *N*,*N*-Diisopropylethylamine (1.68 mL, 9.6 mmol, 4.0 eq.) and boron trifluoride diethyl etherate (1.20 mL, 10.1 mmol, 4.2 eq.) were added to the reaction mixture which was allowed to stir for 24 h. The reaction mixture was concentrated onto silica gel. Flash column chromatography was used to purify the crude mixture (0-35% EtOAc in petroleum ether) giving the title compound as a dark red/green oil (0.70 g, 1.6 mmol, 67%).

$^{1}$H NMR ($CDCl_3$, 500 MHz) δ: 7.74-7.72 (2H, br d, *J* = 8.2 Hz, **2** × $C_{(13)}$**H**), 7.28-7.26 (2H, d, *J* = 8.0 Hz, **2** × $C_{(14)}$**H**), 7.00 (2H, s, $C_{(8)}$**H**), 6.79-6.78 (1H, d, *J* = 3.9 Hz, $C_{(1)}$**H**), 6.12-6.11 (1H, d, *J* = 4.1 Hz, $C_{(2)}$**H**), 6.03 (1H, s, $C_{(6)}$**H**), 4.03 (2H, t, *J* = 6.4 Hz, $C_{(11)}$**H**$_2$), 2.89 (2H, t, *J* = 7.5 Hz, $C_{(9)}$**H**$_2$), 2.47 (3H, s, $C_{(17)}$**H**$_3$), 2.37 (3H, s, $C_{(16)}$**H**$_3$), 2.17 (3H, s, $C_{(18)}$**H**$_3$), 2.02 (2H, t, *J* = 7.7, 6.5 Hz, $C_{(10)}$**H**$_2$). $^{13}$C NMR ($CDCl_3$, 125 MHz) δ: 160.3 (**C**$_{(7a/5)}$), 157.1 (**C**$_{(7a/5)}$), 144.2 (Ar**C**), 143.8 (Ar**C**), 135.2 (Ar**C**), 133.3 (Ar**C**), 133.0 (Ar**C**), 129.9 (**2** × **C**$_{(13)}$), 128.1 (Ar**C**H), 128.0 (**2** × **C**$_{(14)}$), 123.8 (Ar**C**H), 120.4 (Ar**C**H), 116.8 (Ar**C**H), 69.8 (**C**$_{(11)}$), 28.2 (**C**$_{(9/10)}$), 24.6 (**C**$_{(9/10)}$), 21.6 (**C**$_{(16)}$),14.9 (**C**$_{(17)}$), 11.3 (**C**$_{(18)}$). HRMS (ESI) calcd for $BC_{21}F_2H_{23}N_2O_3S$ [(M+Na)$^+$]: 454.1407, found: 454.1419. $\nu_{max}$ ($CDCl_3$)/cm$^{-1}$: 2962.8 (s), 2358.1 (m), 1601.9 (s), 1355.0 (m), 1188.2 (m). λabs,max (MeCN): 509 nm, λem,max (MeCN): 513 nm.

2-(3-Azidopropyl)-1*H*-pyrrole[74]

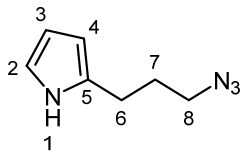


**111**

Alcohol **105** (2.10 g, 16.8 mmol, 1.0 eq.) was dissolved in dichloromethane (60 mL), the solution was cooled to 0 °C and triethylamine (4.60 mL, 33.6 mmol, 2.0 eq.) was added. Methanesulfonyl chloride (1.56 mL, 20.2 mmol, 1.2 eq.) was added dropwise giving a yellow solution. The reaction mixture was allowed to warm to room temperature before being washed with 1 M hydrochloric acid (50 mL), sodium bicarbonate (sat. aq. 50 mL), brine (50 mL), dried ($Na_2SO_4$), filtered and concentrated *in vacuo*. The mesylate was dissolved in dimethyl formamide (60 mL) and sodium azide (3.30 g, 50.4 mmol, 3.0 eq.) was added. The reaction mixture was allowed to stir at 70 °C for 16 hours. The reaction mixture was cooled to room temperature and diluted with ethyl acetate (50 mL) and water (50 mL), the phases were separated and the aqueous layer was extracted with ethyl acetate (50 mL). The combined organic layer was washed with brine (5 × 50 mL), dried ($Na_2SO_4$), filtered, and concentrated *in vacuo* giving the title compound as a colourless oil (1.60 g, 10.6 mmol, 63%).

$^{1}$H NMR ($CDCl_3$, 500 MHz) δ: 8.01 (1H, br s, N**H**), 6.74-6.73 (1H, m, Ar**H**), 6.23-6.21 (1H, m, Ar**H**), 6.03-6.02 (1H, m, Ar**H**), 3.39 (2H, t, J = 6.6 Hz, $C_{(8)}$**H**$_2$), 2.77 (2H, t, J = 7.5 Hz, $C_{(6)}$**H**$_2$), 1.99 (2H, app quint, (dt), J = 7.2, $C_{(7)}$**H**$_2$). $^{13}$C NMR ($CDCl_3$, 125 MHz) δ: 130.8 (**C**$_{(ArQ)}$), 116.6 (**C**$_{(ArQ)}$), 108.5 (**C**$_{(Ar)}$), 105.6 (**C**$_{(Ar)}$), 50.7 (**C**$_{(8)}$), 28.9 (**C**$_{(6)}$), 24.7 (**C**$_{(7)}$).

3-Azido[4,4-difluoro-5,7-dimethyl-4-bora-3a,4a-diaza-*s*-indacene-3-yl]propane[74]

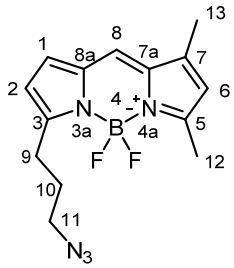


**109**

Method 1: Pyrrole **111** (60 mg, 0.40 mmol, 1.0 eq.) and formylated pyrrole **90** (0.042 g, 0.44 mmol, 1.1 eq.) were dissolved in dichloromethane (3 mL) and the solution was cooled to 0 °C. Phosphorus oxychloride (0.04 mL, 0.44 mmol, 1.1 eq.) was added to the solution dropwise. The solution was allowed to warm to room temperature and stir for 6 h before being cooled to 0 °C. Boron trifluoride diethyl etherate (0.23 mL, 1.8 mmol, 4.5 eq.) and *N*,*N*-diisopropylethylamine (0.31 mL, 1.8 mmol, 4.5 eq.) were added to the dark red solution which was allowed to warm to room temperature and stir for 12 h. The mixture was diluted with water (5 mL) and dichloromethane (5 mL) before being filtered through celite and washed with dichloromethane (2 × 5 mL). The combined organic layer was dried ($Na_2SO_4$), filtered and concentrated *in vacuo*. The resulting solid was filtered through a bed of silica gel and washed with 20% ethyl acetate in 40-60 petroleum ethers (2 × 20 mL) giving the title compound as a red/green oil (0.067 g, 0.22 mmol, 55 %).

Method 2: Tosyl BODIPY **108** (77 mg, 0.18 mmol, 1.0 eq.) was dissolved in ethanol (5.0 mL). Sodium azide (60 mg, 0.90 mmol, 5.0 eq.) was added and the reaction mixture was heated to 45 °C for 72 h. The reaction mixture was concentrated *in vacuo* onto silica gel and the reaction mixture was purified by column chromatography (0-12.5% ethyl acetate in petroleum ether) giving the title compound as a red/green oil (45 mg, 0.15 mmol, 83%).

$^1$H NMR ($CDCl_3$, 500 MHz) δ: 7.11 (1H, s, $C_{(8)}\mathbf{H}$), 6.92 (1H, d, *J* = 3.9 Hz, $C_{(1)}\mathbf{H}$), 6.30 (1H, d, *J*= 3.9 Hz, $C_{(2)}\mathbf{H}$), 6.13 (1H, s, $C_{(6)}\mathbf{H}$), 3.41 (2H, t, *J* = 7.0 Hz, $C_{(11)}\mathbf{H_2}$), 3.05 (2H, t, *J* = 7.4 Hz, $C_{(9)}\mathbf{H_2}$), 2.57 (3H, s, $C\mathbf{H_3}$), 2.27 (3H, s, $C\mathbf{H_3}$), 2.04 (2H, app quintet, (dt), *J* = 7.8, 7.1 Hz, $C_{(10)}\mathbf{H_2}$). $^{13}$C NMR ($CDCl_3$, 125 MHz) δ: 160.3 ($\mathbf{C}_{(Ar)}$), 157.8 ($\mathbf{C}_{(Ar)}$), 143.7 ($\mathbf{C}_{(Ar)}$), 135.1 ($\mathbf{C}_{(Ar)}$), 133.3 ($\mathbf{C}_{(Ar)}$), 128.1 ($\mathbf{C}_{(ArH)}$), 123.7 ($\mathbf{C}_{(ArH)}$), 120.4 ($\mathbf{C}_{(ArH)}$), 116.6 ($\mathbf{C}_{(ArH)}$), 50.9 ($\mathbf{C}_{(11)}$), 28.1 ($\mathbf{C}_{(9)}$), 25.8 ($\mathbf{C}_{(10)}$), 14.9 ($\mathbf{C}_{(12/13)}$), 11.3 ($\mathbf{C}_{(12/13)}$).

3-[4-(pent-4-yn-1-yl)-1H-1,2,3-triazol-1-yl]-1-[4,4-difluoro-5,7-dimethyl-4-bora-3a,4a-diaza-*s*-indacene-3-yl]propane

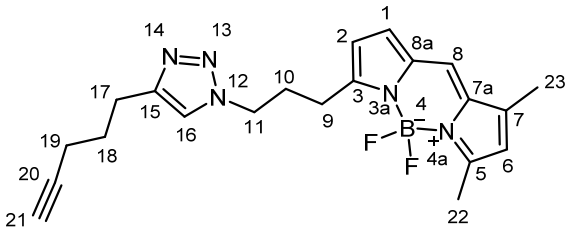

**110**

*N*,*N*-Diisopropylethylamine (0.05 mL, 0.28 mmol, 4.0 eq.) and copper (I) iodide (6 mg, cat.), were added to a solution of 1,6-heptadiyne (0.15 mL, 1.05 mmol, 15.0 eq.) and azide **109** (0.22 g, 0.07 mmol, 1.0 eq.) in tetrahydrofuran (10 mL). The reaction mixture was heated to 50 °C and allowed to stir for 72 h. The reaction mixture was concentrated *in vacuo* onto silica gel and flash column chromatography (10-50% ethyl acetate in petroleum ether) gave the title compound as a dark red/green oil (15 mg, 0.04 mmol, 57%).

$^{1}$H NMR ($CDCl_3$, 500 MHz) δ: 7.28 (1H, s, $C_{(16)}$**H**), 7.02 (1H, s, $C_{(8)}$**H**), 6.81 (1H, d, *J* = 3.9 Hz, $C_{(1)}$**H**), 6.18 (1H, d, *J* = 4.0 Hz, $C_{(2)}$**H**), 6.06 (1H, s, $C_{(6)}$**H**), 4.36 (2H, t, *J* = 7.2 Hz, $C_{(11)}$**H$_2$**), 2.95 (2H, t, *J* = 7.5 Hz, $C_{(9)}$**H$_2$**), 2.76 (2H, t, *J* = 7.6 Hz, $C_{(17)}$**H$_2$**), 2.50 (3H, s, $C_{(22)}$**H$_3$**), 2.30 (2H, apparent quintet, *J* = 7.4 7.4 Hz, $C_{(10)}$**H$_2$**), 2.19 (3H, s, $C_{(23)}$**H$_3$**), 2.77 (2H, td, *J* = 2.7, 7.0 Hz, $C_{(19)}$**H$_2$**), 1.90 (1H, t, *J* = 2.6 Hz, $C_{(21)}$**H**), 1.82 (2H, apparent quintet, *J* = 7.2, 7.6 Hz, $C_{(18)}$**H$_2$**). $^{13}$C NMR ($CDCl_3$, 125 MHz) δ: 160.5 (**C**$_{(5)}$), 156.9 (**C**$_{(3)}$), 147.0 (**C**$_{(15)}$), 144.0 (**C**$_{(7a)}$), 135.2 (**C**$_{(7)}$), 133.2 (**C**$_{(8a)}$), 128.2 (**C**$_{(1)}$),123.8 (**C**$_{(8)}$), 121.1 (**C**$_{(16)}$), 120.5 (**C**$_{(6)}$), 116.7 (**C**$_{(2)}$), 83.9 (**C**$_{(20)}$), 68.8 (**C**$_{(21)}$), 49.6 (**C**$_{(11)}$), 29.5 (**C**$_{(10)}$), 28.0 (**C**$_{(18)}$), 25.7 (**C**$_{(9/17)}$), 24.5 (**C**$_{(9/17)}$), 17.9 (**C**$_{(19)}$), 15.0 (**C**$_{(23)}$), 11.3 (**C**$_{(22)}$). HRMS (ESI) calcd for $BC_{21}F_2H_{24}N_5Na$ [$(M+Na)^+$]: m/z 417.2021, found m/z 417.2004. $\nu_{max}$ ($CDCl_3$)/cm$^{-1}$: 2924 (m), 2853 (m), 2362 (m), 1604 (s), 1139 (m). λabs,max (MeCN): 503 nm, λem,max (MeCN): 513 nm.

3-[4-(pent-4-yn-1-yl)-5-iodo-1H-1,2,3-triazol-1-yl]-1-[4,4-difluoro-5,7-dimethyl-4-bora-3a,4a-diaza-*s*-indacene-3-yl]propane

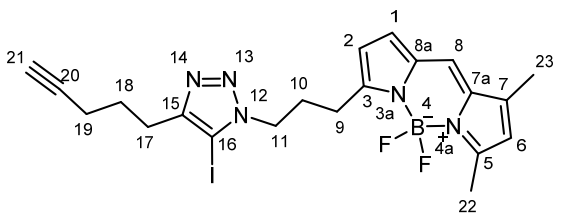

**112**

This compound was isolated as a red/green oil as a by-product in the synthesis of **110** (43%).

$^{1}$H NMR ($CDCl_3$, 500 MHz) δ: 7.03 (1H, s, $C_{(8)}$**H**), 6.83 (1H, d, *J* = 4.0 Hz, $C_{(1)}$**H**), 6.25 (1H, d, *J* = 4.0 Hz, $C_{(2)}$**H**), 6.05 (1H, s, $C_{(6)}$**H**), 4.36 (2H, dd, *J* = 7.6, 7.5 Hz, $C_{(11)}$**H**$_2$), 2.99 (2H, t, *J* = 7.7 Hz, $C_{(9)}$**H**$_2$), 2.71 (2H, t, *J* = 7.6 Hz, $C_{(17)}$**H**$_2$), 2.50 (3H, s, $C_{(22)}$**H**$_3$), 2.28 (2H, tt, *J* = 15.1, 7.7 Hz, $C_{(10)}$**H**$_2$), 2.21-2.19 (5H, m, $C_{(19)}$**H**$_2$ + $C_{(23)}$**H**$_3$), 1.91 (1H, t, *J* = 2.7 Hz, $C_{(21)}$**H**), 1.88 (2H, tt, *J* = 7.3, 7.2 Hz, $C_{(18)}$**H**$_2$). $^{13}$C NMR ($CDCl_3$, 125 MHz) δ: 160.5 (**C**$_{(5)}$), 156.8 (**C**$_{(3)}$), 150.9 (**C**$_{(15)}$), 144.0 (**C**$_{(7a)}$), 135.3 (**C**$_{(7)}$), 133.2 (**C**$_{(8a)}$), 130.9 (**C**$_{(16)}$), 128.1 (**C**$_{(1)}$), 123.8 (**C**$_{(8)}$), 120.5 (**C**$_{(6)}$), 116.7 (**C**$_{(2)}$), 83.9 (**C**$_{(20)}$), 68.9 (**C**$_{(21)}$), 50.2 (**C**$_{(11)}$), 29.1 (**C**$_{(10)}$), 27.6 (**C**$_{(18)}$), 25.6 (**C**$_{(9)}$), 25.1 (**C**$_{(17)}$), 18.0 (**C**$_{(19)}$), 15.0 (**C**$_{(23)}$), 11.3 (**C**$_{(22)}$). HRMS (ESI) calcd for $BC_{21}F_2H_{23}IN_5Na$ [$(M+Na)^+$]: m/z 543.0988, found m/z 543.0970. $v_{max}$ ($CDCl_3$)/cm$^{-1}$: 2925 (s), 2855 (m), 2360 (s), 1734 (w), 2332 (s).

3-[4-(1*H*-1,2,3-triazol-1-yl]-1-[4,4-difluoro-5,7-dimethyl-4-bora-3a,4a-diaza-*s*-indacene-3-yl]propane)-1*H*-1,2,3-triazol-1-yl]-1-[4,4-difluoro-5,7-dimethyl-4-bora-3a,4a-diaza-*s*-indacene-3-yl]propane

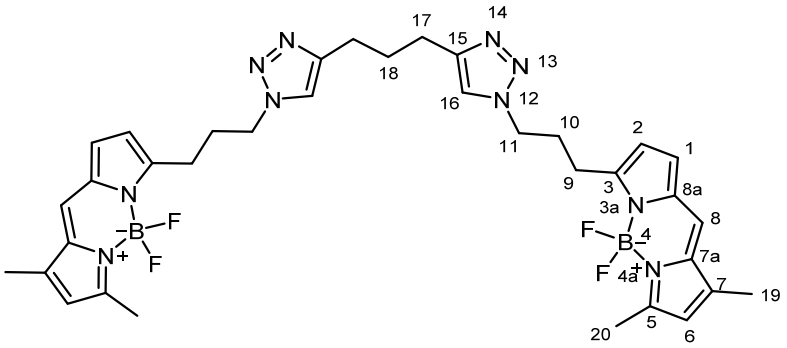

**113**

This compound was isolated as a red/green oil as a by-product in the synthesis of **110**.

$^{1}$H NMR ($CDCl_3$, 500 MHz): 7.28 (2H, s, **2** × $C_{(16)}$**H**), 7.02 (2H, s, **2** × $C_{(8)}$**H**), 6.81 (2H, d, *J* = 4.0 Hz, **2** × $C_{(1)}$**H**), 6.81 (2H, d, *J* = 4.0 Hz, **2** × $C_{(2)}$**H**), 6.05 (2H, s, **2** × $C_{(6)}$**H**), 4.32 (4H, t, *J* = 7.2 Hz, **2** × $C_{(11)}$**H**$_2$), 2.94 (4H, t, *J* = 7.5 Hz, **2** × $C_{(9)}$**H**$_2$), 2.68 (4H, t, *J* = 7.5 Hz, **2** × $C_{(17)}$**H**$_2$), 2.48 (6H, s, **2** × $C_{(19)}$**H**$_3$), 2.29 (4H, apparent quintet, *J* = 7.4, 7.4 Hz, **2** × $C_{(10)}$**H**$_2$), 2.18 (6H, s, **2** × $C_{(20)}$**H**$_3$), 1.97 (2H, apparent quintet, *J* = 7.6 Hz, $C_{(18)}$**H**$_2$). $^{13}$C NMR ($CDCl_3$, 125 MHz): 160.4 (**2** × **C**$_{(5)}$), 156.9 (**2** × **C**$_{(3)}$), 147.5 (**2** × **C**$_{(15)}$), 144.0 (**2** × **C**$_{(7a)}$), 135.2 (**2** × **C**$_{(7)}$), 133.2 (**2** × **C**$_{(8a)}$), 128.2 (**2** × **C**$_{(1)}$), 123.8 (**2** × **C**$_{(8)}$), 121.1 (**2** × **C**$_{(16)}$), 120.5 (**2** × **C**$_{(6)}$), 116.7 (**2** × **C**$_{(2)}$), 49.6 (**2** × **C**$_{(11)}$), 29.5 (**2** × **C**$_{(10)}$), 29.1 (**C**$_{(18)}$), 25.7 (**2** × **C**$_{(9/17)}$), 24.9 (**2** × **C**$_{(9/17)}$), 14.9 (**2** × **C**$_{(23)}$), 11.3 (**2** × **C**$_{(22)}$). HRMS (ESI) calcd for $C_{35}H_{40}B_2F_4N_{10}Na$ [M+Na]: 721.3452, found: 721.3373. $v_{max}$ ($CDCl_3$)/cm$^{-1}$: 2927 (s), 2360 (s), 1717 (m), 1603 (s), 1139 (m).

5-(3-Azidopropyl)-1*H*-pyrrole-2-carbaldehyde

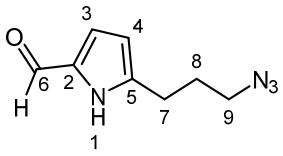


**123**

Dimethylformamide (10 mL) was cooled to 0 °C. Phosphorous oxychloride (4.8 mL, 50.0 mmol, 15.0 eq.) was added and the solution was allowed to stir at 0 °C for ten minutes before being allowed to warm to room temperature and stir for one hour. The solution was cooled to 0 °C and pyrrole **111** (0.50 g, 3.33 mmol, 1.0 eq.) in dimethyl formamide (10 mL) was added. The resulting reaction mixture was allowed to stir at 40 °C for 18 hours. Brine (100 mL) and ethyl acetate (100 mL) were added to the solution and the phases were separated, the aqueous phase was increased from pH 2 to pH 11 (3 M NaOH aq.). The aqueous phase was extracted with ethyl acetate (2 × 50 mL) and the combined organic layer was washed with brine (5 × 100 mL). The organic layer was dried ($Na_2SO_4$), filtered and concentrated onto silica gel. Flash column chromatography was employed to purify to title compound (30% ethyl acetate in 40-60 petroleum ethers), giving the desired product as a low temperature melting solid (0.41 g, 2.3 mmol, 70%).

$^1$H NMR ($CDCl_3$, 500 MHz): 10.20 (1H, s, N**H**), 9.40 (1H, s, $C_{(6)}$**H**), 6.95-6.94 (1H, m, $C_{(3)}$**H**), 6.14-6.13 (1H, m, $C_{(4)}$**H**), 3.36 (2H, t, *J* = 6.6 Hz, $C_{(7)}$**H$_2$**), 2.83 (2H, t, *J* = 7.5 Hz, $C_{(9)}$**H$_2$**), 1.99 (2H, dt, *J* = 7.7, 6.7 Hz,$C_{(8)}$**H$_2$**).$^{13}$C NMR ($CDCl_3$, 125 MHz) δ: 178.4 (**C**$_{(6)}$), 141.4 (**C**$_{(2)}$), 132.2 (**C**$_{(5)}$), 122.8 (**C**$_{(3)}$), 109.8 (**C**$_{(4)}$), 50.5 (**C**$_{(7)}$), 28.3 (**C**$_{(8)}$), 24.9 (**C**$_{(9)}$). HRMS (ESI) calcd for $C_8H_{10}N_4O$ [M$^+$]: *m*/*z* 178.0855, found: *m*/*z* 178.0856. $\nu_{max}$ ($CDCl_3$)/cm$^{-1}$: 3233 (s), 2951 (m), 2167 (m), 2096 (s), 1635 (s).

5-Azidopropane-3-tosylpropane-4,4-difluoro-4-bora-3a,4a-diaza-*s*-indacene

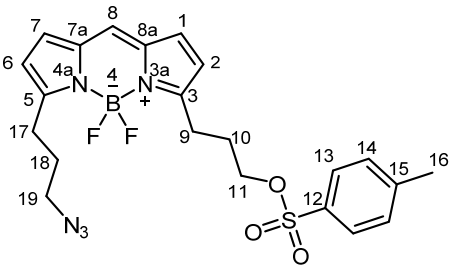


**118**

Azide **123** (0.25 g, 1.4 mmol, 1.0 eq.) and tosylate **106** (0.41 g, 1.54 mmol, 1.1 eq.) were dissolved in dichloromethane (20 mL) and the solution was cooled to 0 °C. Phosphorous oxychloride (0.14 mL, 1.54 mmol, 1.1 eq.) was added and the solution

was allowed to stir at room temperature for 18 h. The reaction mixture was cooled to 0 °C, *N*,*N*-diisopropylethylamine (1.1 mL, 6.16 mmol, 4.0 eq.) and boron trifluoride diethyl etherate (0.76 mL, 6.16 mmol, 4.0 eq.) were added and the resulting reaction mixture was allowed to warm to room temperature and stir for 18 h. The reaction mixture was concentrated onto silica gel and purified by flash column chromatography (0-35% ethyl acetate in petroleum ether) giving the title compound as a red/green oil (0.37 g, 0.76 mmol, 54%).

$^1$H NMR ($CDCl_3$, 500 MHz) δ: 7.73 (2H, d, *J* = 8.1 Hz, **2** × $C_{(13)}$**H**), 7.26 (2H, d, J = 8.0 Hz, **2** × $C_{(14)}$**H**), 7.04 (1H, s, $C_{(8)}$**H**), 6.93 (1H, d, *J* = 4.3 Hz, $C_{(1/7)}$**H**), 6.89 (1H, *J* = 4.1 Hz, $C_{(1/7)}$**H**), 6.27 (1H, d, *J* = 4.1 Hz, $C_{(2/6)}$**H**), 6.20 (1H, d, *J* = 4.1 Hz, $C_{(2/6)}$**H**), 4.04 (2H, t, *J* = 6.3 Hz, $C_{(\mathbf{11/19})}\mathbf{H_2}$), 3.32 (2H, t, *J* = 6.9 Hz, $C_{(11/19)}\mathbf{H_2}$), 2.97(2H, t, *J* = 7.6 Hz, $C_{(9/17)}\mathbf{H_2}$), 2.92 (2H, t, *J* = 7.7 Hz, $C_{(9/17)}\mathbf{H_2}$), 2.38 (3H, s, $C_{(16)}\mathbf{H_3}$), 2.04 (2H, tt, *J* = 7.8, 6.4 Hz, $C_{(10/18)}\mathbf{H_2}$), 1.95 (2H, apparent quintet, *J* = 7.9 Hz, $C_{(10/18)}\mathbf{H_2}$). $^{13}$C NMR ($CDCl_3$, 125 MHz) δ: 161.3 ($\mathbf{C}_{(3/5)}$), 160.5 ($\mathbf{C}_{(3/5)}$), 144.8 ($\mathbf{C}_{(15)}$), 134.7 ($\mathbf{C}_{(12)}$), 133.0 ($\mathbf{C}_{(7a)}$ + $\mathbf{C}_{(8a)}$), 130.6 ($\mathbf{C}_{(2/6)}$), 130.5 ($\mathbf{C}_{(2/6)}$), 129.9 (**2** × $\mathbf{C}_{(14)}$), 127.9 (**2** × $\mathbf{C}_{(13)}$), 127.7 ($\mathbf{C}_{(8)}$), 118.5 ($\mathbf{C}_{(1/7)}$), 118.4 ($\mathbf{C}_{(1/7)}$), 69.6 ($\mathbf{C}_{(11)}$), 50.9 ($\mathbf{C}_{(19)}$), 28.1 ($\mathbf{C}_{(9)}$), 28.0 ($\mathbf{C}_{(18)}$), 26.0 ($\mathbf{C}_{(17)}$), 24.9 ($\mathbf{C}_{(10)}$), 21.6 ($\mathbf{C}_{(16)}$). HRMS (ESI) calcd for $BC_{22}F_2H_{24}N_5NaO_3S$ [$(M+Na)^+$]: *m*/*z* 509.1589, found *m*/*z* 509.1577. $\nu_{max}$ ($CDCl_3$)/$cm^{-1}$: 2930 (m), 2096 (s), 1602 (s), 1256 (s), 1116 (s). λabs,max (MeCN): 510 nm, λem,max (MeCN): 517 nm.

3,5-Azidopropane-4,4-difluoro-4-bora-3a,4a-diaza-*s*-indacene

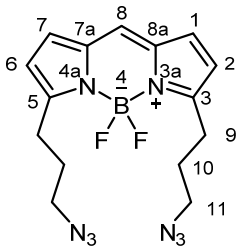


**124**

This compound was isolated as a red/green oil as a by-product in the synthesis of **118** (16%).

$^1$H NMR ($CDCl_3$, 500 MHz): 7.06 (1H, s, $C_{(8)}$**H**), 6.93 (2H, d, *J* = 4.1 Hz, $C_{(1)}$**H** + $C_{(7)}$**H**), 6.28 (2H, d, *J* = 4.1 Hz, $C_{(2)}$**H** + $C_{(6)}$**H**), 3.33 (4H, t, *J* = 6.9 Hz, **2** × $C_{(11)}\mathbf{H_2}$), 3.00 (4H, t, *J* = 7.8 Hz, **2** × $C_{(9)}\mathbf{H_2}$), 1.97 (4H, apparent quintet, *J* = 7.1 Hz, **2** × $C_{(10)}\mathbf{H_2}$). $^{13}$C NMR ($CDCl_3$, 125 MHz): 161.2 (**2** × $\mathbf{C}_{(ArQ)}$), 134.6 (**2** × $\mathbf{C}_{(ArQ)}$), 130.5 (**2** × $\mathbf{C}_{(H)}$), 127.7 ($\mathbf{C}_{(8)}$), 118.3 (**2** × $\mathbf{C}_{(H)}$), 50.9 (**2** × $\mathbf{C}_{(11)}$), 28.0 (**2** × $\mathbf{C}_{(10)}$), 26.0 (**2** × $\mathbf{C}_{(9)}$). HRMS calcd for $BC_{15}F_2H_{17}N_8Na$ [$(M+Na)^+$]: *m*/*z* 380.1566, found: *m*/*z* 380.1551. $\nu_{max}$ ($CDCl_3$): 2930

(w), 2095 (s), 2095 (s), 1605 (s), 1252 (m), 1117 (s). λabs,max (MeCN): 508 nm, λem,max (MeCN): 516 nm.

3,5-Tosylpropane-4,4-Difluoro-4-bora-3a,4a-diaza-*s*-indacene

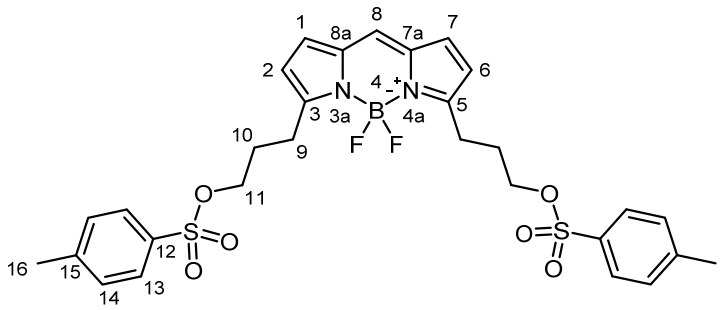

**125**

This compound was isolated as a red/green oil as a by-product in the synthesis of **118** (29%).

$^1$H NMR ($CDCl_3$, 500 MHz): 7.72 (4H, d, *J* = 8.3 Hz, **2** × $C_{(13)}\mathbf{H_2}$), 7.27 (4H, d, *J* = 8.0 Hz, **2** × $C_{(14)}\mathbf{H_2}$), 7.03 (1H, s, $C_{(8)}\mathbf{H}$), 6.89 (2H, d, *J* = 4.1 Hz, **2** × $C_{(1/2)}\mathbf{H}$), 6.20 (2H, d, *J* = 4.1 Hz, **2** × $C_{(1/2)}\mathbf{H}$), 4.03 (4H, t, *J* = 6.4 Hz, **2** × $C_{(11)}\mathbf{H_2}$), 2.99 (4H, t, *J* = 7.6 Hz, **2** × $C_{(9)}\mathbf{H_2}$), 2.37 (6H, s, **2** × $C_{(16)}\mathbf{H_3}$), 2.02 (4H, tt, *J* = 7.9, 6.4 Hz, **2** × $C_{(10)}\mathbf{H_2}$). $^{13}$C NMR ($CDCl_3$, 125 MHz): 160.6 ($\mathbf{C}_{(3)}$ + $\mathbf{C}_{(5)}$), 144.8 (**2** × $\mathbf{C}_{(15)}$), 134.7 (**2** × $\mathbf{C}_{(12)}$), 133.0 ($\mathbf{C}_{(7a)}$ + $\mathbf{C}_{(8a)}$), 130.5 ($\mathbf{C}_{(2)}$ + $\mathbf{C}_{(6)}$), 129.9 (**4** × $\mathbf{C}_{(14)}$), 127.9 (**4** × $\mathbf{C}_{(13)}$), 127.8 ($\mathbf{C}_{(8)}$), 118.6 ($\mathbf{C}_{(1)}$ + $\mathbf{C}_{(7)}$), 69.6 (**2** × $\mathbf{C}_{(11)}$), 28.0 (**2** × $\mathbf{C}_{(9)}$), 24.8 (**2** × $\mathbf{C}_{(10)}$), 21.6 (**2** × $\mathbf{C}_{(16)}$). HRMS (ESI) calcd for $BC_{29}F_2H_{31}N_2NaO_6S_2$ [$(M+Na)^+$]: *m/z* 638.1613, found *m/z* 639.1585. $\nu_{max}$ ($CDCl_3$)/$cm^{-1}$: 2925 (m), 2357 (s), 1733 (m), 1607 (s), 1176 (m). λabs,max (MeCN): 509 nm, λem,max (MeCN): 518 nm.

Bis-(1H-pyrrol-2-yl)-methanethione[72]

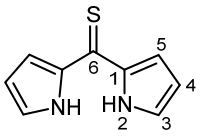

**97**

Pyrrole (5.00 mL, 65.2 mmol, 1.0 eq.) was dissolved in toluene (150 mL) and cooled to 0 °C. Thiophosgene (9.00 mL, 130.4 mmol, 2.0 eq.) was dissolved in diethyl ether (150 mL), added to the toluene solution and allowed to stir for 20 min. Methanol (10% aq.) (150 mL) was added and the reaction mixture was allowed to stir for 45 min. The reaction mixture was concentrated *in vacuo* onto silica gel. Flash column

chromatography (5% toluene and 1% triethylamine in chloroform) gave the title compound as a solid (4.90 g, 27.8 mmol, 43%).

$^1$H NMR ($CDCl_3$, 500 MHz) δ: 9.70 (**2** × N**H**), 7.11-7.10 (2H, m, **2** × Ar**H**), 6.98-6.95 (2H, m, **2** × Ar**H**), 6.33-6.31 (2H, m Hz, **2** × Ar**H**). $^{13}$C NMR ($CDCl_3$, 125 MHz) δ: 193.2 (**C**$_{(6)}$), 138.4 (**2** × **C**$_{(1)}$), 130.6 (**2** × **C**$_{(2)}$), 114.8 (**2** × **C**$_{(4/5)}$), 112.5 (**2** × **C**$_{(4/5)}$).

8-(Methyl-thio)-BODIPY[72]

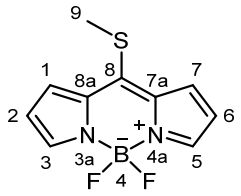


**92**

Pyrrole **97** (1.09 g, 6.2 mmol, 1.0 eq.) was dissolved in dichloromethane (15 mL) giving a red solution. Methyl iodide (2.3 mL) was added and the reaction mixture was allowed to stir at room temperature for 18 h. Triethylamine (2.6 mL, 18.6 mmol, 3.0 eq.) was added to the reaction mixture which was allowed to stir for 30 minutes. Boron trifluoride diethyl etherate (0.77 mL. 6.2 mmol, 1.0 eq.) was added to the reaction mixture which was allowed to stir for 30 min before being concentrated *in vacuo*. Flash column chromatography (0-10% ethyl acetate and 5% DCM in petroleum ether) gave a mixture of compound and triethylamine. $H_2O$ (20 mL) and DCM (20 mL) were added to the concentrate and the phases were separated. The organic phase was washed with brine (20 mL), dried ($Na_2SO_4$) and filtered giving the title compound as a solid in low yield (0.10 g, 0.4 mmol, 6%).

$^1$H NMR ($CDCl_3$) δ: 7.73 (2H, s, **2** × C**H**). 7.35-7.40 (2H, d, *J* = 4.1 Hz, **2** × C**H**), 6.46 (2H, d, *J* = 3.7 Hz, **2** × C**H**), 2.85 (3H, s, C$_{(9)}$**H$_3$**). $^{13}$C NMR ($CDCl_3$) δ: 153.8 (**C**$_{(8)}$). 141.4 (**2** × **C**H), 133.8 (**C**$_{(7a)}$ + **C**$_{(8a)}$), 127.6 (**2** × **C**H), 117.8 (**2** × **C**H), 20.5 (**C**$_{(9)}$).

Methyl-[1-[3-(3-methyl-butoxy)-2-nitro-phenyl]-meth-(*E*)-ylidene]-amine[94]

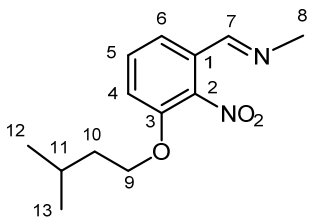


**162**

Aldehyde **18** (1.71 g, 7.2 mmol, 1.0 eq.) was dissolved in heptane (40 mL) and treated with methylamine (40 wt. % solution in water, 1.75 mL, 20.2 mmol, 2.8 eq.). The

biphasic mixture was stirred vigorously at room temperature for 2 h. Heptane was then removed *in vacuo*, and remaining crude imine **162** was taken directly to the next reaction without purification.

$^{1}$H NMR ($CDCl_3$, 500 MHz) δ: 8.19 (1H, d, *J* = 1.5 Hz, $C_{(7)}$**H**), 7.49 (1H, d, *J* = 7.9 Hz, Ar**H**), 7.44 (1H, t, *J* = 8.1 Hz, Ar**H**), 7.10 (1H, d, *J* = 8.2 Hz, Ar**H**), 4.12 (2H, t, *J* = 6.6 Hz, $C_{(9)}$**H₂**), 3.54 (3H, d, *J* = 1.6 Hz, $C_{(8)}$**H₃**), 1.81 (1H, apparent septet, *J* = 6.7 Hz, $C_{(11)}$**H**), 1.69 (2H, q, *J* = 6.7 Hz, $C_{(10)}$**H₂**), 0.95 (6H, d, *J* = 6.6 Hz, $C_{(12)}$**H₃** + $C_{(13)}$**H₃**). $^{13}$C NMR ($CDCl_3$, 125 MHz) δ: 156.0 (**C**$_{(7)}$), 150.3 (Ar**C**q), 141.4 (Ar**C**q), 130.9 (Ar**C**H), 128.6 (Ar**C**q), 119.4 (Ar**C**H), 115.1 (Ar**C**H), 68.2 (**C**$_{(9)}$), 48.6 (**C**$_{(8)}$), 37.5 (**C**$_{(10)}$), 24.9 (**C**$_{(11)}$), 22.4 (**C**$_{(12)}$ + **C**$_{(13)}$). HRMS (CI+) calcd for $C_{13}H_{19}N_2O_3$ [M+H$^+$]: *m/z* 251.1396, found *m/z* 251.1397.

Methyl-[3-(3-methylbutoxy)-2-nitro-benzyl]-amine[94]

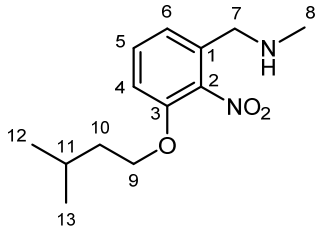


**8**

Imine **162** (1.80 g, 7.2 mmol, 1.0 eq.) was dissolved in methanol (40 mL), sodium borohydride (0.40 g, 10.8 mmol, 1.5 eq.) was added in portions and the reaction mixture was stirred at room temperature for 3 h. The reaction mixture was cooled to 0 °C, slowly quenched with water (40 mL) and stirred for 20 min. Ethyl acetate (80 mL) was added and biphasic mixture was warmed to room temperature. The phases were separated and the aqueous layer was extracted with ethyl acetate (2 × 80 mL). The combined organic phase was dried ($Na_2SO_4$), filtered and concentrated *in vacuo* to give the title compound as an orange liquid (1.72 g, 6.8 mmol, 94%).

$^{1}$H NMR ($CDCl_3$, 500 MHz) δ: 7.38 (1H, t, *J* = 8.0 Hz, Ar**H**), 7.05 (1H, d, *J* = 7.1 Hz, Ar**H**), 6.96 (1H, d, *J* = 8.3 Hz, Ar**H**), 4.09 (2H, t, *J* = 6.6 Hz, $C_{(9)}$**H₂**), 3.72 (2H, s, $C_{(7)}$**H₂**), 2.43 (3H, s, $C_{(8)}$**H₃**), 1.81 (1H, apparent septet, *J* = 6.8 Hz, $C_{(11)}$**H**), 1.68 (2H, q, *J* = 6.6 Hz, $C_{(10)}$**H₂**), 0.95 (6H, d, *J* = 6.7 Hz, $C_{(12)}$**H₃** + $C_{(13)}$**H₃** ).$^{13}$C NMR ($CDCl_3$, 125 MHz) δ: 150.4 (Ar**C**q), 141.8 (Ar**C**q), 133.3 (Ar**C**q), 130.8 (Ar**C**H), 121.2 (Ar**C**H), 112.2 (Ar**C**H), 68.0 (**C**$_{(9)}$), 51.3 (**C**$_{(7)}$), 37.5 (**C**$_{(10)}$), 36.1 (**C**$_{(8)}$), 24.9 (**C**$_{(11)}$), 22.5 (**C**$_{(12)}$ + **C**$_{(13)}$). HRMS (CI+) calcd for $C_{13}H_{21}N_2O_3$ [M+H$^+$]: *m/z* 253.1552, found *m/z* 253.1551.

Methyl-[3-(3-methyl-butoxy)-2-nitro-benzyl]-carbamic acid *tert*-butyl ester[94]

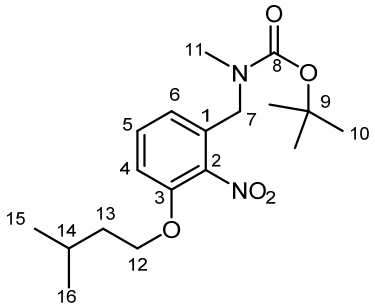


**10**

Amine **8** (4.00 g, 15.9 mmol, 1.0 eq.) was dissolved in dichloromethane (60 mL). Triethylamine (4.4 mL, 31.8 mmol, 2.0 eq.) and di-*tert*-butyl dicarbonate (4.84 g, 22.2 mmol, 1.4 eq.) were added to the solution which was allowed to stir at room temperature for 16 h. The reaction mixture was concentrated *in vacuo* onto silica gel and purified by flash column chromatography (0-30% ethyl acetate in petroleum ether) giving the title compound as an oil (5.61 g, 15.9 mmol, 100%).

$^{1}$H NMR ($CDCl_3$, 500 MHz) δ: 7.29 (1H, t, $C_{(5)}$**H**), 6.88-6.77 (2H, m, $C_{(4)}$**H** + $C_{(6)}$**H**), 4.35-4.32 (2H, m, $C_{(7)}$**H$_2$**), 4.00 (2H, t, *J* = 6.4 Hz, $C_{(12)}$**H$_2$**), 2.77-2.71 (3H, m, $C_{(11)}$**H$_3$**), 1.71 (1H, apparent septet, *J* = 6.7 Hz, $C_{(14)}$**H**), 1.58 (2H, dt, *J* = 6.6, 6.6 Hz, $C_{(13)}$**H$_2$**), 1.42 (3.9H, br s, rotamer of **3** × $C_{(10)}$**H$_3$**), 1.35 (5.1H, br s, rotamer of **3** × $C_{(10)}$**H$_3$**), 0.86 (6H, d, *J* = 6.7 Hz, $C_{(15)}$**H$_3$** + $C_{(16)}$**H$_3$**). $^{13}$C NMR ($CDCl_3$, 125 MHz) δ: 155.5 (**C**$_{(3)}$), 150.4 (**C**$_{(8)}$), 131.6 (**C**$_{(1)}$), 131.0 (**C**$_{(5)}$), 119.7 (rotamer **C**$_{(6)}$), 118.9 (rotamer **C**$_{(6)}$), 112.3 (**C**$_{(4)}$), 80.3 (**C**$_{(9)}$), 68.0 (**C**$_{(12)}$), 48.1 (rotamer **C**$_{(7)}$), 47.3 (rotamer **C**$_{(7)}$), 37.5 (**C**$_{(13)}$), 34.3 (**C**$_{(11)}$), 28.3 (**3** × **C**$_{(10)}$), 24.9 (**C**$_{(14)}$), 22.6 (**C**$_{(15)}$), 22.4 (**C**$_{(16)}$). HRMS (ESI) calcd for $C_{18}H_{28}N_2NaO_5$ [$(M+Na)^+$]: *m/z* 375.1890, found *m/z* 375.1891. $\nu_{max}$ ($CDCl_3$)/cm$^{-1}$: 2959.9 (m), 1696.5 (s), 1533.5 (s), 1367.6 (s).

[2-Amino-3-(3-methyl-butoxy)-benzyl]-methyl-carbamic acid *tert*-butyl ester[94]

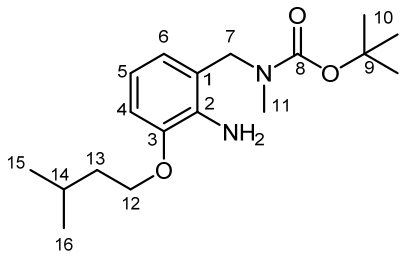


**12**

Carbamate **10** (3.00 g, 8.50 mmol, 1.0 eq.) was dissolved in anhydrous methanol (30 mL) and cooled to 0 °C. 10% Palladium on activated charcoal (0.30 g) and ammonium formate (5.40 g, 85.0 mmol, 10.0 eq.) were added and the reaction mixture was heated to 55 °C for 72 h. The reaction mixture was filtered through celite

and concentrated *in vacuo*. The concentrate was dissolved in ethyl acetate (30 mL) and washed with water (30 mL), brine (30 mL), filtered and concentrated *in vacuo*, giving the desired compound as a colourless oil (2.74 g, 8.50 mmol, 100%).

$^1$H NMR ($CDCl_3$, 500 MHz): 6.78 (1H, d, *J* = 8.7 Hz, $C_{(4/5/6)}$**H**), 6.68 (1H, d, *J* = 6.6 Hz, $C_{(4/5/6)}$**H**), 6.62 (1H, br s, $C_{(4/5/6)}$**H**), 4.69 (1.6H, br s, N$\mathbf{H_2}$), 4.38 (2H, s, $C_{(7)}\mathbf{H_2}$), 4.20 (0.4H, br s, N$\mathbf{H_2}$), 4.02 (2H, t, *J* = 6.7 Hz, $C_{(12)}\mathbf{H_2}$), 2.77 (3H, s, $C_{(9)}\mathbf{H_3}$), 1.88 (1H, m, *J* = 6.7 Hz, $C_{(14)}$**H**), 1.73 (2H, dt, *J* = 6.8, 6.6 Hz, $C_{(13)}\mathbf{H_2}$), 1.50 (9H, br s, **3** × $C_{(10)}\mathbf{H_3}$), 0.99 (6H, d, *J* = 6.7 Hz, $C_{(15)}\mathbf{H_3}$ + $C_{(16)}\mathbf{H_3}$). $^{13}$C NMR ($CDCl_3$, 125 MHz): 156.5 (**C**$_{(8)}$), 146.5 (**C**$_{(3)}$), 136.1 (**C**$_{(2)}$), 123.3 (**C**$_{(6)}$), 120.4 (**C**$_{(1)}$), 115.8 (**C**$_{(5)}$), 110.6 (**C**$_{(4)}$), 79.9 (**C**$_{(9)}$), 66.7 (**C**$_{(12)}$), 49.5 (**C**$_{(7)}$), 38.2 (**C**$_{(13)}$), 33.0 (**C**$_{(11)}$), 28.4 (**3 × C**$_{(10)}$), 25.2 (**C**$_{(14)}$), 22.7 (**C**$_{(15)}$ + **C**$_{(16)}$). HRMS (ESI) calcd for $C_{18}H_{30}N_2NaO_3$ [$(M+Na)^+$]: *m/z* 345.2149, found *m/z* 345.2132. $\nu_{max}$ ($CDCl_3$)/$cm^{-1}$: 3349 (m), 2951 (m), 1664 (s), 1238 (s), 1128 (s).

(*S*)-Dimethyl 2-(2-((*tert*-butoxycarbonyl(methyl)amino)methyl)-6-(isopentoxy)phenylamino)succinate[94]

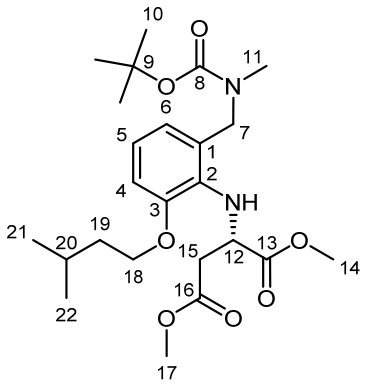


**(S)-14**

Aniline **12** (1.00 g, 3.2 mmol. 1.0 eq.) was dissolved in anhydrous dichloromethane (20 mL), 2,6- lutidine (1.40 mL, 12.4 mmol, 3.9 eq.) was added and the solution was allowed to stir at room temperature for 20 min. Triflate **(*R*)-20** (3.60 g, 12.4 mmol, 3.9 eq.) was dissolved in anhydrous dichloromethane (30 mL) and was added dropwise to the solution. The reaction mixture was heated to 45 ºC and stirred for 48 h. The reaction mixture was quenched with water (20 mL) and the phases were separated. The aqueous phase was extracted with dichloromethane (2 × 20 mL), and the combined organic layer was then washed with copper sulfate solution (aq. sat.) (3 × 20 mL), dried ($Na_2SO_4$), filtered and concentrated *in vacuo*. The resulting mixture was purified by flash column chromatography (0-10% ethyl acetate in petroleum ether) giving the desired compound as a clear oil (1.04 g, 2.20 mmol, 71%).

$^1$H NMR ($CDCl_3$, 500 MHz) δ: 6.77 (1H, br s, $C_{(6)}$**H**), 6.70 (1H, d, *J* = 7.3 Hz, $C_{(4)}$**H**), 6.62 (1H, d, *J* = 8.5 Hz, $C_{(5)}$**H**), 4.81-4.16 (4H, br m, N**H** + $C_{(7)}\mathbf{H_2}$ + $C_{(12)}$**H**), 3.91 (2H, t,

*J* = 6.8 Hz, $C_{(18)}\mathbf{H_2}$), 3.58 (6H, s, $C_{(14)}\mathbf{H_3}$ + $C_{(17)}\mathbf{H_3}$), 2.77 (2H, d, *J* = 5.7 Hz, $C_{(15)}\mathbf{H_2}$), 2.64 (3H, br s, $C_{(11)}\mathbf{H_3}$), 1.77 (1H, apparent septet, *J* = 6.7 Hz, $C_{(20)}\mathbf{H}$), 1.65 (2H, dt, *J* = 6.9, 6.7 Hz, $C_{(19)}\mathbf{H_2}$), 1.40 (9H, s, **3** × $C_{(10)}\mathbf{H_3}$), 0.90 (6H, dd, *J* = 6.5, 1.2, $C_{(21)}\mathbf{H_3}$ + $C_{(22)}\mathbf{H_3}$). $^{13}$C NMR ($CDCl_3$, 125 MHz) δ: 173.4 ($\mathbf{C}_{(16)}$), 171.2 ($\mathbf{C}_{(13)}$), 156.1 ($\mathbf{C}_{(8)}$), 151.0 ($\mathbf{C}_{(3)}$), 134.9 ($\mathbf{C}_{(2)}$), 128.2 ($\mathbf{C}_{(1)}$), 122.9 ($\mathbf{C}_{(6)}$), 121.3 ($\mathbf{C}_{(5)}$), 111.6 ($\mathbf{C}_{(4)}$), 79.9 ($\mathbf{C}_{(9)}$), 66.8 ($\mathbf{C}_{(18)}$), 56.0 ($\mathbf{C}_{(12)}$), 52.0 ($\mathbf{C}_{(14/17)}$), 51.7 ($\mathbf{C}_{(14/17)}$), 48.8 ($\mathbf{C}_{(7)}$), 38.0 ($\mathbf{C}_{(15)}$), 37.9 ($\mathbf{C}_{(19)}$), 33.3 ($\mathbf{C}_{(11)}$), 28.4 (**3** × $\mathbf{C}_{(10)}$), 25.1 ($\mathbf{C}_{(20)}$), 22.7 ($\mathbf{C}_{(21/22)}$), 22.6 ($\mathbf{C}_{(21/22)}$). $\nu_{max}$ ($CDCl_3$)/cm$^{-1}$: 3329 (w), 2955 (m), 1740 (s), 1694 (s), 1674 (s). $[\alpha]_D$: -2.20 (*c* = 1.0, $CHCl_3$, 28.7 ºC).

(*R*)-dimethyl 2-(2-((*tert*-butoxycarbonyl(methyl)amino)methyl)-6-(3-methylbutoxy)phenylamino)succinate[94]

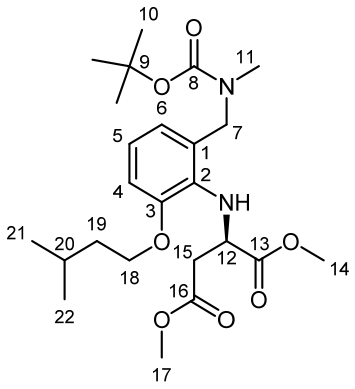

**(*R*)-14**

**(*R*)-14** was synthesised via the method described above (86%). $[\alpha]_D$: +2.72 (*c* = 1.0, $CHCl_3$, 28.7 ºC).

(*R*)-Methyl 2-(9-(3-methylbutoxy)-4-methyl-3-oxo-2,3,4,5-tetraydro-1H-benzo-1,4-diazepin-2-yl)acetate[94]

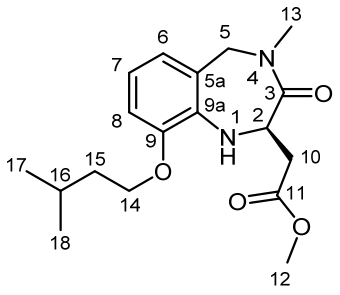

**(*R*)-2**

Succinate **(*R*)-14** (1.00 g, 2.10 mmol) was dissolved in dichloromethane (10 mL). Trifluoroacetic acid (10 mL) was added to the solution and the reaction mixture was allowed to stir at room temperature for 48 h. The reaction mixture was concentrated *in vacuo* and loaded onto a strong cation exchange column with methanol (10 mL).

The column was washed with methanol (3 × 10 mL) and then flushed with 7 M ammonia in methanol. The 7 M ammonia in methanol fractions were allowed to stand at room temperature for 4 h before concentration *in vacuo* giving the desired compound as a colourless oil (0.63 g, 1.90 mmol, 90%).

$^1$H NMR (500 MHz, $CHCl_3$) δ: 6.63 (1H, dd, *J* = 7.5, 1.8 Hz, $C_{(6)}$**H**), 6.52-6.47 (2H, m, $C_{(7)}$**H** + $C_{(8)}$**H**), 5.39 (1H, d, *J* = 16.3 Hz, $C_{(5)}$**H**), 5.01-4.99 (1H, m, $C_{(2)}$**H**), 4.35 (1H, br s, N**H**), 3.94-3.86 (2H, m, $C_{(14)}$**H$_2$**), 3.65 (3H, s, $C_{(12)}$**H$_3$**), 3.63 (1H, d, *J* = 17.5 Hz, $C_{(5)}$**H**), 2.99 (3H, s, $C_{(13)}$**H$_3$**), 2.97 (1H, dd, *J* = 8.3, 7.5 Hz, $C_{(10)}$**H**), 2.61 (1H, dd, *J* = 15.8, 6.3 Hz, $C_{(10)}$**H**), 1.73 (1H, apparent septet, *J* = 6.8 Hz, $C_{(16)}$**H**), 1.60 (2H, dt, *J* = 6.7, 6.6 Hz, $C_{(15)}$**H$_2$**), 0.88 (6H, d, *J* = 6.7 Hz, $C_{(17)}$**H$_3$** + $C_{(18)}$**H$_3$**). $^{13}$C NMR (125 MHz, $CDCl_3$) δ: 171.7 (**C**$_{(7)}$), 169.5 (**C**$_{(3)}$), 146.6 (**C**$_{(9)}$), 135.0 (**C**$_{(9a)}$), 121.3 (**C**$_{(6)}$), 119.3 (**C**$_{(5a)}$), 116.8 (**C**$_{(7)}$), 110.7 (**C**$_{(8)}$), 66.9 (**C**$_{(14)}$), 53.1 (**C**$_{(5)}$), 52.0 (**C**$_{(12)}$), 51.5 (**C**$_{(2)}$), 38.0 (**C**$_{(15)}$), 36.3 (**C**$_{(10)}$), 34.6 (**C**$_{(13)}$), 25.2 (**C**$_{(10)}$), 22.6 (**C**$_{(17)}$ + **C**$_{(18)}$). HRMS (ESI) calcd for $C_{18}H_{26}N_2NaO_4$ [M+Na$^+$]: *m/z* 357.1785, found *m/z* 357.1794. $[\alpha]_D$: 9.32 (*c* = 1%, $CHCl_3$, 28.7 ºC).

(*R*)-Methyl 2-(9-(3-methylbutoxy)-4-methyl-3-oxo-2,3,4,5-tetraydro-1H-benzo-1,4-diazepin-2-yl)acetate[94]

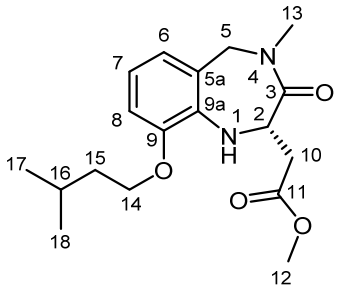


**(S)-2**

**(S)-2** was synthesised via the method described above (88%). $[\alpha]_D$: -7.84 (*c* = 1%, $CHCl_3$, 28.8 ºC).

2-2-2-(*t*-Butyldiphenylsiloxy)ethoxy-ethoxy-ethanol[95]

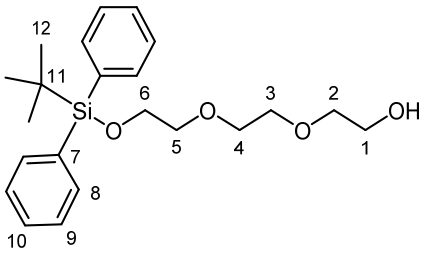


**163**

This compound was isolated as a by-product in the synthesis of **149**.

$^{1}$H NMR ($CDCl_3$, 500 MHz) δ: 7.61-7.60 (4H, m, **4** × $C_{(8)}$**H**), 7.35-7.28 (6H, m, **2** × $C_{(10)}$**H** + **4** × $C_{(9)}$**H**), 3.73 (2H, t, J = 5.4 Hz, C$\mathbf{H_2}$), 3.56-3.49 (8H, m, **4** × C$\mathbf{H_2}$), 2.73 (2H, t, J = 5.5 Hz, C$\mathbf{H_2}$), 2.40 (1H, br s, O**H**), 0.97 (9H, s, **3** × C$\mathbf{H_3}$). $^{13}$C NMR ($CDCl_3$, 125 MHz) δ: 135.6 (**4** × $\mathbf{C_{(8)}}$), 133.7 (**2** × $\mathbf{C_{(7)}}$), 129.6 (**2** × $\mathbf{C_{(10)}}$), 127.6 (**4** × $\mathbf{C_{(9)}}$), 72.4 (**C**$H_2$), 70.7 (**C**$H_2$), 70.5 (**C**$H_2$), 70.5 (**C**$H_2$), 63.4 (**C**$H_2$), 49.2 (**C**$H_2$), 26.8 (**3** × $\mathbf{C_{(12)}}$), 19.2 ($\mathbf{C_{(11)}}$).

2-[2-(2-Azidoethoxy)ethoxy]ethan-1-ol[96]

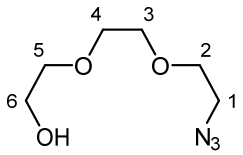


**157**

Triethylene glycol (1.80 mL, 13.3 mmol, 2.8 eq.) was dissolved in tetrahydrofuran (25 mL) and cooled to 0 °C. Methanesulfonyl chloride (0.37 mL, 4.8 mmol, 1.0 eq.) and triethylamine (1.38 mL, 10.0 mmol, 2.1 eq.) were added to the solution which was allowed to stir at 0 °C for 10 min and concentrated *in vacuo*. Ethanol (25 mL) and sodium azide (0.62 g, 9.60 mmol, 2.0 eq.) were added to the concentrate and the reaction mixture was allowed to stir at 70 °C for 18 h. The reaction mixture was concentrated onto silica and purified by flash column chromatography (20-80% ethyl acetate in petroleum ether) giving the title compound as a colourless oil (0.55 g, 3.10 mmol, 65%).

$^{1}$H NMR (500 MHz, $CDCl_3$) δ: 3.66-3.60 (8H, m, **4** × C$\mathbf{H_2}$), 3.54-3.52 (2H, m, $C_{(6)}\mathbf{H_2}$), 3.33 (2H, m, $C_{(1)}\mathbf{H_2}$), 2.97 (1H, br s, O**H**). $^{13}$C NMR (125 MHz, $CDCl_3$) δ: 72.5 (**C**$H_2$), 70.5 (**C**$H_2$), 70.3 (**C**$H_2$), 69.9 (**C**$H_2$), 61.5 ($\mathbf{C_{(6)}}$), 50.6 ($\mathbf{C_{(1)}}$).

2,2,2-(*tert*-Butyldiphenylsiloxy)ethoxy-ethoxy-ethylamine

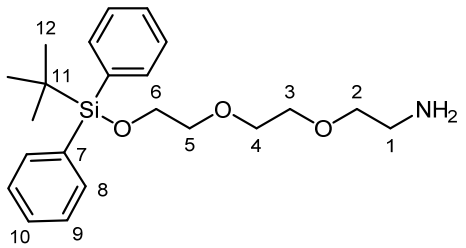


**149**

Alcohol **157** (0.55 g, 3.10 mmol, 1.0 eq.) and *t*-butyldiphenylsilylchloride (2.0 mL, 7.80 mmol, 2.5 mmol) , were dissolved in dichloromethane (20 mL) and cooled to 0 °C. Triethylamine (3.2 mL, 23.3 mmol, 7.5 eq.) was added and the reaction mixture was allowed to warm to room temperature and stir for 48 h giving a red solution. Water

(20 mL) and dichloromethane (20 mL) were added to the solution and the phases were separated. The aqueous layer was extracted with dichloromethane (2 × 20 mL) and the combined organic layers were washed with brine (20 mL), dried ($Na_2SO_4$), filtered, and concentrated *in vacuo* onto silica gel. The mixture was filtered through a plug of silica and washed with 10% ethyl acetate in petroleum ether. The resulting mixture was dissolved in methanol (20 mL). Ammonium formate (2.00 g, 31 mmol, 10.0 eq.) and 10% palladium on activated charcoal (60 mg) were added and the reaction mixture was allowed to stir at room temperature 16 h. The reaction mixture was filtered through celite and purified by flash column chromatography (0-100% ethyl acetate in petroleum ether, then 5 % triethylamine in 95 % ethyl acetate followed by 100% methanol). The methanol fraction was concentrated *in vacuo* and filtered through cotton wool with 100% ethyl acetate (40 mL) giving the desired compound a colourless oil (0.66 g, 1.70 mmol, 55%).

$^1$H NMR (500 MHz, $CHCl_3$) δ: 7.61-7.59 (4H, m, **4** × $C_{(8)}$**H**), 7.37-7.28 (6H, m, **4** × $C_{(9)}$**H** + **2** × $C_{(10)}$**H**), 3.75 (2H, t, *J* = 6.5 Hz, $C_{(6)}$**H**$_2$), 3.59-3.57 (2H, m, C**H**$_2$), 3.55-3.52 (4H, m, **2** × C**H**$_2$), 3.42 (2H, t, *J* = 5.2 Hz, $C_{(2)}$**H**$_2$), 2.78 (2H, br s, $C_{(1)}$**H**$_2$), 1.20 (2H, br s, N**H**$_2$), 0.98 (9H, s, **3** × $C_{(12)}$**H**$_3$). $^{13}$C NMR (125 MHz, $CDCl_3$) δ: 135.6 (**4** × **C**$_{(8)}$), 133.7 (**2** × **C**$_{(7)}$), 129.4 (**2** × **C**$_{(10)}$), 127.6 (**4** × **C**$_{(9)}$), 73.6 (**C**$H_2$), 72.5 (**C**$H_2$), 70.8 (**C**$H_2$), 70.4 (**C**$H_2$), 63.5 (**C**$H_2$), 41.9 (**C**$_{(1)}$), 26.8 (**3** × **C**$_{(12)}$), 19.2 (**C**$_{(11)}$). $\nu_{max}$ ($CDCl_3$)/cm$^{-1}$: 2930.0 (m), 2856.7 (m), 1589.4 (m), 1361.8 (m), 1105.2 (s). HRMS (CI+) calcd for $C_{22}H_{34}NO_3Si$ [(M+H)$^+$] calcd: *m/z* 388.2308, found: *m/z* 388.2308.

2,2,2-(*tert*-Butyldiphenylsilanyloxy)ethoxy-ethoxy-ethyl-[3-(3-methylbutoxy)-2-nitro-benzyl]-amine

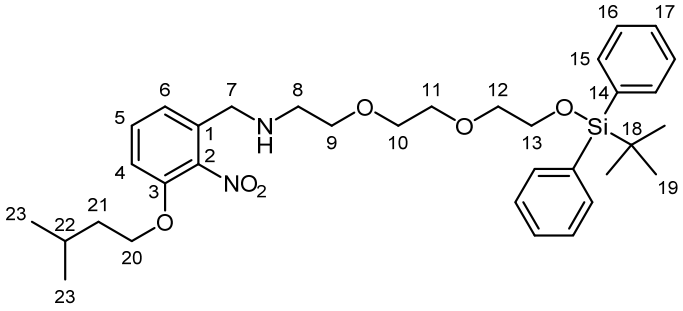


**158**

Aldehyde **18** (0.17 g, 0.7 mmol, 1.0 eq.) and amine **149** (0.32 g, 0.8 mmol, 1.1 eq.) were dissolved in heptane (10 mL). Sodium cyanoborohydride (0.07 g, 1.1 mmol, 1.5 eq.) was added and the reaction mixture was heated to 80 °C for 18 h. The reaction mixture was concentrated *in vacuo* onto silica and the mixture was purified by flash

column chromatography (100% ethyl acetate) giving the title compound as a colourless oil (0.30 g, 0.49 mmol, 70%).

$^{1}$H NMR (500 MHz, $CDCl_3$) δ: 7.61-7.59 (4H, m, **4** × $C_{(15)}$**H**), 7.36-7.28 (6H, m, **4** × $C_{(16)}$**H** + **2** × $C_{(17)}$**H**), 7.25 (1H, t, *J* = 7.9 Hz, $C_{(5)}$**H**), 6.96 (1H, d, *J* = 7.8 Hz, $C_{(4/6)}$**H**), 6.82 (1H, d, *J* = 8.2 Hz, $C_{(4/6)}$**H**), 3.98 (2H, t, *J* = 6.6Hz, C$\mathbf{H_2}$), 3.75 (2H, t, *J* = 5.1 Hz, C$\mathbf{H_2}$), 3.64 (2H, s, $C_{(7)}\mathbf{H_2}$), 3.59-3.56 (4H, m, **2** × C$\mathbf{H_2}$), 3.50-3.48 (2H, t, *J* = 5.1 Hz, C$\mathbf{H_2}$), 2.68 (2H, t, *J* = 5.2 Hz, $C_{(8)}\mathbf{H_2}$), 1.70 (1H, apparent septet, *J* = 6.8 Hz, $C_{(22)}$**H**), 1.57 (2H, q, *J* = 6.6 Hz, $C_{(21)}\mathbf{H_2}$), 0.97 (9H, s, **3** × $C_{(19)}\mathbf{H_3}$), 0.95 (6H, d, *J* = 6.7 Hz, $C_{(23)}\mathbf{H_3}$ + $C_{(24)}\mathbf{H_3}$). $^{13}$C NMR (125 MHz, $CDCl_3$) δ: 150.3 (**C**$_{(3)}$), 141.5 (**C**$_{(2)}$), 135.6 (**4** × **C**$_{(15)}$), 133.7 (**2** × **C**$_{(14)}$), 133.6 (**C**$_{(1)}$), 130.8 (**C**$_{(5)}$), 129.6 (**2** × **C**$_{(17)}$), 127.6 (**4** × **C**$_{(16)}$), 121.0 (**C**$_{(4)}$), 112.1 (**C**$_{(6)}$), 72.5 (**C**$H_2$), 70.7 (**C**$H_2$), 70.5 (**C**$H_2$), 70.4 (**C**$H_2$), 67.9 (**C**$_{(20)}$), 63.5 (**C**$_{(13)}$), 49.0 (**C**$_{(7)}$), 48.6 (**C**$_{(8)}$), 37.6 (**C**$_{(21)}$), 26.8 (**C**$_{(19)}$), 24.9 (**C**$_{(22)}$), 22.5 (**C**$_{(24)}$ + **C**$_{(25)}$), 19.2 (**C**$_{(18)}$). HRMS calcd for $C_{34}H_{49}N_2O_6Si$ ($[M+H]^+$): 609.3354, found: 609.3332. $\nu_{max}$ ($CDCl_3$)/cm$^{-1}$: 2930 (m), 1585 (m), 1584 (m), 1533 (s), 1112 (s).

2,2,2-(*tert*-Butyldiphenylsilanyloxy)ethoxy-ethoxy-ethyl-3-(3-methyl-butoxy)-2-nitro-benzyl]-carbamic acid *tert*-butyl ester

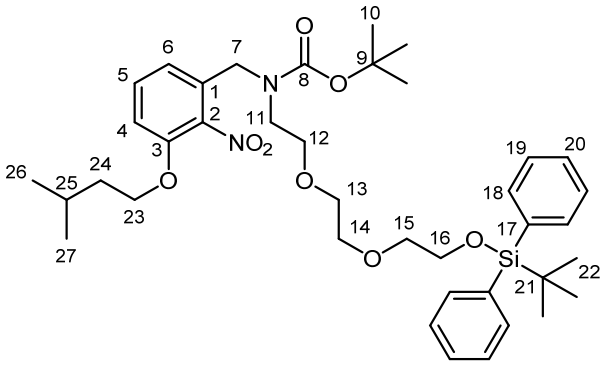


**159**

Amine **158** (0.30 g, 0.49 mmol, 1.0 eq.) was dissolved in dichloromethane (10 mL). Triethylamine (0.14 mmol, 0.98 mmol, 2.0 eq.) and di-*tert*-butyl dicarbonate (0.43 g, 2.0 mmol, 4.0 eq.) were added and allowed to stir at room temperature for 48 h. The reaction mixture was concentrated *in vacuo* onto silica gel. The mixture was purified by flash column chromatography (0-20% ethyl acetate in petroleum ether) giving the title compound as a light brown oil (0.28 g, 0.39 mmol, 80%).

$^{1}$H NMR (500 MHz, $CDCl_3$) δ: 7.66-7.63 (4H, m, **4** × $C_{(18)}$**H**), 7.32-7.19 (7H, m, **4** × $C_{(19)}$**H** + **2** × $C_{(20)}$**H** + Ar$C_{(4/5/6)}$**H**), 6.81-6.76 (2H, m, **2** × Ar$C_{(4/5/6)}$**H**), 4.44-4.40 (2H, m, $C_{(7)}\mathbf{H_2}$), 3.95-3.94 (2H, m, $C_{(23)}\mathbf{H_2}$), 3.72 (2H, t, *J* = 5.2 Hz, C$\mathbf{H_2}$), 3.52-3.49 (5H, m, contains two rotamers: **5H** of several $CH_2$), 3.43 (3H, br s, contains two rotamers: **3H**

of several $CH_2$), 3.33 (1H, br s, rotamer: 56% of $CH_2$ (**1H**)), 3.22 (1H, br s, rotamer: 44% of $CH_2$ (**1H**)), 1.68 (1H, apparent septet, *J* = 6.7 Hz, $C_{(25)}$**H**), 1.55 (2H, dt, *J* = 6.6, 6.5 Hz, $C_{(24)}$**H**$_2$), 1.38 (4H, br s, rotamer: 44% of 3 × $C_{(10)}H_3$ (**4H**)), 1.27 (5H, br s, rotamer: 56% of 3 × $C_{(10)}H_3$ (**5H**)), 0.95 (9H, s, **3** × $C_{(24)}$**H**$_3$), 0.82 (6H, d, *J* = 6.6 Hz, $C_{(26)}$**H**$_3$ + $C_{(27)}$**H**$_3$). $^{13}$C NMR (125 MHz, $CDCl_3$) δ: 155.7 + 155.3 (rotamers $\mathbf{C}_{(8)}$), 150.4 + 150.3 (rotamers $\mathbf{C}_{(3)}$), 141.+ 140.7 (rotamers $\mathbf{C}_{(2)}$), 135.6 (**4** × $\mathbf{C}_{(18)}$), 133.7 (**2** × $\mathbf{C}_{(17)}$), 132.4 + 131.9 (rotamers $\mathbf{C}_{(1)}$), 131.0 + 130.8 (rotamers $\mathbf{C}_{(4/5/6)}$), 129.6 (**2** × $\mathbf{C}_{(20)}$), 127.7 (**4** × $\mathbf{C}_{(19)}$), 119.8 + 119.0 (rotamers $\mathbf{C}_{(4/5/6)}$), 112.2 + 112.0 (rotamers $\mathbf{C}_{(4/5/6)}$), 80.3 + 80.2 (rotamers $\mathbf{C}_{(9)}$), 72.5 ($\mathbf{C}_{(13/14/15/16)}$), 70.8 + 70.7 (rotamers $\mathbf{C}_{(12)}$), 70.5 + 70.4 (rotamers $\mathbf{C}_{(11)}$), 67.9 ($\mathbf{C}_{(23)}$), 67.7 ($\mathbf{C}_{(13/14/15/16)}$), 63.5 ($\mathbf{C}_{(13/14/15/16)}$), 47.5 ($\mathbf{C}_{(13/14/15/16)}$), 46.7 + 46.5 (rotamers $\mathbf{C}_{(7)}$), 37.5 ($\mathbf{C}_{(24)}$), 28.4 + 28.2 (rotamer **3** × $\mathbf{C}_{(10)}$), 26.9 (**3** × $\mathbf{C}_{(22)}$), 24.8 ($\mathbf{C}_{(25)}$), 22.5 ($\mathbf{C}_{(26)}$ + $\mathbf{C}_{(27)}$), 19.2 ($\mathbf{C}_{(21)}$). HRMS (ESI) calcd for $C_{29}H_{56}N_2NaO_8Si$ [$(M+Na)^+$]: *m/z* 731.3698, found *m/z* 731.3669. $\nu_{max}$ ($CDCl_3$): 2957 (s), 1697 (s), 1533 (s), 1142 (s),1113 (s).

[2-Amino-3-(3-methyl-butoxy)-benzyl]- 2,2,2-(*tert*-butyldiphenylsilanyloxy)ethoxy-ethoxy-ethyl-carbamic acid *tert*-butyl ester

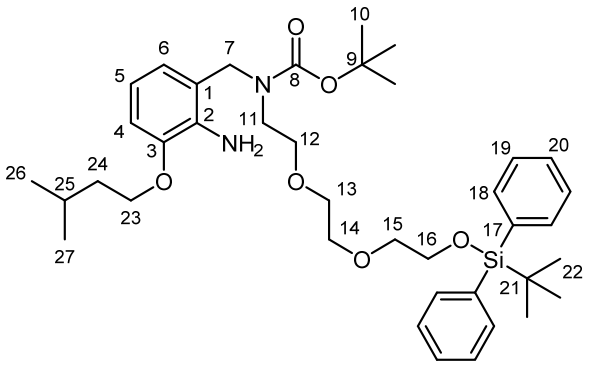


**147**

Carbamate **164** (0.18 g, 0.25 mmol, 1.0 eq.) dissolved in methanol (10 mL). 10 % Palladium on activated charcoal (18 mg) and $NH_4CO_2$ (0.16 g, 2.5 mmol, 10.0 eq.) were added to the solution which was heated to 60 °C and allowed to stir for 15 h. The reaction mixture was filtered through celite, washed with methanol (2 × 10 mL), concentrated *in vacuo*, giving a crude product which was taken onto.subsequent steps with no purification (0.11 g, 0.16mmol, 64%).

$^1$H NMR (500 MHz, $CDCl_3$) δ: 7.61-7.59 (4H, m, **4** × $C_{(18)}$**H**), 7.35-7.28 (6H, m, **4** × $C_{(19)}$**H** + **2** × $C_{(20)}$**H**), 6.64 (1H, dd, *J* = 8.0, 1.0 Hz, $C_{(4/5/6)}$**H**) 6.61 (1H, d, *J* = 7.6 Hz, $C_{(4/5/6)}$**H**), 6.48 (1H, br s, $C_{(4/5/6)}$**H**), 4.39 (2H, s, $C_{(7)}$**H**$_2$), 3.91 (2H, t, *J* = 6.7 Hz, $C_{(23)}$**H**$_2$), 3.73 (2H, t, *J* = 5.2 Hz, $C_{(13/14/15/16)}$**H**$_2$), 3.56-3.52 (4H, m, **2** × $C_{(13/14/15/16)}$**H**$_2$), 3.47-3.44 (4H, m, $C_{(12)}$**H**$_2$ + $C_{(13/14/15/16)}$**H**$_2$), 3.19 (2H, br s, $C_{(11)}$**H**$_2$), 1.76 (1H, apparent septet, *J*

= 6.8 Hz, $C_{(25)}\mathbf{H}$), 1.62 (2H, q, *J* = 6.8 Hz, $C_{(24)}\mathbf{H_2}$), 1.38 (9H, br s, **3** × $C_{(10)}\mathbf{H_3}$), 0.97 (9H, s, **3** × $C_{(22)}\mathbf{H_3}$), 0.88 (6H, d, *J* = 6.6 Hz, $C_{(26)}\mathbf{H_3}$ + $C_{(27)}\mathbf{H_3}$). $^{13}$C NMR (125 MHz, $CDCl_3$) δ: 156.2 ($\mathbf{C}_{(8)}$), 146.4 ($\mathbf{C}_{(3)}$), 136.2 ($\mathbf{C}_{(2)}$), 136.2 (**4** × $\mathbf{C}_{(18)}$), 133.7 (**2** × $\mathbf{C}_{(17)}$), 129.6 (**4** × $\mathbf{C}_{(20)}$), 127.7 (**4** × $\mathbf{C}_{(19)}$), 123.6 ($\mathbf{C}_{(6)}$), 120.7 ($\mathbf{C}_{(1)}$), 115.9 ($\mathbf{C}_{(5)}$), 110.6 ($\mathbf{C}_{(4)}$), 80.0 ($\mathbf{C}_{(9)}$), 72.5 ($\mathbf{C}H_2$), 70.8 ($\mathbf{C}H_2$), 70.5 ($\mathbf{C}H_2$), 69.6 ($\mathbf{C}H_2$), 66.7 ($\mathbf{C}_{(23)}$), 63.5 ($\mathbf{C}H_2$), 48.1 ($\mathbf{C}_{(7)}$), 44.7 ($\mathbf{C}_{(11)}$), 38.2 ($\mathbf{C}_{(24)}$), 28.5 ($\mathbf{C}_{(10)}$), 26.8 (**3** × $\mathbf{C}_{(22)}$), 25.2 ($\mathbf{C}_{(25)}$), 22.7 ($\mathbf{C}_{(26)}$ + $\mathbf{C}_{(27)}$), 19.2 ($\mathbf{C}_{(21)}$). HRMS (ESI) calcd for $C_{39}H_{58}N_2NaO_6Si$ [$(M+Na)^+$]: *m/z* 701.3956, found *m/z* 701.3925. $\nu_{max}$ ($CDCl_3$)/$cm^{-1}$: 2957.0 (m), 2359.0 (m), 1674.3 (s), 1473.7 (m), 1111.0 (s).

(*S*)-Dimethyl 2-(2-((*tert*-butoxycarbonyl(2,2,2-(*tert*-butyldiphenylsilanyloxy)ethoxy-ethoxy-ethyl)amino)methyl)-6-(3-methylbutoxy)phenylamino)succinate

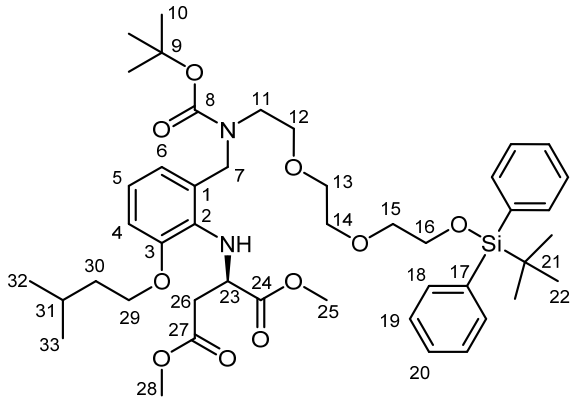


**(*S*)-159**

Aniline **147** was dissolved in dichloromethane (10 mL) and cooled to -78 °C, 2,6-lutidine (0.06 mL, 0.53 mmol, 1.9 eq.) was added to the solution. Triflate **(*R*)-20** (80 mg, 0.28 mmol, 1.7 eq.) was added in dichloromethane (5 mL), the reaction mixture was heated to 40 °C and allowed to stir for 18 h. The reaction mixture was allowed to cool to room temperature and copper sulfate (aq. sat. 15 mL) was added and the phases were separated. The organic phase was washed with copper sulfate (2 × 15 mL), brine, dried ($Na_2SO_4$), filtered and concentrated *in vacuo* onto silica gel. Flash column chromatography was used to purify the resulting mixture (0-30% ethyl acetate in petroleum ether) giving the title compound as a colourless oil (115 mg, 0.14 mmol, 36%).

$^1$H NMR ($CDCl_3$, 500 MHz) δ: 7.61-7.59 (4H, m, **4** × $C_{(18)}\mathbf{H}$), 7.35-7.27 (6H, m, **2** × $C_{(20)}\mathbf{H}$ + **4** × $C_{(19)}\mathbf{H}$), 6.70-6.64 (3H, m, $C_{(4)}\mathbf{H}$ + $C_{(5)}\mathbf{H}$ + $C_{(6)}\mathbf{H}$), 4.81-4.69 (3H, m, $C_{(23)}\mathbf{H}$ + $C_{(6)}\mathbf{H_2}$), 4.30-4.27 (1H, m, N**H**), 3.90 (2H, t, *J* = 6.8 Hz, $C_{(29)}\mathbf{H_2}$), 3.73 (2H, t, *J* = 5.4 Hz, $C_{(16)}\mathbf{H_2}$), 3.61-3.45 (14H, m, $C_{(25)}\mathbf{H_3}$ + $C_{(28)}\mathbf{H_3}$ + $C_{(12)}\mathbf{H_2}$ + $C_{(13)}\mathbf{H_2}$ + $C_{(14)}\mathbf{H_2}$ + $C_{(15)}\mathbf{H_2}$), 3.24-3.15 (2H, m, $C_{(11)}\mathbf{H_2}$), 2.77-2.76 (2H, m, $C_{(26)}\mathbf{H_2}$), 1.76 (1H, apparent septet, *J* = 6.5 Hz, $C_{(31)}\mathbf{H}$), 1.68-1.65 (2H, m, $C_{(30)}\mathbf{H_2}$), 1.38 (9H, s, **3** × $C_{(10)}\mathbf{H_3}$), 0.97 (9H, s, **3** ×

$C_{(22)}\mathbf{H_3}$), 0.89 (6H, dd, *J* = 6.5, 1.3 Hz, $C_{(32)}\mathbf{H_3}$ + $C_{(33)}\mathbf{H_3}$). $^{13}$C NMR ($CDCl_3$, 125 MHz) δ: 173.4 ($\mathbf{C_{(24/27)}}$), 171.2 ($\mathbf{C_{(24/27)}}$), 155.9 ($\mathbf{C_{(8)}}$), 150.8 ($\mathbf{C_{(3)}}$), 135.6 (**4** × $\mathbf{C_{(18)}}$), 133.7 (**2** × $\mathbf{C_{(17)}}$), 129.6 (**2** × $\mathbf{C_{(20)}}$), 127.6 (**4** × $\mathbf{C_{(19)}}$), 122.9 ($\mathbf{C_{(6)}}$), 121.1 ($\mathbf{C_{(5)}}$), 111.7 ($\mathbf{C_{(4)}}$), 80.0 ($\mathbf{C_{(9)}}$), 77.2 (**C**$H_2$), 72.5 (**C**$H_2$), 70.7 (**C**$H_2$), 70.4 (**C**$H_2$), 69.4 (**C**$H_2$), 66.9 (**C**$H_2$), 63.4 (**C**$H_2$), 56.1 ($\mathbf{C_{(23)}}$), 52.0 ($\mathbf{C_{(25/28)}}$), 51.7 ($\mathbf{C_{(25/28)}}$), 47.6 (**C**$H_2$), 44.9 (**C**$H_2$), 38.1 (**C**$H_2$), 28.4 (**3** × $\mathbf{C_{(10)}}$), 26.8 (**3** × $\mathbf{C_{(22)}}$), 25.2 ($\mathbf{C_{(31)}}$), 22.7 ($\mathbf{C_{(32/33)}}$), 22.6 ($\mathbf{C_{(32/33)}}$), 19.2 ($\mathbf{C_{(21)}}$), $\mathbf{C_{(1)}}$ and $\mathbf{C_{(2)}}$ are unresolved. HRMS (ESI) calcd for $C_{45}H_{65}N_2NaO_{10}Si$ [$(M+Na)^+$]: *m*/*z* 845.4379, found *m*/*z*, 845.4339. $\nu_{max}$ ($CDCl_3$)/$cm^{-1}$: 2954 (m), 1741 (s), 1691 (s), 1463 (m), 1111 (s). $[\alpha]_D$: +17.2 (*c* =1.0, $CHCl_3$, 22.8 ºC).

## 5.3 Biology General Information

Dulbecco's Phosphate Buffered Saline (0.0095 M (PO4) without Ca and Mg) (PBS). FBS, DPBS, Trypsin-EDTA, Glutamine, DMEM from Lonza. Corning T75 vented culture flasks from Fisher. Human Dermal Fibroblasts, neonatal (HDFn) from Invitrogen. Images taken with Nikon Eclipse TS100 and Euromex CMEX DC 5000.

## 5.4 General Protocols for Splitting and Maintaining Human Fibroblast Cultures

### 5.4.1 Composition of Media and Buffers

Dulbecco's Modified Eagle's Media with 1 g/L Glucose (DMEM).

cDMEM: DMEM + Glutamine + Penicillin-Streptomycin + Fetal bovine serum

sfDMEM: DMEM + Glutamine + Penicillin-Streptomycin + 0.1% bovine serum albumin.

### 5.4.2 Changing media:

The media (cDMEM) and DPBS were heated to 37$^{o}$C in water bath for about 15 minutes before use. The used media was removed from the cells. The flask was tilted and the cells were washed with 5 ml DPBS. Fresh media was added to the cells (10 mL to T75 flask, 5 ml to T25 flask). The cells were incubated at 37 °C and the media was changed every two days.

### 5.4.3 Splitting flasks of cells:

The media was removed and the cells were washed with warmed DPBS (2 × 5 mL). The cells were treated with trypsin (1 mL) and incubated at 37 °C for 5 minutes. The cells were removed from the base of the flask through physical perturbation and suspended in media (9 mL). The cells were transferred to a universal and centrifuged at 800 rpm for 5 mins. The supernatant was removed and the cells were suspended in media (4 mL). An aliquot of the cell media suspension (1 mL) was added to a T75 flask and media (9 mL) was added. The flask was incubated at 37 °C.

## 5.5 HDFn Scrape Wounds General Procedure

Cells seeded in cDMEM (1.5 × $10^5$ cells/mL) into 12 well plate and allowed to attach for 72 hours. Media removed and cells washed with PBS (5 mL). sfDMEM (0.25 mL) added to each well and cells incubated for 1 hour. Treatment solutions (4 solutions x 3 wells) made from appropriate stock. Diameter scrapes made in each well with

sterile, yellow pipette tip (600 μM). Media removed, cells washed with PBS and treated with appropriate medium (0.25-0.5 mL). Image captured of scrape in each well (× 100 magnification). Cells allowed to incubate for 24 hours, solutions made from stock, media replaced. Images captured at 24 hours. Repeated for 48 and 72 hours time periods.

## 5.6 RNA Extraction Protocol

Reagent Preparation:
*β*-Mercaptoethanol was added to Buffer RLT giving 10 μL/1 ml.
Buffer RPE is supplied as a concentrate, ethanol (96–100%) (4 volumes) was added to Buffer RPE to obtain a working solution.
DNase I (1500 Kunitz units) was dissolved in RNase free water (550 μL).

Procedure:
The media was completely aspirated from the cell culture flask. The cells were disrupted through the addition of Buffer RLT (350 μL) to the cell-culture dish. The resulting lysate was collected with a rubber policeman. The lysate was transferred into a microcentrifuge tube by pipette. The lysate was passed through a 0.9 mm diameter needle fitted to an RNase-free syringe five times. 70% Ethanol (350 μL) was added to the homogenized lysate, and mixed well by pipetting. The sample was transferred to an RNeasy spin column in a 2 ml collection tube and centrifuged for 15 s at ≥8000 x *g* (≥10,000 rpm), the flow-through was discarded. Buffer RW1 (350 μL) was added to the RNeasy spin column. The column was centrifuged for 15 s at ≥8000 x *g* (≥10,000 rpm) to wash the spin column membrane and the flow-through was discarded

DNase I stock solution (10 μL) was added to Buffer RDD (70 μL) and the tube was gently inverted to allow solvation. DNase I incubation mix (80 μL) was added directly to the RNeasy spin column membrane, and allowed to stand at room temperature for 15 min. Buffer RW1 (350 μL) was added to the RNeasy spin column, which was then centrifuged for 15 s at ≥8000 x *g* (≥10,000 rpm) and the flow through was discarded. Buffer RPE (500 μL) was added to the RNeasy spin column which was centrifuged for 15 s at ≥8000 x *g* (≥10,000 rpm) to wash the spin column membrane. The flow-through was discarded. Buffer RPE (500 μL) was added to the RNeasy spin column which was centrifuged for 2min at ≥8000 x *g* (≥10,000 rpm) to wash the spin column

membrane.  The RNeasy spin column was placed in a new 2 ml collection tube,and the old collection tube was discarded with the flow-through. The RNeasy spin column was centrifuged at full speed for 1 min and the RNeasy spin column was placed in a new 1.5 ml collection tube.  RNase-free water (30–50 µL) was added directly to the spin column membrane and the spin column was centrifuged for 1 min at ≥8000 x *g* (≥10,000 rpm) eluting the RNA.

# 6.0 Appendices

## Appendix 6.1: Serum Free vs Complete DMEM Scratch Assay Results

| | Well 1 Wound Area Remaining (%) | Well 2 Wound Area Remaining (%) | Well 3 Wound Area Remaining (%) |
|---|---|---|---|
| Time (hr) | Complete Media Control | | |
| 0. | 100.0 | 100.00 | 100.00 |
| 24. | 80.40 | 45.90 | 72.10 |
| 48. | 53.30 | 36.50 | 47.50 |
| 72. | 0.00 | 51.85 | 38.04 |
| | Complete Media + Compound | | |
| 0. | 100.00 | 100.00 | 100.00 |
| 24. | 81.10 | 97.80 | 36.90 |
| 48. | 84.90 | 83.50 | 42.00 |
| 72. | 33.34 | 0.00 | 0.00 |
| | Serum Free Media Control | | |
| 0. | 100.00 | 100.00 | 100.00 |
| 24. | 65.30 | 90.40 | 92.80 |
| 48. | 68.90 | 101.20 | 77.10 |
| 72. | 69.89 | 71.76 | 66.32 |
| | Serum Free Media + Compound | | |
| 0. | 100.00 | 100.00 | 100.00 |
| 24. | 95.80 | 88.70 | 61.70 |
| 48. | 79.00 | 90.70 | 61.30 |
| 72. | 0.00 | 72.79 | 0.00 |

**Appendix 6.2: Determination of Optimal Dose ((*S*)-Methyl IGD Peptidomimetic ((*S*)-2)))**

| Time (hr) | Control Wound Area Remaining (%) | | | | | | | | |
|---|---|---|---|---|---|---|---|---|---|
| 0. | 100 | 100 | 100 | 100 | 100 | 100 | 100 | 100 | 100 |
| 24. | 68 | 77 | 65 | 65 | 83 | 63 | 44 | 80 | 67 |
| 48. | 47 | 61 | 46 | 55 | 59 | | 32 | 66 | 47 |
| 72. | 37 | 32 | 42 | 37 | 47 | | 10 | 30 | 23 |
| | *S* IGD 0.1 Wound Area Remaining (%) | | | | | | | | |
| 0. | 100 | 100 | 100 | 100 | 100 | 100 | 100 | 100 | 100 |
| 24. | 55 | 66 | 79 | 49 | 63 | 87 | 54 | 49 | 46 |
| 48. | 26 | 38 | 56 | 36 | 52 | 56 | 40 | 43 | 39 |
| 72. | 22 | 57 | 60 | 46 | 40 | 64 | 29 | 26 | 19 |
| | *S* IGD 1 Wound Area Remaining (%) | | | | | | | | |
| 0. | 100 | 100 | 100 | 100 | 100 | 100 | 100 | 100 | 100 |
| 24. | 73 | 60 | 64 | 83 | 77 | 72 | 69 | 62 | 52 |
| 48. | 64 | 43 | 29 | 52 | 59 | 49 | 36 | 42 | 34 |
| 72. | 48 | 41 | 46 | 35 | 40 | 21 | 25 | 28 | 23 |
| | *S* IGD 10 Wound Area Remaining (%) | | | | | | | | |
| 0. | 100 | 100 | 100 | 100 | 100 | 100 | 100 | 100 | 100 |
| 24. | 56 | 74 | 63 | 71 | 54 | 90 | 63 | 54 | 63 |
| 48. | 50 | 48 | 29 | 41 | 37 | 68 | 40 | 24 | 32 |
| 72. | 65 | 39 | 59 | 39 | 39 | 51 | 27 | 29 | 15 |

**Appendix 6.3: Determination of Optimal Dose ((*R*)-Methyl IGD Peptidomimetic ((*R*)-2))**

| Time (hr) | Control Wound Area Remaining (%) | | | | | | | | |
|---|---|---|---|---|---|---|---|---|---|
| 0. | 100 | 100 | 100 | 100 | 100 | 100 | 100 | 100 | 100 |
| 24. | 61. | 65 | 59 | 59 | 65 | 60 | 69 | 60 | 59 |
| 48. | 48 | 37 | 50 | 40 | 56 | | 52 | 48 | 44 |
| 72. | 38 | 42 | 35 | 46 | 39 | | 39 | 20 | 27 |
| | *R* IGD 0.1 Wound Area Remaining (%) | | | | | | | | |
| 0. | 100 | 100 | 100 | 100 | 100 | | 100 | 100 | 100 |
| 24. | 65 | 59 | 56 | 57 | 43 | | 64 | 60 | 47 |
| 48. | 41 | 37 | 42 | 36 | 38 | | 40 | 60 | 44 |
| 72. | 49 | 35 | 32 | 27 | 28 | | 25 | 13 | 17 |
| | *R* IGD 1 Wound Area Remaining (%) | | | | | | | | |
| 0. | 100 | 100 | | 100 | | 100 | 100 | 100 | 100 |
| 24. | 59 | 66 | | 62 | | 52 | 51 | 56 | 54 |
| 48. | 39 | 45 | | 53 | | 49 | 27 | 37 | 37 |
| 72. | 30 | 34 | | 19. | | 33 | 18 | 23 | 5 |
| | *R* IGD 10 Wound Area Remaining (%) | | | | | | | | |
| 0. | 100 | 100 | 100 | 100 | 100 | 100 | 100 | 100 | 100 |
| 24. | 71 | 61 | 68 | 62 | 67 | 63 | 59 | 66 | 56 |
| 48. | 45 | 44 | 60 | 37 | 52 | 54 | 46 | 44 | 49 |
| 72. | 36 | 32 | 44 | 27 | 45 | 48 | 25 | 45 | 24 |

## Appendix 6.4: High Resolution Magic Angle Spinning NMR of Solid Supported IGD Peptidomimetic.

All high-resolution magic-angle spinning (HRMAS) NMR experiments were recorded at room temperature on a Bruker Avance 700 spectrometer operating at 700.26 MHz for $^{1}H$, using a 4 mm H-X solid-state NMR probe from Bruker. About 1-2 mg of sample was placed at the center of the HRMAS rotor and covered with 2-3 drops of deuterated $CDCl_3$ before sealed. The sample was spun at a spinning frequency of 10000 Hz. A 5.0 μs 90° pulse and a recycle time of 2 s were used. The $^{1}H$ HRMAS spectrum was obtained with a spectral width of 5580 Hz and 32 scans.

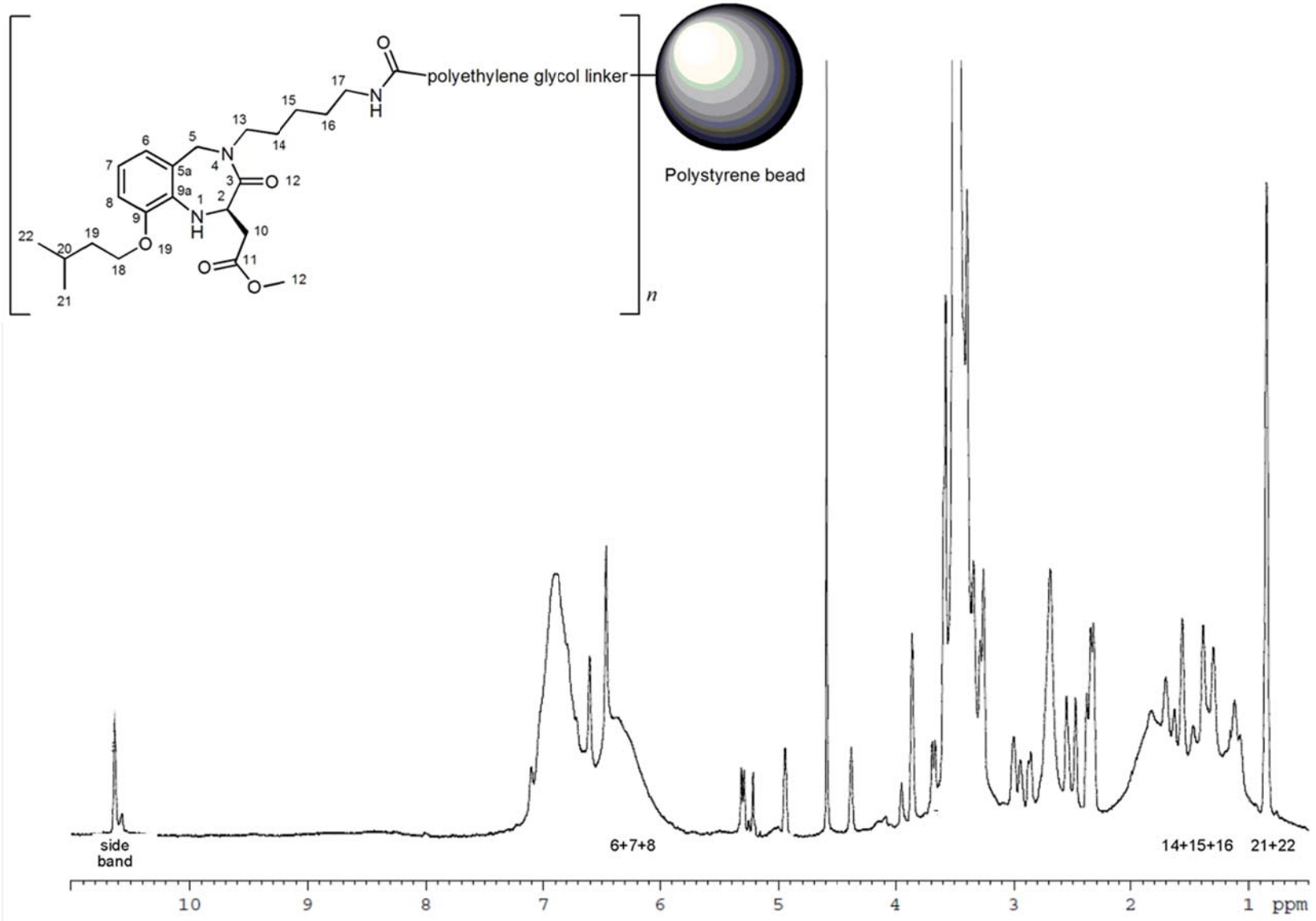
polyethylene glycol linker
Polystyrene bead
n
side band
6+7+8
14+15+16
21+22
10
9
8
7
6
5
4
3
2
1
ppm

## Appendix 6.5: Absorption and Emission Spectra

### 6.5.1: Absorption and Emission Spectra for Difunctionalised BODIPYs

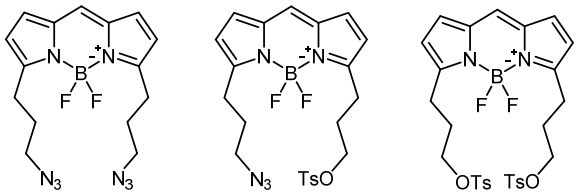


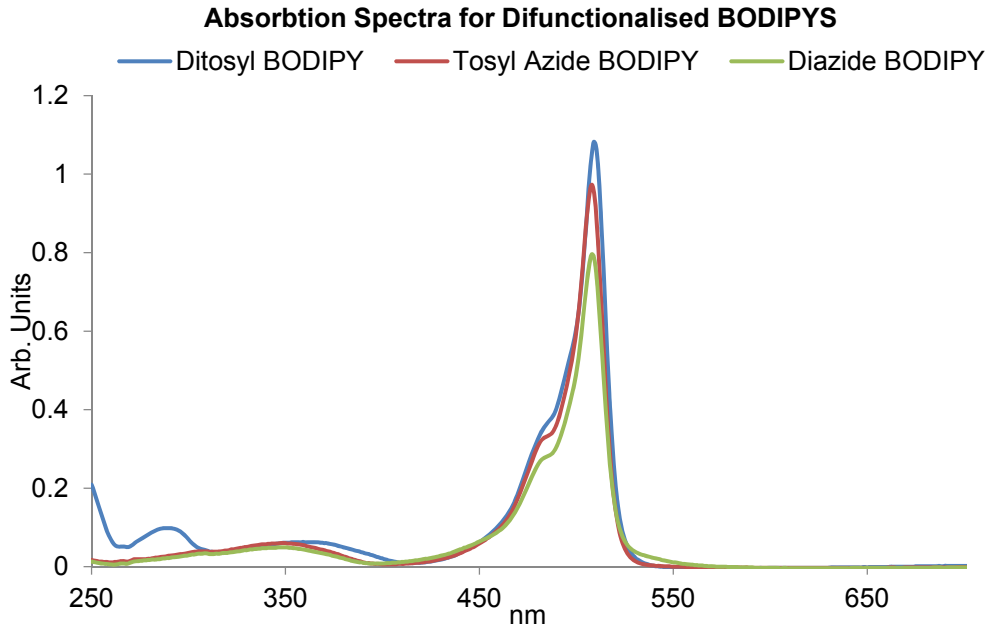


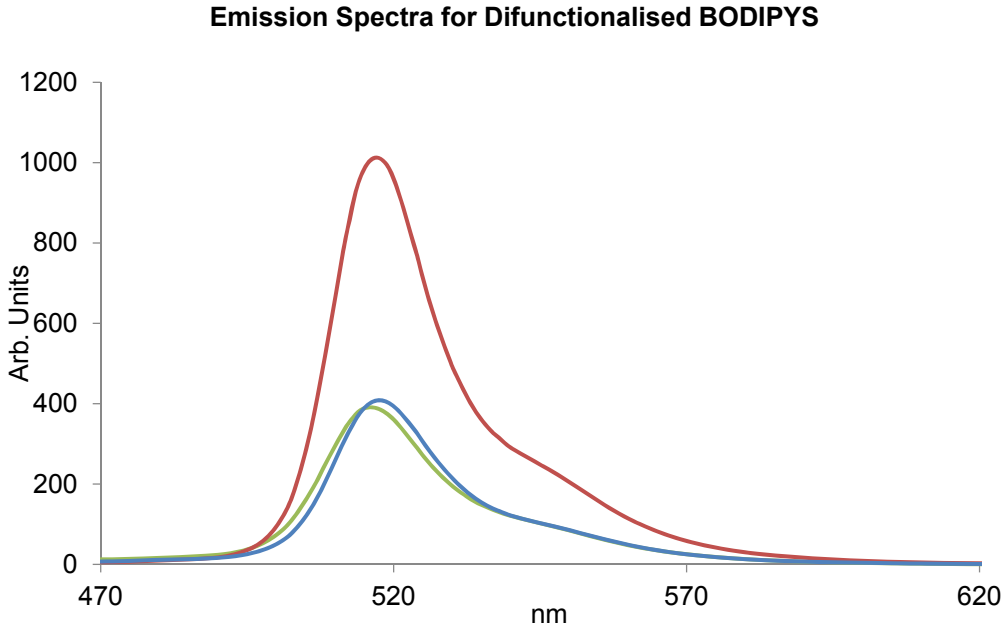

Appendix 6.5.2: Absorption and Emission Spectra for IGD peptidomimetic BODIPYs

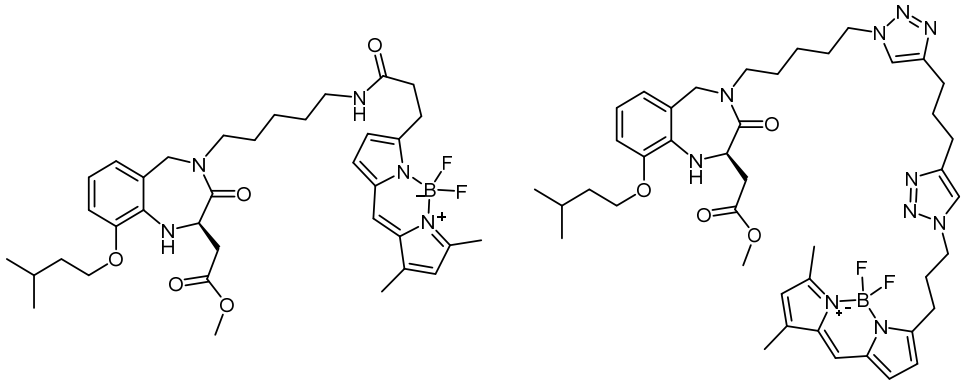

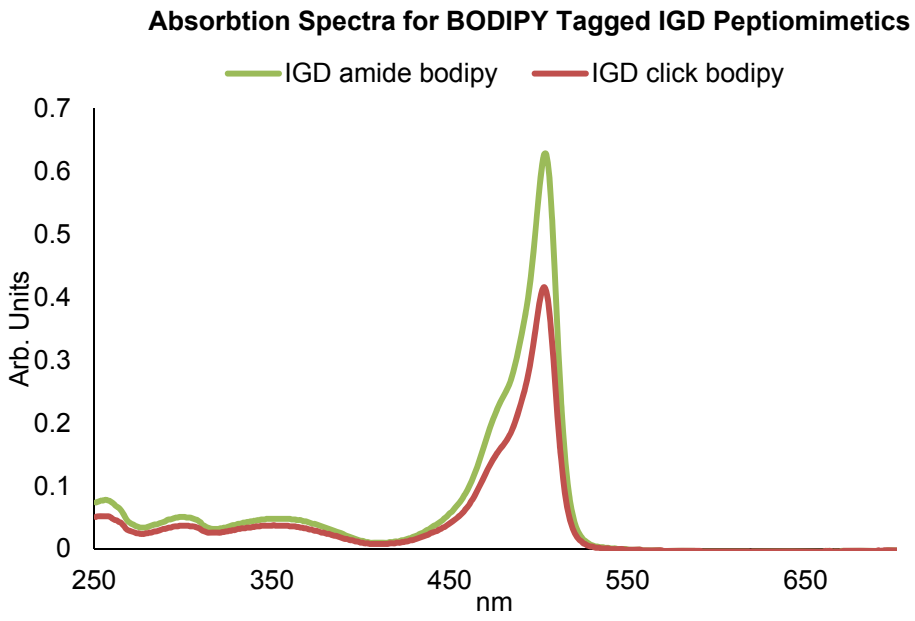


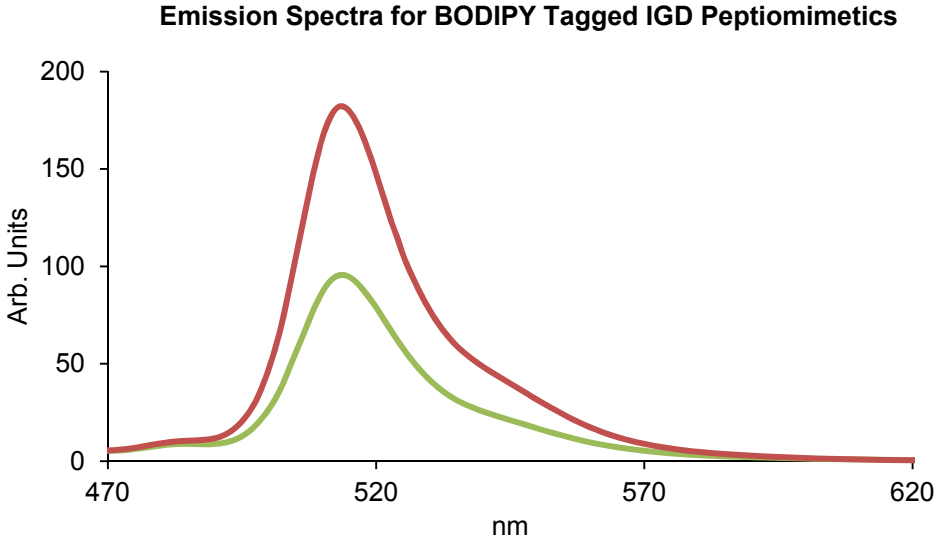

Appendix 6.5.3: Absorption and Emission Spectra for Novel BODIPYs

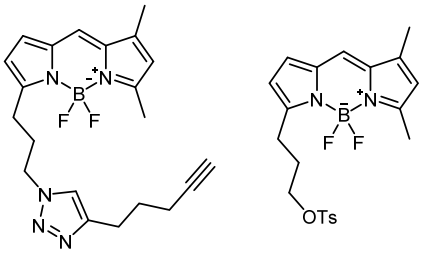


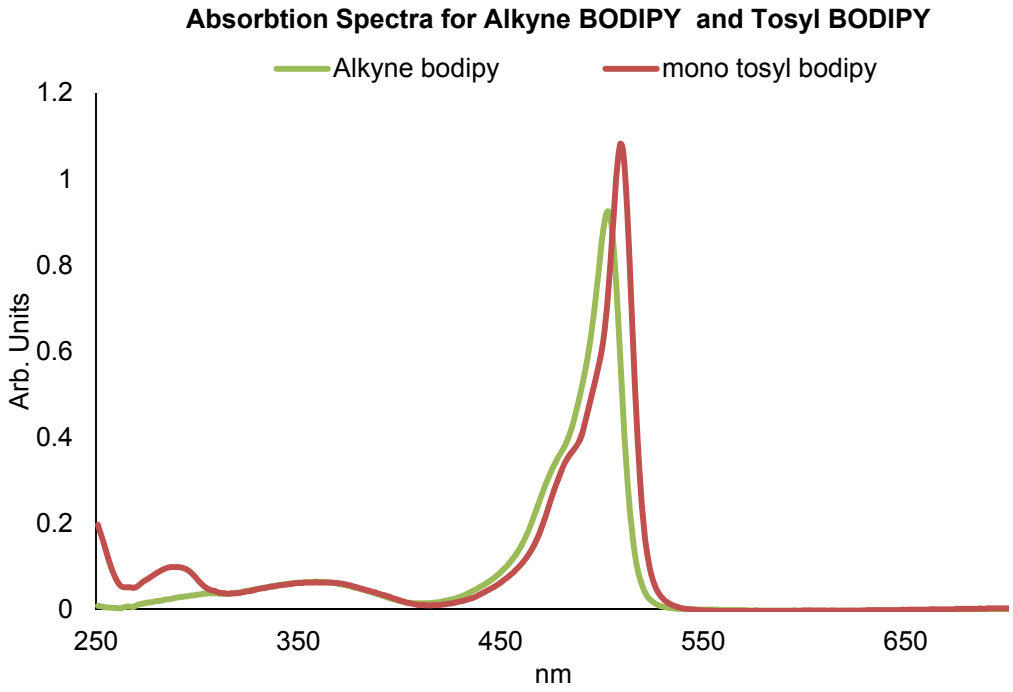


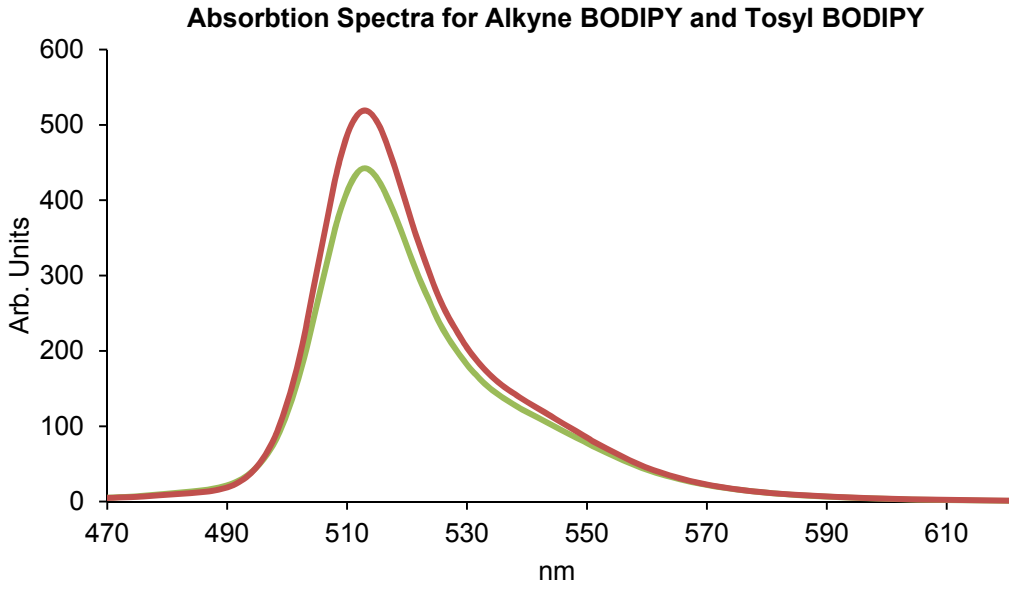

Appendix 6.6: Genes Investigated in qRT-PCR Array

| Relevance to Cell Motility | Genes Investigated in Human Cell Motility RT-qPCR Array |
|---|---|
| Chemotaxis | FGF2 (BFGF), ITGB2, MAPK1 (ERK2), MYH10, MYH9, PLAUR (UPAR), PLD1, PRKCA, RAC2, TGFB1, VEGFA, WASF2, WIPF1. |
| Receptors | EGFR (ERBB1), IGF1R, ITGA4 (CD49D), ITGB1, ITGB2, ITGB3, MET, PLAUR (UPAR), RHO. |
| Growth Factors | CSF1 (MCSF), EGF, FGF2 (BFGF), HGF, IGF1, TGFB1, VEGFA. |
| Rho Family GTPases | RHO Signaling: ACTR2, ACTR3, ARHGDIA, LIMK1, MSN, MYL9, MYLK, PLCG1, PLD1, PRKCA, PTEN, PTPN1 (PTP1B), RHO, RHOA, RHOB, RHOC, RND3, ROCK1, VIM. |
| | RAC Signaling: ACTR2, ACTR3, BAIAP2, CFL1, CRK, PAK1, PAK4, PLD1, PRKCA, RAC1, RAC2, STAT3, WASF1, WASF2, WASL. |
| | CDC42 Signaling: ACTR2, ACTR3, CDC42, PFN1, WASF1, WASF2, WASL. |
| Cell Adhesion Molecules | Cell-Cell Adhesion: DPP4, EGFR (ERBB1), EZR, ITGA4 (CD49D), ITGB1, ITGB2, MSN, MYH9, ROCK1, TGFB1. |
| | Cell-Extracellular Matrix (ECM) Adhesion: ACTN1, ACTN3, CSF1 (MCSF), ILK, ITGB1, ITGB2, ITGB3, MMP14, PTEN, PTK2B (PYK2), PXN, RASA1, RHOA. |
| | Focal Adhesions: ACTN1, ACTN3, ARHGEF7, BCAR1, CAPN1, CAPN2, CAV1, ENAH, ILK, ITGB1, MYL9, PTK2 (FAK), PTK2B (PYK2), PXN, TLN1, VASP, VCL. |
| | Leukocyte Adhesion & Rolling: EZR, ITGA4 (CD49D), ITGB1, ITGB2, MSN, ROCK1. |
| Integrin Signaling | BCAR1, ILK, ITGA4 (CD49D), ITGB1, ITGB2, ITGB3, MYH9, PTK2 (FAK). |
| Cellular Projections | Filopodia: BAIAP2, CDC42, DIAPH1, EGFR (ERBB1), ENAH, EZR, MSN, RDX, SVIL, VASP. |
| | Lamellipodia: CTTN, DPP4, EGFR (ERBB1), ENAH, FAP, PIK3CA (p110-alpha), PLD1, PTK2 (FAK), PXN, RDX, SVIL, VASP, VCL, WASF1, WASF2, WASL.. |
| | Stress Fibers: ACTN4, DIAPH1, MYH10, MYH9, RHOA, RHOB, RHOC |
| | Membrane Blebs: ACTN1, ACTN3, ACTN4, EZR, MYH10, MYH9, MYLK, RND3, ROCK1. |
| | Invasive Projections: ACTR2, ACTR3, ARF6, CDC42, CFL1, CTTN, DPP4, EGF, EZR, FAP, MMP14, MMP2, MMP9, MSN, MYH9, PLAUR (UPAR), RAC2, RASA1, SH3PXD2A, SRC, SVIL, TGFB1, VEGFA, WASL, WIPF1. |
| | Growth Cones: ARHGEF7, CDC42, CFL1, PTK2B (PYK2).. |
| | Membrane Ruffles: ACTR2, ACTR3, ARF6, BAIAP2, BCAR1, CTTN, DIAPH1, EZR, ITGB1, MYH9, RAC1, RAC2, RDX, RHOA, TLN1, WASF2 |
| Cell Polarity | CDC42, CFL1, EZR, IGF1R, ILK, MYH9. |
| Proteases & Protease Inhibitors | AKT1, CAPN1, CAPN2, DPP4, FAP, HGF, MMP14, MMP2, MMP9, MYH9, PLAUR (UPAR), TIMP2. |

## 7.0 References


[1] S. Schreml, R.-M. Szeimies, L. Prantl, M. Landthaler and P. Babilas, *J. Am. Acad. Dermatol. 63*, 866.
[2] N. B. Menke, K. R. Ward, T. M. Witten, D. G. Bonchev and R. F. Diegelmann, *Clin. Dermatol.* **2007**, *25*, 19.
[3] V. Falanga, *Lancet.* **2005**, *366*, 1736.
[4] G. I. Broughton, J. E. Janis and C. E. Attinger, *Plast. Reconstr. Surg.* **2006**, *117*, 12S.
[5] N. T. Bennett and G. S. Schultz, *Am. J. Surg.* **1993**, *165*, 728.
[6] P. Singh, C. Carraher and J. E. Schwarzbauer, *Annu. Rev. Cell Dev. Bi.* **2010**, *26*, 397.
[7] N. S. Greaves, K. J. Ashcroft, M. Baguneid and A. Bayat, *J. Dermatol. Sci.* **2013**, *72*, 206.
[8] N. B. Menke, K. R. Ward, T. M. Witten, D. G. Bonchev and R. F. Diegelmann, *Clin. Dermatol. 25*, 19.
[9] S. Wild, G. Roglic, A. Green, R. Sicree and H. King, *Diabetes Care.* **2004**, *27*, 1047.
[10] E. Mannucci, *JAMA-J. Am. Med. Assoc.* **2010**, *304*, 1615.
[11] B. Buchberger, M. Follmann, D. Freyer, H. Huppertz, A. Ehm and J. Wasem, *GMS Health Technology Assessment,* **2010**, *6*, Doc12.
[12] H. Brem and M. Tomic-Canic, *The Journal of Clinical Investigation*, **2007**, *117*, 1219.
[13] L. Poretsky, D. Shavelson, J. S. Steinberg and B. W. Bakotic in *The Diabetic Foot*, Springer US, pp. 381-399.
[14] H. Brem, P. Sheehan, H. J. Rosenberg, J. S. Schneider and A. J. M. Boulton, *Plast. Reconstr. Surg.* **2006**, *117*, 193S.
[15] N. Papanas and E. Maltezos, *Clin. Interv. Aging*, **2008**, *3*, 233.
[16] C.-F. Cheng, D. Sahu, F. Tsen, Z. Zhao, J. Fan, R. Kim, X. Wang, x, K. Brien, Y. Li, Y. Kuang, M. Chen, D. T. Woodley and W. Li, *J. Clin. Invest.* **2011**, *121*, 4348.
[17] R. Longtin, *J. Natl. Cancer I.* **2004**, *96*, 6.
[18] E. L. George, E. N. Georges-Labouesse, R. S. Patel-King, H. Rayburn and R. O. Hynes, *Development*, **1993**, *119*, 1079.
[19] M. K. Magnusson and D. F. Mosher, *Arterioscler. Thromb. Vasc. Biol.* **1998**, *18*, 1363.
[20] R. A. Fox, D. S. Gregory and J. D. Feldman, *J. Immunol.* **1974**, *112*, 1861.
[21] S. L. Schor, I. R. Ellis, S. J. Jones, R. Baillie, K. Seneviratne, J. Clausen, K. Motegi, B. Vojtesek, K. Kankova, E. Furrie, M. J. Sales, A. M. Schor and R. A. Kay, *Cancer Res.* **2003**, *63*, 8827.
[22] S. L. Schor, A. M. Schor, A. M. Grey and G. Rushton, *J. Cell Sci.* **1988**, *90*, 391.
[23] A. M. Schor and S. L. Schor, *Eye* **2009**, *24*, 450.
[24] I. R. Ellis, S. J. Jones, D. Staunton, I. Vakonakis, D. G. Norman, J. R. Potts, C. M. Milner, N. A. G. Meenan, S. Raibaud, G. Ohea, A. M. Schor and S. L. Schor, *Exp. Cell Res.* **2010**, *316*, 2465.
[25] I. R. Ellis, S. J. Jones, Y. Lindsay, G. Ohe, A. M. Schor, S. L. Schor and N. R. Leslie, *Cell. Signal.* **2010**, *22*, 1655.
[26] S. L. Schor, I. Ellis, J. Banyard and A. M. Schor, *J. Cell Sci.* **1999**, *112 ( Pt 22)*, 3879.
[27] N. Shpiro, I. R. Ellis, T. J. Dines, A. M. Schor, S. L. Schor, D. G. Norman and R. Marquez, *Mol. BioSyst.* **2005**, *1*, 318.
[28] K. Czosnyka, Thesis, University of Glasgow (Glasgow) **2010**.
[29] G. R. Waitkins and C. W. Clark, *Chem. Rev.* **1945**, *36*, 235.
[30] K. C. Nicolaou, T. Montagnon, P. S. Baran and Y. L. Zhong, *J. Am. Chem. Soc.* **2002**, *124*, 2245.
[31] A. Vázquez Sánchez and J. G. Ávila Zárraga, *J. Mex. Chem. Soc.* **2007**, *51*, 213.
[32] N. Inoue. *Vol.* WO2002087578 A1, (Ed: E. P. Office), **2002**.
[33] M. Estévez, E. Martínez, S. J. Yarwood, M. J. Dalby and J. Samitier, *J. Biomed. Mater. Res. Part A.* **2015**, *103*, 1659.

[34] C. S. Wright, M. A. M. Van Steensel, M. B. Hodgins and P. E. M. Martin, *Wound Repair Regen.* **2009**, *17*, 240.
[35] C. S. Wright, S. Pollok, D. J. Flint, J. M. Brandner and P. E. M. Martin, *J. Cell. Physiol.* **2012**, *227*, 77.
[36] C. S. Wright, R. F. Berends, D. J. Flint and P. E. M. Martin, *Exp. Cell Res.* **2013**, *319*, 390.
[37] C.-C. Liang, A. Y. Park and J.-L. Guan, *Nat. Protoc.* **2007**, *2*, 329.
[38] K. B. Mullis, *Sci. Am.* **1990**, *262*, 56.
[39] L. Garibyan and N. Avashia, *J. Invest. Dermatol.* **2013**, *133*, e6.
[40] M. Kubista, J. M. Andrade, M. Bengtsson, A. Forootan, J. Jonák, K. Lind, R. Sindelka, R. Sjöback, B. Sjögreen, L. Strömbom, A. Ståhlberg and N. Zoric, *Mol. Aspects Med.* **2006**, *27*, 95.
[41] T. Nolan, R. E. Hands and S. A. Bustin, *Nat. Protoc.* **2006**, *1*, 1559.
[42] H. Wedler, *Project Report QSA1066. Gene expression analysis using RT² Profiler™ Arrays: Human Cell Motility PCR Array (PAHS-128Z)*, *Vol.* **2015**.
[43] Z. Laron, *Molecular Pathology* **2001**, *54*, 311.
[44] E. De Wolf, R. Gill, S. Geddes, J. Pitts, A. Wollmer and J. Grotzinger, *Protein Sci.* **1996**, *5*, 2193.
[45] S. Werner and R. Grose, *Physiol. Rev.* **2003**, 835.
[46] J. A. Janssen and S. W. Lamberts, *Clin. Endocrinol.* **2000**, *52*, 1.
[47] S. Balaji, M. LeSaint, S. S. Bhattacharya, C. Moles, Y. Dhamija, M. Kidd, L. D. Le, A. King, A. Shaaban, T. M. Crombleholme, P. Bollyky and S. G. Keswani, *J. Surg. Res. 190*, 367-377.
[48] M. G. Slomiany and S. A. Rosenzweig, *J. Pharmacol. Exp. Ther.* **2006**, *318*, 666.
[49] D. G. MacArthur and K. N. North, *BioEssays* **2004**, *26*, 786.
[50] S. Ebashi, F. Ebashi and K. Maruyama, *Nature* **1964**, *203*, 645.
[51] B. Yuruker and V. Niggli, *J. Cell Sci.* **1992**, *101*, 403.
[52] F. M. Pavalko, C. A. Otey, K. O. Simon and K. Burridge, *Biochem. Soc. Trans.* **1991**, *19*, 1065.
[53] H. Li, R. Aneja and I. Chaiken, *Molecules* **2013**, *18*, 9797.
[54] Z. Kupihár, Z. Schmél, Z. Kele, B. Penke and L. Kovács, *Bioorg. Med. Chem.* **2001**, *9*, 1241.
[55] W. E. Bondinell, R. M. Keenan, W. H. Miller, F. E. Ali, A. C. Allen, C. W. De Brosse, D. S. Eggleston, K. F. Erhard, R. C. Haltiwanger, W. F. Huffman, S.-M. Hwang, D. R. Jakas, P. F. Koster, T. W. Ku, C. P. Lee, A. J. Nichols, S. T. Ross, J. M. Samanen, R. E. Valocik, J. A. Vasko-Moser, J. W. Venslavsky, A. S. Wong and C.-K. Yuan, *Bioorg. Med. Chem.* **1994**, *2*, 897.
[56] W. H. Miller, K. A. Newlander, D. S. Eggleston and R. C. Haltiwanger, *Tetrahedron Lett.* **1995**, *36*, 373.
[57] W. H. Miller, T. W. Ku, F. E. Ali, W. E. Bondinell, R. R. Calvo, L. D. Davis, K. F. Erhard, L. B. Hall, W. F. Huffman, R. M. Keenan, C. Kwon, K. A. Newlander, S. T. Ross, J. M. Samanen, D. T. Takata and C.-K. Yuan, *Tetrahedron Lett.* **1995**, *36*, 9433.
[58] R. M. Keenan, W. H. Miller, L. S. Barton, W. E. Bondinell, R. D. Cousins, D. F. Eppley, S.-M. Hwang, C. Kwon, M. A. Lago, T. T. Nguyen, B. R. Smith, I. N. Uzinskas and C. C. K. Yuan, *Bioorg. Med. Chem. Lett.* **1999**, *9*, 1801.
[59] A.-K. C. Schmidt and C. B. W. Stark, *Org. Lett.* **2011**, *13*, 4164.
[60] S. K. Thompson and C. H. Heathcock, *J. Org. Chem.* **1992**, *57*, 5979.
[61] J.-M. Vatèle, *Tetrahedron Lett.* **2006**, *47*, 715.
[62] Y. Sasano, S. Nagasawa, M. Yamazaki, M. Shibuya, J. Park and Y. Iwabuchi, *Angew. Chem. Int. Ed.* **2014**, *53*, 3236.
[63] S. Kapić, H. Čipčić Paljetak, S. Alihodžić, R. Antolović, V. Eraković Haber, R. L. Jarvest, D. J. Holmes, J. P. Broskey and E. Hunt, *Bioorg. Med. Chem.* **2010**, *18*, 6569.
[64] F. Grinnell and B. Geiger, *Exp. Cell Res.* **1986**, *162*, 449.
[65] S. Foillard, P. Dumy and D. Boturyn, *Org. Biomol. Chem.* **2009**, *7*, 4159.
[66] E. Bayer, *Angew. Chem. Internat. Ed.* **1991**, *30*, 113.

[67] C. J. Daly and J. C. McGrath, *Pharmacol.Therapeut.* **2003**, *100*, 101.
[68] G. Ulrich, R. Ziessel and A. Harriman, *Angew. Chem. Int. Ed.* **2008**, *47*, 1184.
[69] S. F. Malan, A. v. Marle, W. M. Menge, V. Zuliana, M. Hoffman, H. Timmerman and R. Leurs, *Bioorg. Med. Chem.* **2004**, *12*, 6495.
[70] K. Gießler, H. Griesser, D. Göhringer, T. Sabirov and C. Richert, *Eur. J. Org. Chem.* **2010**, *2010*, 3611.
[71] J. O. Flores-Rizo, I. Esnal, C. A. Osorio-Martínez, C. F. A. Gómez-Durán, J. Bañuelos, I. López Arbeloa, K. H. Pannell, A. J. Metta-Magaña and E. Peña-Cabrera, *J. Org. Chem.* **2013**, *78*, 5867.
[72] T. V. Goud, A. Tutar and J.-F. Biellmann, *Tetrahedron* **2006**, *62*, 5084.
[73] M. Verdoes, U. Hillaert, B. I. Florea, M. Sae-Heng, M. D. P. Risseeuw, D. V. Filippov, G. A. van der Marel and H. S. Overkleeft, *Bioorg. Med. Chem. Lett.* **2007**, *17*, 6169.
[74] A. M. Hansen, A. L. Sewell, R. H. Pedersen, D.-L. Long, N. Gadegaard and R. Marquez, *Tetrahedron* **2013**, *69*, 8527.
[75] J. Raushel and V. V. Fokin, *Org. Lett.* **2010**, *12*, 4952.
[76] N. Seus, M. T. Saraiva, E. E. Alberto, L. Savegnago and D. Alves, *Tetrahedron* **2012**, *68*, 10419.
[77] V. V. Rostovtsev, L. G. Green, V. V. Fokin and K. B. Sharpless, *Angew. Chem. Int. Ed.* **2002**, *41*, 2596.
[78] F. Grinnell, *J. Cell Biochem.* **1984**, *26*, 107.
[79] W. T. McGaw and A. R. T. Cate, *J. Investig. Dermatol.* **1983**, *81*, 375.
[80] S. D. Blystone, I. L. Graham, F. P. Lindberg and E. J. Brown, *J. Cell Biol.* **1994**, *127*, 1129.
[81] C. J. Millard, I. R. Ellis, A. R. Pickford, A. M. Schor, S. L. Schor and I. D. Campbell, *J. Biol. Chem.* **2007**, *282*, 35530.
[82] R. Yan, K. Sander, E. Galante, V. Rajkumar, A. Badar, M. Robson, E. El-Emir, M. F. Lythgoe, R. B. Pedley and E. Årstad, *J. Am. Chem. Soc.* **2013**, *135*, 703.
[83] L. Wu and K. Burgess, *Chem. Commun.* **2008**, 4933.
[84] J. E. Falk and K. M. Smith, *Porphyrins and Metalloporphyrins*, (Elsevier), **1975**, 37.
[85] J. S. Boateng, K. H. Matthews, H. N. E. Stevens and G. M. Eccleston, *J. Pharm. Sci.* **2008**, *97*, 2892.
[86] S. Sarabahi, *Indian J. Plast. Surg.* **2012**, *45*, 379.
[87] M. Zhou, A. M. Smith, A. K. Das, N. W. Hodson, R. F. Collins, R. V. Ulijn and J. E. Gough, *Biomaterials* **2009**, *30*, 2523.
[88] F. Schmidt, I. C. Rosnizeck, M. Spoerner, H. R. Kalbitzer and B. König, *Inorg. Chim. Acta* **2011**, *365*, 38.
[89] S. W. Jeong and D. F. O'Brien, *J. Org. Chem.* **2001**, *66*, 4799.
[90] K. Hubel, Le and H. Waldmann, *Chemical Society Reviews* **2008**, *37*, 1361-1374.
[91] T. P. Soares da Costa, W. Tieu, M. Y. Yap, O. Zvarec, J. M. Bell, J. D. Turnidge, J. C. Wallace, G. W. Booker, M. C. J. Wilce, A. D. Abell and S. W. Polyak, *ACS Med. Chem. Lett.* **2012**, *3*, 509.
[92] Y. Abouelhassan, A. T. Garrison, F. Bai, V. M. Norwood, M. T. Nguyen, S. Jin and R. W. Huigens, *ChemMedChem.* **2015**, *10*, 1157.
[93] A. García-Rubia, R. G. Arrayás and J. C. Carretero, *Angew. Chem. Int. Ed.* **2009**, *48*, 6511.
[94] K. Czosnyka, Thesis, University of Glasgow (Glasgow) **2010**.
[95] C. J. Forsyth, L. Ying, J. Chen and J. J. La Clair, *J. Am. Chem. Soc.* **2006**, *128*, 3858.
[96] T. Uppal, N. V. S. D. K. Bhupathiraju and M. G. H. Vicente, *Tetrahedron* **2013**, *69*, 4687.